The Afterglows of *Swift*-era Short and Long Gamma-Ray Bursts

Dissertation
zur Erlangung des akademischen Grades
Dr. rer. nat.

vorgelegt dem Rat der Physikalisch-Astronomischen Fakultät
der Friedrich-Schiller-Universität Jena

eingereicht von Dipl.-Phys. David Alexander Kann
geboren am 15.02.1977 in Trier

Gutachter

1. Prof. Dr. Artie Hatzes, Thüringer Landessternwarte Tautenburg, Sternwarte 5, 07778 Tautenburg

2. Prof. Dr. Jörn Wilms, Dr. Remeis-Sternwarte, Sternwartstraße 7, 96049 Bamberg

3. PD Dr. Hans-Thomas Janka, Max-Planck-Institut fr Astrophysik, Karl-Schwarzschild-Str. 1, 85748 Garching

Tag der letzten Rigorosumsprüfung: 13. 07. 2011

Tag der öffentlichen Verteidigung: 13. 07. 2011

Zusammenfassung

Das Phänomen der Gammastrahlenausbrüche (Englisch: Gamma-Ray Bursts, kurz: GRBs) war auch lange nach ihrer Entdeckung vor über vier Jahrzehnten ein großes Rätsel. Selbst heute, über ein Jahrzehnt seit Beginn der "Ära der Nachglühen" (engl.: Afterglows) sind noch viele Fragen unbeantwortet. Das akzeptierte Bild, welches einen Großteil der Daten erklären kann ist, dass GRBs erzeugt werden, wenn ein massereicher Himmelskörper (entweder ein Stern, der die Hauptreihe verlassen hat, oder miteinander verschmelzende kompakte Objekte) in kosmologischer Distanz zu einem schnell rotierenden Objekt kollabiert (ein Schwarzes Loch oder vielleicht ein kurzlebiger Magnetar), welches ultrarelativistische Materieauswürfe (sogenannte "Jets") entlang der Polachse ausschleudert. Die interne Dissipation von Energie in dem Jet führt zu kollimierter nicht-thermischer Strahlung bei hohen Energien (der eigentliche GRB), während Schockfronten, die bei der Interaktion des Jets mit der interstellaren Materie erzeugt werden, zu einem langlebigen abklingenden Afterglows führen. Die gesammelten physikalischen Prozesse, die die GRB-Emission beschreiben, werden als das Standard-Feuerballmodell bezeichnet. GRBs sind für kurze Zeiträume nachweislich die leuchtkräftigsten elektromagnetischen Quellen des Universums.

Noch vor der Entdeckung der Afterglows wurde festgestellt, dass es (mindestens) zwei Klassen von GRBs gibt welche, ihren Zeitverläufen und Spektren nach, als kurze/harte und lange/weiche GRBs bezeichnet werden. In den letzten Jahren wurde offensichtlich, dass diese klassischen Definitionen nicht universell gültig sind, und die Begriffe Typ I GRB (nicht mit massereicher Sternentstehung verknüpft, vermutlich durch die Verschmelzung kompakter Objekte ausgelöst) und Typ II GRB (mit massereicher Sternentstehung verknüpft, die optische Emission zu späten Zeiten enthält eine Komponente, die einer Typ Ic Supernova mit hoher Ausbreitungsgeschwindigkeit zuzuschreiben ist) wurden vorgeschlagen.

Während die Untersuchung der Afterglows von Typ II GRBs seit ihrer Entdeckung Anfang 1997 schnell voranschritt, und inzwischen große Samples untersucht werden können, wurde kein Afterglows eines Typ I GRBs in irgendeinem Wellenlängenbereich entdeckt, bis im Jahre 2005 der dedizierte Satellit *Swift* in Betrieb ging. Die ersten Afterglows wurden in Galaxien mit geringer Sternentstehungsrate gefunden, was sofort bestätigte, dass Typ I GRBs durch alte Sternpopulationen erzeugt werden können, was das Verschmelzungsmodell unterstützt. Des weiteren sind Typ I GRBs signifikant weniger energiereich als Typ II GRBs, sowohl was die GRB-Emission angeht als auch die Leuchtkraft des Afterglows. Weitere Detektierungen zeigten jedoch, dass das Bild nicht so einheitlich war, da sich viele Typ I GRBs in Galaxien mit aktiver Sternentstehung ereignen und sie doch energeireicher sein können, als zu Beginn angenommen.

In dieser Dissertation präsentiere ich meine Untersuchungen zu den Afterglows von Typ I und Typ II GRBs, und vergleiche sie miteinander, insbesondere, was die Extinktion durch Staub in den Muttergalaxien sowie die Leuchtkraftverteilung angeht. Um dies zu ermöglichen, habe ich das weltweit größte Archiv an photometrischen Daten zu Afterglows zusammengestellt und habe aus diesem GRBs selektiert, die ausreichende Daten für eine weitergehende Analyse

boten. Die Dissertation is folgendermaßen geordnet: Das erste Kapitel gibt eine Einleitung zu der Geschichte der GRB-Forschung und präsentiert die Beobachtungen, die zu dem heutigen Bild geführt haben, wie GRBs erzeugt werden. Das zweite Kapitel beinhaltet die theoretischen Grundlagen und Vorhersagen des Standard-Feuerballmodells. Im dritten Kapitel stelle ich die Analysemethoden vor und erläutere, wie ich die Samples erstellt habe. Im vierten Kapitel diskutiere ich die Eigenschaften der Afterglows von Typ II GRBs, während im fünften Kapitel diese mit den Afterglows von Typ I GRBs verglichen werden. Im sechsten Kapitel komme ich zum Schluß, fasse meine Ergebnisse zusammen und gebe einen Ausblick auf weitere Arbeit, an der ich beteiligt bin. Im Anhang schließlich prsentiere ich zustzliche Ergebnisse zu den Afterglows von Type I und Typ II GRBs, diskutiere weitere Untersuchungen an diversen GRBs, an denen ich beteiligt war, und führe die Beobachtungen auf, die wir mit dem Tautenburger Teleskop gewonnen haben und an denen ich beteiligt war.

Abstract

The phenomenon of Gamma-Ray Bursts (GRBs) has been a great mystery since their discovery four decades ago. Even today, over a decade into the "afterglow age", many questions are still unanswered. The canonical picture which satisfies most of the data is that GRBs are produced when a massive celestial body (either a post-main sequence star or merging compact objects) at cosmological distances collapses to a rapidly rotating compact object (a black hole or possibly a short-lived massive magnetar) which launches ultra-relativistic polar jets. The internal dissipation of energy within the jets leads to collimated non-thermal high-energy emission (the actual GRB), whereas shocks created from the interactions of the jets with the interstellar medium create a long-lasting fading afterglow. The collected physical processes describing this emission are called the standard fireball model. GRBs have been found to be the most luminous electromagnetic sources in the universe for short time periods.

Even before the discovery of afterglows, it was established that GRBs exist in (at least) two classes, which, according to their temporal and spectral properties, have been labelled short/hard and long/soft GRBs. In the last years, it has become obvious that these classical definitions do not apply universally, and the terms Type I GRB (not associated with massive star formation, probably due to the merger of compact objects) and Type II GRB (associated with massive star formation, the late optical emission includes a component due to a Type Ic supernova with high expansions speeds) have been suggested instead.

While the study of afterglows of Type II GRBs has progressed rapidly since their discovery in early 1997, and large samples can be studied today, no Type I GRB afterglow was detected at any wavelength until the advent of the dedicated *Swift* satellite in 2005. The first afterglows were localized in early-type galaxies, immediately confirming that Type I GRBs can be produced by an old stellar population, and supporting the merger model. Furthermore, Type I GRBs were clearly significantly less energetic than Type II GRBs, both in the GRB emission as well as the afterglow luminosity. Further detections, though, showed that the picture was not so clear, as many Type I GRBs occur in star-forming galaxies and are more energetic than initially expected.

In this Thesis, I present my study of the afterglows of Type I and Type II GRBs, and compare them with each other, especially in terms of host-galaxy dust extinction and the luminosity distribution. To accomplish this, I have collected the largest sample of photometric afterglow data available worldwide, and from this, selected GRBs with data sufficient for a more detailed analysis. The Thesis is ordered as follows: Chapter 1 gives an introduction into the history of GRB science, and presents the observations which have given us our current picture of how GRBs are generated. Chapter 2 presents the basic equations and predictions of the standard fireball model. In Chapter 3, I present the analysis methods and explain how I created the samples. In Chapter 4, the properties of Type II GRB afterglows are discussed, and in Chapter 5, they are compared with those of Type I GRBs. In Chapter 6, I conclude and sum up my results, and give an outlook on further research in progress. Finally, in the Appendix, I present additional results on the afterglows of Type I and Type

II GRBs, observational results on multiple GRB events which I was involved in, and also list the observations performed with our Tautenburg telescope which I was involved in.

Contents

Chapter 1

The History of GRB Research

Gamma-Ray Bursts (GRBs) are, from a purely observational standpoint, short flare-ups of hard X-rays to soft gamma-rays (keV to MeV region) lasting from milliseconds to several thousand seconds, with the typical range being a few tenths of a second to one hundred seconds. They can be very intense, outshining all other cosmic sources combined at these wavelengths over the short period of time that they are active.

1.1 The discovery of GRBs and the first two decades

Klebesadel et al. (1973) reported the first discovered GRBs. Since they did not seem to have any low-energy counterparts and were only detected in gamma-rays, they could not have been discovered until the first satellites were launched which were able to detect photons in this wavelength regime. These were the U.S. *Vela* military satellites, designed to register the gamma flashes of nuclear detonations both on Earth and in space and monitor compliance of the Limited Nuclear Test Ban Treaty which prohibited atmospheric and exospheric nuclear detonations. On the 2nd of July 1967, two *Vela* satellites detected a strong outburst of gamma-rays which had a time history very different from what was expected from a nuclear explosion. Further events were found in the following years. The *Vela* satellites gave only inaccurate localizations (on the order of tens of degrees), so the GRBs could not be linked to any known sources, on the other hand, the Sun, the Earth and the Moon were excluded. A new cosmic phenomenon had been found. And while the other big discoveries of this era, such as the cosmic microwave background, quasars and pulsars were rapidly explained, or even predicted by theory, GRBs would remain a mystery for a long time.

Over the next two decades, the number of missions capable of detecting GRBs rose. Toward the end of the 1970s, multiple spacecraft, some in low-earth orbit, some orbiting other planets (e.g., the Pioneer Venus Orbiter), formed the first *InterPlanetary Network (IPN)*, which allowed the localization of GRBs with a henceforth unknown precision (e.g., GRB 790406, a short-duration event localized to 0.26 arcmin^2, Schaefer 2006). These precise positions were not available until weeks or months after the event, though, and searches for any remarkable objects (bright stars or nearby galaxies, for example) came up empty. This was the so-called "no-host problem", and it was part of the greatest barrier in understanding the nature of these high-energy events. Without any kind of distance scale, the energetics were unknown, and thus a large number of theories were developed, covering distance (and

2704 BATSE Gamma-Ray Bursts
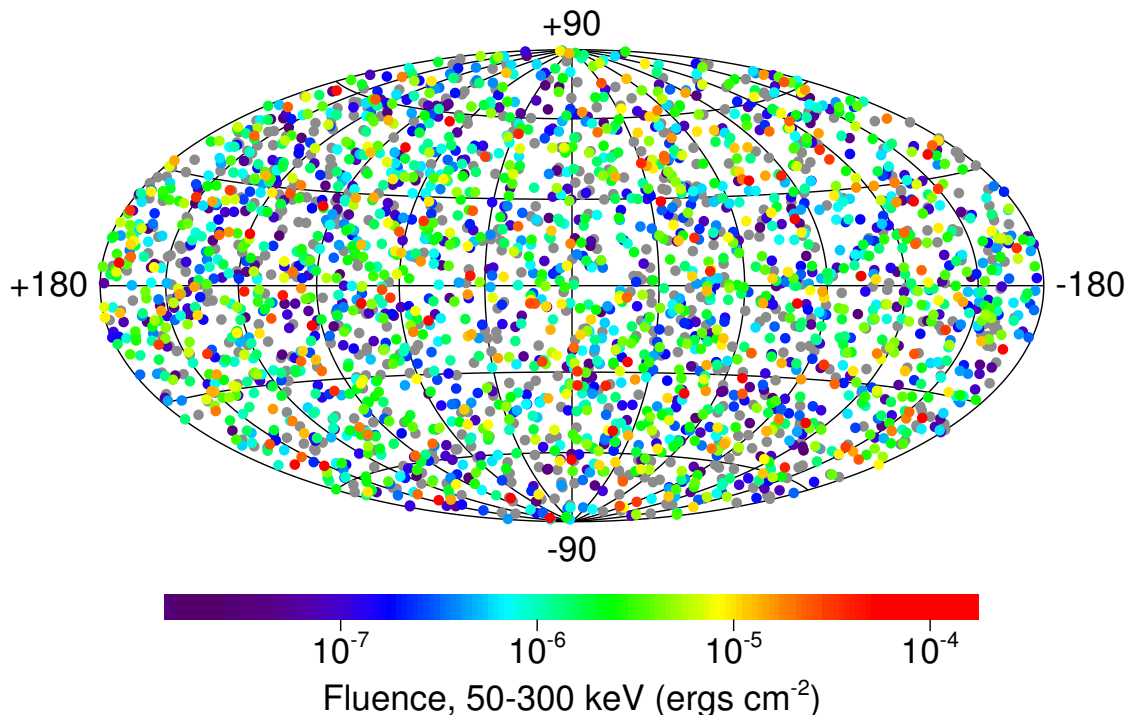
Figure 1.1: *The distribution of the 2704 GRBs in the final catalog (5B) of the* BATSE *experiment on the* CGRO *satellite. The locations are plotted in Galactic coordinates. The locations are color-coded according to fluence (gray dots imply no fluence could be measured). Clearly, there is no clustering toward the Galactic plane, the distribution of GRBs is isotropic. Taken from:* http://www.batse.msfc.nasa.gov/batse/grb/skymap/

energy) scales from the solar system up to extreme redshifts. For an overview of this early phase of research, see Higdon & Lingenfelter (1990).

1.2   The *BATSE* era – creating a large GRB sample

With the launch of the second of NASA's "Great Observatories", the *Compton Gamma-Ray Observatory*, the study of GRBs was revolutionized for the first time since their discovery. While the other instruments on board (*COMPTEL*, *OSSE*, and *EGRET* [*TASC* and the spark chamber]) made some contributions to GRB science, the main instrument for gamma-ray bursts was *BATSE*, the *Burst And Transient Source Experiment*. It consisted of eight detectors arranged on the corners of the spacecraft, giving it an all-sky view (except for Earth occultation due to the low-Earth orbit). During its nine-year life span, BATSE triggered on a total of 2704 GRBs (Figure 1.1), with hundreds more found by ground-analysis of the telemetry data. Figure 1.2 shows the diverse shapes of GRB high-energy emission. Any model which explains GRBs must be able to explain the strong diversity of the prompt emission.
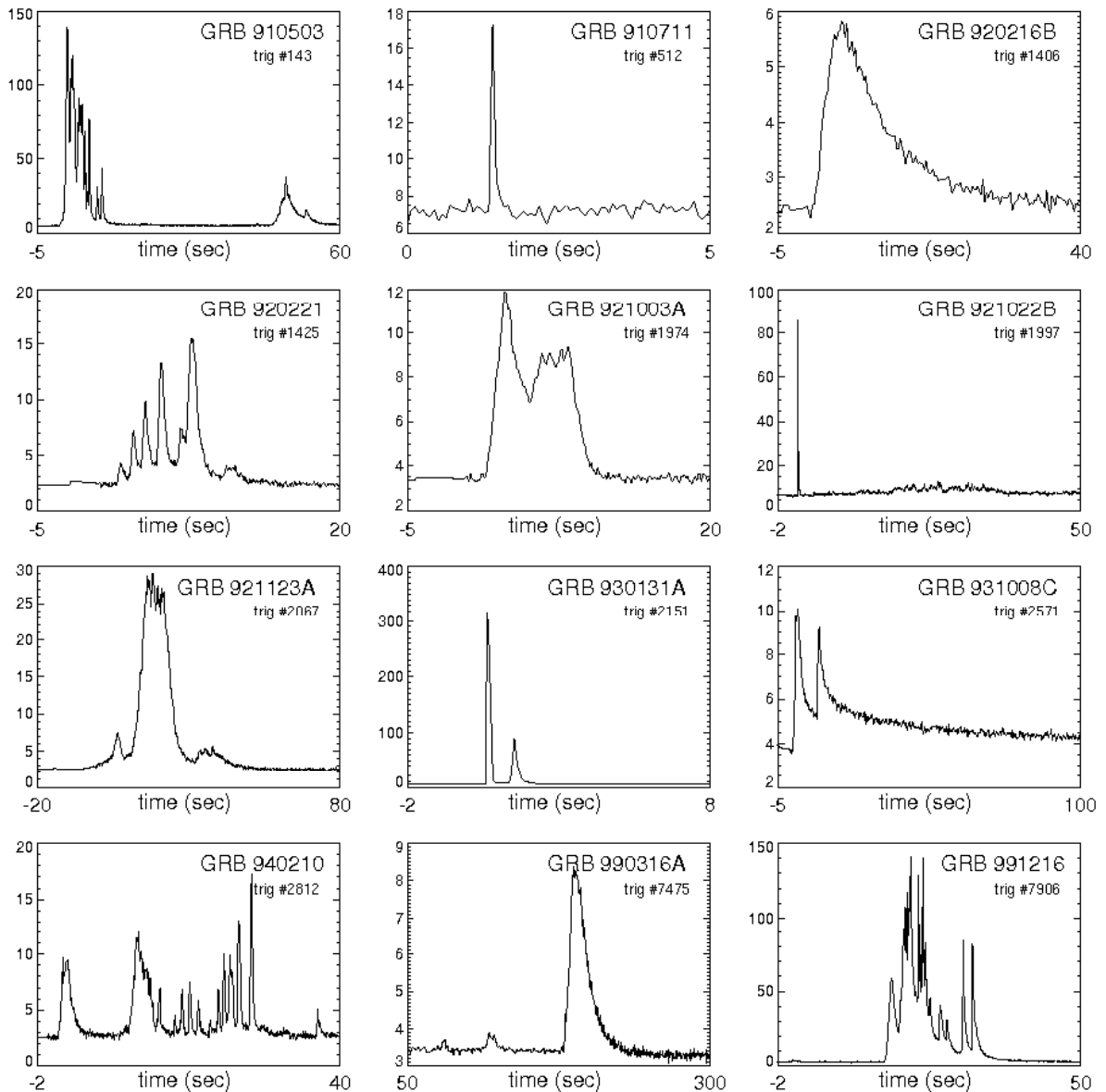
Figure 1.2: *Examples of GRBs detected by* BATSE. *There are complex long GRBs (e.g., GRB 910503, GRB 991216), fast rise, exponential decline (FRED) long GRBs (GRB 920216B), and short GRBs (GRB 910711, GRB 930131A). The y-axis is kilocounts/s.   Taken from: http://upload.wikimedia.org/wikipedia/commons/e/ef/GRB_BATSE_12lightcurves.png*

The uniform, broad spectral coverage of *BATSE* and the other *CGRO* instruments allowed detailed statistical studies of the high-energy emission of GRBs to be performed. Kouveliotou et al. (1993) found that two populations of GRBs must exist, which not only separate into short (duration roughly less than two seconds) and long (duration longer than roughly two seconds) GRBs (as already found by Mazets & Golenetskii 1981), but also spectrally into harder (the short ones) and softer (the long ones) events[1]. Band et al. (1993) introduced an empirical equation, in the form of a smoothly broken power-law (henceforth called the

---

[1]Spectral hardness here is defined as the ratio of the fluence in two separate energy bands, e.g. $20 - 50$ keV vs. $50 - 100$ keV

"Band"-Function), which could be used to fit almost all prompt emission spectra.

The localization accuracy of *BATSE* (usually several degrees) was still not good enough to produce positions fit for rapid ground-based follow-up. But they were accurate enough to allow for a statistical analysis of the sky distribution, which resulted in an isotropic distribution, in accordance with GRBs lying at cosmological distances (Meegan et al. 1992; Hartmann & Narayan 1996)[2]. The search for the sources of GRBs, the progenitors, still had not made any advances, though. *CGRO* was deorbited June 2000 while still functional.

1.3   *BeppoSAX* and the Beginning of the Afterglow Era

In 1996, two satellites were launched with the express purpose of providing better localizations for GRBs: the NASA *HETE* mission, and the Italian-Dutch *BeppoSAX* satellite. The former satellite failed to separate from the last rocket stage, and therefore it was up to *BeppoSAX* to finally settle the debate on the distance and energy scale of GRBs. *BeppoSAX* had one detector for soft gamma-rays (*GRBM*, $40 - 700$ keV) and two wide-field X-ray cameras (*WFC*, $2 - 28$ keV) with a localization accuracy of around $5'$. The unique capability of this satellite was its ability to slew within a few hours and observe the WFC localization with another set of X-ray detectors, the Narrow Field Instruments (*NFI*), especially the X-ray telescopes *LECS* and *MECS* ($0.1 - 10$ keV), which had arcminute localization accuracy. The mission detected GRBs until April 2002.

Ten months after launch, *BeppoSAX* detected the first significant X-ray afterglow of a GRB, that of GRB 970228 (Costa et al. 1997), and this precise position finally also lead to the discovery of the first GRB optical afterglow (van Paradijs et al. 1997). In this case, though, the discovery of the afterglow was not made immediately, but only after over a week, when images taken 0.9 days after the GRB were compared with late observations which showed a single stellar source had disappeared. While spectroscopy was not obtainable, van Paradijs et al. (1997) already report a faint galaxy at the position of the afterglow, a strong hint that GRBs were indeed cosmological sources.

Final confirmation came with the next discovered afterglow, that of GRB 970508. Spectroscopy of the optical afterglow with the Keck telescope established that the GRB must lie at a redshift of at least $z = 0.835$, immediately validating their cosmological origin and implying that they are the most powerful explosions in the universe (Metzger et al. 1997). Here, a bright radio afterglow was also discovered (Frail et al. 1997), which was found to be variable over short time periods. This was interpreted as interstellar scintillation due to a very small angular source size. The fluctuations stopped a month after the event, leading to an estimate of the source expansion speed as being close to the speed of light – a strong indication that relativistic speeds are involved in the GRB phenomenon, in accordance with earlier theoretical work (see Chapter 2). The third identified afterglow, that of GRB 971214, pointed to a host galaxy which was found to lie at $z = 3.42$, implying GRBs were at least an order of magnitude more energetic than thought before, assuming their energy release is isotropic (Kulkarni et al. 1998).

---

[2]It should be noted that for the following years, a Galactic model involving neutron stars in an outer halo as GRB sources had many proponents, leading to the famous "Great Debate" (see Rees 1995, for a summary), but this is more of historical interest only from today's perspective.
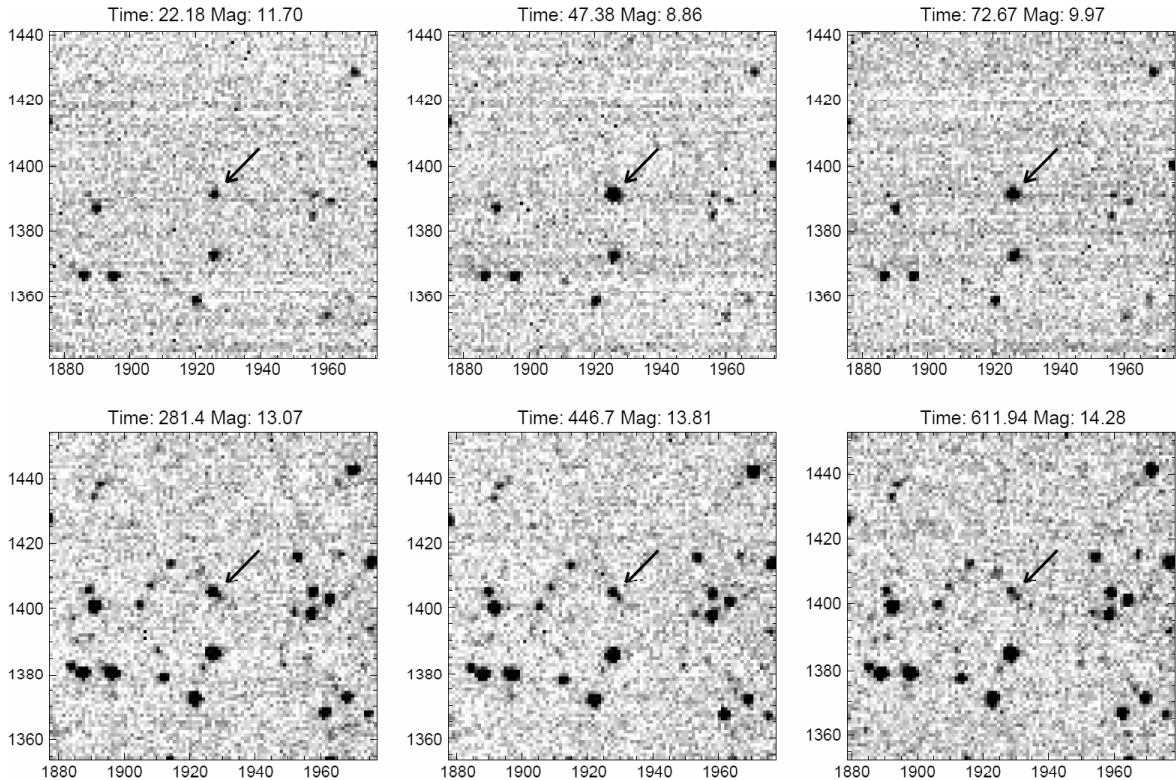
Figure 1.3: *The prompt optical flash of GRB 990123, as measured by the* ROTSE-I *telescope (Akerlof et al. 1999). Clearly, especially at early times, GRB afterglows are extremely variable, and rapid, precise localizations coupled with rapid-reacting, sensitive telescopes are necessary to catch them. Just one day after the GRB, the afterglow was already fainter than 20th magnitude.*

Many of the GRBs detected by *BeppoSAX* were also detected by *CGRO BATSE* (as well as other mission of the *IPN*). An exceptional event was GRB 980425. While no actual optical afterglow was discovered for this source, the *BeppoSAX* error circle encompassed a nearby spiral galaxy, and within days of the GRB, a peculiar supernova, SN 1998bw, was discovered in the galaxy (Galama et al. 1998), which was of Type Ic (core collapse and deficient in hydrogen and helium) with broad lines, indicating expansion speeds of around $0.1c$, leading to it being labeled a "hypernova" (Iwamoto et al. 1998). Together with the first results on their host galaxies, this led to a first link between (long/soft) GRBs and massive star-formation (Paczyński 1998).

On the 23rd of January 1999, one of the brightest GRBs ever detected occurred, triggering both satellites. The *BeppoSAX* localization led to the discovery of the afterglow of GRB 990123, but the initial, degree-wide *BATSE* position triggered a rapid robotic telescope, *ROTSE-I*, which caught a brilliant optical flash (reaching $V = 8.9$ mag, in range of binoculars, see Figure 1.3) contemporaneous with the GRB emission (Akerlof et al. 1999). In combination with the redshift ($z = 1.6004$, Kulkarni et al. 1999), it became clear that an isotropic explosion would have implied the transformation of almost two solar masses of matter into energy ($E_{iso} > 10^{54}$ erg). But the discovery of a break in the light curve (henceforth called a "jet break") implied that the emission was strongly collimated, strongly reducing the energy requirements (Kulkarni et al. 1999). A few months later, the well-monitored afterglow of

GRB 990510 exhibited not a sharp break, but a soft turnover from one power-law decay to another. Of all the empirical equations used to describe this behavior, the one given by Beuermann et al. (1999) became widely used in the community as the "Beuermann equation", it is given in Zeh et al. (2006a) as:

$$F_\nu(t) = const. \cdot \left[\left(\frac{t}{t_b} \right)^{\alpha_1 n} \left(\frac{t}{t_b} \right)^{\alpha_2 n} \right]^{-\frac{1}{n}} + F_\nu^{SN}(t) + F_\nu^{Host} \qquad (1.1)$$

Here, F_ν is the flux density of the optical transient at frequency ν, t is the time measured after the GRB (usually the trigger time), t_b is the time of the jet break, $\alpha_{1,2}$ are the power-law indices of the decay before and after the break, n measures the smoothness of the break ($n = \infty$ is a completely sharp break, $n \approx 1$, as in the case of GRB 990510, indicates a smooth and slow transition), F_ν^{SN} is the contribution of the underlying supernova, and F_ν^{Host} is the constant contribution from the underlying host galaxy.

1.4 *HETE II* and *INTEGRAL* – rapid localization

In October 2000, the *HETE II* satellite was launched, the follow-up mission to the lost 1996 spacecraft. It was followed up two years later by ESA's *INTErnational Gamma-Ray Astrophysics Laboratory (*INTEGRAL*)*. *HETE* was dedicated to the detection of GRBs, while *INTEGRAL* is a gamma-ray observatory with the additional ability to localize GRBs. The *HETE* mission came to an end in 2006, whereas *INTEGRAL* is still working fully. While these satellites did not possess *BeppoSAX's* ability to slew, they were both capable of localizing GRBs within less than a minute to error circles $1' - 2'$ in diameter. This opened up the possibility of finally observing the early optical emission of GRBs.

This promise was fulfilled by the rapid optical detection of the *HETE* GRBs 021004 (Fox et al. 2003b) and GRB 021211 (Vestrand et al. 2004; Li et al. 2003; Fox et al. 2003a). While GRB 021004 remains one of the brightest afterglows at late times, it was rather faint (15th magnitude) a few minutes after the trigger. The afterglow of GRB 021211 was two magnitudes brighter, but decayed rapidly. Clearly, not all GRB afterglows were as bright as that of GRB 990123 at early times. Finally, the extremely bright and long GRB 041219A (also detected by *Swift*) was rapidly localized by *INTEGRAL*, allowing the discovery of early optical emission, contemporaneous with the prompt gamma-ray emission, which evolved in lockstep, implying it was a low-energy tail of the prompt emission (Vestrand et al. 2005; Blake et al. 2005).

The greatest achievement of *HETE* was the discovery of the nearby ($z = 0.1687$, Thöne et al. 2007), very bright GRB 030329. Follow-up of this GRB yielded the largest amount of afterglow data on any event, as the afterglow was extremely bright. The highly variable afterglow (e.g., Lipkin et al. 2004), which is still not satisfactorily explained to this day, revealed the spectroscopic signature of a "hypernova", SN 2003dh, starting several days after the GRB (Hjorth et al. 2003; Stanek et al. 2003), yielding concrete evidence that "normal" GRBs (GRB 980425 remains a mostly unique low-luminosity event) are created in core-collapse explosions of massive stars. A special class of GRBs which exhibit only low-energy X-ray emission and are thus called X-Ray Flashes (XRFs, Heise et al. 2001), were also found to be cosmological (Soderberg et al. 2004a) and linked to broad-lined Type Ic SN (Soderberg
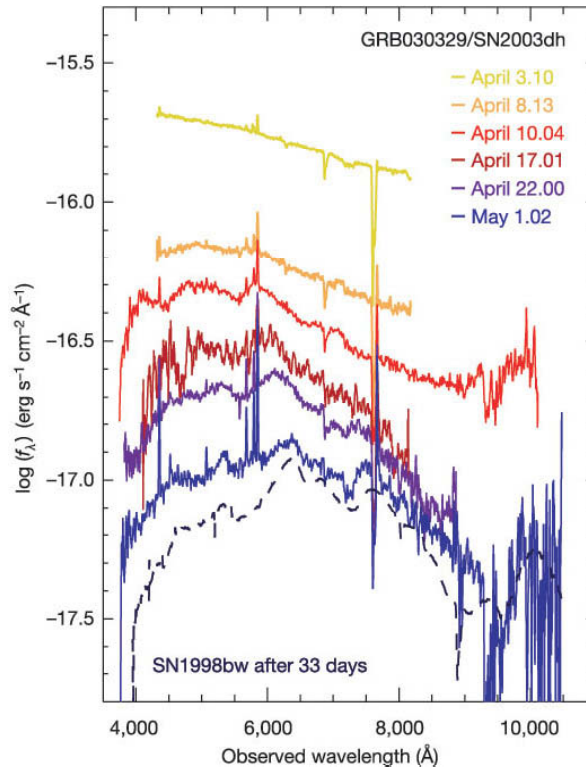
Figure 1.4: *The evolution of the spectrum of the optical transient of GRB 030329, initially exhibiting an almost pure power-law with superposed host galaxy emission lines, which then transforms into the spectrum of the broad-lined Type Ic supernova SN 2003dh, directly linking GRBs to core-collapse SNe (Hjorth et al. 2003).*

et al. 2005). Furthermore, *INTEGRAL* discovered a second low-redshift ($z = 0.105$, e.g., Prochaska et al. 2004) event, GRB 031203, which was similar to GRB 980425 (Soderberg et al. 2004b) and also exhibited powerful SN emission (Malesani et al. 2004).

1.5 *Swift* – afterglows and redshifts become common

In November 2004, the Explorer-class NASA *Swift* satellite, dedicated to the rapid localization and follow-up of GRBs (Gehrels et al. 2004), was launched. It remains up to now *the* "workhorse" mission for GRB science, and has led to many discoveries, but also many additional questions. It is equipped with a coded-mask gamma-ray imaging telescope, the *Burst Alert Telescope BAT* ($15 - 350$ keV), which, similar to *IBIS* on *INTEGRAL*, can deliver GRB positions with a radius of $3'$ within seconds. As soon as the position has been determined on-board, the satellite rapidly slews (typically within $60 - 120$ seconds), pointing its narrow-field instruments at the localization: The *X-Ray Telescope XRT* (0.3 – 10 keV) is able, for the first time, to deliver early X-ray observations, and further localizes the afterglow to a few arcseconds withing a few minutes. The *UltraViolet and Optical Telescope UVOT* contains six filters allowing observations from the mid-UV (190 nm) the the *V* band (550 nm), as well as a filterless mode ("*white*") which is sensitive even further into the red.

These capabilities have allowed the *Swift* satellite to make or support many discoveries.

Some of the highlights are:

- *Swift* has opened up the discovery space of the early X-ray afterglow, which contains steep decays (Tagliaferri et al. 2005b), bright X-ray flares (Burrows et al. 2005) and often a flat "plateau phase", leading to the description of the "canonical X-ray afterglow" (Nousek et al. 2006; O'Brien et al. 2006).

- The discovery of the afterglows of short/hard GRBs and their placement in the cosmological context. *Swift* discovered the faint X-ray afterglow of GRB 050509B, which is associated with a giant elliptical galaxy at $z = 0.225$ (Gehrels et al. 2005; Bloom et al. 2006). The discovery of the first optical afterglow of a short GRB, that of GRB 050709 (Hjorth et al. 2005b; Fox et al. 2005), is actually due a localization from *HETE*. GRB 050724 was also associated with an early-type galaxy and featured a radio afterglow (Berger et al. 2005c). Thus, it was established that short GRBs can derive from old stellar populations, in agreement with the model that they are produced by the merger of compact objects.

- *Swift* GRBs have thrice broken the redshift record for GRBs, with GRB 050904 at $z = 6.3$ (Kawai et al. 2006; Haislip et al. 2006), GRB 080913 at $z = 6.7$ (Greiner et al. 2009b) and finally the momentary distance record-holder for any spectroscopically confirmed source, GRB 090423 at $z \approx 8.2$ (Tanvir et al. 2009; Salvaterra et al. 2009).

- The discovery of the ultra-long (≈ 2700 s) XRF 060218, which featured no afterglow, but a UV-luminous peak and another broad-lined Type Ic SN, SN 2006aj, at a redshift $z = 0.033$ (Mirabal et al. 2006), expanding the sample of peculiar low-luminosity local GRBs (Campana et al. 2006a; Pian et al. 2006; Ferrero et al. 2006). Very recently, a very similar event, XRF 100316D/SN 2010bh, has been discovered (Chornock et al. 2010; Starling et al. 2010).

- Two very nearby temporally long GRBs, GRB 060505 ($z = 0.0889$, Thöne et al. 2008a) and GRB 060614 ($z = 0.125$, Della Valle et al. 2006), were monitored deeply and no associated SNe were discovered down to highly significant limits, implying that the classification scheme for GRBs was incomplete and that new explosion channels must exist (Gehrels et al. 2006; Fynbo et al. 2006b; Gal-Yam et al. 2006; Della Valle et al. 2006; Ofek et al. 2007).

- The serendipitous discovery of an X-ray outburst (XRO 080109) in a nearby galaxy (NGC 2770) which preceded a Type Ib SN, SN 2008D, establishing a "missing link" between GRB-associated SNe and "normal" core-collapse SNe (Soderberg et al. 2008; Malesani et al. 2009b; Mazzali et al. 2008).

- On a day which featured five *Swift*-localized GRBs within 24 hours, the temporal and spatial coincidence with GRB 080319A allowed several wide-field cameras to observe the location of GRB 080319B as it occurred. This event had the second-highest fluence in the last two decades and was accompanied by an extremely variable prompt flash which reached fifth magnitude from a redshift of $z = 0.937$, making it the most luminous transient ever observed (Bloom et al. 2009; Racusin et al. 2008; Woźniak et al. 2009).

- With a localization rate of ≈ 100 GRBs per year, many of which have ground-based follow-up, *Swift* has allowed the creation of samples of hitherto unobtainable size, for example in terms of X-ray afterglows (e.g., Racusin et al. 2009), early optical afterglows (e.g., Rykoff et al. 2009; Cenko et al. 2009), and spectroscopy/redshifts (Fynbo et al. 2009). The work I present in this thesis will make use of the large number of well-observed optical afterglows.

1.6 *Fermi* and *AGILE* – exploring the high-energy regime

The high-MeV/GeV regime of GRBs, unobserved since *CGRO EGRET*, moved back into focus with the launch of the Italian *AGILE* (*Astro-rivelatore Gamma ad Immagini ultra LEggero*, in April 2007) and the NASA *Fermi* (formerly *GLAST, Gamma-Ray Large Area Space Telescope*, in June 2008) satellites. *AGILE* is able to localize GRBs with the hard X-ray imager *SuperAGILE* ($18 - 45$ keV) to precisions smaller than $10'$; its main instrument is the *Gamma-Ray Imaging Detector* (*GRID*), which works in the energy range of 30 MeV – 50 GeV, and has thus far detected several GRBs. The much larger *Fermi* satellite is able to detect a large number of GRBs with the *Gamma-Ray Burst Monitor* (*GBM*, 8 keV – 40 MeV), but this instrument has only low spatial resolution, similar to *CGRO BATSE*. The main *Fermi* instrument is the *Large Area Telescope* (*LAT*), which covers an energy range 30 MeV – 300 GeV and is able to localize strong GeV sources to better than $10'$.

The contribution of *AGILE* to GRB science so far has been small, but *Fermi* has made several important discoveries. The first optical afterglow of a *Fermi LAT* GRB, that of GRB 080916C, revealed that this very bright GRB lay at $z = 4.35$ (Greiner et al. 2009a), implying that it has (over a broad energy range) the highest isotropic energy release ever measured, $E_{iso} \approx 10^{55}$ erg (Abdo et al. 2009c). The extremely luminous short GRB 090510 (also localized immediately by *Swift*) was detected by *Fermi* up to 31 GeV, yielding stringent limits on linear quantum gravity theories (Abdo et al. 2009b), and the highest fluence *Fermi* GRB so far, GRB 090902B, featured a 33 GeV photon and a prompt emission spectrum described by the superposition of a typical Band function and a power-law rising toward GeV energies without any visible cutoff (Abdo et al. 2009a).

The study of the optical afterglow of GeV-detected GRBs is just beginning, but the first results I present in Appendix C indicate that their afterglows are not exceptional.

Swift will possibly function until 2017, and the missions of *AGILE* and *Fermi* both will extend for at least several more years, barring any accidents. With the afterglow-hunting capabilities of *Swift* combined with the broadband high-energy coverage of missions like *Fermi*, a multitude of further discoveries will keep the community busy in the next years.

Chapter 2

The Physics of GRBs: a Primer

In this chapter, I wish to give a short overview of the basic physics, as they are understood today, behind the GRB phenomenon. These relate both to how GRBs as well as their afterglows are produced (the so-called "standard fireball model"), as well as to which astrophysical sources are capable of creating GRBs (the GRB progenitors: "collapsars" and, probably, merging compact objects). As the topic of this thesis deals mostly with observational data and not the underlying theory, I will not go into deep detail. The physics of GRBs as well as the wide variety of observational data are described in a multitude of reviews in the last years, e.g., Zhang & Mészáros (2004); Piran (2005); Woosley & Bloom (2006); Zhang (2007); Mészáros (2006); Nakar (2007a); Lee & Ramirez-Ruiz (2007); Gehrels et al. (2009).

2.1 The Fireball Model

2.1.1 The Compactness Problem – the Need for a Relativistic Fireball

Even before it was clear at which distance GRBs occurred, the information gleaned from the prompt emission light curves pointed to the need for relativistic physics. For example, the extremely short BATSE GRB 910711 (see also Fig. 1.2) showed microsecond variability in its light curve (Bhat et al. 1992). This rapid variability indicates the emitting region can not be larger than 60 km, the distance light can travel in 200 μs. Furthermore, the discovery that GRBs are distributed isotropically in the sky (Meegan et al. 1992) and must therefore lie at large distances (at least in a wide halo around the Milky Way, or even at cosmological distances) implies a very large amount of energy confined to a small volume. Such a source should be optically thick and emit hot blackbody radiation, as $\gamma\gamma$ interactions should produce electron-positron pairs (e.g., Piran 1997). Instead, broadband high energy observations reveal the prompt emission spectra (usually described with a smoothly broken power-law, the Band-function, Band et al. 1993) are non-thermal, and can show emission beyond the rest mass of electrons and positrons at 511 keV.

This conundrum can be solved by assuming that the emitting source is moving toward us at a relativistic speed, with a Lorentz factor $\Gamma = \frac{1}{\sqrt{1-\frac{v^2}{c^2}}} \gg 1$. Indeed, this can be used to place lower limits on the necessary Lorentz factor if the distance of the GRB is known (Lithwick & Sari 2001). Two factors contribute: For one, the spatial extent of the source can be larger by a factor Γ^2. Secondly, as the emitter is moving toward us at relativistic speeds,

the energy of the photons, which get blueshifted, is lower by a factor of Γ in the rest frame of the emitter. If the observed spectrum can be described by $N(\nu)\mathrm{d}\nu \sim \nu^{-\alpha}\mathrm{d}\nu$, where $N(\nu)$ is the number of photons (within the frequency range $[\nu, \nu + \mathrm{d}\nu]$) in the fireball which have enough energy to create electron-positron pairs, then the optical depth is found to be smaller by a factor $\Gamma^{2(1+\alpha)}$. The typical low-energy power-law slope of the Band function is $\alpha = -1$, which leads to an estimation of $\Gamma > 100$ so that the emitting region is optically thin.

2.1.2   Creating the GRB – the Formation of Internal Shocks

Rees & Mészáros (1992) first studied the effect of an ultra-relativistic fireball expanding into a typical galactic environment. After being accelerated to relativistic speeds by an unseen (as the fireball is still optically thick at this distance scale, which is $\approx 10^6$ cm) central engine (see Chapters 2.2 and 2.3) through the transformation of thermal energy into kinetic energy, the fireball coasts to a distance of $\Gamma^2 c\Delta t \approx 10^{13}$ cm (roughly 1 AU) from the central engine. The exact nature of the fireball is not yet known. While it is clear that the baryon loading must be low (such "dirty fireballs" would not achieve high Lorentz factors due to the high rest-masses of the involved baryons), it is unclear if the fireball is mostly an electron-positron plasma or if it is Poynting-flux dominated. As soon as the fireball becomes optically thin, the photons can escape, being beamed into a narrow cone in the propagation-direction of the fireball due to relativistic aberration.

If one assumes that the process which powers the central engine is in some form or fashion unstable, the emitted fireball will consist of thin shells which travel at slightly different Lorentz factors. When a faster shell emitted at a later time catches up with a slower shell (recall that, due to special relativity, the collision speed will be $\Gamma_2 - \Gamma_1$, which is still typically $\Delta\Gamma \gg 1$), the collision will produce so-called "internal shocks" which are thought to power the prompt emission of the GRB itself. While the natural candidate for the prompt emission is synchrotron emission (the measured spectra are almost always non-thermal), this has several problems, see Ghisellini (2010) for a recent overview of prompt emission models. Recently, it was also suggested that the prompt emission is not produced by internal dissipation at all, but by relativistic turbulence (Kumar & Narayan 2009a). Precise measurements of the polarization of the GRB itself would be a powerful tool to discern between models, but no dedicated instrument has yet been flown, and the measurements presented so far are controversial (Coburn & Boggs 2003; Willis et al. 2005; Kalemci et al. 2007; McGlynn et al. 2007; Götz et al. 2009a).

Independent of the actual mechanism of prompt emission, relationships have been found between measured parameters of the prompt emission (if the redshift of the GRB is known). The first is the so-called "Amati relation", first found for a small sample of *Beppo-SAX* GRBs by Amati et al. (2002). It was found that the peak energy of the Band spectrum of the prompt emission correlates with the isotropic energy release in the "bolometric bandpass" (the rest-frame 1 keV - 10 MeV bandpass, Bloom et al. 2001). A larger sample revealed an intrinsic scatter but confirmed the correlation (Amati 2006), and further updates show that it is even valid for very energetic *Fermi* GRBs (Amati et al. 2009a; McBreen et al. 2010). If one corrects for the collimation of the jet (see Chapter 2.1.4), one finds the "Ghirlanda relation" (Ghirlanda et al. 2004, 2007) between the rest-frame peak energy (as in the Amati correlation)

and the collimation-corrected energy release E_γ, which includes several additional parameters, of which the jet break time t_b is the most important. This correlation has a reduced scatter in comparison to the Amati correlation, but it needs deep late-time measurements of the afterglow to work. The use of these correlations in the quest to make GRBs and their afterglows standard candles for cosmology is hotly debated (e.g., Friedman & Bloom 2005a; Amati et al. 2008), and even the existence of the correlations themselves (physical origin vs. selection effects) is still not clear (e.g., Butler et al. 2007a, 2009; Campana et al. 2007a; Ghirlanda et al. 2008). Recently, I was part of a studied which found some energetic *Fermi* LAT GRBs, while being in accordance with the Amati relation, are outliers of the Ghirlanda relation (McBreen et al. 2010). The status of cosmology with GRBs has been reviewed recently by Amati (2009).

2.1.3   Creating the Broadband Afterglow – the External Shock Mechanism

Especially for long GRBs linked to the explosion of massive stars (Chapter 2.2), the surrounding medium into which the jet propagates will contain matter of a density of typically $n \approx 1 - 10$ cm^{-3}. This matter is swept up by the jet, creating so-called "external shocks". The luminosity of the afterglow increases with $L \propto t^2$, while the jet is braked at the same time, and reaches a maximum when $\Gamma \approx 0.5\Gamma_0$, when the rest mass of the swept-up matter is the same as the kinetic energy of the ejecta. The distance at which this occurs is called the deceleration radius, and it is typically at $\approx 10^{17}$ cm (around 10,000 AU) from the central engine. From the engine rest frame, the propagation of the jet to this point takes roughly 50 days (and the collisions which create the GRB occur over the time frame of minutes to hours), but the observer who is looking right into the fireball sees all these event happen almost simultaneously due to the ultra-relativistic approach speed. The rapid rise of optical emission has by now been observed for multiple GRBs, and, conversely, this "rise of the forward shock" can be used to derive the initial Lorentz factor of the outflow (Molinari et al. 2007).

The forward shock rise may be hidden by an even more luminous, short-lived optical phenomenon, the reverse shock flash (of which the most famous example is that of GRB 990123, Akerlof et al. 1999; Sari & Piran 1999a; Mészáros & Rees 1999a), which stems from a sub-relativistic shock which propagates backward into the expanding fireball. Powerful reverse shock flashes need specific conditions to develop, and are expected to be associated with large-scale magnetic fields. Magnetic fields assuredly play a large, yet still uncertain role in GRB afterglows. Late-time measurements of the (non-thermal) optical afterglow radiation (e.g., Covino et al. 1999, who reported the first detection, or Greiner et al. 2003, who presented the polarizationally variable light curve of GRB 030329) positively detect polarization, strong evidence that the emission is synchrotron radiation from shocked electrons. The polarization of the very early afterglow should give clues to the origin and structure of magnetic fields. In the case of GRB 060418, which showed a forward shock rise but no sign of reverse shock emission (Molinari et al. 2007), an early upper limit ruled out a large-scale magnetic field (Mundell et al. 2007b), whereas the early reverse shock flash of GRB 090102 showed a clearly polarized signal (Steele et al. 2009), showing that large-scale magnetic field can be advected from the central engine itself.
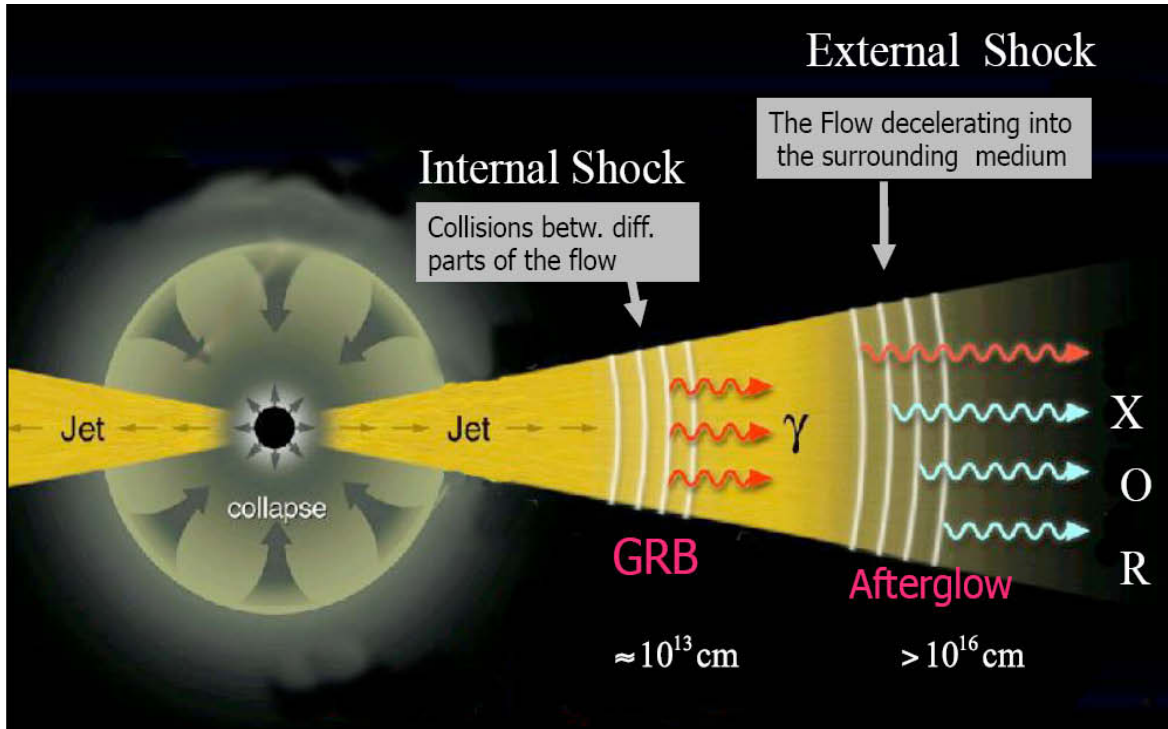
Figure 2.1: *A schematic diagram illustrating the main components of a GRB. A central engine, composed of a newly created black hole, which is surrounded by a rapidly accreting disk (see Chapter 2.2), emits twin ultra-relativistic, collimated jets (see Chapter 2.1.4). Internal dissipation within these jets occurs when shells with different speeds collide (see Chapter 2.1.2), creating the prompt emission of the GRB, while at later times, the jet gets decelerated, producing external shocks which propagate into the circumstellar matter (forward shock) and possibly back into the jet (reverse shock) (see Chapter 2.1.3), producing the long-lasting, broadband afterglow emission (forward shock) and possibly a rapidly decaying prompt flash (reverse shock). Source: Mészáros (2001).*

Sari et al. (1998) derived the temporal and spectral evolution of GRB afterglows. For synchrotron radiation, the energy spectrum of the radiating electrons is described by $N(E)dE \propto E^{-p}dE$, here, $N(E)$ is the number of electrons in the energy interval $(E, \ E + dE)$, and p is the electron distribution index. Numerical simulations, such as those performed by Kirk et al. (2000) and Achterberg et al. (2001), indicate that p should have a "canonical" value of ≈ 2.2, although multiple observational approaches show that this can not be correct (e.g., Kann et al. 2006b; Shen et al. 2006; Starling et al. 2008; Curran et al. 2010). To prevent an ultraviolet catastrophe, $p > 2$ is needed, though there is evidence for smaller values (e.g., Zeh et al. 2006a), and special methods to support hard electron distribution indexes have been studied (Dai & Cheng 2001; Bhattacharya 2001; Resmi & Bhattacharya 2008). To prevent an infrared catastrophe (which would occur even for $p > 2$), a low-energy cutoff must be invoked, which is determined by the available energy density, it is $E_{min} = \frac{(p+2)e_e}{(p+1)n_e}$. Here, n_e is the electron density and e_e is the electron energy density. Most electrons are found around this energy, so E_{min} is the characteristic electron energy, and the frequency at which these electrons radiate is the characteristic frequency ν_m. Therefore, the GRB afterglow will radiate the most energy at this frequency.

The spectrum is described by two further frequencies: The cooling frequency ν_c is the frequency at which an electron which cools during the local hydrodynamic timescale emits, whereas the synchrotron self-absorption frequency ν_a is the frequency below which the emitter becomes optically thick, leading to a rapid decrease in luminosity toward even lower frequencies. The synchrotron self-absorption frequency is usually in the radio band and will not play any further role in this work, and the characteristic frequency ν_m also usually moves rapidly beneath the optical regime, and can typically be found in the hardly accessible FIR/THz/-submm region. The cooling frequency ν_c will play a large role in the spectral analysis, though, as it is often between the optical and the X-ray regime (Panaitescu et al. 2006b,a; Starling et al. 2007; Curran et al. 2010), and can also lie above the X-rays still (Zhang et al. 2007a). The evolution of these frequencies is described by

$$\nu_m = (6 \times 10^{15} \text{ Hz}) \, (1+z)^{1/2}((p-2)/(p-1))^2(\epsilon_e/\zeta_e)^2\epsilon_B^{1/2}E_{52}^{1/2}t_d^{-3/2} \tag{2.1}$$

$$\nu_c = (9 \times 10^{12} \text{ Hz}) \, (1+z)^{-1/2}\epsilon_B^{-3/2}n^{-1}E_{52}^{-1/2}t_d^{-1/2} \tag{2.2}$$

$$\nu_a = (2 \times 10^{9} \text{ Hz}) \, (1+z)^{-1}(\epsilon_e/\zeta_e)^{-1}\epsilon_B^{1/5}n^{3/5}E_{52}^{1/5} \tag{2.3}$$

$$F_{\nu,max} = (20 \text{ mJy}) \, (1+z)\epsilon_B^{1/2}n^{1/2}E_{52}d_{L,28}^{-2} \tag{2.4}$$

where $t_d = (t/\text{day})$, ϵ_e is the energy fraction in electrons, ϵ_B the energy fraction in magnetic fields, $\zeta_e \leq 1$ is the fraction of shocked thermal electrons which is able to achieve the initial equipartition value, E_{52} is the isotropic energy release in units of 10^{52} erg, n is the circumburst density in units of cm^{-3}, and $d_{l,28}$ is the cosmological luminosity distance in units of 10^{28} cm. While most of the values in these equations are unchanging parameters, it is important to note that ν_m and ν_c evolve with time.

The final broadband GRB spectrum is described by four power-laws which break at the three frequencies described above. There are two different cases. If the characteristic frequency ν_m still lies above the cooling frequency ν_c, a large number of electrons cool rapidly, making this the "fast-cooling" case (ν_M is the maximum synchrotron frequency):

$$F_\nu = F_{\nu,max} \begin{cases} (\nu_a/\nu_c)^{1/3}(\nu/\nu_a)^2 & \nu < \nu_a \\ (\nu/\nu_c)^{1/3} & \nu_a \leq \nu < \nu_c \\ (\nu/\nu_c)^{-1/2} & \nu_c \leq \nu < \nu_m \\ (\nu_m/\nu_c)^{-1/2}(\nu/\nu_m)^{-p/2} & \nu_m \leq \nu \leq \nu_M \end{cases} \tag{2.5}$$

ν_m usually moves rapidly beneath ν_c ($t_d^{-3/2}$ vs. $t_d^{-1/2}$), and at typical observing times, the afterglow is in the "slow-cooling" regime:

$$F_\nu = F_{\nu,max} \begin{cases} (\nu_a/\nu_m)^{1/3}(\nu/\nu_a)^2 & \nu < \nu_a \\ (\nu/\nu_m)^{1/3} & \nu_a \leq \nu < \nu_m \\ (\nu/\nu_m)^{-(p-1)/2} & \nu_m \leq \nu < \nu_c \\ (\nu_c/\nu_m)^{-(p-1)/2}(\nu/\nu_c)^{-p/2} & \nu_c \leq \nu \leq \nu_M \end{cases} \tag{2.6}$$

The broadband spectrum is shown for both cases in Fig. 2.2. As can be seen, in the slow-cooling regime, the spectral slopes below and above the cooling break depend upon the electron index p, but it is always $\Delta\beta = 0.5$ ($F_\nu \propto \nu^{-\beta}$). These equations are those for
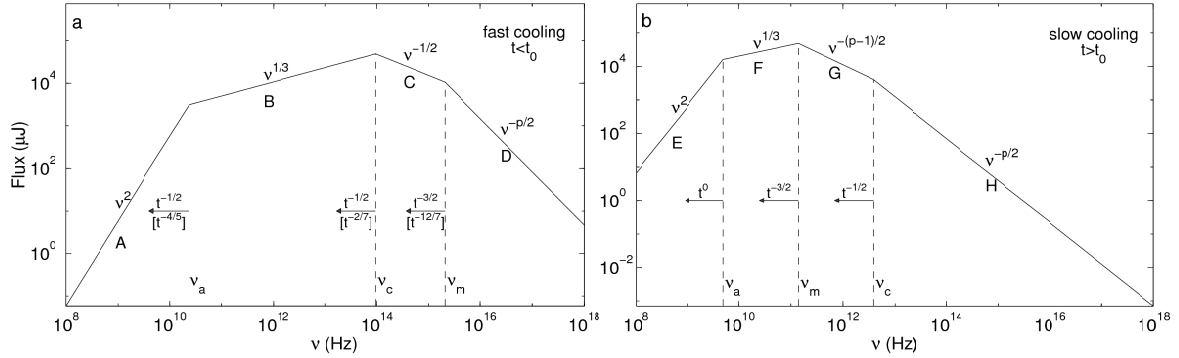
Figure 2.2: *The broadband spectrum of GRB afterglow emission. It is described by four power-laws which are separated by three specific frequencies: The synchrotron self-absorption frequency ν_a, the characteristic frequency ν_m and the cooling frequency ν_c. The fast-cooling regime (left), where $\nu_m > \nu_c$, is usually only important at very early times. The slow-cooling regime is typical for the late-time afterglow observations studied in this work. See the text for more details. Adopted from Sari et al. (1998).*

the case of a constant density medium, similar equations can be derived for a wind-shaped medium $\rho \propto r^{-2}$ (Chevalier & Li 1999, 2000). While it would be logical to assume that such a wind-shaped medium is the norm for the massive-star progenitors of long GRBs, it turns out that actually only few GRBs show this density profile (e.g., Zeh et al. 2006a).

The temporal evolution of the above-mentioned frequencies is linked to the temporal evolution of the afterglow itself. In the simplest approach, it can be described as

$$F_\nu(t) \propto t^{-\alpha}\nu^{-\beta} \tag{2.7}$$

Due to the rapid evolution of the characteristic frequency, afterglow observations are typically taken in the slow-cooling regime, and the spectrum can be described by a simple power-law. Spectral evolution is not expected and the temporal evolution of the afterglow is achromatic. If the cooling break does pass through the optical range, a shallow light curve break, with $\Delta\alpha = 0.25$, is expected. Such shallow breaks have only been found in a few cases, such as GRB 030329 (Sato et al. 2003), GRB 050502A (Yost et al. 2006), XRF 050824 (Sollerman et al. 2007), and I found two further possible cases in my work, for GRB 050401 and GRB 080721. In no case is the broadband optical data good enough to study the SED before and after the break, though, or to detect a temporally variable break time.

Several processes have been discussed which can alter the smooth decay $F \propto t^{-\alpha}$ of a GRB afterglow. Ioka et al. (2005) study these different processes. One possibility, that a sudden increase in the density of the ISM which the forward shock is propagating into will cause a rebrightening in the light curve, has been all but ruled out (Nakar & Granot 2007). Another model is the "patchy-shell" model, where the surface of the jet is inhomogeneous in luminosity and the slowly expanding relativistic emission cone crosses bright and dark "spots", creating short-term low-amplitude light curve fluctuations, such a model has been invoked to explain the early variability of GRB 011211 (Jakobsson et al. 2004). One of the most successful models especially for large-scale rebrightenings is the energy-injection model (also called "refreshed shocks"), in which late central-engine activity emits further, slower

shells, which catch up with the forward shock front after it has been sufficiently braked. Such an injection will usually create a "step-ladder structure" in which the light curve rises and then commences decaying again with the same slope as before. Several GRBs I have worked on show such structures, for example GRB 070125 (Updike et al. 2008), XRF 071010A (Covino et al. 2008) (see Chapter C.4) and GRB 080913 (Greiner et al. 2009b) (see Chapter 3.3.1), and multiple injections have been used to model the variability of the afterglow of GRB 060526 (Thöne et al. 2010) (see Chapter C.3). Further examples of highly variable light curves are GRB 021004 (e.g., de Ugarte Postigo et al. 2005) and the "ultimate" case, GRB 030329, which still has not been modeled successfully (Huang et al. 2006), though recently, an approach has been tried which involves stronger collimation of the late shells (Deng et al. 2010) (I am involved in a further project to model GRB 030329 which should be finished this year). Finally, strong early optical variability can be attributed to a low-frequency extension of the prompt emission itself, such flares were first discovered by Vestrand et al. (2005) and Blake et al. (2005) for the extremely long and bright GRB 041219A. GRB 060526, mentioned above, also shows strong early variability, and the most impressive case is that of GRB 080129 (Greiner et al. 2009c) (which probably also features multiple energy injections), though in this case, no high-energy data have been recorded contemporaneously to the extreme optical flare.

2.1.4   Evidence for Collimated Emission – the Jet and its Break

The phenomenon of relativistic aberration leads to the emission of the relativistic fireball to be beamed into a small solid angle $\Omega_j < 4\pi$, so that the observer is unaware of what lies outside the light-cone, and is not able to discern if the fireball is a spherical explosion (and the released energy is thus equal to the isotropic energy release E_{iso}) or if it is collimated, as the jet boundary lies outside the light-cone and is causally disconnected, which occurs as long as $\Gamma \gtrsim \Omega_j^{-1/2}$. Rhoads (1997) first proposed (see also Rhoads 1999) that the light curve evolution should be influenced by a collimated explosion. In colliding with the ISM, the fireball is braked and the reduction of Γ leads the condition above to not be met anymore after a certain time, and the causal (light-cone) angle $\Gamma(t)^{-1}$ becomes comparable to (and then larger than) the jet half-opening angle θ_j. As soon as this occurs (at the jet break time $t_{j,d}$), the "dark", non-emitting region around the jet becomes visible, and the integrated luminosity of the shock front starts to decay steeper than before. Under the assumptions of adiabatic dynamics and a homogeneous external medium (a similar equation can be derived for a wind-shaped medium), the jet opening half-angle is found to be (e.g., Piran 2005)

$$\theta_j \sim 5\text{deg } t_{j,d}^{3/8} E_{53}^{-1/8} n^{1/8} (\eta_\gamma/0.2)^{1/8} ([1+z]/2)^{-3/8} \qquad (2.8)$$

Here, η_γ is the radiative efficiency. As can be seen, the dependence on the isotropic energy release and the external medium density n is low. This equation is fundamental to the Ghirlanda relation (Chapter 2.1.2), as it is used to correct the energy release for collimation, which implies "guesstimates" for the density and radiative efficiency, as these are usually not known (Friedman & Bloom 2005a). In the pre-*Swift* era, the detection of optical jet breaks was relatively common. The first afterglow with a detected break is that of GRB 980519 (Jaunsen et al. 2001), though it was not reported with confidence until 2001. The first GRB

for which a jet break was reported was GRB 990123 (Kulkarni et al. 1999), where collimation
of the fireball was necessary, as an isotropic explosion would have implied the conversion of
$> M_\odot$ into energy within a very short time span. In Appendix C.4 several cases of optical
jet breaks in the *Swift* era are presented, but the expectation that the X-ray observations
would yield many more breaks (as a geometric effect, the jet break should be achromatic)
has not materialized. Instead, the X-ray light curve has revealed an additional break, the
transition from the "shallow decay phase" to the normal afterglow (Nousek et al. 2006; Liang
et al. 2007b, which can be used to yield a Ghirlanda-like relation, Willingale et al. 2007),
breaks have been found to be chromatic (Panaitescu et al. 2006a), and jet breaks in general,
both in the optical as well as the X-ray regime, have been found to be rare in the *Swift* era
(Willingale et al. 2007; Liang et al. 2008; Racusin et al. 2009).

2.2   Collapsars – the Progenitors of long GRBs

Especially after the resolution of the distance debate on GRBs (Metzger et al. 1997), it became
clear that these explosions had enormous energy outputs (Paczynski 1986), and the outflow
speeds must be ultrarelativistic, the Lorentz factor must be in the region of several hundred.
The only astrophysical source which is known to be capable of releasing such extreme amounts
of energy within a short time (and be the "central engine" powering the outflow) is a compact
object, usually a black hole, which undergoes a phase of super-Eddington accretion (called
"hyperaccretion"). As a single black hole or neutron star, even one in a binary system with a
star (X-ray binary) would never be able to reach such accretion rates (up to several $M_\odot$ per
second), it makes sense that GRBs occur when black holes (or possibly magnetars, as inferred
in the case of the low-luminosity event XRF 060218, Mazzali et al. 2006a, see Appendix C.1
for more on this source) are created. Even before the discovery of GRBs was reported, Colgate
(1968) surmised supernovae could release gamma-rays and X-rays upon explosion (though the
mechanism is different than what actually powers a GRB). It was Woosley (1993) who created
the model in which a Wolf-Rayet star emits paired matter jets upon core collapse, earning
this model the name "collapsar model". In this model, the death of the star actually did not
create a supernova ("failed supernova", see also MacFadyen & Woosley 1999), and further
infall supported the creation of the long, complex GRB emission. Only with the discovery of
the GRB-SN link GRB 980425/SN 1998bw were the models changed to permit both a GRB
and a powerful supernova with rapid expansion speed ("hypernova" or broad-lined Type Ic
supernova).

The exact process which launches the jet is still debated today. The original model by
Woosley (1993) launched the outflow (which was also assumed to not have a strong degree
of collimation) through $\nu\overline{\nu}$ annihilation and electron-neutrino scattering. A second theory
uses the Blandford & Znajek (1977) mechanism to extract rotational energy from the rapidly
spinning black hole itself. In both cases, a jet is accelerated along the polar axes of the
collapsing star, becoming collimated as it punctures the outer layers of the star. This process
makes it important for the star to be a Wolf-Rayet star, which has shed at least its outer
layer of hydrogen (resulting in a Type Ib SN) or even the helium layer (a Type Ic SN). If
the star possessed an extended outer envelope (i.e., was a red supergiant), the jet would be
quenched, and no GRB would be produced. And indeed, so far all spectroscopic evidence

shows that GRBs are associated with a special class of Type Ic SNe (Galama et al. 1998; Hjorth et al. 2003; Stanek et al. 2003; Malesani et al. 2004; Pian et al. 2006; Chornock et al. 2010).

Studies of the evolution of massive stars have shown that the creation of GRBs is dependent upon a delicate balance. As mentioned, the progenitor star must shed its outer layers to enable the jet to break out and interact with the ISM. Typically, this is accomplished by a powerful stellar wind during the Wolf-Rayet phase which is driven by the line opacity of metals in the star's outer layers. Therefore, a very low metallicity will imply that only few massive stars reach the Wolf-Rayet phase, and indeed, the low-metallicity SMC contains way fewer Wolf-Rayet stars in comparison to red supergiants than the Milky Way. On the other hand, the strong stellar wind transports away angular momentum, braking the rotation of the star. Numerical simulations of accreting black holes show that the freshly created compact object must spin extremely rapidly to allow the creation of polar jets, therefore, the large Wolf-Rayet population in high-metallicity galaxies like our own is not expected to produce GRBs (Stanek et al. 2006). Studies of metallicities derived from the GRB environment via afterglow spectroscopy show that the environment of GRBs is of moderately low metallicity, but typically more metal-enriched than galaxies along quasar sightlines at similar redshifts (e.g., Fynbo et al. 2006a). An immediate solution to this problem is that GRBs occur in binary systems, where the close interaction of the two stars removes the outer envelope without robbing the progenitor of angular momentum. A single star progenitor model has been proposed by Yoon et al. (2006), they examine a fully convective star which subsumes its complete outer layer through convection and fusion. Since GRBs occur at cosmological distances, so far no progenitor star has been observed before the explosion, something which has now been achieved for several kinds of "normal" core-collapse SNe (see, e.g., Smartt 2009, for a review).

Studies of the host galaxies of GRB (e.g., Le Floc'h et al. 2003; Christensen et al. 2004; Savaglio et al. 2009; Levesque et al. 2010) have found them to usually be subluminous, blue star-forming dwarf galaxies. They are less massive than field galaxies at similar redshifts, and stick out especially in terms of their specific star-formation rate (i.e., star-formation rate per unit luminosity or mass, depending on definition). Furthermore, GRB host galaxies are often morphologically disturbed or even merging systems, which tend to have very high star-formation rates (Conselice et al. 2005; Wainwright et al. 2007). Within their host galaxies, they are concentrated in the brightest regions, which are most likely due to large HII regions (Fruchter et al. 2006). This is in contrast to the distribution of Type II core-collapse SNe, but similar to Type Ic SNe (Kelly et al. 2008). A study of the distribution of Wolf-Rayet stars in two nearby galaxies (Leloudas et al. 2010) finds tentative evidence that the WC class (thought to be the progenitors of Type Ic SNe) is more concentrated on the host light than the WN class (thought to be the progenitors of Type Ib SNe), which is not in conflict with GRBs stemming from Type Ic SNe, which are thought to have even more of their envelope removed than Type Ib SNe.

The (long) GRB-SN connection has been reviewed in Woosley & Bloom (2006).

2.3   Mergers – the viable Progenitors of Short GRBs

Historically, models involving neutron stars as the sources of GRBs, either through coalescence (e.g., Paczynski 1986; Eichler et al. 1989) or through the catastrophic braking of a freshly formed magnetar (Usov 1992), have preceded models involving massive star collapse. Spectroscopic studies of bright BATSE short and long GRBs have shown that the first seconds of the bright long GRBs often spectrally resemble short GRBs, indicating that the same central engine process is at work (Ghirlanda et al. 2009), and the differences between short and long GRBs in terms of duration and spectral hardness result from the difference in the progenitor surrounding the central engine and the circumburst medium (Eichler et al. 2009). General relativistic hydrodynamical simulations have shown the viability of compact object mergers to create short GRBs (Aloy et al. 2005).

In 2001, Panaitescu et al. (2001) already predicted that it would be very difficult to detect the afterglows of short GRBs. Optical afterglows should be 10 - 40 times fainter assuming similar radiative efficiencies and microphysical parameters, and possibly even fainter if short GRBs exploded in low-density surroundings, as expected from the merger model. Radio afterglows should be almost impossible to detect, and the best chances would be rapid X-ray observations. These predictions have mostly come true, although it has turned out that detections are even more difficult to achieve, as I will show (Chapter 5). As mentioned in the introduction (Chapter 1.5), the first localized short GRB, GRB 050509B, was found in the outskirts of a giant elliptical galaxy at a cosmological distance ($z = 0.225$, Gehrels et al. 2005), its X-ray afterglow was barely detected, and it had no optical or radio afterglow at all. The following two event allowed the first detections of optical (GRB 050709, Hjorth et al. 2005b; Fox et al. 2005) and radio (GRB 050724, Berger et al. 2005c) afterglows (since then, only a single further short GRB, GRB 051221A, had a detectable radio afterglow, Soderberg et al. 2006a).

The discovery rate of short GRBs is lower for *Swift* than for BATSE (roughly 10% vs. 25%). The reason is that *Swift* GRBs almost always are reported only if they have been flight-localized (ground-analysis-detected GRBs are rare), and the combination of a usually harder spectrum as well as the low numbers of photons short GRBs emit means they are usually only localized if the are near the detector axis and the coded mask is 100% illuminated. Still, so far several dozen short GRBs have been localized to the precision of some arcseconds (a small number have no X-ray afterglows at all, despite immediate observations by *Swift*). Even after five years, no absorption spectrum of a short GRB afterglow has been successfully performed[1], and all redshifts have been derived from spectroscopy of the associated host galaxies (e.g., Berger et al. 2007a; D'Avanzo et al. 2009), though such associations can be questionable, as some short GRBs have extremely faint host galaxies (e.g., Levan et al. 2006; Berger et al. 2007a; Stratta et al. 2007b; Piranomonte et al. 2008; Fong et al. 2010; Berger 2010). Studies of larger samples have shown that only few short GRB host galaxies are part of clusters (Berger et al. 2007b), and the host galaxies, while often being actively star-forming (Berger et al. 2007a; D'Avanzo et al. 2009), are more luminous than the host galaxies of long GRBs, and typical of the field galaxy population (Berger 2009). Morphological studies reveal

---

[1]Very recently, low signal-to-noise absorption lines were discovered in the afterglow of GRB 100816A (Tanvir et al. 2010; Gorosabel et al. 2010), but it is still unclear if this is a short/hard GRB or not.

a high abundance of exponential-disk dominated galaxies (that is, probably spirals), and the offest distribution (with offsets much larger than typical for long GRBs) is in accordance with the progenitors being compact object mergers (Fong et al. 2010).

Initially, it was thought that the redshift distribution of short GRBs was much lower than that of long GRBs, as the first events were found to lie at $z \lesssim 0.25$ (Gehrels et al. 2005; Hjorth et al. 2005b; Berger et al. 2005c), but by now, it is clear that both the redshift as well as the prompt energy release distribution is much larger than initially thought, as very energetic events have been discovered at $z \approx 1$ (Berger et al. 2007a; Perley et al. 2007a; Cenko et al. 2008a; Graham et al. 2009; McBreen et al. 2010). The original models of short GRBs predicted that they should not be collimated strongly, and while some evidence has been found for large opening angles (Grupe et al. 2006), other, especially energetic, short GRBs have shown evidence for strong collimation (Burrows et al. 2006; Berger 2007; De Pasquale et al. 2010; McBreen et al. 2010). Another challenge for the merger model is the evidence of extended central engine activity, a canonical case being GRB 050724, which exhibits both an "extended soft emission component" (Barthelmy et al. 2005) and a late flare seen both in the X-rays (Campana et al. 2006b) and the optical (Malesani et al. 2007). Within the *Swift* BAT energy range, this implies that this short GRB (and others with similar light curves) break the old T_{90} paradigm. This will be discussed in more detail in Chapter 3.3.1.

A "smoking gun" like the spectroscopic detection Type Ic SN emission at the position of long GRBs and their afterglows has not yet been found for short GRBs. The gravitational wave signature of a merger would be unmistakable, though (e.g., Kiuchi et al. 2010, and references therein), but such a signal has not yet been found (Abadie et al. 2010).

Short GRBs and their progenitors have been reviewed by Nakar (2007a) and Lee & Ramirez-Ruiz (2007).

2.4   GRB Environments and Dust Extinction

2.4.1   Dust Extinction and Extinction Laws

As was established in Chapter 2.1, within such a small spectral region as the optical/NIR window, the afterglow spectrum is a pure power-law $F_\nu \propto \nu^{-\beta}$, with β usually constant over the typical times of observation. The association of (long) GRBs with massive stars (Chapter 2.2), though, indicates that they should explode within their host galaxies, in dense environments, which implies that the afterglow light has to pass through the interstellar medium before it reaches us. Absorption lines in the ISM allow the spectroscopic derivation of the redshift, and interstellar dust will create wavelength-dependent extinction along the line of sight. Adding dust, the equation for the flux density transforms to

$$F_\nu = F_0 \cdot \nu^{-\beta} \cdot e^{-\tau(\nu_{\mathrm{host}})}, \tag{2.9}$$

with

$$\tau(\nu_{host}) = \frac{1}{1.086} \cdot \mathrm{A_V} \cdot \eta(\nu_{host}) \,. \tag{2.10}$$

Here, β is the intrinsic power-law slope of the SED, and F_0 a normalization constant (I choose the unextinguished flux density at $5 \cdot 10^{14}$ Hz in the host galaxy frame). The function
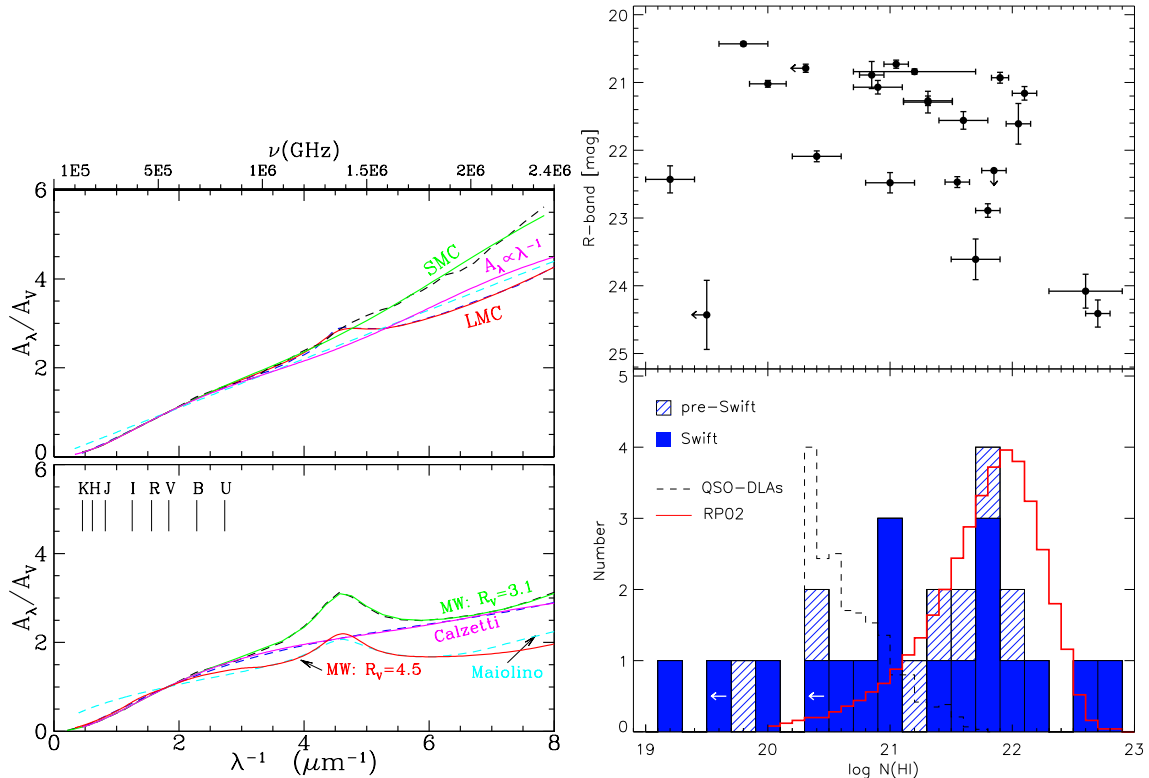
Figure 2.3: Left*: Extinction laws. The actual extinction laws are given as dashed lines, while the "Drude" model fits to them are given as colored solid lines. The 2175 Å bumps in the MW and LMC extinction laws are clearly seen (as "emission bumps" in the extinction laws, which imply additional extinction dips in source light). The MW, LMC and SMC extinction laws are used in my work. Figure taken from Li et al. (2008).* Right*: The distribution of hydrogen column densities* N_H *as derived from afterglow spectroscopy for GRBs at sufficient redshift for Lyα to be detected in the spectrum (typically* $z \geq 2$*), as of late 2006. The top panel shows the afterglow magnitudes in the* R_C *band at twelve hours after the GRB in the source frame, all shifted to* $z = 3$*. They have* not *been corrected for host galaxy extinction, to show the link between hydrogen column density and dust extinction. While there is a trend, there is clearly a large amount of scatter, indicating there is no "canonical" dust-to-gas ratio in GRB host galaxies. Figure taken from Jakobsson et al. (2006a).*

$\eta(\nu_{host}) = A_{\lambda_{\text{host}}}/A_V$ is the extinction law assumed for the interstellar medium (ISM) of the GRB host galaxy. An intrinsic problem in GRB science is that this extinction law is basically unknown. In one case, a special extinction law, which is probably due to dust produced in supernovae (instead of AGB stars) was derived from spectroscopy of a high-z quasar (Maiolino et al. 2004), and such dust has been used to successfully model the anomalous spectral energy distribution of GRB 071025 (Perley et al. 2010).

In lieu of the true extinction laws (which are assuredly different for each host galaxy), the usual procedure is to use well-defined extinction laws derived from galaxies in the local universe, specifically the Milky Way (MW) itself, as well as the Large and Small Magellanic Clouds (LMC and SMC, respectively) (see Figure 2.3). Especially the latter resembles typical GRB host galaxies in terms of size, luminosity and metallicity Z (which is $1/8$ $Z_\odot$). A special feature in the extinction curves of the MW and (less so) the LMC is the 2175 Å bump, an

absorption feature of mysterious origin (there is a possible link to organic molecules and amorphous silicates, Bradley et al. 2005, but many other carriers have been suggested) which is clearly linked to the mean metallicity of the ISM. It does not exist in the SMC extinction law. A second sequence is the strength of FUV absorption, this is high for SMC extinction, but less and less so for LMC and then MW extinction. These three extinction laws have been fitted analytically by Pei (1992). He gives them in the following form:

$$\frac{A_\lambda}{A_B} = \sum_{i=1}^{6} \frac{a_i}{\left(\frac{\lambda}{\lambda_i}\right)^{n_i} + \left(\frac{\lambda_i}{\lambda}\right)^{n_i} + b_i} \tag{2.11}$$

λ_i, a_i, b_i and n_i are free parameters, dimensionless except for $\lambda_i(\mu m)$. a_i weighs the contribution of each addend to the sum. They are different for each addend and galaxy. The first addend represents a background, the second the far ultraviolet (FUV) rise, the third addend represents the 2175 Å bump, while the fourth and fifth are two bumps in the MIR, at 9.7 μm and 18 μm, and the last addend is the far infrared (FIR) extinction. These two bumps and the FIR extinction will not be relevant for the data analyzed in my thesis (as no measurements go beyond the $K-$band at 2.2 μm and all bursts are redshifted), but I include them to preserve the overall shape of the extinction curve.

More specifically, for the MW, LMC and SMC extinction laws, respectively, the equations are as the following:

$$\frac{A_\lambda}{A_B} = \frac{165}{\left(\frac{\lambda}{0.047}\right)^2 + \left(\frac{0.047}{\lambda}\right)^2 + 90} + \frac{14}{\left(\frac{\lambda}{0.08}\right)^{6.5} + \left(\frac{0.08}{\lambda}\right)^{6.5} + 4}$$
$$+ \frac{0.045}{\left(\frac{\lambda}{0.22}\right)^2 + \left(\frac{0.22}{\lambda}\right)^2 - 1.95} + \frac{0.002}{\left(\frac{\lambda}{9.7}\right)^2 + \left(\frac{9.7}{\lambda}\right)^2 - 1.95}$$
$$+ \frac{0.002}{\left(\frac{\lambda}{18}\right)^2 + \left(\frac{18}{\lambda}\right)^2 - 1.8} + \frac{0.012}{\left(\frac{\lambda}{25}\right)^2 + \left(\frac{25}{\lambda}\right)^2} \tag{2.12}$$

$$\frac{A_\lambda}{A_B} = \frac{175}{\left(\frac{\lambda}{0.046}\right)^2 + \left(\frac{0.046}{\lambda}\right)^2 + 90} + \frac{19}{\left(\frac{\lambda}{0.08}\right)^{4.5} + \left(\frac{0.08}{\lambda}\right)^{4.5} + 5.5}$$
$$+ \frac{0.023}{\left(\frac{\lambda}{0.22}\right)^2 + \left(\frac{0.22}{\lambda}\right)^2 - 1.95} + \frac{0.005}{\left(\frac{\lambda}{9.7}\right)^2 + \left(\frac{9.7}{\lambda}\right)^2 - 1.95}$$
$$+ \frac{0.006}{\left(\frac{\lambda}{18}\right)^2 + \left(\frac{18}{\lambda}\right)^2 - 1.8} + \frac{0.02}{\left(\frac{\lambda}{25}\right)^2 + \left(\frac{25}{\lambda}\right)^2} \tag{2.13}$$

$$\frac{A_\lambda}{A_B} = \frac{185}{\left(\frac{\lambda}{0.042}\right)^2 + \left(\frac{0.042}{\lambda}\right)^2 + 90} + \frac{27}{\left(\frac{\lambda}{0.08}\right)^{4.0} + \left(\frac{0.08}{\lambda}\right)^{4.0} + 5.5}$$
$$+ \frac{0.005}{\left(\frac{\lambda}{0.22}\right)^2 + \left(\frac{0.22}{\lambda}\right)^2 - 1.95} + \frac{0.01}{\left(\frac{\lambda}{9.7}\right)^2 + \left(\frac{9.7}{\lambda}\right)^2 - 1.95}$$
$$+ \frac{0.012}{\left(\frac{\lambda}{18}\right)^2 + \left(\frac{18}{\lambda}\right)^2 - 1.8} + \frac{0.03}{\left(\frac{\lambda}{25}\right)^2 + \left(\frac{25}{\lambda}\right)^2} \tag{2.14}$$
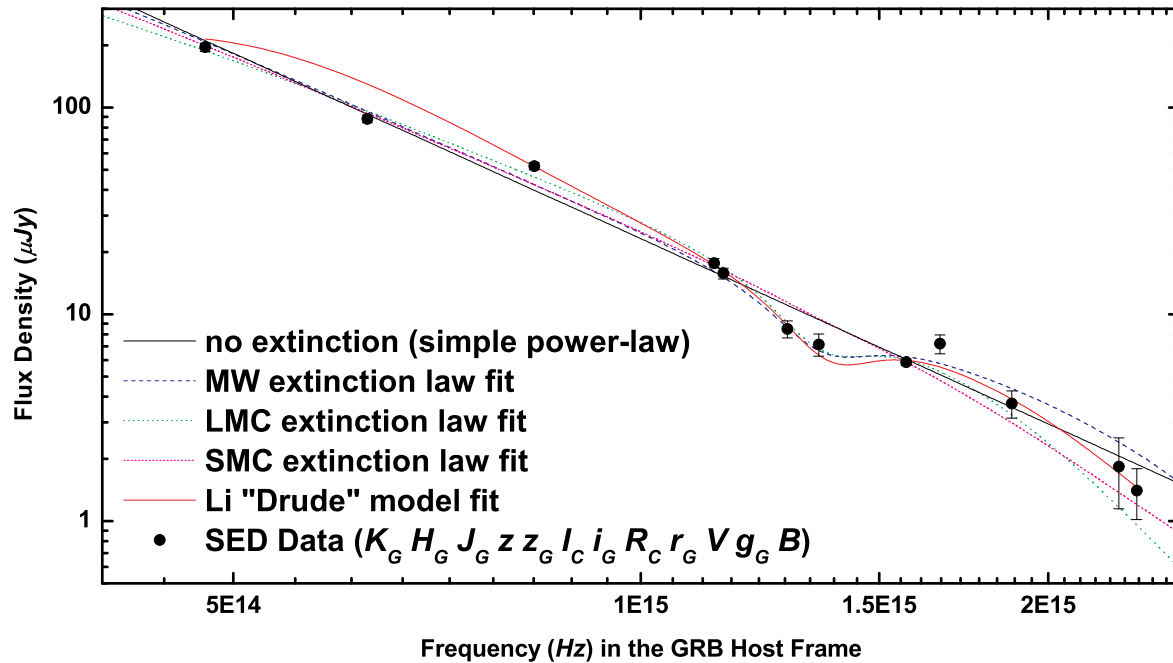
Figure 2.4: *The SED of the GRB 070802 afterglow, measured during the peak at 0.03 days, which shows a strong 2175 Å bump feature at a redshift of $z = 2.4549$ (Krühler et al. 2008a; Elíasdóttir et al. 2009), at the time of discovery the highest redshift such a feature had been detected at. It has been fit with different extinction laws. Clearly, both the fit with no extinction (simple power-law, straight black line) and SMC dust (magenta short-dashed line) completely fail to approximate the spectral shape. MW (blue dashed line) and LMC dust (green dotted) fit better, with especially the latter yielding an acceptable result with $\beta = 1.07 \pm 0.31$ and $A_V = 1.18 \pm 0.19$ mag. The fit with the "Drude" model of Li et al. (2008) is even better but yields completely unphysical results (see text for details).*

In Pei (1992), the laws are defined as the ratio of the extinction at the wavelength λ (in the host galaxy rest frame) to the extinction in the B band, $A_{\lambda_{\text{host}}}/A_B$. In GRB literature, usually the rest-frame V-band extinction A_V is used. To convert, one needs the parameters $E_{(B-V)}$ and R_V. The parameter $E_{(B-V)}$ is defined by the difference between the extinction in the blue band (A_B) and the visual band (A_V):

$$E_{(B-V)} = A_B - A_V \tag{2.15}$$

The parameter R_V (the ratio of total-to-selective extinction) is given by:

$$R_V = \frac{A_V}{E_{(B-V)}}, \tag{2.16}$$

and therefore:

$$A_B = \frac{A_V \cdot (1 + R_V)}{R_V} \tag{2.17}$$

R_V has been found to be 3.08 for MW-type dust, 3.16 for LMC-type dust, and 2.93 for SMC-type dust (e.g., Pei 1992). Note that these are mean values, R_V can differ strongly (ranging from $\approx 2 - 6$) for different sightlines, though these mostly involve high extinction.

2.4.2   The "Drude" Approach

While I will later show that these local extinction curves are usually adequate in fitting GRB afterglow SEDs, in recent years, efforts have been undertaken to derive the intrinsic dust extinction laws from afterglow SEDs. In the framework of Li et al. (2008), I helped in developing a more physical approach. In an analogy to the equations Pei (1992) used to model the extinction data of local galaxies, we constructed a Drude" model (as it resembles a sum of Drude functions):

$$
\begin{aligned}
A_\lambda / \mathrm{A_V} \;=\;& \frac{c_1}{(\lambda/0.08)^{c_2} + (0.08/\lambda)^{c_2} + c_3} \\
&+ \frac{233\left[1 - c_1/(6.88^{c_2} + 0.145^{c_2} + c_3) - c_4/4.60\right]}{(\lambda/0.046)^2 + (0.046/\lambda)^2 + 90} \\
&+ \frac{c_4}{(\lambda/0.2175)^2 + (0.2175/\lambda)^2 - 1.95} \; .
\end{aligned}
\tag{2.18}
$$

The first term in the right-hand side of the model equation represents the far-UV extinction rise, the second term accounts for the near-IR/visible extinction, and the third term creates the 2175 Å extinction bump. c_1 to c_4 are additional free parameters. We showed that this single equation is able to recover the Pei (1992) extinction laws for local galaxies. Furthermore, fitting the SED data of GRB afterglows should allow the derivation of the intrinsic extinction laws. Several pre-*Swift* SEDs (which I derived) were fitted in Li et al. (2008), and additional analysis has been done (with no contribution by myself) by Liang & Li (2009, 2010).

In the work I present here, one of the GRBs I analyzed was GRB 070802, which is extraordinary because it features high extinction and a prominent 2175 Å bump at a redshift $z = 2.4549$ (Krühler et al. 2008a; Elíasdóttir et al. 2009). Of the local galactic laws, I found (in accordance with Krühler et al. 2008a; Elíasdóttir et al. 2009) that LMC dust fits best, but there are still discrepancies. Therefore I employed the Drude model of Li et al. (2008). The fits are all displayed in Figure 2.4. With the exception of the GROND H band which is slightly too low even in the LMC fit, the Drude model fits best. The problem is that I have found that the model is extremely flexible, and GRB afterglow SEDs are usually not broad enough in wavelength range to prevent the best fit from being unconstrained at the ends. A fit without the H band finds: $\chi^2 = 6.62$ for 4 d.o.f., $F_0 = 5022677 \pm 30347844$, $\beta = -11.83 \pm 10.95$, $\mathrm{A_V} = 12.22 \pm 7.61$, $c_1 = 0.41 \pm 3.78$, $c_2 = -0.82 \pm 4.46$, $c_3 = -1.68 \pm 2.75$, $c_4 = 0.0031 \pm 0.0019$. With the exception of c_4, the c parameters are unconstrained, and the the intrinsic spectral slope is found to be very negative. Even fixing the spectral slope to the value from the X-rays ($\beta = 1.02$) leads to unconstrained results: $F_0 = 590.1 \pm 1112$, $\mathrm{A_V} = 1.35 \pm 2.04$, $c_1 = 0.22 \pm 22.6$, $c_2 = -0.60 \pm 31.8$, $c_3 = -1.94 \pm 6.15$, $c_4 = 0.033 \pm 0.054$. Therefore, it is unclear if the Drude model can be used to produce sensible results.

2.4.3   The Hydrogen and Metal Columns

The interstellar as well as intergalactic environment along the line of sight influence the GRB afterglow in two further ways. At 121.6 nm in the rest frame, the Lyman α absorption

line of hydrogen often causes a broad absorption line in afterglow spectra (e.g. Fynbo et al. 2009), and even more into the blue, the Lyman series creates further absorption lines. The Lyman α lines of hydrogen clouds in the IGM at lower redshift create the Lyman forest, which becomes strongly dominant for very high redshift GRBs (e.g., GRB 050904 and GRB 080913, Kawai et al. 2006; Greiner et al. 2009b). Finally, at 91 nm in the rest frame, the universe becomes opaque at the Lyman cutoff. The flux suppression through hydrogen absorption shows strongly in the SEDs of afterglows at higher redshifts (especially with the UV-capability of *Swift*), and it can be used to determine photometric redshifts (e.g., Rossi et al. 2008; Greiner et al. 2009a; Perley et al. 2010) or support the typically low signal-to-noise afterglow spectroscopy of high-z GRBs (e.g., Haislip et al. 2006; Greiner et al. 2009b; Tanvir et al. 2009). Examples of such "dropout" SEDs are presented in the Appendix, those of GRB 060526 (Figure C.4) and of GRB 080514B (Figure C.7).

Since the absorption cross section for ionization is $\propto \lambda^{8/3}$, the universe becomes transparent again in the soft X-ray regime. In the range of 0.1 - 1 keV, which is covered by the *Swift* XRT, the transitions in the inner shells of metals such as Fe and O create absorption edges which dampen the X-ray emission. Beyond a few keV, the emission is barely influenced by absorption. Along typical sightlines in the Milky Way and other galaxies, there is a reasonably fixed ratio between the column density of metals and that of hydrogen, so that the X-ray absorption can be used to derive an equivalent hydrogen column density N_H under the assumption of a certain metallicity, usually fixed to solar metallicity, which is very probably incorrect for GRB host galaxies. It has been found the the hydrogen column density N_H can differ strongly between the one derived from Lyman α and the equivalent one derived from the metal column (Watson et al. 2007), probably due to the absorption occurring at different distances from the GRB (e.g. Prochaska et al. 2006b). The ratio of gas to dust has been shown to typically be much higher than even in the SMC (Galama & Wijers 2001; Stratta et al. 2004), and I extended this in my own pre-*Swift* work (Kann et al. 2006b). This is thought to be due to the typically low metallicites of GRB host galaxies (the original hypothesis of dust destruction still has no evidence to support it). I was also part of the first systematic study of hydrogen column densities based only on Lyman α absorption (Jakobsson et al. 2006a), something that had been almost impossible in the pre-*Swift* era, as GRBs during that time rarely occurred at redshifts high enough to allow the measurement of N_H. From my optical afterglow sample, I derived the magnitudes at twelve hours after the GRB in the source frame (all afterglow magnitudes were furthermore shifted to a redshift of $z = 3$ so they became directly comparable), in this case *not* correcting for the host galaxy extinction (in contrast to my main work presented in Chapter 4). It would be expected that a rough correlation exists between the afterglow magnitude and the hydrogen column density if one assumes both a standard intrinsic afterglow luminosity as well as a standard gas-to-dust ratio in GRB host galaxies. The plot in Figure 2.3 shows that this is clearly not the case. There is a slight trend visible, afterglows whose spectra show strong Damped Lyman Alpha (DLAs, $log\ N_H \geq 20.3$) systems are usually fainter, but clearly, the scatter is very large and there are strong outliers.

Chapter 3

Background, Analysis Methods and Sample Creation

3.1 Introduction

Early this decade, the number of detected afterglows had become large enough to allow first statistical studies on the properties of afterglows to be done. By compiling all available data on GRB afterglow light curves, it should be possible to derive better parameters even for single afterglows, as well as study the distributions of the derived parameters. Sylvio Klose initiated this project and, together with his student Andreas Zeh, as well as Dieter Hartmann, first studied the late-time afterglows to search for the photometric signature of supernovae (Zeh et al. 2004). They came to the conclusion that all GRB afterglows (up to the end of 2002) at $z < 0.7$ which had sufficient late-time data exhibited bumps which could be modeled with a light curve model based on the light curve of the first GRB-supernova, SN 1998bw (Galama et al. 1998), as long as one introduces two further parameters, k and s, which modify the luminosity and the temporal stretch of the light curve, respectively.

During my diploma thesis, the work was expanded. I compiled further light curve data for 2003 GRBs (especially GRB 030329), and finalized the earlier data sets compiled by Andreas Zeh. Using the multicolor light curves of GRBs with well-detected afterglows, I analyzed the spectral energy distributions of the afterglows for signatures of dust in the line-of-sight. Andreas Zeh led the effort to fit the light curves, deriving parameters like decay slopes and break times and studying their distributions. We published this analysis in two papers written at the beginning of my PhD thesis, Zeh et al. (2006a) (henceforth Z06) and Kann et al. (2006b) (henceforth K06). These studies encompassed all GRBs with afterglows of the pre-*Swift* era, up to GRB 041006.

The pertinent results from Z06 are:

- The distributions of both the pre-break slopes α_1 as well as the post-break slopes α_2 are broad and even overlap. There are afterglows in which $\alpha_2 < 2$ at high significance. The light curve steepening $\Delta\alpha = \alpha_1 - \alpha_2$ also has a broad distribution. None of these values show a clear preferred peak value. The mean values are $\overline{\alpha_1} = 1.05 \pm 0.10$, $\overline{\alpha_2} = 2.12 \pm 0.14$.

- The afterglow break times (in the GRB rest-frame) are also broadly distributed, but

with a clustering around 0.3 days. This indicates that breaks in the pre-*Swift* era may have been missed due to follow-up being initiated too late.

- From the analysis of the afterglow parameters alone, about half the GRB afterglows propagate into a wind-swept environment, but there are also clear cases where a constant-density surrounding medium is preferred.

- Similar to the jet break times, the jet opening angles show a distribution with a clustering at small angles ($2° - 5°$) but extend to larger values. We reproduce the Ghirlanda relation with out sample, for which we determined the opening angles after individually determining if a wind- or an ISM-medium was more appropriate, this was the first study to do so.

- A search for correlations among other parameters did not yield any other strong correlations, especially not with the redshift.

- The residuals from the light curve fitting show only small variations of ± 0.1 magnitudes for almost all GRBs, with GRBs 021004 and 030329 being the only strongly variable light curves. We reference the time against the break time, and find no differences pre- and post-break.

The pertinent results from K06 are:

- The distribution of line-of-sight extinctions is strongly clustered toward low extinctions, with $\overline{A_V} = 0.21 \pm 0.04$. There are no secure cases with $A_V > 0.8$, creating a "dark burst desert" in comparison with the high lower limits on extinction from dark GRBs, like GRB 970828. In part, this can be accounted for by sample selection bias: As I derived extinctions only for afterglows with good multiband data, highly extinguished afterglows would typically fall out of the sample automatically due to no afterglows, or no redshifts, or detections in only a few (red) bands.

- For a few cases where data quality is less good, moderately high extinction values of $A_V \approx 1$ can be derived under reasonable assumptions on the intrinsic spectrum.

- The line-of-sight extinction drops toward higher redshifts. Similar to the generally low extinction values, this must in part be due to an observational bias, as high-z afterglows are affected much more strongly by the same amount of rest-frame extinction as afterglows at low-z, due to the extinction-sensitive UV region being redshifted into the optical.

- The distribution of intrinsic spectral slopes is broad, from $\beta = 0.2 - 1.2$, with $\overline{\beta} = 0.57 \pm 0.05$. Several afterglows have an intrinsic slope significantly below $\beta = 0.5$, the cutoff in the standard model. This is a further indication that p is not universal and that hard electron spectral indices exist.

- Further to the results of Galama & Wijers (2001) and Stratta et al. (2004), I find that in most cases, the dust-to-gas ratios for GRB host galaxies lie even lower than for the SMC.

- At one day after the burst in the observer frame, the distribution of afterglow magnitudes is 7.5 magnitudes. GRB 030329 has the brightest afterglow at any time after one hour (when it was first observed), and GRB 990123 has the brightest afterglow at early times (the prompt optical flash).

- Using the method detailed in K06, the afterglows are shifted to a common redshift of $z = 1$, which incorporates a shift in time as well as magnitude, the latter includes a correction for the line-of-sight extinction as well as the distance. This reduces the spread of luminosity at one day (12 hours in the host frame) to 5.7 magnitudes, and 56% or all afterglows lie in a cluster only two magnitudes wide. If split along the mean redshift of the *HETE II* sample, $z = 1.4$, a bimodal distribution is seen, with nearby ($z < 1.4$) afterglows being less luminous than more distant ones, with mean absolute magnitudes of $\overline{M_B} = -22.4 \pm 0.6$ and $\overline{M_B} = -24.1 \pm 0.5$, respectively. This clustering and bimodality was also discovered independendtly by Liang & Zhang (2006) and Nardini et al. (2006), both using A_V values from the literature only.

In the following work, I will expand my study of afterglows to those of the *Swift* era. Early studies of the first *Swift* afterglows showed that these were fainter than those of the pre-*Swift* era (Berger et al. 2005a,b). Furthermore, *Swift* and *HETE II* allowed the first discoveries of short GRB afterglows, finally allowing a comparison with the afterglows of long GRBs. Therefore, the goals of this study were:

- Expand the sample to leave the realm of low-number statistics and find more cases with extreme values (high A_V, sub- or superluminous afterglows).

- Compare the intrinsic properties of pre-*Swift* and *Swift*-era long GRB afterglows (Kann et al. 2010, hereafter Paper I).

- For the first time, research the properties of short GRB (optical) afterglows, and compare them to the long GRB sample (Kann et al. 2008e, hereafter Paper II).

3.2 Analysis Methods

3.2.1 Light-curve analysis

In the course of my diploma work as well as the PhD work of Andreas Zeh, he developed fitting scripts within the commercial mathematical analysis package *Origin*. These scripts generally employ a built-in Levenberg-Marquardt least-squares fitting algorithm to derive non-linear fits to the error-weighted data and produce results along with the associated parameter errors. The light-curve fitting procedure allows the choice of a simple power-law, a Beuermann equation (Equation 1.1), and an additional SN component (the mathematical structure of the analytic equation which models the SN emission is given in the PhD thesis of Andreas Zeh), as well as the host galaxy component (an unvarying "base level"). In a script window, all the parameters can be chosen to be fixed or left free to vary. The fitting is improved if good guesses at the initial parameters are made. We found that the break strength n almost always had to be fixed. With this script, usually a single waveband (that with the best data,

usually R_C) is fit, then the derived parameters are fixed for the other wavebands, which assumes an achromatic evolution of the afterglow – a fact which is almost always given (and in the case color changes are detected, such data are excluded from the fitting procedure, of course).

A more advanced and realistic method of fitting (using the same equations as above as well as the Levenberg-Marquardt algorithm within *Origin*) involves the simultaneous fit of all wavebands. Here again, achromaticity is assumed/checked, which allowed me to fix the light-curve parameters as shared values in the fit, whereas the normalization values (and possibly the host galaxy values if multicolor data exists, as the galaxies have SEDs which can differ strongly from those of the afterglow) are different for each band. These normalization values are derived either at one day after the GRB (for a simple power-law fit) or at the break time (for a fit with the Beuermann equation).

The actual light curve parameter values were of lesser importance in my study, results for single GRBs are given in the extensive appendix of Paper I and are not further reproduced here. A project to expand the results of Z06 to the *Swift*-era is planned.

3.2.2   SED analysis

Publications on GRB afterglows usually derive the SED of the afterglow at a certain time, typically when the data density is highest and/or the amount of extrapolation needed for different bands (often, the bluest and reddest bands have less dense sampling than the "core bands" VR_CI_C) is lowest. In my approach, unless clear achromaticity is found, I always use the entire available light-curve data set to derive the SED using the light curve fits as described in Chapter 3.2.1, with the normalizations. Usually, this leads to a reduction of the errors of the SED data points. Of course, in cases where some bands are given only as single data points, special care has to be taken, but experience has shown me that chromatic evolution in GRB afterglows is a rare phenomenon usually associated with the early afterglow (e.g., Perley et al. 2008a; Bloom et al. 2009).

The fitting script then uses a filename mask and information from several database files (Galactic extinction, GRB redshift, zero-point in Jy of the associated filter, mid-wavelength of the filter; initially compiled by Andreas Zeh but greatly expanded by myself over the last six years) to transform the magnitudes into flux densities in the GRB rest frame, which are then fitted with the MW, LMC and SMC analytical models described in Chapter 2.4.1. Next to these three fits, a fit with no extinction (simple power-law) is possible (yielding a slope I call β_0), furthermore fits with fixed intrinsic spectral slopes β as derived from light-curve fits and the $\alpha - \beta$ relations are possible, as well as just fixing β to an arbitrary value (useful if the spectral slope is assumed to be related to the slope of the X-ray afterglow either as $\beta_O = \beta_X$ or as $\beta_O = \beta_X - 0.5$, the two possibilities which depend on the position of ν_c). The fits with the "Drude" model were performed within the non-linear curve fitting tool of *Origin*, similar to the multi-band light curve analysis.

These fits have three parameters with their associated 1σ errors as output: a normalization flux density F_0 (which is of no real interest, as it just reflects at which time the SED was derived), the intrinsic spectral slope β (which is the spectral slope which would be measured if there was no dust extinction along the line of sight) and the extinction in the rest-frame

V band A_V (which can be an extrapolation for high-z events). Especially in the case of low extinction or at low redshift (K06), the fit quality (in terms of $\chi^2/d.o.f.$) does not differ strongly between the three extinction laws, and I am not able to determine, at least with strong significance, which of the extinction models fits the SED best.

3.2.3   Further procedures

The procedure to shift the afterglows to a common redshift of $z = 1$ (correcting for the line-of-sight extinction and taking the different intrinsic spectral slopes β into account), so that they are readily comparable, was developed and programmed by Sylvio Klose. It is described in detail in the Appendix of K06.

The procedure to derive the cosmological k-correction of the prompt emission of the GRBs in my sample is based upon the work of Bloom et al. (2001) and was implemented in a program by Amelia Wilson. I wrote a script to get from the measured fluence of a GRB to the isotropic energy release which includes the input of this correction. In these calculations a flat universe with matter density $\Omega_M = 0.27$, cosmological constant $\Omega_\Lambda = 0.73$, and Hubble Constant $H_0 = 71$ km s^{-1} Mpc^{-1} (Spergel et al. 2003) is assumed. The luminosity distance is derived using Ned Wright's Cosmology Calculator[1].

The Galactic extinction toward the GRBs has been taken from the NED (NASA Extragalactic Database) Galactic Extinction Calculator[2]. For the non-parametric Kendall rank correlation test, I used an online calculator[3]. Significance values σ for the null hypothesis are derived in *Origin*. For the Spearman's rank correlation test, I used another online calculator[4]. An implementation of the Kolmogoroff-Smirnov Test has been programmed by Sylvio Klose, who also implemented the Monte Carlo analysis to perform log-log fitting of data with asymmetric error bars.

3.3   Sample Selection and Data Mining

3.3.1   On the Problems of Classification – the Type I/II Denomination

To derive meaningful statistical conclusions on the different samples of GRB afterglows (i.e., short/hard vs. long/soft), it is necessary to think about how to classify the GRBs within the sample. In this regard, I have been involved in several studies, some of which pointed to weaknesses in the old classification scheme, and one which devised a new classification scheme which I will use henceforth in my work.

In the *BATSE* era, after the discovery of the classes of short/hard and long/soft GRBs (Kouveliotou et al. 1993), the "2 second divide" became canonical. This was despite the fact that the defining characteristics, T_{90} and the hardness ratio, are instrument- and redshift-dependent. Since GRB prompt emission often exhibits hard-to-soft evolution and differing pulse widths in different energy bands (Ford et al. 1995), the duration at lower energies is often longer. Hardness ratios are defined in certain bands, another detector may not even

---

[1] http://www.astro.ucla.edu/~wright/CosmoCalc.html
[2] http://nedwww.ipac.caltech.edu/forms/calculator.html
[3] http://www.wessa.net/rwasp_kendall.wasp
[4] http://www.spearmansrank.com/

have detection capabilities in that energy range. Unless the peak energy lies strongly outside the detector range (so that the spectrum is almost a pure power law) different redshifts will create different HRs for the same intrinsic spectrum, and of course T_{90} changes with redshift. With the beginning of the afterglow era and the measurement of distances, the dividing line has become weaker, and GRBs have been discovered which are not easily placed in either category, or clearly associated with a certain class of progenitor.

GRB 040924 was a temporally short but spectrally soft event (an XRR GRB) localized rapidly be *HETE* (Fenimore et al. 2004) and also detected by *Konus-Wind*, which measured a T_{90} of 1.5 seconds (Golenetskii et al. 2004). Ground-based follow-up rapidly found a faint afterglow, which turned out to be one of the most intrinsically faint known to that date (K06). Late-time follow-up with the HST revealed an accompanying supernova (Soderberg et al. 2006c), which was confirmed by a study I was part of (Wiersema et al. 2008). My fitting found that the SN is detected only marginally, and is probably the faintest GRB-SN discovered so far (Figure 3.1). While it has been labeled a short GRB in the literature (Huang et al. 2005), the combination of spectral softness and the SN emission clearly implies that this is a collapsar-induced GRB – it is just not "long".

The third short/hard GRB with an afterglow was the *Swift* GRB 050724. Its prompt emission turned out to be peculiar. The main prompt emission was already ≈ 4 seconds long in the lowest *BAT* energy channel, and this was followed by a long soft emission "bump" (Barthelmy et al. 2005), which went over seamlessly into a steeply decaying X-ray afterglow (Campana et al. 2006b). A similar feature had already been seen, albeit with much lower signal-to-noise and without X-ray follow-up, for GRB 050709 (Villasenor et al. 2005). T_{90} of the complete event is 152 seconds. On the other hand, there is clear evidence the GRB is not associated with current star formation (Barthelmy et al. 2005; Berger et al. 2005c; Gorosabel et al. 2006), implying it cannot be collapsar-induced. Analysis showed that this GRB would have had $T_{90} < 2$ s if it had been detected by *BATSE*, though. Soon afterward, Norris & Bonnell (2006) reported that several similar events (which had been thought to be long GRBs) had been detected by *BATSE*. They labeled the two distinct emission parts (often, there are some seconds of negligible emission in between) the Initial Pulse Complex (IPC) and the Extended Soft Emission Component (ESEC). It had now become clear that not all short/hard GRBs need be temporally short, though the special IPC+ESEC light curve shape is a characteristic. Furthermore, Norris & Bonnell (2006) found that all the IPCs had negligible spectral lag – the emission peak appears at the same time within errors in different energy bands (which is almost never the case for long/soft GRBs, Ford et al. 1995). "Zero spectral lag" thus became a positive indicator for short/hard GRBs, though the most luminous long GRBs (which often have hard spectra and high peak energies too) can also have negligible spectral lags. Donaghy et al. (2006) were the first to suggest a new classification scheme based on multiple observable criteria.

A year later, the situation became even more complicated when two temporally long, nearby events were discovered which were observed deeply but yielded no sign of the expected supernova emission: GRB 060505 and GRB 060614 (Fynbo et al. 2006b; Gal-Yam et al. 2006; Della Valle et al. 2006; Ofek et al. 2007). GRB 060505 is about 4 seconds long, but also shows a faint precursor which extends the total duration to 10 seconds (McBreen et al. 2008), whereas GRB 060614 was a bright event lasting over 100 seconds (Gehrels et al. 2006). A study of the
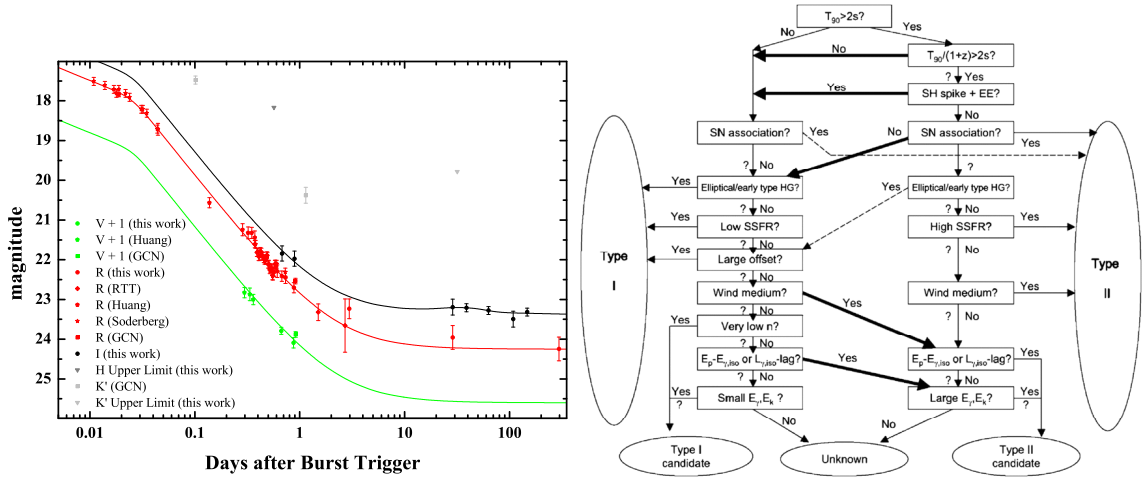
Figure 3.1: Left: *The optical light curve of GRB 040924. At late times, a shallow SN bump is visible. Despite being temporally short, this GRB resulted from the core collapse of a massive star. From Wiersema et al. (2008).* Right: *The flow chart of Zhang et al. (2009), used to determine whether a GRB belongs to the Type I or Type II class (or is at least a candidate for one of the two classes). As the observables are not given in many cases, the question marks indicate the option if no conclusion can be drawn. The dashed lines indicate possible directions which have never been observed before. I have used this flow chart in the selection of my samples.*

prompt emission of GRB 060614 showed that not only was the light curve of the IPC+ESEC shape (though the IPC lasts an uncommon 5 seconds), but both the IPC as well as the ESEC showed negligible lag (Gehrels et al. 2006), indicating a new classification scheme was needed. It was either possible that "short/hard" GRBs could be temporally long after all, or there are "long/soft" GRBs in which the expulsion of large amounts of radioactive elements is strongly suppressed, preventing a supernova from forming. This "fallback black hole" scenario was the preferred explanation of several groups (Fynbo et al. 2006b; Gal-Yam et al. 2006; Della Valle et al. 2006; Thöne et al. 2008a). Zhang et al. (2007c) made a comparison of the light curves of GRB 050724 and GRB 060614, and found that if one made GRB 060614 less luminous by a factor of 8, its light curve strongly resembled that of GRB 050724. GRB 060505 is an even more complicating case, as was shown, amongst others, by two studies I was involved in. Thöne et al. (2008a) analyzed the spatially resolved spectroscopy of the spiral host galaxy GRB 060505 occurred in, and found that the GRB exploded in a massive HII region, which by itself shared many of its properties with the host galaxies of long/soft GRBs. I analyzed the SED of the optical afterglow, finding no evidence for dust, which is evidence that the GRB was not a background event. Furthermore, McBreen et al. (2008) (following an idea I originally had) analyzed the *Suzaku/WAM* data of GRB 060505, which is of better quality than the *Swift* data (the GRB occurred while *Swift* was entering the South Atlantic Anomaly, preventing the satellite from flight-localizing it or slewing to it), and found significant evidence for spectral lag, something which "should not occur" for short/hard GRBs. GRB 060505 and GRB 060614 will be discussed in more detail in Chapter 5.

In September 2008, Andrea Rossi of the Thüringer Landessternwarte Tautenburg (TLS) GRB team discovered the afterglow of the *Swift* GRB 080913 through rapid follow-up with GROND detector (a seven-channel simultaneous imager mounted on the 2.2m telescope at

La Silla, Chile, Greiner et al. 2008). A z' dropout indicated a high redshift, and spectroscopic follow-up with the VLT found that the GRB lies at $z = 6.695$, at this time the most distant GRB discovered (Greiner et al. 2009b). Half a year later, an even more distant GRB was discovered, GRB 090423 at $z \approx 8.2$ (Tanvir et al. 2009; Salvaterra et al. 2009). My analysis of their afterglows (Greiner et al. 2009b, this work) showed that both were of average luminosity, typical for long/soft GRBs. Their prompt emission, on the other hand, indicated that they could be short/hard GRBs, in both cases, $T_{90} < 2$ seconds if their light curves were transformed into the rest frame. Zhang et al. (2007c) had introduced a new classification labeling, expanding the work of Donaghy et al. (2006). Basing the GRB classes on the different kinds of progenitors, they labeled GRBs which are due to collapsing massive stars "Type II" (formerly "long/soft", though clearly some of them can be temporally quite short, and some have very hard spectra and high peak energies), whereas those not associated directly with exploding stars (and probably due to the mergers of compact objects) are labeled "Type I" (formerly "short/hard", though the extended emission can create $T_{90} \gg 2$ s, and some "short/soft" events have been found, like GRB 070724A in this work) – these labels are in analogy to the types of SNe. In the following, I shall use these designations. The short durations of GRBs 080913 and 090423 – which occurred at redshifts where Type I GRBs are expected to be very uncommon – triggered a deeper study into the possibility of classifying GRBs along the progenitor divide, using multiple observational criteria (Zhang et al. 2009). Analysis of the joint BAT/XRT light curves of the two bursts showed that at $z = 1$, both would have appeared as IPC+ESEC GRBs, although the ESEC components would have shown more structure than is typical for these events. Following a review of the different possible selection criteria and the physics underlying them, we created two samples of GRBs which we considered to be Type I or Type II with high confidence. Any GRB with an associated supernova (either spectroscopically, or with a strong bump signature, like GRBs 011121 and 020405) and/or a high star-formation rate of the host galaxy, small offset and no deep limits on a SN is considered a Type II GRB. A Type I GRB is either associated with an elliptical or otherwise low-SFR host galaxy, and/or a large offset (which always implies an insecurity in associating the GRB with the correct host galaxy, see Chapter 5) and deep observations have revealed no associated SN emission. These selection criteria ignore the prompt emission completely. Since the Type I GRB sample contained only five events, we created an additional "other short/hard GRBs" sample for comparison purposes. My involvement in this work consisted of helping select these samples and comparing the optical afterglows of the two samples (see Chapter 5 for more details). As an end result, we created a flow-chart to allow the identification of the class a GRB belongs too (Figure 3.1). While this chart does begin with the "classical" T_{90} divide, it allows several crossovers. In most cases, the observational evidence is not strong enough to place a GRB clearly into the type I or Type II category, but almost all are found to be either Type I or II candidates.

This flow chart is used to select the samples in this Chapter as well as Chapter 5. Almost all events in my work are classified as Type II GRB/Type II GRB candidates as well as Type I GRB/Type I GRB candidates (e.g., any that do not have host associations cannot fulfill the definite Type I criteria of Zhang et al. 2009) without controversy. Furthermore, an earlier, rougher classification scheme (which relied mostly on the analysis presented in GCNs and papers for more controversial cases) yielded exactly the same results as the use of the Zhang

et al. (2009) flowchart. The two controversial GRBs 060505 and 060614 mentioned above are both classified as Type I (GRB 060614, due to low SSFR as well as large offset) and Type I candidate (GRB 060505, due to very low E_{iso}). The single truly controversial case is GRB 060121. This GRB was localized by *HETE* with $T_{90} \leq 2$ s, negligible lag and an IPC+ESEC (very faint) prompt emission evolution (Donaghy et al. 2006). A faint optical afterglow was discovered by my Italian collaborators, which was associated with an extremely faint host galaxy (Levan et al. 2006) and was found to be strongly reddened. de Ugarte Postigo et al. (2006) modeled the afterglow and derived two photometric redshift solutions, $z = 4.6$ (the more likely one) and $z = 1.7$. According to the Zhang et al. (2009) flowchart, GRB 060121 must, in all consequence, be classified as "unknown". It follows the Type I path well ($T_{90} \leq 2$ s, and also the IPC+ESEC light curve shape), but, at least for the $z = 4.6$ solution, energetics arguments imply it is not of Type I, but more similar to GRB 080913 and GRB 090423. Also, it obeys the Amati relation (Zhang et al. 2009). Still, it was seen as a traditional "short/hard" burst, so I will discuss it in the context of the Type I sample (see Chapter 5).

Furthermore, I have also compared my sample with the recent ε-classification criterium of Lü et al. (2010). These authors define ε as a ratio between the isotropic energy release and the rest-frame peak energy of the spectrum (this implies the redshift must be known), then plot $\log \varepsilon$ versus $\log T_{90,z}$, the rest-frame duration. They find that GRBs tend to cluster in three groups: The first group follows the Type II (and candidates) from Zhang et al. (2009), the second the Type I GRBs (if only the IPC component is used in IPC+ESEC GRBs), and a third group (low ε but large $T_{90,z}$) consist of nearby low-luminosity events which are often associated with SNe but show no classical afterglow emission. I determined ε for all of my candidates and find that they separate exactly along the dividing lines already established using the Zhang et al. (2009) flowchart, *again* with the exception of GRB 060121 which belongs to the high-ε (i.e., Type II GRBs) class, albeit being the leftmost event, with even lower $T_{90,z}$ than GRBs 080913 and 090423.

3.3.2 Data Mining and Additional Photometry

Data acquisition was begun during his diploma and PhD Thesis by Andreas Zeh, extending to mid-2001, and was used to search for late SN bumps (Zeh et al. 2004). I began expanding the data base, adding additional old GRBs with sparser measurements (though only those with detected afterglows, I have not researched dark GRBs), as well as adding 2002 and 2003 GRBs. Since then, I have strongly expanded the data base to over 150 afterglows (both of Type I and Type II GRBs). In Z06 we analyzed all GRBs with reported afterglows in the pre-*Swift* era (only XRF 040812 was published later, and the actual data have not been published), but this is not feasible anymore now. *Swift* has strongly increased the rate of burst localization as well as afterglow recovery, with the consequence that the community must perform triage, both in assigning valuable observation time as well as working preferentially on GRBs that are egregious in some sense (bright afterglow, high or very low redshift, etc.). Similarly, it is not useful to collect data on *all* GRBs with an afterglow right now, as many will only have very few points published in the GCN. Such afterglows yield hardly any information (and rarely have redshifts, as well). Of course, such a situation is often given with Type I GRB afterglows, but here I relaxed my criteria to increase the sample size.

The data are taken from journal publications and the GCN Circulars, and in some cases, were also supplied to me by private communication. Photometry from journals is always preferred over that in the GCNs, as the latter are usually "quick-shot" calibrated against astrometric catalogs like USNO-B1.0, which may deviate from Landolt/SDSS calibrations by up to two magnitudes. The sources of all *Swift*-era photometry are given in the Appendices of Paper I and Paper II. In most cases, data was used "as is". Unfiltered data is usually calibrated to the R_C band, and only in rare cases are significant offsets found to well-calibrated R_C data. In the K band, I usually do not differentiate between slightly different filters like K, K_S, and K' – my experience is that any color shifts between these filters are smaller than their typical statistical errors found in this band (Kann et al. 2007f). The same is true for the long-wavelength UVOT filters *ubv*, which are close to the Johnson-Cousins filter system as well. Filters that are treated on their own are the Sloan filter system *ugriz* (also Gunn filters, though these are rarely used anymore) as well as the seven-color GROND filter system, these are achieved with dichroics and can have quite significantly different central wavelengths and zero points from the Sloan/2MASS filter system.

In addition to published data from other sources, I have compiled further unpublished photometry on the GRBs in my sample and published it in Papers I and II (unpublished photometry will be included in the revised version of the latter paper which is not yet re-submitted). In total, I publish 840 data points on 42 (Type II) GRB afterglows in Paper I (two of these GRBs, 040924 and 041006, are the last two pre-*Swift* GRBs), see Table 1 of that paper (available in complete form either in the arXiv preprint or as a machine-readable table on the ApJ Web page). Most of this photometry has been analyzed by the co-authors of Paper I (indeed, a large number of co-authors are part of the paper for the exact reason of having supplied this data), but for a small number (≈ 20) I did the analysis myself. In many cases, only a few data points (or even just one) are given for a GRB, often, these are revised GCN magnitudes (in some cases, the GCN magnitude was deemed final and was taken over unchanged). For a few GRBs, though, I obtained large data sets, with several "firsts". For GRB 050319, I present late-time, deep data which shows a smooth jet break, as well as the only NIR detection. For GRB 050502A, I present a very deep late detection ($R_C = 25.3$) which also yields evidence of a jet break occurring. For GRB 050820A, I present a large amount of JHK data, the only NIR data published on this GRB. For GRB 050802, I present a large ground-based data set, so far the only ground-based data published on this event, including the late detection of a faint host galaxy. Dense early as well as deep late data is also presented for GRB 050922C. For GRB 061007, I present the only available NIR data, which allows me to derive a much better-constrained SED than was possible beforehand. Further large data sets are included for GRBs 050408, 060418, 080413A, and 080810.

The analysis of additional unpublished Type I GRB afterglow data is not yet complete, but so far, I have the deepest reported limits for GRBs 050911, 051105A, and 060801, as well as the discovery observations of the afterglow of GRB 060121.

Chapter 4

The Afterglows of Type II GRBs

In this Chapter, I will present the results my work on the comparison between the pre-*Swift* afterglow sample I published in K06 and the *Swift*-era afterglow sample. The complete results are presented in Paper I.

4.1 The Type II GRB Afterglow Samples

All in all, I compiled data on a total of 79 GRBs with redshifts (three of them photometric, all others spectroscopic) and good light curve coverage (extending to about 1 day in the observer frame if the GRB were at $z = 1$, with a few exceptions) from the *Swift* era (from the end of 2004 to 2009 September), a few of which have been localized by missions other than *Swift*, such as *HETE II*, *INTEGRAL*, the *Third Interplanetary Network* (*IPN*) and most recently *Fermi*. This is to be compared with a total of 251 Type II GRB afterglows in the *Swift*-era as of the end of 2009 September, of these, 146 have redshifts (122 spectroscopic, 6 photometric, 18 host galaxy-derived)[1]. All the remaining GRBs did not have redshifts and/or sufficient light curve coverage to be included in the sample. Depending on the data quality, I have sorted the 79 GRB afterglows into a further three different samples (with one further split temporally). All afterglow data are corrected for Galactic extinction using the maps of Schlegel et al. (1998).

4.1.1 The pre-*Swift* era "Golden Sample" updated

This sample comprises three GRBs. These were all included in the complete sample of K06, but not in my Golden Sample due to the SEDs not conforming to the sample selection criteria. Additional data (GRB 990510) and a more diligent re-analysis (GRB 011211, GRB 030323) led me to be able to include them in the pre-*Swift* Golden Sample. Details are given[2] in Appendix B.1 of Paper I.

---

[1] http://www.mpe.mpg.de/~jcg/grbgen.html

[2] I have not included these appendices even in the Appendix of this thesis as doing so would add an enormous amount of references without yielding any truly relevant information

4.1.2   The *Swift*-era "Golden Sample"

This sample comprises 48 GRBs. These GRBs fulfill the criteria of the Golden Sample of K06, allowing me to directly compare them. The criteria (as taken from K06) are:

1. The 1σ error in β ($\Delta\beta$) and the 1σ error in A_V (ΔA_V) should both be ≤ 0.5.

2. $A_V + \Delta A_V \geq 0$.

3. I do not consider GRBs where all fits (MW, LMC, and SMC) find $A_V < 0$, even if the previous criterion is fulfilled[3].

4. $\beta > 0$ (although I do not reject cases with $\beta - \Delta\beta \leq 0$).

5. A known redshift (derived from absorption line spectroscopy in most cases, with some GRBs having redshifts from host galaxy spectroscopy [e.g., XRF 050416A, GRB 061126], and some being photometric redshifts [e.g., GRB 050801, GRB 080916C]).

Details on the GRB afterglows, including light-curve analysis results, can be found in Appendix B.2 of Paper I.

4.1.3   The *Swift*-era "Silver Sample"

This sample comprises 14 GRBs. These GRBs have well-detected multi-color afterglow light curves but the derived SEDs do not conform to the quality standards of the "Golden Sample". Certain reasonable assumptions are made to derive β and thus A_V using the theoretical relations derived from the fireball model (e.g., Zhang & Mészáros 2004). I treat different cases individually, see Appendix B.3 in Paper I for the exact assumptions I used. In some cases, β is derived from the measured pre-break afterglow decay slope α, in other cases, I use the X-ray spectral slope β_X as given on the XRT repository Web page[4] (Evans et al. 2007, 2009), with the assumed optical spectral slope being either $\beta = \beta_X$ or $\beta = \beta_X - 0.5$.

4.1.4   The *Swift*-era "Bronze Sample"

The sample selection criteria used to define the Golden and Silver Samples includes a significant selection bias against dust obscured systems (Fynbo et al. 2009). In limiting myself to afterglows that have good multicolor observations (which is usually only the case for observationally bright afterglows), I may be missing out a population of fainter afterglows that would increase the spread of luminosities, in principle possibly bringing Type II GRB afterglows closer to those of Type I GRBs (Chapter 5). Reducing this selection bias is a complicated task, though. I expect no significant rest frame dust extinction along the line of sight to Type I GRB afterglows (but see Chapter 5 for caveats on this), and only a small spread in redshift, ranging (for now) from $z = 0.1$ to roughly $z = 1$ for those events where associations

---

[3]Such negative extinction is usually found when scatter in the SED results in data points in the blue region being too bright, or an overbright data point creating a "2175 Å emission bump". In such cases, the fitting program determines that the best fit is then "emissive dust" which creates an upward curvature, $A_V < 0$ and $\beta > \beta_0$.

[4]http://www.swift.ac.uk/xrt_curves/

are significantly secure. Both assumptions are clearly invalid for Type II GRBs, which have been detected up to $z = 8.2$ (Tanvir et al. 2009; Salvaterra et al. 2009), and can be strongly extinguished by dust in their host galaxies (e.g., GRB 051022: Rol et al. 2007; Castro-Tirado et al. 2007; Nakagawa et al. 2006, GRB 060923A: Tanvir et al. 2008a, GRB 061222A, GRB 070521: Perley et al. 2009a, GRB 070306: Jaunsen et al. 2008, GRB 080607: Prochaska et al. 2009 and GRB 090417B: Holland et al. 2010). An unknown redshift can have a strong influence on the magnitude shift (denoted dRc, see K06), that is applied when transforming an afterglow from its observed redshift to a common redshift of $z = 1$. An unknown rest frame extinction can only make the afterglow more luminous if it were corrected for[5].

For this reason I have created a third Type II GRB afterglow sample which I denote the "Bronze Sample". The selection criteria are the following: First, the GRB must have a well-constrained redshift. In all selected GRBs, this is a spectroscopic redshift, though I would not exclude GRBs with well-constrained photometric redshifts. The knowledge of the redshift removes the strongest uncertainty in the luminosity derivation. Second, the redshift must be $z \leq 4$, to keep the R_C band (which is usually the band with the best measurements) unaffected by host galaxy Lyα absorption or intergalactic Lyα blanketing. Third, the GRB must have sufficient afterglow data in the R_C band (in some cases, I created composite light curves by shifting other colors to the R_C zero point if sufficient overlap exists) to allow at least a confident extrapolation of the light curve to 0.5 rest frame days after the corresponding burst, where I will be determining the optical luminosity. This final criterion removes many GRBs that only have very early detections published, usually *Swift* UVOT observations. In total, I find 14 additional GRBs that fulfill these selection criteria. Clearly a selection bias against very faint afterglows still applies, but if one sets the sample selection threshold even lower (e.g., including also optically dark GRBs with no afterglow detection and no redshift), hardly any useful information can be gleaned.

Details on the photometry sources of the "Bronze Sample" are listed in the Appendix B.4 of Paper I. In shifting these afterglows, I assume a spectral index in the optical/NIR bands of $\beta = 0.6$ and a host galaxy extinction of $A_V = 0$ (a single exception is GRB 060605, where an extrapolation of the X-ray slope finds that the optical slope must be identical, and also that the R_C band is unaffected by Lyman α absorption, Ferrero et al. 2009). A value of $\beta = 0.6$ was found to be the mean value for pre-*Swift* afterglows (see, e.g., K06), and I also find a similar value for the *Swift*-era Golden Sample (4.2.2). These afterglows suffer from host frame extinction as well, as has been shown by an analysis of mostly unpublished UVOT data by Schady et al. (2010), so the derived luminosities are lower limits, and the mean absolute magnitude of this sample is a lower limit only as well.

4.2   Results on the observed Light Curves of *Swift*-era GRB Afterglows

The results of the SED fits with no extinction as well as a MW, LMC, and SMC extinction curve are given in Table A.1 for the Golden Sample (for the Silver Sample, approximative

---

[5]Note that an unknown redshift also implies an additional uncertainty in the host galaxy extinction, but this effect will usually be minor compared to the pure distance effect.

results can be found in the individual GRB descriptions in Appendix B.3 of Paper I). Apparent and absolute magnitude at 1 and 4 days after the GRB can be found in Table A.3. The magnitude of a selected sample of GRBs with early observations and/or well-defined peaks in the afterglow evolution can be found in Table A.4. The energetics, including the bolometric isotropic energies, for the complete sample (including the 19 GRBs from K06) can be found in Table 2 of Paper I.

4.2.1   Observed Light Curves of *Swift*-era GRB Afterglows

In Figure 4.1 I present (analogous to Figure 7 in K06), the observed light curves of afterglows of *Swift*-era GRBs (after correcting for Galactic extinction and also host galaxy contribution, if the latter is possible), in comparison with the Golden Sample of K06. The most immediate result is that the rapid and precise localization capabilities of *Swift*, as well as the proliferation of rapid-slewing autonomous robotic telescopes, have strongly increased the number of afterglows that are detected at early times, typically starting within the first minutes after the GRB trigger. A strong spread in early magnitudes is also evident. Only a few GRBs of the *Swift* era are observationally as bright as the brightest pre-*Swift* afterglows. At early times, the prompt optical flash of the "naked-eye" GRB 080319B (Racusin et al. 2008; Bloom et al. 2009; Woźniak et al. 2009; Beskin et al. 2010) lies several mag above all other afterglows. Otherwise, only the afterglow of GRB 061007 is comparable to the optical flash of GRB 990123 (Akerlof et al. 1999). Several further early afterglows reach mag $\approx$ 12. At later times, beyond 0.1 days, the afterglows of GRB 050603, GRB 090926A, GRB 070125 and, at very late times, GRB 060729, are among the brightest observed, the latter due to a long plateau phase and a slow, unbreaking decline (Grupe et al. 2007). At early times, the faintest afterglows are GRB 071122 (which has a long plateau phase, Cenko et al. 2009), GRB 080129 (which was undetected down to 23rd mag in the beginning before rising to a huge optical flare, Greiner et al. 2009c), GRB 080913 (at very high redshift, assuming a fully transparent universe, Greiner et al. 2009b) and GRB 070802 (which exhibited a late rise and a highly extinguished afterglow, Krühler et al. 2008b; Elíasdóttir et al. 2009). After 0.1 days, several further afterglows (GRB 050401, XRF 050416A, GRB 060927, GRB 070419A, GRB 050502A) are considerably fainter than the faintest afterglow in the pre-*Swift* sample, GRB 040924 (K06). This confirms the early reports about the faintness of the afterglows of *Swift* GRBs (Berger et al. 2005a,b).

4.2.2   Results from SED Fitting – Low Host Extinctions at High Redshifts

SMC dust is preferred for most GRBs in my Golden Sample, which strengthens the results of K06. Clear exceptions are GRB 060124 (which features a small 2175 Å bump, Kann et al., in preparation) and GRB 070802 (Krühler et al. 2008b; Elíasdóttir et al. 2009), and several other GRBs are better fit, though not with high statistical significance, with LMC or MW dust. In several cases, especially for MW dust, the fitting process finds unphysical "negative extinction" which I see as evidence that the corresponding dust extinction curve is ruled out. I find a total of 17 GRBs for which the preference for SMC dust is strong, whereas the preference for SMC dust is weak for a further 17 events. For a total of six afterglows, I find no evidence at all for dust and I just use the spectral slope without extinction correction
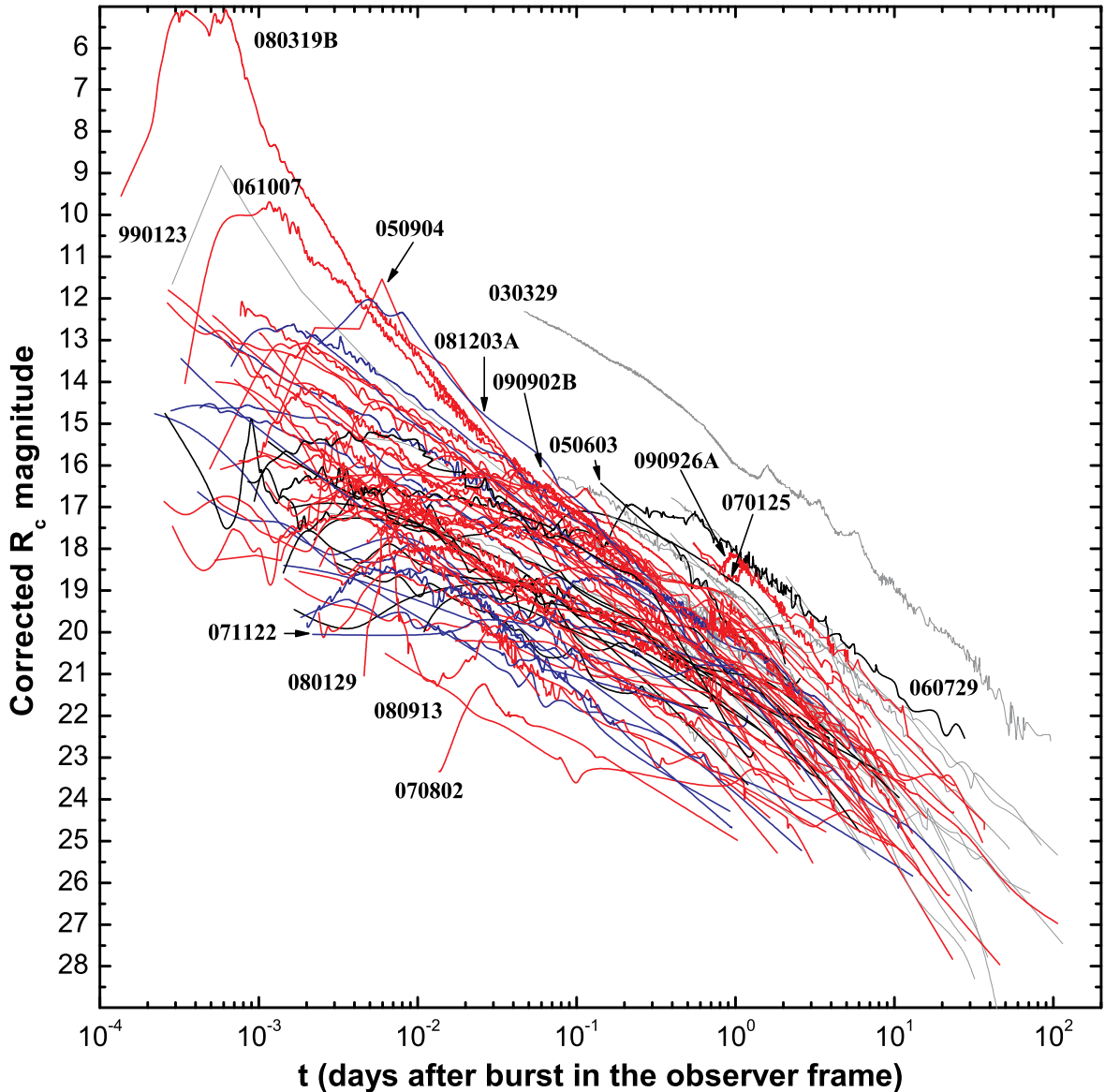
Figure 4.1: *Afterglows of Type II GRBs in the observer frame. All data have been corrected for Galactic extinction and, where possible, the contribution of the host galaxy has been subtracted. Thin gray lines are Type II GRBs from the pre-Swift era, taken from K06 (three further GRBs were re-analyzed in my work and are added to the pre-Swift sample, now denoted K06+3). Thick red lines are the Swift-era Golden Sample. The Silver Sample is blue, and the Bronze Sample is black. The large number of early afterglow detections is evident. Clearly, there are several afterglows that are significantly fainter than the pre-Swift sample. At late times, the non-breaking afterglow of GRB 060729 is brighter than any other except for GRB 030329. At very early times, the prompt flash of the "naked-eye" GRB 080319B reaches four mag brighter than the previous record-holder, GRB 990123. GRB 061007 comes close to the magnitude of the optical flash of GRB 990123, making it the third-brightest afterglow ever detected. At late times, the afterglow of the nearby GRB 030329 still remains brighter than any other afterglow discovered since.*

(in further cases, the amount of dust is negligible within errors), most of these events (four out of six) lie at high redshift, $z > 4$ (see below). A total of seven GRBs have $A_V > 0.5$
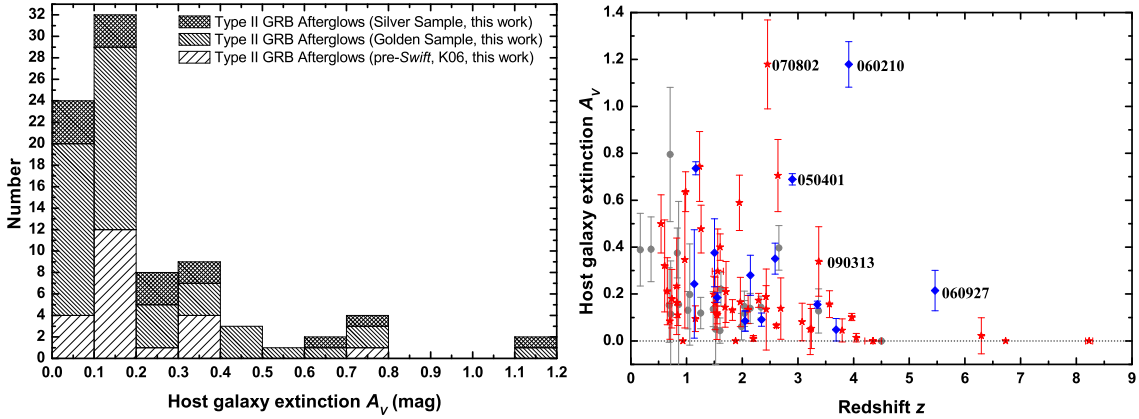
Figure 4.2:   Left*: Distribution of the derived host galaxy visual extinction* A_V *in the source frame for the bursts of the Golden Sample of K06+3 and the values I derive in my work (Golden Sample and Silver Sample). In contrast to the sample presented in K06, I now find two bursts with* $A_V \geq 0.8$*, GRB 070802 with* $A_V = 1.18 \pm 0.19$ *and GRB 060210 with* $A_V = 1.18 \pm 0.10$*, the latter case being unsure, though. Most bursts have* $A_V \leq 0.2$*, just as in the pre-*Swift *sample.* Right*: Derived host galaxy visual extinction* A_V *in the source frame for the Golden Sample of K06+3 bursts (grey circles) and the values derived for the GRBs in this work (Golden Sample, red stars, and Silver Sample, blue diamonds) plotted as a function of the redshift z. A trend of lower extinctions toward higher redshifts is visible but only weakly supported (Kendall's* $\tau = -0.34$*, Spearman's* $\rho = -0.42$*). Note that for most Silver Sample GRBs, the errors of the derived extinction are underestimated due to parameter fixing in the fitting process. Several exceptional GRBs are indicated.*

within 1σ errors, two of these, GRB 070802 with $A_V = 1.18 \pm 0.19$ and GRB 060210 with $A_V = 1.18 \pm 0.10$ (though there are caveats on this event, as given in Appendix B.3 of Paper I), lie significantly above the highest value in K06, that of GRB 991208 ($A_V = 0.80 \pm 0.29$). The further GRBs are GRB 050408 ($A_V = 0.74 \pm 0.15$), XRF 071010A ($A_V = 0.64 \pm 0.09$), and GRB 080210 ($A_V = 0.71 \pm 0.15$, though the data are sparse on this event) in the Golden Sample, and GRB 050401 ($A_V = 0.69 \pm 0.02$) and GRB 070208 ($A_V = 0.74 \pm 0.03$) in the Silver Sample, note here that the errors are underestimated due to the spectral slope in the fit not being a variable. Furthermore, evidence for high extinction of an uncommon type is found for GRB 071025, here I just follow Perley et al. (2010). Otherwise, all afterglows show very low extinction (Figure 4.2). The mean extinction value for the 48 GRB afterglows of the Golden Sample is $\overline{A_V} = 0.21 \pm 0.03$ (FWHM 0.24), identical to the pre-*Swift* sample value of $\overline{A_V} = 0.20 \pm 0.04$ (K06, with the additional three GRBs presented here). Similarly, the mean value for the extinction-corrected spectral slope, $\overline{\beta} = 0.66 \pm 0.04$ (FWHM 0.25), is also in decent agreement within errors with the value from K06, $\overline{\beta} = 0.54 \pm 0.05$. The reason for the offset may be due to the higher number of *Swift* GRB afterglows that have SEDs which include NIR data, see Paper I for more details.

For the Silver Sample, I find a strong preference for SMC dust in some cases (e.g., GRB 051109A and GRB 051111), but even for SMC dust, these fits are still not good and formally rejected. Such strongly curved SEDs were also found for some pre-*Swift* GRB afterglows (e.g., GRB 971214, K06). A free fit to such an SED results in very high extinction and a negative spectral slope β. I deduce a mean host extinction which is slightly higher than that

of both my Golden Samples ($\overline{A_V} = 0.32 \pm 0.08$), but note that the derived extinctions depend upon fixed spectral index values derived from theoretical relations only.

One big difference between the *Swift*-era sample and the sample of K06 is that there was only one burst (GRB 000131, Andersen et al. 2000) in the pre-*Swift* sample which had $z \geq 3$ (as GRB 030323 [Vreeswijk et al. 2004] has only been included in the pre-*Swift* sample in this work), while in the present Golden Sample, 27% (13 out of 48) of the GRBs lie at such high redshifts (an additional 36%, five out of 14, in the Silver Sample). Like GRB 000131, almost all these high-z GRBs show very small host extinction (Fig. 4.2). This seems to confirm the initial suspicion in K06 that host extinction declines with higher redshift. Exceptions are GRB 060210 (see above, and Cenko et al. 2009), GRB 071025 (see Perley et al. 2010), GRB 090313 with a moderate extinction of $A_V = 0.34 \pm 0.15$, and possibly GRB 060927, but the result here is unsure. Also, GRB 050401, at $z \approx 3$, clearly shows signs of moderate line-of-sight reddening (see Watson et al. 2006), and an extreme event not included in my sample so far is the $z = 3$ GRB 080607 with $A_V \approx 3$ (D. A. Perley et al., in preparation, Prochaska et al. 2009). To check the significance of this possible result, I used two rank correlation tests, Kendall's τ and Spearman's ρ, on the combined Golden Sample bursts of this work and K06. I find $\tau = -0.34$ and $\rho = -0.42$, both results indicate that while there is a (negative, as expected) correlation, it is only weakly significant at best. To estimate the influence of the errors, I do the same tests on the maximum ($A_V + \Delta A_V$) and minimum possible ($A_V - \Delta A_V$) values. I find $\tau = -0.14... - 0.39$ and $\rho = -0.25... - 0.52$ (with the minimum extinction yielding the lowest rank correlation coefficient, and vice versa). Furthermore, a Kolmogorov-Smirnov (K-S) test on two samples (taken from the Golden Samples only), divided by $z < 2$ and $z > 2$, shows that they are likely to be taken from the same distribution ($P = 0.039$). While this low-extinction result might be expected from several evolutionary factors, such as the metallicity evolution of the universe (Lapi et al. 2008; Li 2008), different dust depletion patterns at high redshift (Savaglio 2006) or the lack of dust-producing AGB stars (Fiore et al. 2007; Stratta et al. 2007c), several biases might be involved (K06; Fiore et al. 2007) and the evidence is thus not conclusive at all. A higher redshift implies that what is oberved in the optical (and measured with a spectrograph) lies further and further into the rest-frame ultraviolet, which is much more affected by dust (especially if it is similar to SMC dust, which is usually found). Therefore, unless rapidly observed, highly extinct high redshift afterglows are much more likely to not be observed successfully spectroscopically, thus excluding them from my sample.

4.3   Results on the rest-frame Light Curves of *Swift*-era GRB Afterglows

4.3.1   Clustering and Bimodality of the Luminosity Distribution in the *Swift*-Era

It was independently found by three groups (K06; Liang & Zhang 2006; Nardini et al. 2006) studying pre-*Swift* afterglows that the magnitude distribution becomes tighter (clusters) compared to the observed distribution if the afterglows are corrected for host-frame extinction and transformed to a common redshift ($z = 1$ was used). Closer study revealed that this

clustering was best described by two populations (a bimodality) which were separated in redshift. Nearby afterglows were, in the mean, less luminous than more distant ones (K06).

In Figure 4.3 I show (analogous to Figure 8 in K06) the light curves of all optical afterglows shifted to $z = 1$. The additional 76 afterglows of the *Swift*-era samples seem to confirm the clustering of intrinsic afterglow luminosities. Only three afterglows, those of XRF 050416A, XRF 060512 and GRB 070419A, are fainter than the one of GRB 040924 at one day, but the difference is only large for XRF 050416A, ≈ 1.3 mag. Furthermore, also only three afterglows exceed the previously brightest one, GRB 021004, these being GRB 090313, GRB 090926A and especially GRB 080129, which is 0.7 mag brighter. This was an extremely peculiar afterglow which exhibited a long plateau phase and multiple rebrightenings (Greiner et al. 2009c), and something similar was seen for GRB 090926A (Cenko et al. 2010; Rau et al. 2010). In K06, a bimodality in the afterglow luminosities was found after dividing the samples into two redshift bins, with $z = 1.4$ as a dividing line. The new afterglows further bolster this finding, with the faintest afterglows at early times (GRB 060729, GRB 060904B, GRB 071122) and at later times (XRF 050416A, XRF 060512, GRB 070419A) all lying at $z \lesssim 1$. A quantitative analysis has lead me to be cautious about this result, though. While I find that the total spread of pre-*Swift* afterglows is indeed reduced (7 to 5.7 mag for those detected at one day), the FWHM of the two samples is identical, though (1.51 vs. 1.54 mag). For the *Swift* era sample, I even find that both the spread (6.9 vs. 7.8 mag) as well as the FWHM (1.48 vs. 1.63 mag) actually *increases*. Only for a complete sample of all afterglows, the range is still reduced (8.9 vs. 7.8 mag) while the FWHM is similar (1.56 vs. 1.61 mag). The effect of the reduced spread is mostly due to a single afterglow, that of the very nearby GRB 030329, whereas the increase in spread in the *Swift*-era data is due to the very faint afterglow of XRF 050416A.

While *Swift* has clearly allowed the detection of observationally fainter afterglows (I find $\overline{R_C} = 20.08 \pm 0.36$ for the pre-*Swift* GRBs, and $\overline{R_C} = 21.30 \pm 0.18$ for the *Swift*-era GRBs), are these afterglows also less luminous? In Figure 4.4, on the left, I show the distribution of afterglow magnitudes measured in the host frame at one day after the GRB assuming a common redshift of $z = 1$ (Table A.3). Evidence for the bimodality is not directly evident. Indeed, several recent works (Melandri et al. 2008; Cenko et al. 2009; Oates et al. 2009), working on small, homogeneous samples derived from single instruments, do not report finding a bimodality. As a whole, the clearer bimodality of the pre-*Swift* sample has disappeared (if one does not do the redshift separation), though see Nardini et al. (2008). Indeed, while the magnitude distribution is not fit very well with a unimodal distribution (both Gaussian or Lorentzian distributions yield χ^2/d.o.f. > 2 for both the *Swift*-era data set as well as the complete data set [see below]), I was also unable to find a bimodal distribution which significantly improved the fit. Thus, working on a larger sample, I find agreement with above-mentioned works, in contrast to the clear bimodality seen by Nardini et al. (2008).

It is also evident that my four samples are not significantly different from each other. K06 found a mean absolute magnitude of $\overline{M_B} = -23.3 \pm 0.4$ for their Golden Sample, to which I now add three further GRBs, and find $\overline{M_B} = -23.44 \pm 0.36$ (FWHM 1.59 mag). This value is almost identical to my new Golden Sample, where I find $\overline{M_B} = -23.02 \pm 0.27$ (FWHM 1.82 mag). A K-S test shows that both data sets are consistent with being drawn from the same distribution ($P = 0.78$). The Silver Sample is slightly more luminous on average, with
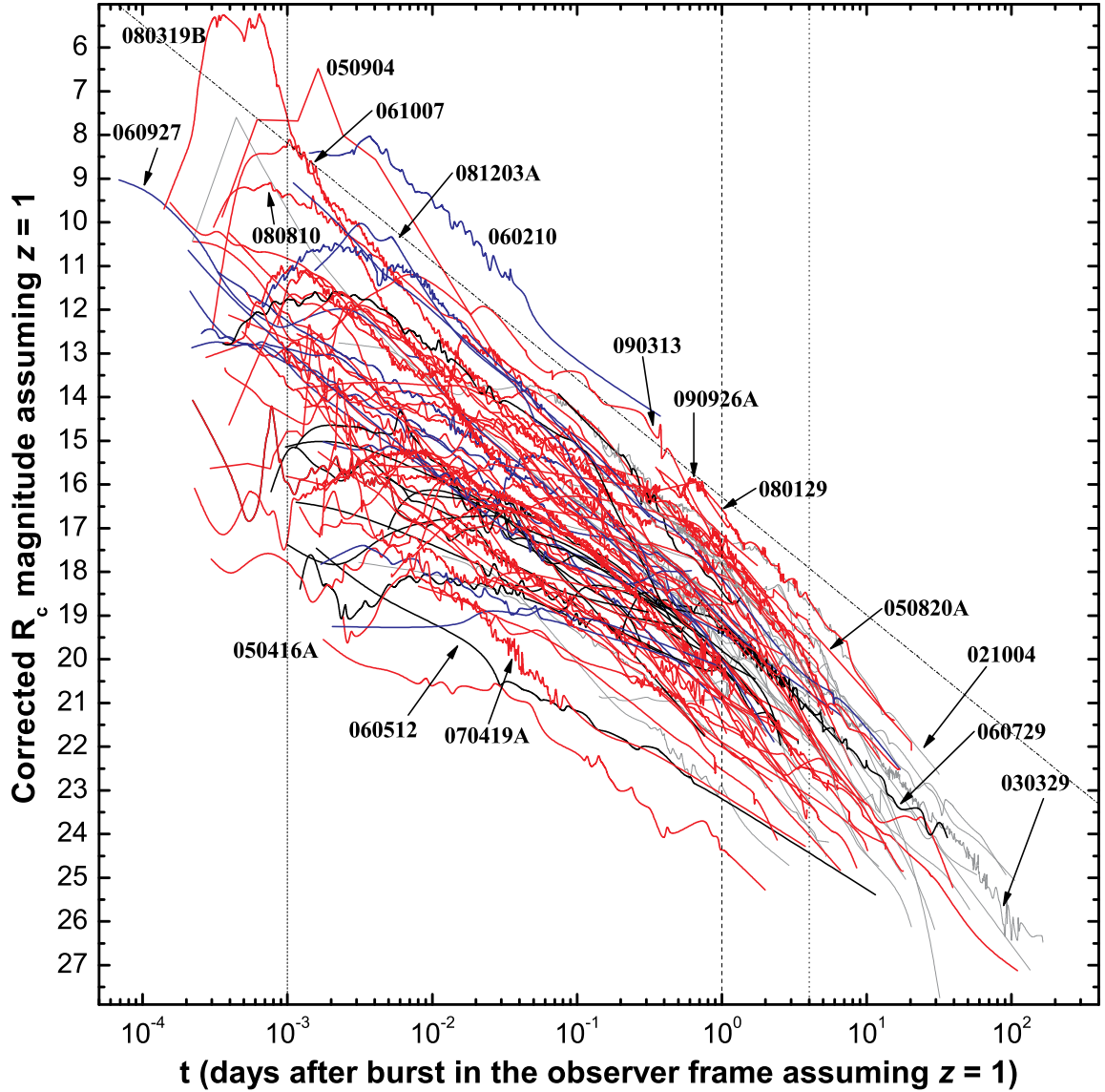
Figure 4.3: *Afterglows of Type II GRBs in the observer frame after transforming them to a common redshift of z = 1. The labeling is identical to Fig. 4.1. The vertical lines denote 10^{-3}, 1 and 4 days, times at which the luminosities were determined. The width of the distribution expands slightly, with XRF 050416A, XRF 060512 and GRB 070419A being fainter than the faintest afterglow of the pre-Swift era, GRB 040924. At very early times, a large spread is visible, as well as several cases of strong variability beyond a simple decay. The brightest bursts at early times are GRBs 080319B, 050904, 061007 and 060210, and several more GRBs exceed 10th mag. The dot-dashed, slanted line (α ≈ 1) indicates what may be an upper ceiling for the afterglow luminosity at later times. Similar to the afterglow of GRB 030329 (K06), the afterglow of GRB 060729 is now seen to be of average luminosity at one day, and quite subluminous at early times. Exceptional afterglows are indicated.*

$\overline{M_B} = -23.69 \pm 0.32$ (FWHM 1.11 mag), whereas the Bronze Sample is slightly less luminous on average, with $\overline{M_B} = -22.53 \pm 0.33$ (FWHM 1.25 mag), respectively. The difference is not statistically significant, though, a K-S test shows that they are taken from the same distribution as the *Swift*-era Golden Sample ($P = 0.15$ and $P = 0.43$ for the Silver and Bronze
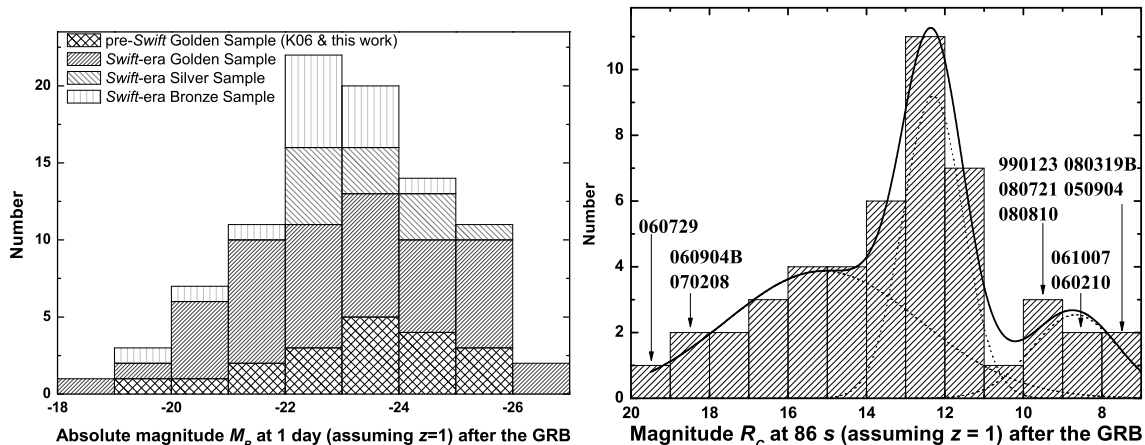
Figure 4.4: Left*: Absolute magnitude of Type II GRB afterglows at one day after the burst assuming* $z = 1$*. The* Swift*-era Type II GRB afterglows in the Golden Sample analyzed in my work (mean magnitude* $\overline{M_B} = -23.02 \pm 0.27$*, FWHM 1.82 mag) are very similar to those of the K06+3 sample (mean magnitude* $\overline{M_B} = -23.44 \pm 0.36$*, FWHM 1.59 mag). The Silver Sample afterglows are identical in luminosity with the pre-*Swift *sample (mean magnitude* $\overline{M_B} = -23.69 \pm 0.32$*, FWHM 1.11 mag). The Bronze Sample afterglows represent the least luminous afterglows (mean magnitude* $\overline{M_B} = -22.53 \pm 0.34$*, FWHM 1.25 mag), and the assumption of a small amount of rest frame extinction makes them as bright as the Golden Sample afterglows.* Right*: Distribution of optical transient magnitudes at 86 seconds* $(10^{-3}$ *days) after the GRB trigger in the observer frame, after shifting all afterglows to* $z = 1$*. While the complete spread is very wide (12 mag), there is a strong clustering around* 13th *mag. These GRB afterglows can be interpreted as those where the forward shock emission dominates already at early times. In some cases, an additional component dominates strongly, making the afterglow even brighter, while many other afterglows suffer from early suppression. The complete distribution is trimodal and well-fit by three overlapping Gaussians. The brightest and faintest afterglows are indicated.*

Samples, respectively). Furthermore, as no extinction correction has been applied to the Bronze Sample, its mean absolute magnitude is a lower limit only (Chapter 4.1.4). Assuming $A_V = 0.3$ for all afterglows of this sample, a value just slightly above the mean extinction of the Golden Samples (Chapter 4.2.2), I find a mean magnitude $\overline{M_B} = -23.45 \pm 0.38$ (FWHM 1.42 mag), identical with to the Golden Samples of both papers. Therefore, a small amount of host extinction is sufficient to explain the slightly fainter mean mag.

As the Golden Samples of K06 and this work can be readily compared, I create one total Golden Sample and split it along the $z = 1.4$ division used by K06. In this case, I find clear evidence for bimodality, it is $\overline{M_B} = -21.89 \pm 0.32$ (FWHM 1.52 mag) for the low-z and $\overline{M_B} = -23.78 \pm 0.23$ (FWHM 1.51 mag) for the high-z sample. The difference is statistically significant, a K-S test shows that they are probably not taken from the same distribution ($P = 2.9 \times 10^{-4}$). Using the *Swift*-era sample only, and dividing it along the $z = 1.4$ line, I find $P = 8.4 \times 10^{-4}$, further strengthening the result. Non-parametric rank correlation tests find further, albeit relatively weak, evidence for the magnitude increase toward higher redshifts; it is Kendall's $\tau = -0.41$ and Spearman's $\rho = -0.53$ for the *Swift*-era-only sample, and Kendall's $\tau = -0.31$ and Spearman's $\rho = -0.51$ for the complete sample, these very similar values also show that mixing the two samples is not problematic.

While *Swift* has increased the recovery rate of afterglows, and also the percentage of

afterglows with successful spectroscopy in follow-up observations, *Swift* GRBs that actually did meet my selection criteria, especially those of the Golden Sample, are quite rare events. These bursts usually not only have a lot of optical follow-up, but are also interesting in such a manner that publications with data on these bursts are preferred over the many others *Swift* has delivered. For example, GRB 050904 held the record for highest redshift ever discovered for a burst for several years, the afterglow of GRB 060206 showed a very powerful rebrightening, that of GRB 060526 showed a complex optical light curve, and GRB 061007, GRB 070125 and especially GRB 080319B were exceptionally bright, both in gamma-rays and in the optical. GRB 050408, one of the observationally faintest afterglows in the new Golden Sample, was very well observable from both hemispheres, leading to a lot of observations. In other words, my Golden Sample contains mostly GRBs that are not typical of the faint *Swift*-era bursts, but more typical of the *Beppo-SAX* era. While the selection criteria of the Silver and especially the Bronze Sample are less stringent, the amount of derived information is also reduced.

Still, it seems clear that for the GRBs in my combined *Swift* sample (i.e., Golden, Silver and Bronze), the larger amount of faint afterglows is an effect based mostly on the increased mean ensemble redshift (Jakobsson et al. 2006b). This is mainly a result of *Swift* BAT's low-energy sensitivity and novel triggering methods, such as image triggers, which find GRBs whose light curves are strongly stretched due to redshift (e.g., Campana et al. 2007b). Another factor is the rapid localization capability of *Swift* combined with rapid ground-based follow-up, which is crucial for long-slit spectroscopy of faint high-z targets. But the need for a spectroscopic redshift and decent light curve coverage is, of course, still a strong restriction for inclusion into my samples (see Fiore et al. 2007, for a discussion on these selection effects). There are afterglows which are clearly strongly extinguished by host extinction, as mentioned in Chapter 4.1.4. In such cases, I would not be able to derive the afterglow luminosity. More highly extinguished or intrinsically faint afterglows very probably can be found among those *Swift* afterglows that did not match my selection criteria, even for the Bronze Sample. Therefore, the question if "dark" GRBs are usually optically undetected due to strong host extinction or intrinsic faintness remains unsolved as yet, though several recent works find evidence for dust attenuation being the main factor (Gehrels et al. 2008; Cenko et al. 2009; Perley et al. 2009a). It therefore remains possible that a population of afterglows would remain that are significantly less luminous than all in my complete sample. In this case, the clustering of afterglow luminosities itself (evidence for which has already been reduced now with my larger sample) may be an observational bias, both due to optical sampling criteria (good multicolor light curves and redshift) and gamma-ray detection criteria, similar to what has been proposed for the existence of high-energy correlations (e.g., Butler et al. 2007b). On the whole, a combination of factors makes the *Swift* afterglow sample less biased than that of the pre-*Swift* era, and thus more representative of the (unknown) true luminosity distribution. That I find only weak evidence for clustering with my less biased sample may indicate that an unknown observational bias has played a role in the pre-*Swift* data.

4.3.2   The Luminosity Distribution at Early Times – Diversity and Clustering

As mentioned before, many of the *Swift*-era GRBs in my sample have afterglows that have been detected at very early times, when they were for the most part still bright. This allows me to derive the luminosity distribution at early times, an exercise that was not possible in the pre-*Swift* era. To do this, I choose 10^{-3} days (86.4 seconds) at $z = 1$, which is equivalent to only 43.2 seconds after the GRB trigger in the rest frame (in several cases, GRB prompt high-energy emission is still ongoing at this time). The sample comprises 48 afterglows, with GRB 990123 being the only burst from the pre-*Swift* era . The distribution is presented in Figure 4.4 on the right. It is, on the one hand, very broad, which was already apparent from Figure 4.3. The total width is 11.5 mag, almost twice as wide as the luminosity distribution at one day. On the other hand, 50% of all afterglows (24 out of 48) cluster within only three mag (a similar tight clustering has been found by Oates et al. 2009 at 100 seconds after the GRB onset in the rest-frame). Eight afterglows (GRBs 080319B, 050904, 061007, 060210, 080810, 080721, 990123 and 080413B) are brighter than this cluster (albeit significantly, in some cases). Most of these are probably dominated by additional emission components at early times (see below), although the unbroken decay from very early times on in the case of GRB 061007 may speak against an additional component (Mundell et al. 2007a; Schady et al. 2007a). GRB 080721 is a similar case (Starling et al. 2009). The strongly clustered afterglows would then be those that are dominated by the forward shock emission already at early times, while the fainter afterglows may suffer from optical supression (Roming et al. 2006a) or a late afterglow onset (e.g. Molinari et al. 2007; Nysewander et al. 2009b). In some cases (e.g., GRB 060729, Grupe et al. 2007), there are also indications that significant long-term energy injection similar to what may cause the shallow decay/plateau phase of the "canonical" X-ray afterglow (Nousek et al. 2006; Zhang et al. 2006; Panaitescu et al. 2006b) occurs, although in most cases the plateau phase in X-rays and the following break to a "classical" afterglow decay is not mirrored in the optical (Panaitescu et al. 2006a). This highlights the possibility that there are afterglows that start at a similar faintness to, e.g., GRB 060729, and then follow a straightforward decay instead of remaining roughly constant. These optical afterglows would be too faint to be included in my sample due to the selection criteria, and might also be much less luminous at 0.5 rest-frame days than the afterglows presented here.

Fitting the complete distribution with a single Gaussian does not yield an acceptable result, it is $\chi^2/\text{d.o.f.} = 1.58$, and, more importantly, the fit finds that a constant $y_0 \approx 2$ has to be added, which is unphysical. Instead, following the idea that three different types of early behavior exist, I am able to fit the distribution with three overlapping Gaussians (see Figure 4.4, right). This yields a significantly improved fit, it is $\chi^2/\text{d.o.f.} = 0.58$, no constant term is needed ($y_0 = 0$), and the three Gaussians are centered at 8.67 ± 0.48 (FWHM 2.20) mag, 12.31 ± 0.09 (FWHM 1.52) mag, and 15.11 ± 1.23 (FWHM 4.95) mag, for the "overluminous", "standard" and "subluminous" types, respectively.

Several caveats apply, however, and the picture is not so simple. In Kann et al. (2007f), I discussed the possibility of different spectral slopes at early times, in application to the prompt optical emission of GRB 050904. I found that assuming achromaticity (and thus the

spectral slope derived from the late-time, forward-shock dominated afterglow), the luminosity of the prompt flash was higher than in the case that spectral slopes more appropriate for early emission were considered (e.g., fast cooling phase, or injection frequency still above the optical band). Therefore, such color evolution may also apply to other afterglows in my early sample, possibly widening the clustering in one photometric band. For some GRBs, early multicolor afterglow data are available, but these yield an inconclusive picture. For example, the prompt optical flare of GRB 061121 (Page et al. 2007) is more pronounced in the *V* band (*Swift* UVOT) than in unfiltered observations (ROTSE). On the other hand, the color evolution of the afterglow of GRB 061126 (Perley et al. 2008a) goes from redder to bluer, similar to the case of the very-well sampled early afterglow of GRB 080319B (Bloom et al. 2009; Racusin et al. 2008; Woźniak et al. 2009). Several other afterglows show no early color changes at all, e.g., those of GRB 060418 and GRB 060607A (Molinari et al. 2007; Nysewander et al. 2009b) and GRB 061007 (Mundell et al. 2007a; Schady et al. 2007a).

Furthermore, several cases in the "cluster" exist where a detailed study has shown additional emission components. An early reverse shock component has been proposed for GRB 050525A (Klotz et al. 2005; Shao & Dai 2005), this is also an interpretation for the early steep decay of GRB 061126 (Perley et al. 2008a) and GRB 060908 (Covino et al. 2010). In the case of GRB 051111, an early steep decay is associated with the tail of the prompt emission (Yost et al. 2007; Butler et al. 2006). Once again, there are counterexamples, e.g. for GRB 060418, early upper limits on the polarization of the optical afterglow point to a weak (or even negligible) reverse shock component (Mundell et al. 2007b; Jin & Fan 2007), in agreement with a dominating forward shock at very early times.

Panaitescu & Vestrand (2008) have presented a study of early afterglow behavior, investigating different classes and finding a possible correlation between peak luminosity and peak time for afterglows with fast rises (which can be both reverse-shock flashes and forward-shock peaks; from their sample, Oates et al. 2009 find the rises are consistent with forward-shock evolution), which they claim might even be used as a redshift indicator. My large sample allows me to further study this possible correlation. In total, I find 72 afterglows (including several more from the pre-*Swift* era) which have either very early detections, or show later peaks. I have gathered these afterglows in Table A.4, where I give the relevant time (peak or earliest detection) and the R_C magnitude in the extinction-corrected $z = 1$ frame (errors are statistical only). Here, I discern between six classes, and indicate additional noteworthy features in the comments to Table A.4:

- **Afterglow peak followed by a fast decay:** These afterglows show a fast rise to a peak, followed by a fast decay ($\alpha \approx 1.5 - 2$), which usually becomes flatter later. This behavior is interpreted as an additional component superposed on the forward-shock afterglow, which, due to its rapid decay, quickly becomes less luminous than the forward-shock afterglow, leading to the steep-to-shallow transition. Often, this component is attributed to a reverse-shock flash, with the classical example being GRB 990123 (Mészáros & Rees 1997; Mészáros & Rees 1999b; Sari & Piran 1999b). In other cases, it is probably tied to optically emissive internal shocks, that is, direct central engine activity, as for GRB 080319B[6] (Racusin et al. 2008; Beskin et al. 2010), GRB

---

[6]Racusin et al. (2008) interpret the intermediately rapid decay in the early light curve of this afterglow as

060526 (Thöne et al. 2010), GRB 061121 (Page et al. 2007), and GRB 080129 (Greiner et al. 2009c), making this a diverse class. These afterglows (or, more correctly, optical transients), are the most luminous among GRB or any other phenomena (Kann et al. 2007f; Bloom et al. 2009). I find seven afterglows (10%) in this category.

- **Initial fast decay:** These afterglows show a similar steep-to-shallow transition as described above, but the observations did not begin until after the peak, implying it must be very early. An example is GRB 090102 (Gendre et al. 2010). To my knowledge, an early steep decay for GRB 090424 is reported by myself for the first time. This category contains six afterglows (8%), and the combined fast decay categories make for 18% of all afterglows, in agreement with Klotz et al. (2009).

- **Afterglow peak followed by a slow decay:** In these cases, after a usually fast rise and a turnover, the decay index is typical for a forward-shock afterglow with constant blastwave energy (aside from the radiative losses, and opposed to a forward shock with energy injection), and there is no further transition between different decay indices. This has been interpreted as the rise of the forward-shock afterglow at deceleration time, with classical examples being GRBs 060418 and 060607A (Molinari et al. 2007; Nysewander et al. 2009b). Panaitescu & Vestrand (2008), from afterglow modeling, also favor this explanation, with a second valid interpretation being non-uniform jets beamed off-axis with respect to the observer. Such an interpretation is favored for late peaks (if the initial Lorentz factor is also a function of angle), as in the case of GRB 080710 (Krühler et al. 2009). Some special cases also exist, like the extreme rebrightening (following a standard forward-shock decay) of GRB 060206, which has been interpreted as an extreme energy injection event (Woźniak et al. 2006; Monfardini et al. 2006). This group contains the most afterglows, 30 (41%).

- **Initial slow decay:** In these cases, the decay index is typical for a forward-shock dominated afterglow, and no peak is seen. All afterglows in my total sample which I do not discuss here would fit into this category, but have been detected at such late times (e.g., almost all afterglows of the pre-*Swift* era) that no real conclusions can be gathered about their early behavior. Intriguingly, some afterglows with very early detections already feature a typical forward-shock decay from the first detection on. While once seen as the most typical behavior, most forward-shock dominated afterglows peak late enough that their peaks are detected in early observations (see above), putting less afterglows in this category, a total of 15 (21%). In total, the early dominance of the forward shock is found to be the most common case, with 45 afterglows (62%).

- **A plateau with a discernible peak mag:** In these cases, a rising-to-decaying transition is seen as well, but the rise and initial decay are very shallow, leading to a plateau phase where the afterglow luminosity barely changes over long times. Such a behavior has often been seen in connection with the spectrally soft X-Ray flashes, and may indicate a jet viewed off-axis (e.g., XRF 080310 and XRF 080330, Guidorzi et al. 2009a analyze the latter in detail). Several special cases are included in this category,

---

a reverse shock flash component that becomes dominant over the very rapidly fading prompt optical emission.
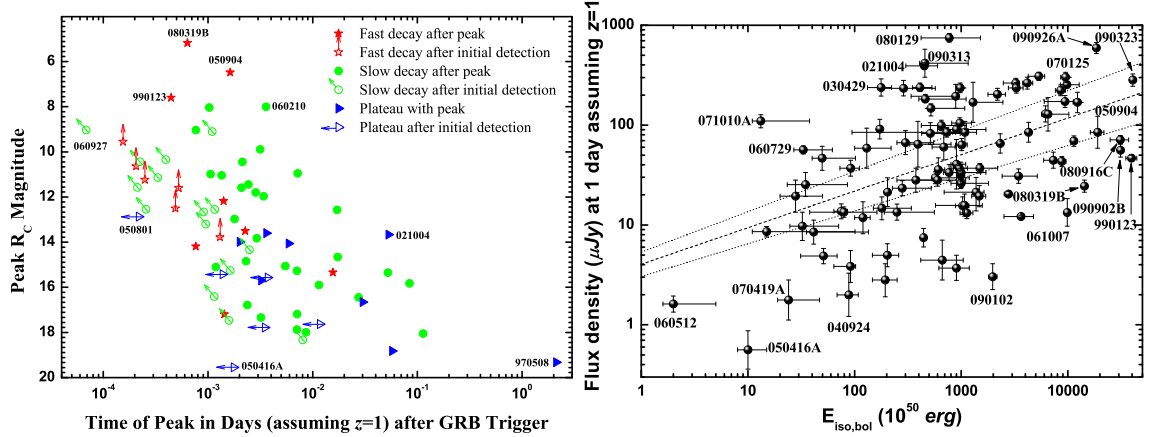
Figure 4.5: Left: *Peak magnitude of 72 afterglows from my samples, as derived from the extinction-corrected $z = 1$ light curves (Fig. 4.3). I discern between six groups: Those with early peaks followed by rapid decays (possibly of reverse-shock origin, filled red stars), those where the peak is before the earliest detection, but the early decay is also steep (empty red stars with upward-pointing arrows), those with early peaks followed by slower decays (probably of forward-shock origin, filled green discs), those where the peak is before the earliest detection, but the early decay is also slower (green rings with slanted arrows), those with early plateau phases which also show magnitude peaks (very slow rise and decay, filled blue triangles), and those where the early decay is very slow, but the peak lies before the first detection (empty blue triangles with left-pointing arrows). While there is clearly an envelope seen, the scatter is very large. Several outstanding events have been labeled. See text for more details on special cases.* Right: *Flux density in the R_C band at one day (in the host frame assuming $z = 1$) plotted against the bolometric isotropic energy of the prompt emission for all GRBs in the optically selected sample which had data at this time. While no tight correlation is visible, there is a trend of increasing optical luminosity with increasing prompt energy release. This is confirmed by a linear fit (in log-log space), using a Monte Carlo analysis to account for the asymmetric errors. The dashed line shows the best fit, while the dotted line marks the 3σ error region. Several special GRBs are marked.*

like GRB 021004, which is dominated by multiple energy injections at early times (de Ugarte Postigo et al. 2005), and the highly peculiar afterglow of GRB 970508, which begins with a very faint plateau followed by a very late, strong rebrightening. This category contains nine afterglows (12%).

- **An early very shallow decay:** Here, the afterglow decays from the first observation onwards, but the decay index is very shallow, less than is expected from a classical forward shock ($\alpha \approx 0 - 0.4$), creating a plateau phase. A classical example of such behavior is GRB 050801 (Rykoff et al. 2006; de Pasquale et al. 2007), and it has also been seen in the highest redshift GRB 090423 (Tanvir et al. 2009). These very slow decays are quite rare, with only six afterglows in the sample showing them (8%).

I show a plot of all 73 data points (GRB 060729 has resulted in two measurements) in Figure 4.5 on the left, discerning between the six classes. Clearly, an envelope is seen which traces the correlation found by Panaitescu & Vestrand (2008), but the scatter is much larger than what they find in their small sample, indicating that the significance of the correlation is much smaller than assumed. Applying rank correlation tests, I find Kendall's $\tau = 0.43$, and Spearman's $\rho = 0.62$, indicating the existence of a correlation with only moderate significance.

A similar result was found by Klotz et al. (2009) using observations of the TAROT robotic telescopes. In mag, the width of the scatter is around ten mag even if I only choose those afterglows which exhibit a fast rise (and fast or slow decay). Intriguingly, those afterglows which are already decaying at first detection cluster more strongly than those with detected peaks (especially those with rapid decays), on the left hand side of the correlation, indicating an extension in this direction and even larger scatter, were the optical follow-up to be even more rapid. All afterglows not included in my sample of 72 (most of the pre-*Swift* afterglows) would be found in the lower right hand corner, usually beyond 0.1 days and fainter than 16th mag.

4.3.3   A Correlation between Optical Luminosity and Isotropic Energy

In Figure 4.5, on the right, I show the flux density in the R_C band at one day in the host frame assuming $z = 1$ (Figure 4.3, Table A.3) plotted against the bolometric isotropic energy of the prompt emission (Table 2 of Paper I). This plot is similar to that of Kouveliotou et al. (2004, see also Freedman & Waxman 2001; Liang & Zhang 2006; Amati et al. 2007; Kaneko et al. 2007; Gehrels et al. 2008, and Nakar 2007a; Berger et al. 2007a for Type I GRBs), who used the X-ray luminosity at 10 hours (for a detailed discussion, see Granot et al. 2006; Fan & Piran 2006), as well as Nysewander et al. (2009a), who also studied the $R-$band luminosity (as well as the X-ray luminosity) at 11 hours. Similar to the correlations found by the aforementioned authors, a trend is visible in Figure 4.5: The optical luminosity increases with increasing prompt energy release. But the scatter is very large, especially in contrast to the often very well constrained flux densities (i.e., the offset from the best fit in units of the individual flux density errors σ_F is much larger than one in many cases, $\frac{|F - F_{Fit}|}{\sigma_F} \gg 1$, with F_{Fit} being the flux density expected from the correlation). This can be clearly seen both in flux density and in isotropic energy. GRB 061007 and GRB 070125 have almost identical isotropic energy releases, but the flux densities of their optical afterglows differ by a factor of 23^{+12}_{-8}. The span between GRB 080129 and GRB 050502A is even larger, over two orders of mag. GRB 990123 has an isotropic energy release roughly 1000 times higher than GRB 060729, but its optical afterglow has a slightly fainter luminosity at one day. The trend is almost non-existent except for three faint bursts: XRF 060512, XRF 050416A and GRB 070419A have been mentioned in Chapter 4.3.1, and here it can be seen that these events are also sub-energetic in their prompt emission. The faintest optical afterglow of the K06 sample, GRB 040924, is seen to be among the least energetic GRBs too, but it is still part of the "cloud". In log-log space, a linear fit is used, accounting for the asymmetric error bars with a Monte Carlo simulation; and in 30000 runs, the following correlation is found:

$$\frac{F_{\text{opt}} \ (\text{at } t = 1 \text{ day})}{1\mu\text{Jy}} = 10^{(0.607 \pm 0.041)} \times \left(\frac{E_{iso,bol}}{10^{50} \ erg} \right)^{(0.366 \pm 0.013)} . \qquad (4.1)$$

Using an unweighted fit, exactly the same slope and a slightly smaller (though identical within 1σ errors) normalization is found, indicating that the intrinsic scatter dominates over the errors of the data points. I find $\tau = 0.29$ (significance 4.1σ) for the complete data set using Kendall's rank correlation. Therefore, the correlation is only of low significance. As would be expected, removing the three sub-energetic events reduces the significance even

more, it is $\tau = 0.24$ (significance 3.3σ). I conservatively estimate the errors on τ by creating maximally tight and maximally scattered data sets. In the first case, I shift data beneath the best fit closer by $-\delta E_{iso,bol}$ and $+\delta F_{\mathrm{opt}}$, and data above the best fit closer by $+\delta E_{iso,bol}$ and $-\delta F_{\mathrm{opt}}$. In the latter case, the data are shifted away from the correlation in the reverse way. For the maximally tight data set, I find $\tau = 0.44$ (significance 6.1σ) for the complete data set and $\tau = 0.40$ (significance 5.5σ) if I remove the three sub-energetic events. For the maximally scattered data set, the values are $\tau = 0.18$ (significance 2.6σ) and $\tau = 0.13$ (significance 1.8σ), respectively.

Nakar (2007a) and Berger et al. (2007a) argue that as the cooling frequency is usually beneath the X-ray range (but see Zhang et al. 2007b, who find that 30% (9 of 31) of the X-ray afterglows they studied to still have $\nu_c > \nu_X$ at up to ten hours after the GRB), the X-ray luminosity is independent of the circumburst density and it thus represents an acceptable proxy for the kinetic energy, $L_X \propto \epsilon_e E_K$ (with ϵ_e being the fraction of energy in relativistic electrons). Clearly this is not the case here, as the cooling break lies above the optical bands in most cases (e.g, K06; Panaitescu et al. 2006b,a; Starling et al. 2007; Schady et al. 2007b; Curran et al. 2010). Therefore, the strong spread in optical luminosities may be explained by the effect of the spread in the circumburst density, which, while typically lying at $1-10 \ \mathrm{cm}^{-3}$ (cf. Friedman & Bloom 2005b), can reach several hundred cm^{-3}, e.g. in the case of GRB 050904 (Frail et al. 2006) or GRB 060526 (Thöne et al. 2010). Still, the existence of this trend is intriguing, and further observations will hopefully reveal more subluminous GRBs. A second possibility is to discuss the addition of Type I GRBs, which brings me to the next Chapter.

Chapter 5

The Afterglows of Type I GRBs

In the previous Chapter, I compared the optical afterglows of an older pre-*Swift*-era sample (K06) with those I have gathered during the *Swift* era. One of the pertinent results was that the two samples do not differ strongly in their intrinsic properties. I will use this to combine them into a large Type II GRB afterglow sample, and compare them with the optical afterglows of Type I GRBs in this Chapter. Studies of moderately large samples of Type II GRB afterglows were done before K06, my first study, e.g., Stratta et al. (2004), and next to the study I present in this work (which still remains the largest from the data up" study so far), multiple other authors have also studied different samples of Type II GRB afterglows as well as their extinction properties (Liang & Zhang 2006; Nardini et al. 2006, 2008; Starling et al. 2007; Melandri et al. 2008; Schady et al. 2007b, 2010; Oates et al. 2009; Cenko et al. 2009). The study of Type I GRB afterglows I present in the following Chapter, though, was completely unique at the time it was first made public (2008 April, before that, only a preliminary study had been done myself on a very small sample within our study of GRB 050813 Ferrero et al. 2007). In the following months, two other studies came out (Gehrels et al. 2008; Nysewander et al. 2009a) which present similar results to what I find in Chapter 5.3.3, though I will also comment on how my study differs from theirs, and where my results are superior.

5.1   The Light Curves of Type I GRB Afterglows

As for the Type II GRB afterglow sample, data was mostly derived from the literature (publications as well as GCN circulars), with some additional data published in Paper II for the first time (Chapter 3.3.2). This sample takes into account events up to 2009 December. The selection criteria to separate the two samples have been described in Chapter 3.3.1. Sources of photometry as well as specific information of all the GRBs of the Sample is given in Appendix B of Paper II, there, I also list additional Type I GRBs (or Type I GRB candidates) which were not included in my sample, usually because the data situation even in terms of upper limits was too sparse to work with. All in all, my sample comprises 37 GRBs, and I will now delineate which additional procedures had to be undertaken to work with this data. As with the Type II GRB afterglow sample, I have derived the energetics of the Type I GRB sample, these values, together with the host galaxy offsets, if such could be determined, are given in Table 2 of Paper II.

In many cases (16 of 37, 43%), no optical afterglows were discovered, so that only upper limits are available, either ground-based or by *Swift* UVOT. In order to maximize the available light curve information for my study, I transformed the data of all filters to the R_C band (after correcting for the individual foreground extinction for each GRB and each filter, Schlegel et al. 1998) by making the following assumptions: First, I assume that the intrinsic spectral slope of the optical/NIR afterglow of each GRB is $\beta = 0.6$, unless the data were sufficient to measure it. In the standard fireball model[1], if the cooling frequency ν_c lies blueward of the optical bands, it is $\beta = (p-1)/2$ (e.g., Sari et al. 1998; Zhang & Mészáros 2004; Piran 2005, and references therein), with the canonical value $p = 2.2$ (Kirk et al. 2000; Achterberg et al. 2001), implying $\beta = 0.6$. Observations of Type II GRB afterglows show that this situation has the highest probability (K06), and the mean and median values of the complete sample of Paper I are close to 0.6. As I have already pointed out, it has been shown that p is not universal (K06, Shen et al. 2006; Starling et al. 2008), and that ν_c can also lie redward of the optical bands (e.g., the case of GRB 060505, Xu et al. 2009), this assumption should be valid in the majority of cases. The influence of a different spectral slope on the shift dRc is dependent on redshift, e.g., for $z = 0.2$, $\Delta dRc = 0.3$ mag between $\beta = 0.5$ and $\beta = 1.1$, for $z = 0.8$, it is only $\Delta dRc = 0.07$ mag. For the luminosity distribution, these small differences are not critical. The second assumption is that the observed SED is unaffected by wavelength-dependent extinction through dust in the GRB host galaxies. As merger-induced events are typically expected to occur far from star-forming regions (but see, e.g., Belczynski et al. 2006, 2007; Dewi et al. 2006; van den Heuvel 2007; D'Avanzo et al. 2009), this assumption is reasonable[2]. In those cases where no afterglow has been detected and I only have upper limits, I choose successively deeper limits, as the afterglows are not expected to rebrighten significantly and follow a typical monotonic decay (see Figure 5.1).

Many Type I GRBs do not have measured redshifts. So far, no absorption spectroscopy of a Type I GRB afterglow has been successful (see Chapter 2.3), so that redshifts can only be determined from host galaxy spectroscopy. In some cases, no galaxies (or only extremely faint ones) are found in the *Swift* XRT or optical afterglow error circles (e.g., Piranomonte

---

[1]While Type I GRBs clearly derive from a different type of progenitor as Type II GRBs, most of the physics behind the GRB and the afterglow are expected to be identical (Nakar 2007a; Nakar & Granot 2007; Nysewander et al. 2009a), i.e., a hyperaccreting accretion torus around a black hole which powers an ultrarelativistic fireball that propagates into the external medium (Eichler et al. 2009; Lazzati et al. 2010). The viability of both neutron star-neutron star and neutron star-black hole mergers to create Type I GRBs has been shown in numerical simulations (e.g., Rosswog et al. 2003; Aloy et al. 2005; Rosswog 2005; Oechslin & Janka 2006; Lee et al. 2010), though BH-NS mergers may account only for small numbers of Type I GRBs (Belczynski et al. 2008; O'Shaughnessy et al. 2008).

[2]I need to point out several notes of caution, however. At least one Type I GRB afterglow SED, that of GRB 050709, seems to show line-of-sight extinction even though the GRB is located in the outskirts of its host galaxy (Ferrero et al. 2007). While Gehrels et al. (2008) did not find any dark Type I GRBs, Zheng et al. (2009) show that the highly reddened afterglow of GRB 070809 (Perley et al. 2007b) is dark, and also suspect this could be the case for GRB 070724A, which was later confirmed by the discovery of the very red afterglow of this event by Berger et al. (2009). I find that extinction along the line of sight to these two GRBs, if it is the source of the steep spectral slope, must be high ($A_V \approx 0.9 - 1.5$). Therefore, there must be cases where Type I GRB progenitors are surrounded by significant local extinction. Discerning such cases when no optical afterglows are detected and even the X-ray afterglows can be extremely faint is difficult, though, therefore I assume no extinction along the line of sight, as for the Bronze Sample GRBs of the Type II GRB afterglow sample (Chapter 4.1.4)

et al. 2008; Perley et al. 2009b; Fong et al. 2010; Rowlinson et al. 2010a; Berger 2010), and the GRBs are instead assumed to be associated with bright nearby galaxies, such as in the case of GRB 050509B (localized in the outskirts of a bright elliptical galaxy which itself is part of a cluster, Gehrels et al. 2005), GRB 060502B (Bloom et al. 2007), GRB 061201 (Stratta et al. 2007b) and GRB 070809 (Perley et al. 2008b; Berger 2010), or galaxy clusters, as for GRB 050813 (Prochaska et al. 2006a; Ferrero et al. 2007), GRB 050911 (Berger et al. 2007c), and GRB 090515 (Berger 2010). Finally, if no association can be made at all, I choose a redshift $z = 0.5$, which is the (rounded) median value of all measured redshifts which I consider secure (see also Nysewander et al. 2009a). In four cases (GRB 051227, GRB 060313, GRB 070707 and GRB 080503), I choose $z = 1$ instead, as the host galaxies of these GRBs (localized to subarcsecond precision through their optical afterglows) are exceedingly faint ($R \gtrsim 26$, D'Avanzo et al. 2009; Roming et al. 2006b; Fong et al. 2010; Piranomonte et al. 2008; Perley et al. 2009b). While there is evidence that these GRBs do not lie much beyond $z = 1$ (e.g., the detection of the afterglow of GRB 060313 in all UVOT filters, Roming et al. 2006b), they may lie significantly closer, with their host galaxies lying at the faint end of an as yet unknown luminosity distribution (usually, though, the host galaxies of Type I GRBs are typical for field galaxies, Berger 2009). The effect of an unknown redshift on the shift dRc is stronger than that of an unknown spectral slope. Compared with the true but unknown values for the needed parameters, the magnitudes or upper limits of some GRBs may be fainter or brighter. The effect is stronger for low redshifts, for $z = 0.2$ in comparison to $z = 0.5$, it is $\Delta dRc = 2.1$, for $z = 0.8$ in comparison to $z = 0.5$, it is $\Delta dRc = 1.1$. Still, in a statistical sense, the effect will not be strong as it is expected that the true redshifts of the GRBs to be distributed relatively evenly around $z = 0.5$.

5.2   Results on the observed Type I GRB Afterglows

The light curves of the afterglows of my Type I GRB sample are presented in comparison with the pre-*Swift* and *Swift*-era Type II GRB afterglow light curves (K06, Chapter 4) in Figure 5.1. Upper limits are marked with downward pointing triangles connected by thin straight dashed lines, while detections are squares connected with thicker splines. All the afterglow data have been corrected for Galactic extinction (which is often small) and in some cases, the contribution of the host galaxy was subtracted. I label only a few special afterglows. It is visible immediately that observationally, the optical afterglows of Type I GRBs are typically much fainter than those of Type II GRBs (see also Gehrels et al. 2008; Nysewander et al. 2009a). Many optical afterglows are not detected at all, to upper limits that would have clearly detected almost all Type II GRB afterglows in my sample (again, I must caution that this sample is biased, there are upper limits on dark Type II GRB afterglows which are similarly deep as the limits shown here on Type I GRB afterglows). This is especially the case for early times (< 0.01 days), where only a few Type II GRB afterglows (e.g. GRB 050820A, XRF 050416A, GRB 070110, GRB 070419A) are fainter than most limits.

The most constraining upper limits at early times are on GRB 050509B, which was observed rapidly by ROTSE (Rykoff et al. 2005) and RAPTOR (Woźniak et al. 2005), an upper limit of $R_C > 18.75$ is found after just 30 s. Furthermore, Bloom et al. (2006) give an upper limit $R_C > 24.4$ at only 0.09 days after the GRB, over 1 mag deeper than needed
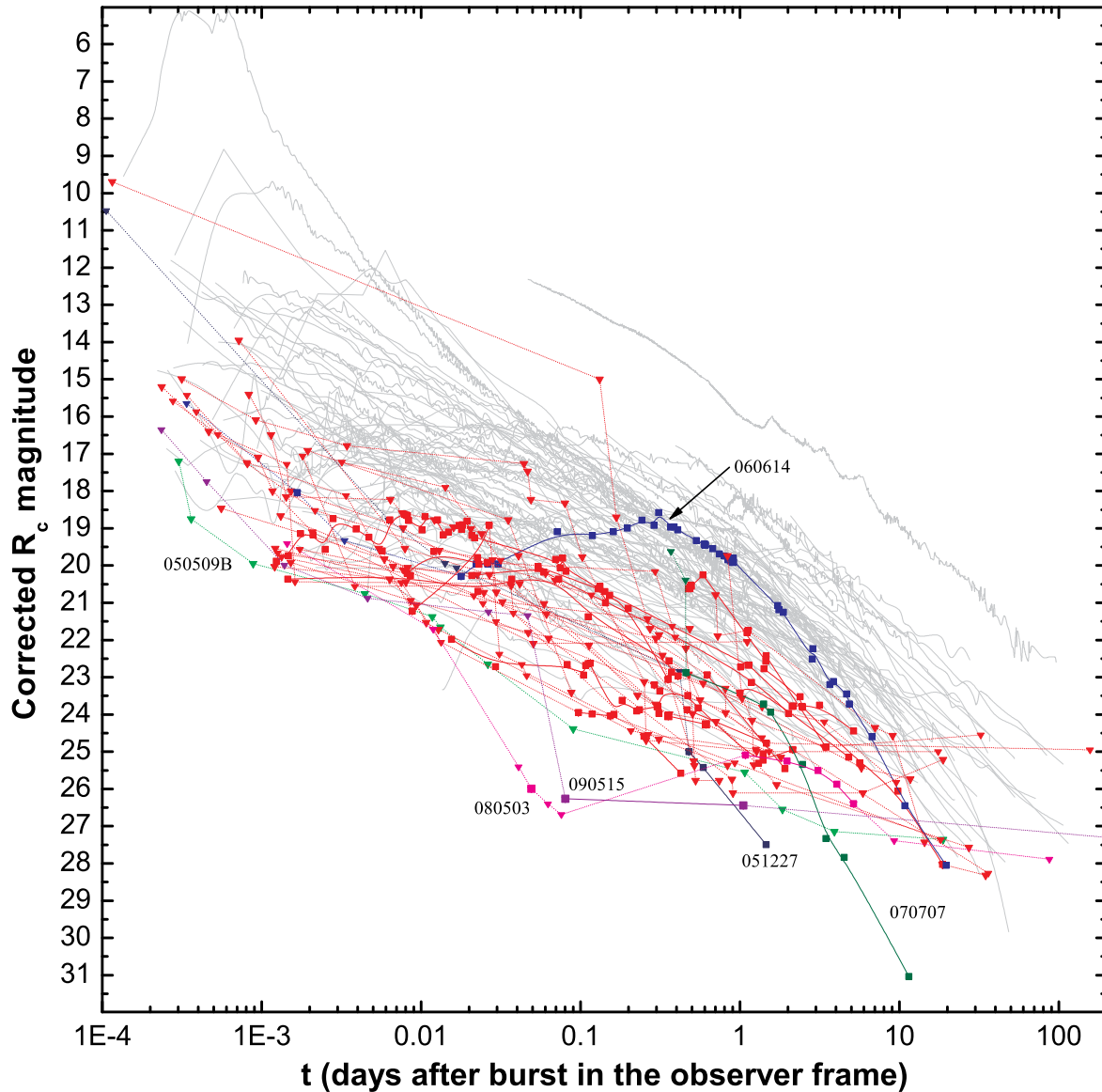
Figure 5.1: *Afterglows of Type I and Type II GRBs in the observer frame. All data have been corrected for Galactic extinction and, where possible, the contribution of the host galaxy has been subtracted. Thin gray lines are Type II GRB afterglows. Red lines with data points are upper limits (straight lines, downward pointing triangles) or detections (splines, squares) of Type I GRB afterglows. It is already clear from this figure that Type I GRB afterglows are fainter than Type II GRB afterglows, as most of the upper limits would have easily detected all Type II GRB afterglows presented here. The single detected Type I GRB afterglow that is comparable in brightness to the Type II GRB afterglow sample is that of GRB 060614. Several other exceptional GRB afterglows (or limits thereon) mentioned in the text are highlighted in color and labeled.*

to detect any Type II GRB in my sample (note that the two faintest GRBs at this time are GRB 080913, which was at an extremely high redshift, and GRB 070802, which was highly extincted). At about 0.05 days after the GRB, one GRB, 080503, sticks out, with both upper limits and a single detection at ≈ 26th mag, these are the deepest early detections and non-detections achieved for an afterglow so far (Perley et al. 2009b). At ≈ 0.1 days, the afterglow

of GRB 090515 is also found to be exceedingly faint (Rowlinson et al. 2010a). In both cases, detections were achieved only due to the combination of 8 m-class telescopes and excellent observing conditions. The faintest Type I afterglow in my sample around one day is that of GRB 051227, discovered by the VLT (D'Avanzo et al. 2009) and seen to decay very rapidly, possibly due to post-jet-break decay (Berger et al. 2007a; D'Avanzo et al. 2009). At later times, another extremely faint and rapidly decaying afterglow is that of GRB 070707, which also had a very faint host galaxy which has been subtracted here (Piranomonte et al. 2008). The only afterglow of a Type I GRB (and a controversial one at that) that is comparable to the typical Type II GRB afterglows is that of GRB 060614 (Della Valle et al. 2006; Fynbo et al. 2006b; Gal-Yam et al. 2006; Mangano et al. 2007; Xu et al. 2009). This afterglow starts out faint but rises to a peak at about 0.25 days (Gal-Yam et al. 2006), followed by a typical afterglow decay that includes a jet break (Mangano et al. 2007; Xu et al. 2009).

5.3   Results on the rest-frame Type I GRB Afterglows

5.3.1   The Luminosity Distribution of Type I GRB Afterglows

After shifting all afterglows to $z = 1$, I am now able to compare the afterglows of Type I and Type II GRBs. The results are shown in Figure 5.2, the labeling is identical to that in Figure 5.1. Several afterglows (partly different ones from Figure 5.1) have been highlighted with color. Magnitude shifts dRc and absolute magnitudes M_B at one day after the burst are given in Table A.5. It is immediately apparent that the afterglows of Type I GRBs spread even further apart, whereas the distribution of Type II GRB afterglows retains about the same width (Chapter 4.3.1). At 0.1 days, the total span is greater than 11 mag, from GRB 060121 at 17th mag (assuming $z = 4.6$, de Ugarte Postigo et al. 2006) to the afterglow of GRB 090515 at $R_C = 28.5$ mag (note that this is a case with insecure redshift, though, but an upper limit on the GRB 050509B afterglow is almost as deep). Assuming $z = 1.7$ for GRB 060121, the spread is about 1.5 mag less. At the same time, the spread of Type II GRB afterglows is about 8 mag, from 13th (the insecure case of GRB 060210) to 21st mag (XRF 050416A), and these afterglows tend to cluster even more strongly at later times. The variance of the complete Type II GRB afterglow sample of Paper I at one day is 3.1 mag, whereas the variance of the Type I GRB afterglow detections is 7.4 mag (4.2 mag without GRB 060121), that of the upper limits 4.4 mag. For the complete Type I GRB afterglow sample (detections and upper limits, but without GRB 060121), the variance is at least 4.1 mag. Furthermore, the Type I GRB afterglows are much fainter than those of Type II GRBs, as has been predicted by Panaitescu et al. (2001). GRB 060121, which probably lies at high redshift and is strongly collimated (de Ugarte Postigo et al. 2006; Levan et al. 2006), is comparable to typical Type II GRB afterglows if $z = 4.6$, and comparable to faint Type II GRB afterglows if $z = 1.7$. The afterglow of the extremely energetic GRB 060313 (Roming et al. 2006b), assuming $z = 1$, is also comparable to the faintest Type II GRB afterglows of the sample, the same is the case for the also extremely energetic *Fermi*-LAT GRB 090510, though it fades rapidly after 0.02 days (De Pasquale et al. 2010; McBreen et al. 2010). At about one day, the afterglow of GRB 060614, by far the brightest observed Type I GRB afterglow, is just slightly brighter than the afterglow of XRF 050416A (the faintest
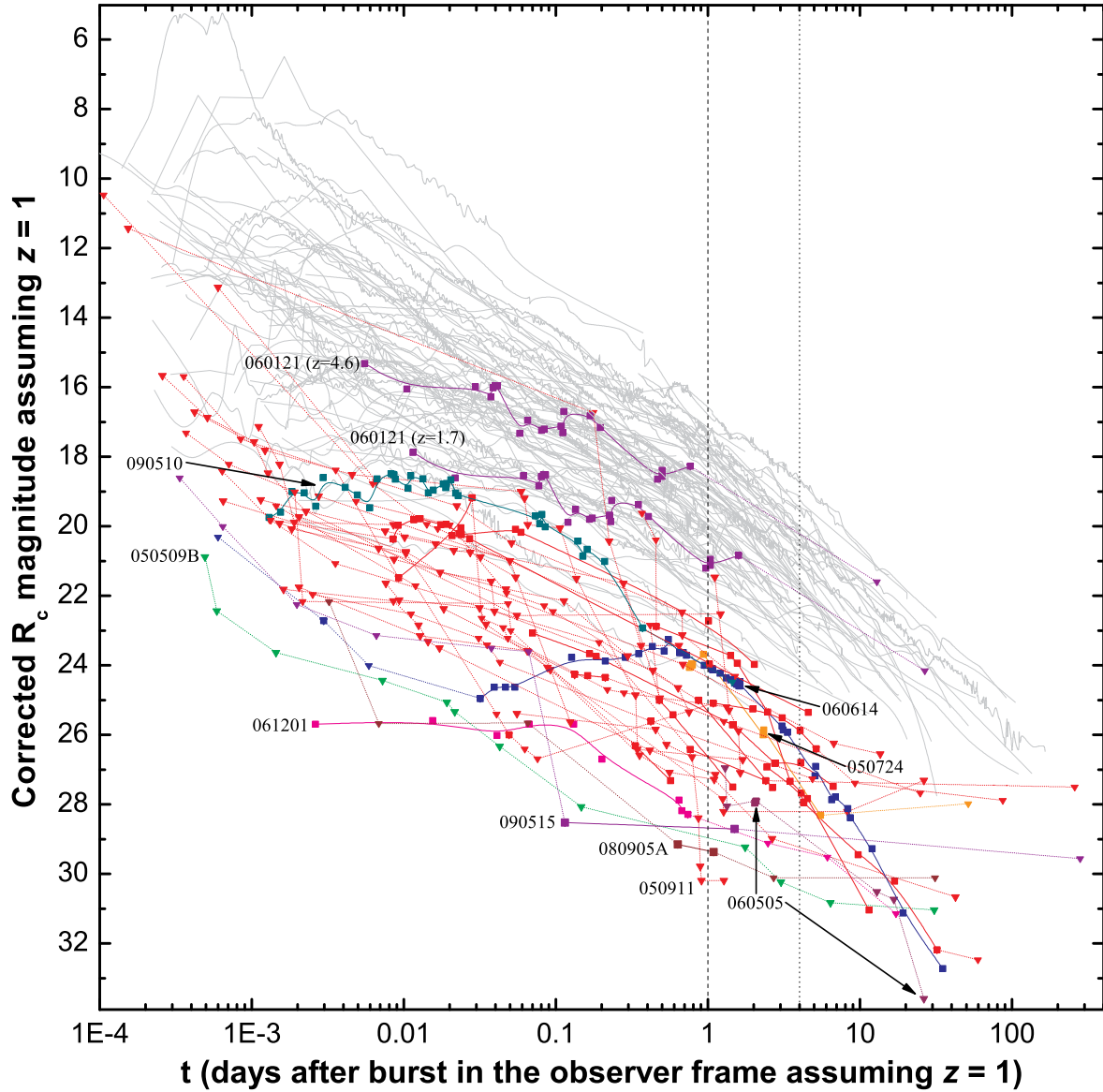
Figure 5.2: *Afterglows of Type I and Type II GRBs in the observer frame after transforming all afterglows to z = 1. With the exception of the afterglow of GRB 060121, which is comparable to bright Type II GRB afterglows for z = 4.6 and faint Type II GRB afterglows for z = 1.7, the afterglows of Type I GRBs, including that of GRB 060614, are fainter than those of Type II GRBs at one day, except for the very faint afterglow of XRF 050416A. At early times, the afterglow of GRB 090510 is also comparable to faint Type II GRB afterglows. The afterglow of GRB 060505, which is a unique, unclear case, is extremely faint. The faintest early afterglow is that of GRB 061201, assuming z = 0.111 (Stratta et al. 2007b). This is about 11 mag fainter than typical Type II GRB afterglows detected at this time. Assuming GRB 060121 to lie at z = 4.6, the total span at 1 day is around 12 mag, otherwise (GRB 060121 lies at z = 1.7), it is around 9 mag, still larger than the span of Type II GRB afterglows.*

Type II GRB afterglow), and then it becomes even fainter rapidly. The late optical flare of GRB 050724 (Malesani et al. 2007) is seen to peak at a similar magnitude. Assuming the association with a galaxy at z = 0.111 (Stratta et al. 2007b; Berger 2010), the afterglow

of GRB 061201 has a magnitude of $R_C \approx 25.5$ just a few minutes after the GRB, which is about 11 mag fainter than the typical early Type II GRB afterglows. The faintest detected afterglow at one day (in the $z = 1$ frame) is that of GRB 080905A (Rowlinson et al. 2010b), at $R_C = 29.3$; the redshift for this GRB is secure. Even fainter are the upper limits (derived in my work) on GRB 050911, if one assumes an association with a galaxy cluster at $z = 0.1646$ (Berger et al. 2007c). The afterglow of GRB 060505, for which it is unclear if it is a Type I GRB (Ofek et al. 2007) or a Type II GRB (Fynbo et al. 2006b; Thöne et al. 2008a; McBreen et al. 2008), is here seen to be about 3 mag fainter than the faintest Type II GRB afterglows, but well comparable to the other Type I GRB afterglows or upper limits thereon. It is thus clearly not a classical Type II GRB, but also not of the subluminous Type II family, such as GRB 980425 (Galama et al. 1998), GRB 031203 (Sazonov et al. 2004; Soderberg et al. 2004b; Malesani et al. 2004) and XRF 060218 (Campana et al. 2006a; Pian et al. 2006; Soderberg et al. 2006b), as these GRBs, while possessing very faint afterglows, were also accompanied by energetic SNe. I will discuss this GRB in more detail below (Chapter 5.3.7). Three afterglows which were seen to be exceptional observationally, namely GRBs 051227, 070707 and 080503, are all not remarkable any more. In all three cases I caution that the redshift is unknown, but I have assumed $z = 1$ due to the fact that all three have very faint host galaxies – and in this case, their exceptional observational faintness is mostly a distance effect (though they are all still much fainter than Type II GRB afterglows).

A histogram of the absolute magnitudes M_B (at one day after the burst assuming $z = 1$) is shown in Figure 5.3. As mentioned, I can "mix" the pre-*Swift* and *Swift*-era Golden Samples, for the combined Golden Sample (for which the extinction corrections are well-defined), I find $\overline{M_B} = -23.14 \pm 0.22$ (FWHM 1.76 mag). The Type I GRB afterglows which are detected are found to be over 5 mag fainter in the mean, it is $\overline{M_B} = -17.61 \pm 0.61$ (FWHM 2.71 mag), thus, about a factor of 160 less luminous than Type II GRB afterglows. If GRB 060121 (for which the high redshift is insecure) is removed, the mean absolute magnitude goes down to $\overline{M_B} = -17.00 \pm 0.48$ (FWHM 2.00 mag), yielding a factor about 290. (Note that in the case of GRB 070429B, there is an afterglow detected at early times, but only an upper limit can be given at one day.) Note that in the sample with detections, there are five GRBs with assumed redshifts (as well as several where the association with a nearby galaxy is not strongly significant, e.g., GRB 061201, GRB 070809, GRB 090515). But four of these, GRBs 051227, 060313, 070707, and 080503 are assumed to lie at $z = 1$ (only GRB 091109B is assumed to lie at $z = 0.5$). Almost all other Type I GRBs with redshifts are closer than this, so it is more likely that the true redshifts of these two GRBs will be $z < 1$ than $z > 1$, making their absolute magnitudes even fainter and the strong bimodality of Type I and Type II GRB afterglows even more secure. For the upper limits, the percentage of GRBs with an estimated redshift ($z = 0.5$ in all cases) is higher, and thus the upper limit on the mean magnitude, which is even lower than the mean magnitude of the detections, $\overline{M_B} \geq -16.94 \pm 0.52$ (FWHM 2.09 mag), is to be taken with caution. Taking all Type II GRB afterglow absolute magnitudes (91 data points) and all Type I GRB afterglow absolute magnitudes (36 data points), including the upper limits, a K-S test shows that the two samples are inconsistent with being drawn from the same distribution with a high significance ($P = 2.5 \times 10^{-17}$). As the basic fundamental principles of afterglow emission are not expected to be different for Type II and Type I GRB afterglows (i.e., both are external forward shock emission from a relativistic fireball, Nakar
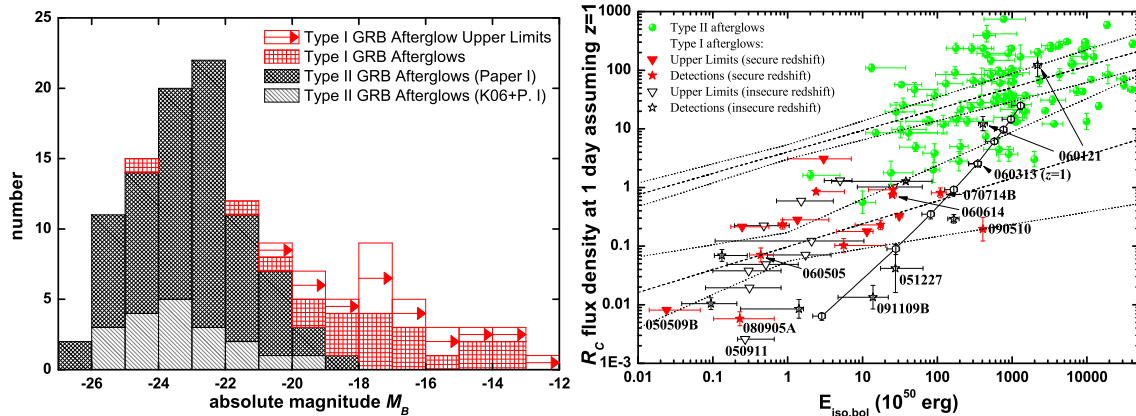
Figure 5.3: Left: *Absolute B-band magnitudes of Type II and Type I GRB afterglows or upper limits thereon. They are measured at one day after the burst in the observer frame after shifting the afterglows to z = 1. The Type I GRB afterglows are typically 5 mag fainter than the Type II GRB afterglows (mean mag $\overline{M_B} = -17.61 \pm 0.61$ versus $\overline{M_B} = -23.14 \pm 0.22$, respectively). The upper limits are even more constraining ($\overline{M_B} = \geq -16.94 \pm 0.52$). Note that some redshifts of the Type I GRB afterglow detection sample are estimates. Right: R_C flux densities of the Type I and Type II GRB afterglows measured in the observer frame at 1 day after shifting the afterglows to z = 1 plotted against the isotropic energy of the GRBs. I differentiate between Type II GRB afterglows (green circles), Type I GRB afterglow detections (stars) and upper limits (triangles). Type I GRBs with redshifts which I consider to be secure have filled red symbols, those with insecure redshifts have black open symbols. There is a clear trend visible. Bursts with higher isotropic energy tend to have more luminous afterglows at a fixed time. I plot two Monte Carlo fits, one to the Type II sample and one to the Type I sample with detections and secure redshifts, as well as their confidence intervals, 3σ for the Type II GRB afterglows and 1σ for the Type I GRB afterglows. Both fits have very similar slopes but a different normalization, indicating different typical circumburst densities. I also illustrate the effect of different redshifts (from z = 0.1, bottom, to z = 2.0, top) for GRB 060313.*

2007a; Nakar & Granot 2007; Nysewander et al. 2009a), the reason for this bimodality must lie elsewhere, as I will discuss below.

5.3.2   Luminosities of Type I GRB versus Type II GRB Afterglows

Several years before the first detection of a Type I GRB afterglow, Panaitescu et al. (2001) predicted that the discovery and follow-up of Type I GRB afterglows would be a big observational challenge. Based on the observational fact that typical Type I GRBs show a fluence more than an order of magnitude smaller than typical Type II GRBs, they predicted that the afterglows should be 10 to 40 times fainter, with radio afterglows hardly detectable and X-ray afterglows giving the best chance for detection. Furthermore, a low density external medium, as might be expected from merger progenitor models (Nakar & Granot 2007, but see Nysewander et al. 2009a), would further complicate the chances for follow-up, as would less collimated jets. Basically, their predictions have been observationally confirmed. I show here, however, that the factor is around 160 (90 to 300), not only 10 to 40. One reason for this discrepancy is that many *Swift*-detected Type I GRBs have up to orders of magnitude less isotropic energy release than the 5×10^{51} erg Panaitescu et al. (2001) used in their modeling (of the GRBs with secure redshifts, only two, namely GRB 070714B and GRB 090510, exceed

this energy, with GRB 051221A coming close, see Table 2 in Paper II). The additional detrimental effects of low density external media (e.g., Panaitescu 2006; Nakar 2007b) and large jet opening angles (e.g., Grupe et al. 2006) have also been shown to play crucial roles. Even very energetic Type I GRBs at redshifts comparable to typical Type II GRBs, such as GRB 060313, and the aforementioned GRB 070714B and GRB 090510, have optical afterglows that are comparable to faint Type II GRB afterglows only. The predictions of Panaitescu et al. (2001) concerning radio and X-ray afterglows have also proven to be correct, as only two Type I GRBs have been detected in the radio (Berger et al. 2005c; Soderberg et al. 2006a), whereas most of those which *Swift* was able to slew to immediately have X-ray afterglows (e.g., Nakar 2007a; Nysewander et al. 2009a).

To access the reason of the faintness of Type I GRB optical afterglows, I employ the standard external shock model (Mészáros & Rees 1997; Sari et al. 1998). For merger-like events, the circumburst medium is expected to have a constant density. With typical parameters, the optical band should satisfy $\nu_m < \nu_{opt} < \nu_c$, where ν_m and ν_c are the minimum injection synchrotron frequency and cooling frequency of relativistic electrons, respectively. The optical afterglow flux density in this regime is (Panaitescu et al. 2001)

$$F_\nu \propto \epsilon_B^{(p+1)/4} \epsilon_e^{p-1} E_{K,iso}^{(p+3)/4} n^{1/2} f_p D_L^{-2}, \tag{5.1}$$

where $f_p \propto [(p-2)/(p-1)]^{(p-1)}$ (Zhang et al. 2007b). Other notations follow the convention of the standard afterglow model: $E_{K,iso}$ is the isotropic kinetic energy of the blastwave, n is the circumburst medium density, ϵ_e and ϵ_B are the fractions of the shock internal energy carried by electrons and magnetic fields, respectively, p is the spectral index of the relativistic electrons, and D_L is the luminosity distance of the burst. The fainter afterglows of Type I GRBs are due to the combination of a lower fluence and a lower energy density as expected for the merger scenarios (Panaitescu et al. 2001; Nysewander et al. 2009a). The derivation of Panaitescu et al. (2001) was based on two assumptions: Type I GRBs have similar radiative efficiency as Type II GRBs, and $E_{K,iso}$ of Type I GRBs is on average 20 times smaller than that of Type II GRBs. With the recent observations of Type I GRBs, it is clear that the first assumption holds, i.e., for a sample of Type I GRBs studied, the radiative efficiency is not very different from that of Type II GRBs (Zhang et al. 2007b; Nakar 2007a; Berger 2007; Nysewander et al. 2009a). However, the second assumption, which was based on the fact that Type I GRBs have a ~ 20 times smaller fluence than Type II GRBs and the implicit assumption that both populations have a similar mean redshift, is no longer justified. Leaving out the $E_{K,iso}/D_L^{-2}$ factor in eq. (5.1) which takes account for the fluence factor discussed by Panaitescu et al. (2001), there is an additional $\propto E_{K,iso}^{(p-1)/4}$ dependence. This accounts for another factor of $100^{0.3} \sim 4$ reduction of Type I GRB flux (assuming a typical value of $p \sim 2.2$) with respect to the estimate of Panaitescu et al. (2001). This is in agreement with the results I present here. In some cases, an even lower density n (to be consistent with the intergalactic medium outside the host galaxy, as expected to happen for some Type I GRBs with large kick velocities) is needed to account for the faintness of the afterglows (Nakar 2007a). Nysewander et al. (2009a), though, have derived results which can be interpreted as that Type I GRBs and Type II GRBs occur in similarly dense environments.

The larger spread of F_ν for Type I GRBs than Type II GRBs is less straightforwardly interpreted. Both types of GRBs should follow the same parameter dependences as shown

in eq.(5.1). One has to argue that the scatter of the parameters is larger for Type I GRBs than Type II GRBs. One factor of F_ν scatter is due to that of $E_{\mathrm{K,iso}}$ (with a dependence of $\propto E_{\mathrm{K,iso}}^{(p+3)/4}$). The possibly high-$z$ GRB 060121 is an example that has a much larger $E_{\mathrm{K,iso}}$ than its low-z brethren. It may be highly collimated (Levan et al. 2006; de Ugarte Postigo et al. 2006), or may not actually be a Type I GRB at all (see Chapter 5.3.7). A second factor that causes the larger scatter of F_ν for Type I GRBs is the circumburst medium n (with a dependence $\propto n^{1/2}$). Since merger events can happen in all types of galaxies and either inside and outside the hosts, as suggested by the data, the ambient density could have a large scatter (but see Nysewander et al. 2009a). While mergers inside star-forming galaxies may have a medium density comparable to that of Type II GRBs, those events outside the hosts (due to large kicks received during the births of one or two neutron stars in the system) could have a tenuous medium, which tends to give rise to a "naked" burst (e.g. La Parola et al. 2006; Perley et al. 2009b). Another possibility that leads to a low density circumburst medium and a large offset without the need for high kick velocities are mergers in globular clusters (Grindlay et al. 2006; Salvaterra et al. 2008, 2010; Guetta & Stella 2009; Berger 2010; Lee et al. 2010), though at least some Type I GRBs show high X-ray column densities and thus cannot reside in globular clusters (D'Avanzo et al. 2009). A more speculative possibility is the scatter of shock parameters. While for Type II GRBs ϵ_B may be mainly determined by the post-shock instabilities that generate the in-situ fields (Medvedev & Loeb 1999), the existence of a pulsar wind bubble before the merger events would introduce a background magnetic field which would be compressed by the shock to power synchrotron emission (for GRBs and pulsar wind nebulae, see Königl & Granot 2002; Guetta & Granot 2004). This extra complication may introduce a larger scatter of ϵ_B and hence F_ν (with a dependence $\propto \epsilon_B^{(p+1)/4}$). But the existence of such a bubble can be ruled out for all but the youngest merging systems, though such young systems may make up a significant fraction of the population (e.g., Belczynski et al. 2006, 2007).

5.3.3   The Bolometric Isotropic Energy versus the Optical Luminosity

My unique sample of Type I and Type II GRB afterglow luminosities allows me to look for correlations between different parameters. By now, there is significant evidence (Amati et al. 2007, 2009b; Piranomonte et al. 2008; Ohno et al. 2008; Krimm et al. 2009; Ghirlanda et al. 2009; Zhang et al. 2009) that Type I GRBs do *not* obey the relationship between the peak energy of the gamma-ray spectrum and the isotropic energy release (the "Amati relation", Amati et al. 2002, though possibly they lie on a parallel relation at an offset to that of the Type II GRBs), while it seems they do obey (Ghirlanda et al. 2009) the relation between the peak energy and the isotropic peak luminosity (the "Yonetoku relation", Yonetoku et al. 2004). Therefore, I have also compiled the energetics of the Type I GRB sample and determined k-corrections and the isotropic energy release (see Chapter 3.2.3 and Table 2 of Paper II). In total, the sample now encompasses 38 Type I GRB events (or 37, as GRB 060121 is included twice at different redshifts) and 95 Type II GRB events.

The plot of bolometric isotropic energy release versus the flux density of the afterglow at one day after the GRB assuming $z = 1$ (converted from Table A.5) is shown in Figure 5.3 on the right, which is an expansion of Figure 4.5 (right). I differentiate between five data

sets. All Type II GRB afterglows have detections and a secure redshift (while a few are photometric, their errors are small). In the case of Type I GRB afterglows, I differentiate between detected afterglows and upper limits, and between secure and insecure redshifts[3]. Clearly, the afterglows of Type I GRBs extend the correlation for Type II GRB afterglows shown in Chapter 4.3.3 (which was significant at the 4.1σ level), and I find a tighter correlation in this case. Using only the Type I GRB afterglow detections with secure redshifts, I find $\tau = 0.42$ and $\rho = 0.64$. Due to the much lower number of data points, the significance is still very low, though, only 1.7σ. I also derive maximally tight and maximally scattered data sets (see Chapter 4.3.3 for more details), and find $\tau = 0.47$, $\rho = 0.76$, and $\tau = 0.29$, $\rho = 0.56$ for the maximally tight and maximally scattered data sets, respectively. The significances are not overly different this time, 1.9σ, and 1.2σ, respectively.

Two further teams presented similar results to mine after I had initially submitted Paper II, Gehrels et al. (2008) and Nysewander et al. (2009a). Both added X-ray data to their studies. The sample of Gehrels et al. (2008) is *Swift*-era only and smaller than my total sample, whereas Nysewander et al. (2009a) use a Type I GRB sample very similar to mine, but a much larger Type II GRB sample which also includes upper limits. In comparison to my study, both neither perform extinction correction of the afterglows in the source frame (which would not be possible in many cases anyway), nor do they derive the bolometric isotropic energy release, especially the latter may influence their results.

At first glance, the Type I and Type II samples seem to form a homogeneous sample, with the brightest and most powerful Type I GRBs (e.g., GRB 060121, GRB 060313, GRB 070714B) overlapping with the faintest Type II GRBs (e.g., XRF 060512, XRF 050416A, GRB 070419A, see Chapter 4.3.3). One exception is the most energetic (of those with secure redshifts) of all Type I GRBs, GRB 090510, which lies a whole order of magnitude under the faintest Type II GRBs of comparable energy. Again, I use a Monte Carlo method (30,000 runs each) to fit the Type I GRB afterglows with detections and secure redshifts while accounting for the two-dimensional asymmetric error bars. Analog to the fit presented in Chapter 4.3.3, I find the following correlation:

$$\frac{F_{\mathrm{opt}} \ (\text{at } t = 1 \text{ day})}{1\mu\mathrm{Jy}} = 10^{(-1.011\pm0.242)} \times \left(\frac{E_{iso,bol}}{10^{50} \ erg}\right)^{(0.390\pm0.182)}. \qquad (5.2)$$

This shows that while the slope is similar (0.37 and 0.39 for Type II and Type I afterglows, respectively), the normalization is different. At 10^{50} erg, the difference in flux density is a factor 41^{+55}_{-24}; and 39^{+112}_{-29} at 10^{51} erg, where the two data clouds overlap.

As discussed before, assuming the radiative efficiencies and blastwave physics to be similar

---

[3]Admittedly, the dividing line between "secure" and "insecure" is something of a personal choice. Type I GRBs with optical afterglows, i.e., that have subarcsecond localizations, which are found in or near the light of a galaxy with a spectroscopic redshift are generally considered secure (e.g., GRB 050709, GRB 050724, GRB 051221A, GRB 061006, GRB 070429B, GRB 070714B, GRB 071227, GRB 080905A, GRB 090510). I also consider GRBs with only X-ray positions, but a bright (i.e., the brightest within a large radius) galaxy in or close to the error circle to be secure (e.g., GRB 050509B, GRB 060801, GRB 061210, GRB 061217). I do not consider secure associations where several galaxies lie nearby with similar chance probabilities, even if there is a subarcsecond afterglow position (e.g., GRB 070809, GRB 090515, see Berger 2010), or there is only a position far away from a large galaxy (e.g., GRB 060502B, GRB 061201), or there is just a possible cluster association (e.g., GRB 050813, GRB 050906, GRB 050911).

for both central engine types (also, the jet opening angle distribution needs to be similar, it is as yet unclear if this is the case), this is an indication that the typical circumburst density around Type I GRB progenitors is lower than for collapsar-induced GRBs. As the normalization difference is $\propto n^{1/2}$, this implies that the typical ambient density around Type I GRB progenitors is roughly a factor of ≈ 1700 less, albeit with very large error margins (in the range of 300 to 10000). This result is markedly in contrast to that of Nysewander et al. (2009a), they perform a very similar fit and find that the normalization for the Type I and Type II GRBs is extremely similar, the afterglow luminosities scale almost exclusively with the prompt energy release. If I assume all afterglows (Type II and Type I detection with secure redshift) to be one population, I derive $\tau = 0.41$ (significance 6.0σ), $\rho = 0.58$, significantly higher than for the Type II GRBs alone. As pointed out above, Nysewander et al. (2009a) do not use bolometric energy releases. Since Type I GRBs typically have harder spectra and higher peak energies (Barat & Lestrade 2007; Ghirlanda et al. 2009; Nava et al. 2010), their bolometric corrections would be higher, moving them further to the right in the plot in comparison to their position as derived by Nysewander et al. (2009a). On the other hand, a correction for line-of-sight extinction, which Nysewander et al. (2009a) also do not perform, moves data points up in the plot, partly canceling the aforementioned effect (but typically, this correction will be more significant for the Type II GRB afterglow sample, moving it away from the Type I GRB afterglow sample). Furthermore, Nysewander et al. (2009a) show that the optical-to-X-ray flux ratios also point to a similar circumburst density for both types of GRB. Though again, one must be cautious, as these will be influenced by a correction for extinction. Any extinction correction will increase the optical-to-X-ray flux ratio, and this effect may again be stronger for Type II GRBs. On the other hand, most Type II GRBs from the sample of Paper I exhibit only low line-of-sight extinction, so the effect cannot be too strong. Finally, a spread of efficiencies is also possible (for a detailed analysis, see Zhang et al. 2007b), which may also induce the large scatter in the Type II sample. Note that since many Type I GRBs only have upper limits on the optical luminosity, the reduced scatter that seems to be visible in Figure 5.3 is probably not real (indeed, GRB 080905A already represents a strong outlier).

I also research the effect of an unknown redshift. Here, I use GRB 060313 as an example, since it has a well-determined prompt emission spectrum and a well-observed afterglow too. I determine the isotropic bolometric energy release assuming the GRB actually lies at $z = 0.1, 0.3, 0.5, 0.7, 1.0, 1.3, 1.5, 1.7$, and 2.0, as well as the magnitude shift dRc for these redshifts (ignoring the fact that UVOT detections in all bands imply $z \lesssim 1.3$, Roming et al. 2006b), and then use the shifted light curve to determine the flux density at 1 day assuming $z = 1$. The results are shown as data points connected by a spline. They rise more rapidly than the slope of the correlations, implying that an unknown redshift will have a significant effect on the scatter and on the fit results if one were to add these additional GRBs.

5.3.4   The Optical Luminosity versus the Host Galaxy Offset

In the case of Type II GRBs, it has been shown that they occur almost exclusively at small offsets from their host galaxies (Bloom et al. 2002), and that their locations usually mark the brightest pixels in the host-light distribution, pointing to their origin in star-forming
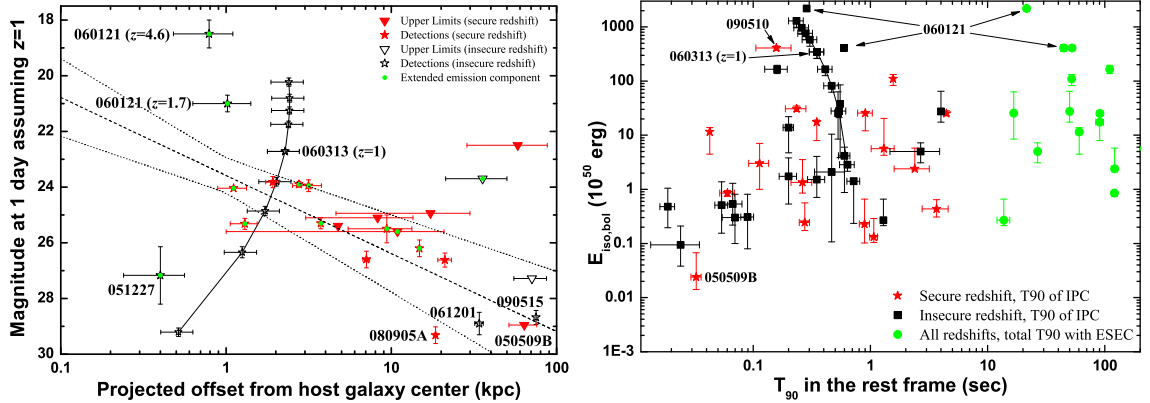
Figure 5.4: Left*: Magnitude of the Type I GRB afterglows measured in the observer frame at one day after shifting the afterglows to z = 1 plotted against the offset to the (assumed) host galaxy of the GRB. The labeling is identical to Figure 5.3. For the Type I GRB afterglow detections with secure redshifts, I find a correlation between the two quantities, which could be expected, since larger offsets typically imply lower circumburst densities and thus lower afterglow luminosities. The upper limits with secure redshifts are also in agreement with the correlation. But there are strong outliers (with uncertain redshifts) such as GRB 051227 or the high redshift solution of GRB 060121. Again, I illustrate the effect of different redshifts (from z = 0.1, bottom, to z = 2.0, top) for GRB 060313. Clearly, an uncertain redshift has a strong effect on the scatter of the correlation. GRBs with green dots are those with an extended emission component. While most of these are found at small offsets, as claimed by Troja et al. (2008), there are several at much larger offsets, and, conversely, several GRBs without an ESEC at small offsets. Right*: Bolometric isotropic energy of Type I GRBs plotted against the T_{90} of the Type I GRBs. I differentiate between the duration of the Initial Pulse Complex (IPC) and the total duration in those cases where an Extended Soft Emission Complex (ESEC) exists (green circles). For the IPC T_{90}, I furthermore differentiate between those GRBs with a redshift which I consider secure (red stars) and with an insecure redshift (black squares). While there is a trend visible, where longer GRBs have higher isotropic energies, it is not statistically significant. Once more, I illustrate the effect of different redshifts (from z = 0.1, bottom, to z = 2.0, top) for GRB 060313. Again, an uncertain redshift has a strong effect on the scatter of a possible correlation.

regions (Fruchter et al. 2006). Right from the first Type I GRB localization, it was clear that this paradigm would not hold for this class of GRBs, as GRB 050509B was localized to the outskirts of its host galaxy (Gehrels et al. 2005). While some Type I GRBs lie at small offsets, within their host light, which may point to low kick velocities or fast merger channels (Graham et al. 2009; Piranomonte et al. 2008; D'Avanzo et al. 2009), typically, the offsets have been found to be much larger than for Type II GRBs, indeed in agreement with predictions from the NS-NS merger models (Fong et al. 2010; Berger 2010). Furthermore, they trace their host light uniformly, indicating no preferred explosion environments. On the other hand, Fong et al. (2010) caution that Type I GRB host galaxies are also larger, so the relative offsets of Type I and Type II GRBs are very similar, actually. Salvaterra et al. (2010) study the detectability of Type I GRB afterglows in different scenarios, from primordial binaries with high kick velocities to dynamically formed binaries in different types of globular clusters, including intra-cluster globular clusters. They find the afterglows in the latter cases should be detectable, as the gas density within such ICGCs is still appreciably higher than the inter-cluster medium (ICM). Berger (2010) present several recent examples

of Type I GRBs with optical afterglows which do not have any underlying host galaxies down to very deep limits (though note that almost none of the observations would have detected the host galaxy of GRB 070707, Piranomonte et al. 2008). They obtained spectroscopy of multiple galaxies in the surroundings and find that often, very faint galaxies (without redshifts) lie close to these GRBs, but these are statistically less likely to be the host galaxies than more distant, bright galaxies. Therefore, it is likely these GRBs exploded in globular clusters in the outer halos of nearby galaxies.

Figure 5.4 (left) shows the afterglow magnitude of Type I GRBs (the same data as in Figure 5.3, right) plotted against the offset from their host galaxy. Once again, I differentiate between detections and upper limits and secure and insecure redshifts. Concentrating on the secure redshifts only, a clear correlation emerges, with larger offsets implying fainter magnitudes. Another Monte Carlo analysis, using the detections with secure redshifts only (additionally, note that the upper limits with secure redshifts all agree with the fit), finds in 30,000 runs:

$$m_{\mathrm{R_C}} \text{ (at } t = 1 \text{ day, } z = 1 \text{) mag} = (23.59 \pm 0.62) \text{ mag} + \left(\frac{\text{Offset}}{kpc} \right) \times (2.80 \pm 0.77). \quad (5.3)$$

The high significance of the correlation is shown by non-parametric rank correlation tests, I find $\tau = 0.64$, and $\rho = 0.84$. Due to the low number of data points, the significance is still not very high (2.7σ). The correlation (of which GRB 080905A is once again an outlier) once again indicates the probable effect of the density of the circumburst medium on the kinetic-energy conversion efficiency and thus the afterglow magnitude. For the cases with insecure redshift, the scatter is much larger, with GRB 051227 (faint afterglow centered on the host) and the high-redshift solution of GRB 060121 (extremely bright afterglow with a moderate host offset) being the strongest outliers. As I am only able to measure the offset in projection, this can have a strong effect, e.g., GRB 051227 may have occurred at a much larger offset but right in front of its host galaxy.

Again, I employ GRB 060313 to analyze the effect of an unknown redshift. The derived track is roughly perpendicular to the correlation, implying a strong dependency on redshift. The track of GRB 060313 crosses the correlation at roughly $z \approx 0.6$. Interestingly enough, the $z = 1.7$ solution of GRB 060121 is quite close in both afterglow magnitude and host offset to GRB 060313 at a similar redshift, at first glance implying a similar track for GRB 060121 and a naive "prediction" of a redshift around $z \approx 0.6$. Independent of the validity of the correlation as a rough redshift indicator, the track for GRB 060121 would be different, though, as the red afterglow would imply a strong extinction correction at such a low redshift (de Ugarte Postigo et al. 2006), which would correct the afterglow magnitude up again (no extinction correction has been assumed for GRB 060313).

Troja et al. (2008) claim that "all SHBs with extended-duration soft emission components lie very close to their hosts." and posit that this is an indication of two different progenitor classes of Type I GRBs, with the low-offset GRBs being NS-BH mergers (as stated before, simulations show that the fraction of NS-BH mergers should be low, O'Shaughnessy et al. 2008; Belczynski et al. 2008, whereas the result of Troja et al. 2008 would imply a large fraction). Fong et al. (2010) use their sample of afterglow offsets derived from HST observations to place doubt on this claim, finding no strong dichotomy. Using my large sample of

offsets (of which many have been taken from Fong et al. 2010), I similarly find only marginal evidence for the claim of Troja et al. (2008). In Figure 5.4 (left), I indicate the GRBs with extended faint emission with green dots (note that in some cases, it is unclear of extended emission exists, Norris et al. 2010). Of those with secure redshifts, the largest offsets are for GRB 071227 (though this event does still lie in the light of its host galaxy, an edge-on spiral galaxy, D'Avanzo et al. 2009; Fong et al. 2010) and GRB 061210 (though this offset has a large error bar). GRB 051210 has an even larger offset, though its redshift is not secure. Perley et al. (2009b) also point out that GRB 080503, the epitome of Type I GRBs with extended emission, lies at a large offset to any possible host galaxy detected in deep HST imaging. Conversely, GRB 051221A has a relatively small offset and no extended emission.

5.3.5   The Bolometric Isotropic Energy versus the Duration

Berger et al. (2007a) researched a possible correlation between T_{90} and E_{iso}, and found tentative evidence for a correlation between the two parameters. With my larger sample, I repeat this analysis. I correct the T_{90} times for the redshift[4], and, in contrast to Berger et al. (2007a), the isotropic energies I use are bolometric. In the case of GRBs which have an extended soft emission component (ESEC), I separate this total T_{90} from the duration of the initial pulse complex (IPC) only, which is shorter than 5 s in all cases. Figure 5.4 (right) shows the plotted data. Disregarding the T_{90} values which include an ESEC, a trend seems to be visible, both in the sample with secure redshifts only and in the complete sample, but the scatter is very large, and I caution that biases may be involved. Rank correlation tests also show that no significant correlation exists, it is $\tau = 0.06$ (significance 0.33σ), $\rho = 0.26$ for the cases with secure redshifts, and $\tau = 0.18$ (significance 1.6σ), $\rho = 0.32$ for the whole sample. GRB 090510 is a strong outlier, indicating an extremely high peak luminosity.

Once more, I use GRB 060313 to derive a redshift track. Again, this GRB is very suited for this analysis, as it was exceedingly bright and had the highest (lower limit) ratio of IPC to ESEC emission (Roming et al. 2006b), therefore my naive T_{90} transformation with redshift is expected to be adequate. Similar to the effect of an unknown redshift on host galaxy offset (Figure 5.4, left), the track is roughly perpendicular to the trend seen in Figure 5.4 (right) and thus redshift uncertainty may strongly contribute to scatter. In this case, GRB 060313 agrees with the values of other GRBs only for low redshifts $z \lesssim 0.5$. If a redshift $z \approx 1$ is confirmed spectroscopically, it will be a strong outlier in this plot, indicating the lack of a true correlation, similar to GRB 090510, which it resembles.

5.3.6   The Optical Luminosity as a Function of Redshift

In Figure 5.5, I plot the absolute magnitude M_B of all Type I and Type II GRBs in my sample over the redshift of the GRBs. There is clearly a "zone of avoidance" in the lower right corner. If I plot the constant observer frame luminosity, shown as a dashed line, it becomes clear

---

[4]Note that, in lieu of a complicated analysis of the prompt emission, I simply derive $T_{90}/(1 + z)$. A more correct approach would need to involve the modeling of detector thresholds and a temporally resolved spectral analysis of the prompt emission to determine which parts would still be detectable at different redshifts. This is especially important for the ESEC component, which typically has both a very low peak flux as well as soft emission, and thus rapidly becomes undetectable with rising redshift.

that this effect is due to the optical detector threshold, in this case the limiting magnitude that the telescopes used for observations can reach. This is similar to the detector threshold bias in high-energy observations (Butler et al. 2007b). Another point, different from detector thresholds, is how much effort is (can be) actually invested into obtaining deep observations. GRB 050509B is a good example, being the first well-localized Type I GRB, it triggered an unprecedented observing campaign, yielding very deep early limits (Figure 5.2). Sometimes even luck plays a role, for example, the extremely deep detection and upper limits of GRB 080503 at early times were mostly due to exceptional seeing during the observations (Perley et al. 2009b), the same is true for GRB 090515 (Rowlinson et al. 2010a). Another strong bias in the case of Type II GRB afterglows comes from the sample selection criteria, especially the need for a spectroscopic redshift, which favors afterglows that are bright in the observer frame (Chapter 4). For Type I GRBs, this bias is reduced, as all redshifts have been derived from host galaxy spectroscopy, but here, the need for (at least) an X-ray afterglow detection to determine the host identification with sufficient significance yields a similar effect. Several outliers under this threshold are visible, GRB 090515 at $z = 0.403$, GRB 091109B at $z = 0.5$ (assumed) and GRB 051227 at $z = 1$ (assumed). These afterglows were only discovered due to very deep and quite rapid observations with 8m-class telescopes (Rowlinson et al. 2010a; Levan et al. 2009; Malesani et al. 2009a; D'Avanzo et al. 2009; Berger et al. 2007a, also note the ultra-deep limit on GRB 050911 from VLT observations presented in Paper II). In these cases, the redshift assumption is almost irrelevant, as changing the redshift will move the data point more or less parallel to the threshold line. I illustrate this again with GRB 060313. Interestingly, the absolute magnitudes of two Type I GRB afterglows with uncertain redshifts, both of them bright high-fluence events, lie exactly on this line: GRB 061201 (which is quite similar to GRB 060313) at $z = 0.111$, and the $z = 1.7$ solution of GRB 060121. GRB 070707 at $z = 1$ also lies not far beneath it.

5.3.7   Contested GRBs in the Light of their Optical Afterglow Luminosities

In this final chapter, I will focus on three events that are in my Type I GRB sample which are contested. They have "hybrid indicators", with some of the population indicators pointing to a Type I (merger population) origin and some pointing to a Type II (collapsar population) origin. Next to the indicators already discussed in Chapter 3.3.1, I can now add the optical afterglow luminosity at one day after the GRB assuming $z = 1$, as I have shown (Chapter 5.3.2) that Type I GRB afterglows are typically a factor $100 - 300$ fainter than Type II GRB afterglows.

5.3.7.1   GRB 060121

Donaghy et al. (2006) present a detailed analysis of the prompt emission properties of this GRB. They find $T_{90} = 1.60 \pm 0.07$ s in the energy range $85 - 400$ keV, close to the "borderline" but still within the classic BATSE short GRB definition. Furthermore, the spectral lag is negligible, and the prompt light curve shows the IPC + ESEC shape (although the ESEC has a significance of only $\approx 4\sigma$). The fluence is among the highest in the Type I sample, but much smaller than bright Type II GRBs. The observed afterglow is extremely faint and very red. The host galaxy offset is larger than for a typical Type II GRB (Fong et al. 2010).
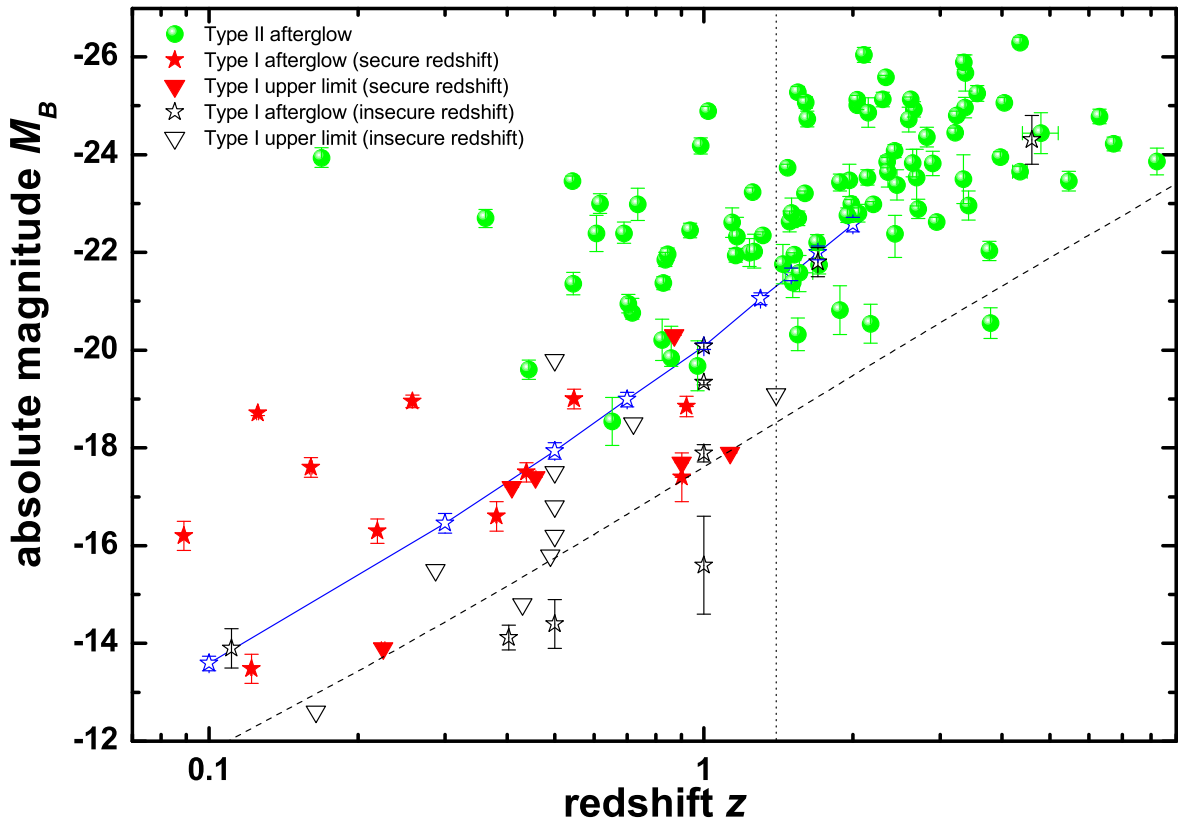
Figure 5.5: *Absolute magnitude* M_B *of the Type I and Type II GRBs at one day (assuming $z = 1$) versus their redshift z. A "zone of avoidance" for faint afterglows at high redshifts is visible, indicating a bias, both due to the detectors (telescope) and selection criteria. This is supported by plotting (dashed line) the line of constant observer frame luminosity, which parallels the detection edge. Deep, dedicated observations with 8m-class telescopes are able to find even fainter afterglows, though, such as those of GRB 090515, GRB 091109B and GRB 051227. I plot the redshift track of GRB 060313, in this case, an uncertain redshift has almost no influence on the position compared to the detection edge. The vertical dotted line lies at $z = 1.4$ and denotes the separation between "type A" and "type B" GRBs (low-z and high-z, respectively, see K06). Clearly, with three exceptions (GRB 030329 at $z = 0.17$, GRB 071010A at $z = 0.99$ and GRB 991216 at $z = 1$), the nearby afterglows are fainter than the more distant ones. The very faint afterglow at $z = 3.8$ is GRB 050502A, which decayed rapidly (Yost et al. 2006, and this work).*

Zhang et al. (2009) find that this event obeys the Amati relation, in contrast to other Type I GRBs, and I find that applying the ε-criterion of Lü et al. (2010), this GRB lies in the same region as the ultra-high-z GRBs 080913 and 090423, and clearly above the Type I GRB region.

What makes this event extraordinary is the implied very high redshift (de Ugarte Postigo et al. 2006; Levan et al. 2006; Berger et al. 2007a). If the GRB really lies at $z \sim 4$, then the isotropic energy release is comparable to the more powerful Type II GRBs, and the afterglow luminosity is typical for a Type II GRB too (this includes a significant extinction correction). Even if one assumes $z = 1.7$ (de Ugarte Postigo et al. 2006), the event is an outlier in comparison to the other Type I GRBs, and the additional problem of the even higher line-of-sight extinction that is needed (de Ugarte Postigo et al. 2006) emerges, which would be

rather peculiar at the large offset. A yet lower redshift (e.g., $z = 0.5$ which I assume for some other GRBs in the sample) eases the energy problem, but the extinction has to be increased even more, and the inferred low luminosity of the host galaxy becomes an additional factor to consider. In any case, the afterglow light curve points to extreme collimation (de Ugarte Postigo et al. 2006, find a half-opening angle $\theta_0 = 0.°6$ for the $z = 4.6$ case from broadband modeling), which is hardly achievable within the context of compact object mergers (Aloy et al. 2005).

If this is a Type I GRB, it indicates that in rare cases the isotropic energy release is comparable to Type II GRBs (note that at least the $z = 1.7$ solution is similar in terms of energetics to the bona fide Type I GRB 090510, though the latter is a truly extreme event), and the afterglow luminosity is not an indicator of the progenitor population. If this is a Type II GRB, then the problem emerges of how to explain the extremely short prompt emission, ~ 0.3 s at high energies in the rest frame assuming $z = 4.6$, in the framework of the collapsar model. Zhang et al. (2003) show that, under special conditions, the jet breakout from the massive star can produce a bright short emission spike, which is then followed by the lower-luminosity long GRB (see also Lazzati et al. 2010). This is exactly the IPC+ESEC light curve[5] seen for GRB 060121 (but also for events like GRB 050724 which are clearly not associated with massive stars). But these authors also note that the initial bright spike should dominate only in flux, not in fluence, as is the case for GRB 060121. Note that the negligible spectral lag is not evidence against a GRB being Type II, as extremely luminous long GRBs can have negligible spectral lag (e.g., GRB 050717, Krimm et al. 2006). A host galaxy redshift might help to solve the affiliation of this enigmatic event, but the extremely faint host ($R_C \approx 26.5$, Levan et al. 2006; Berger et al. 2007a) may prevent such a measurement before the next generation of large optical telescopes. In any case, independent of which population it actually belongs to, this event probes the envelope of known progenitor models.

5.3.7.2   GRB 060614

GRB 060614 is the much-discussed example of a temporally very long GRB ($T_{90} = 102 \pm 5$ s) that nonetheless seems to belong to the Type I GRB population, having negligible spectral lag while being subluminous at the same time (Gehrels et al. 2006; Mangano et al. 2007), a host galaxy with a small specific star-formation rate (Gal-Yam et al. 2006; Della Valle et al. 2006), a large offset in terms of half-light radius and brightest pixel distribution (Gal-Yam et al. 2006) and a missing SN component down to $M_R \gtrsim -13.6$ (Fynbo et al. 2006b; Gal-Yam et al. 2006; Della Valle et al. 2006, and my work). The medium the GRB jet propagates into is of constant density, but this finding carries no weight as most Type II GRBs also show constant density surroundings. The prompt emission light curve has been shown to be an extreme IPC+ESEC form, similar to other Type I GRBs but at higher luminosity (Zhang et al. 2007d). One difference to other Type I GRBs is that it does obey the Amati relation (Amati et al. 2007), although only in terms of the integrated spectrum, the IPC alone is

---

[5]Also note that the two highest-redshift GRBs 080913 and 090423 showed X-ray flaring activity for several 100 s (in the observer frame) after the temporally short prompt spike (Greiner et al. 2009b; Tanvir et al. 2009), such activity might be detected as a low-level extended emission component in soft γ-rays.

strongly offset as is the case for other Type I GRBs (Amati 2008). Lü et al. (2010) find the IPC lies in the Type I GRB region, though at the temporally long edge. Furthermore, it clearly does not follow other luminosity indicators (Schaefer & Xiao 2006). Perley et al. (2009b) also state that the strong resemblance of light curve shapes between GRB 080503 and GRB 060614 is a further indicator that this is a Type I event.

My new result is that in accordance with the relatively high isotropic energy release, the afterglow luminosity at late times is also quite high – for a Type I GRB. Even so, it does not become more luminous than the faintest Type II GRB afterglows. Therefore, I do not contradict earlier interpretations, and while no absolute consensus can be reached, there are more indications that this GRB did not result from massive stellar death than evidence supporting such an SN-less demise. Still, the extreme light curve shows the need to develop merger models that are able to accommodate such long periods of sustained bright emission. Mergers involving white dwarfs may be a solution (King et al. 2007; Lee et al. 2010).

5.3.7.3   GRB 060505

With the discovery of significant spectral lag for this event (McBreen et al. 2008), this event has become of crucial importance. In light of all data on this GRB, one of two "gold indicators" of progenitor affiliation (Donaghy et al. 2006) must be incorrect in at least some cases. Either not all merger-population GRBs show negligible spectral lag, or not all collapsar population GRBs show a SN component. Either way, this GRB breaks with the Type I and Type II classification as proposed by Zhang et al. (2007d), and also poses a problem for the flowchart of Zhang et al. (2009), as it does not obey the Amati relation, typical of Type I GRBs (Krimm et al. 2009), but conversely has a spectral lag (McBreen et al. 2008, though it does not lie on the lag-luminosity relation, but so do several of the "SN-GRBs"). These two indicators are summarized in a single point in Zhang et al. (2009). The ε-criterion of Lü et al. (2010) places this GRB into the "cloud" of Type I GRBs, though on the right edge due to the high T_{90}, beneath GRBs 051227 and 060614.

In comparison to the extreme length of GRB 060614, the $T_{90} = 4.8$ s of GRB 060505 (McBreen et al. 2008) is still marginally in agreement with a long tail of the Type I GRB distribution (Donaghy et al. 2006). The fact that the host environment, a low-metallicity super starcluster in a spiral galaxy, strongly resembles the typical blue starburst host galaxies of Type II GRBs (Thöne et al. 2008a) is also not a definitive argument against this being a Type I event (Ofek et al. 2007), as by now the majority of Type I GRB host galaxies have been found to be actively star-forming (Berger et al. 2007a)[6]. Also, the negligible offset from the star-forming region is not a conclusive argument for a Type II event, as Belczynski et al. (2006) show that compact object mergers can occur within just a few million years after a starburst via a common envelope phase channel (see also Belczynski et al. 2010). On the other hand, the fact that the GRB does not obey the Amati relation (Amati et al. 2007;

---

[6]Note, though, that the redshifts derived from host galaxy observations are strongly biased toward star-forming galaxies, as their emission lines are detectable at much higher significance than absorption lines in non-star-forming hosts (see the case of GRB 051210 in Berger et al. 2007a). Furthermore, there are indications that offsets are larger in the case of massive elliptical hosts (such as for GRB 050509B and possibly GRB 060502B, Gehrels et al. 2005; Bloom et al. 2007), making the association with these galaxies less secure (Troja et al. 2008).

Krimm et al. 2009) is also not a strong indication of this being a Type I event, as several clear collapsar events (GRB 980425, GRB 031203) are also not in accordance with the Amati relation. The one strong argument for this being a Type II GRB is the significant spectral lag, and the one strong argument for this being a Type I GRB is the deepest non-detection of a SN in a GRB-afterglow light curve ever.

From a theoretical standpoint, there is no compelling reason for Type I GRBs to have negligible spectral lag. Salmonson (2000) and Ioka & Nakamura (2001) interpret the lag-luminosity correlation (Norris et al. 2000) as a kinematic effect, dependent on the viewing angle from which the jet is seen, and on the Lorentz factor. One may now speculate that the jets of Type I GRBs have higher Lorentz factors, and thus smaller lags, as they propagate into a cleaner environment, since they do not have to penetrate a heavy stellar envelope and are thus less affected by baryon loading. A test of this hypothesis awaits the measurement of the Lorentz factors of Type I GRB jets, something that is non-trivial even for the much brighter afterglows of Type II GRBs (e.g., Molinari et al. 2007). Recent estimations of an extremely high Lorentz factor for GRB 090510 ($\Gamma \gtrsim 1000$, Ghirlanda et al. 2010; Ackermann et al. 2010b) may point toward a verification of this hypothesis, but GRB 090510 was anything but a typical Type I GRB. Concerning a missing SN component, I have already pointed out that several authors have proposed the "fallback black hole" scenario which results in a GRB without a bright accompanying SN (Fryer et al. 2006, 2007; Moriya et al. 2010). Tominaga et al. (2007) show that GRB-producing relativistic jets can be launched with negligible Ni^{56} production, leading to the absence of SN emission. But it seems that such events must be either rare or usually very subluminous, thus evading detection.

Xu et al. (2009) study both GRB 060614 and 060505 with broadband modelling, and come to the conclusion: "Hence, from the properties of the afterglows there is nothing to suggest that these bursts should have another progenitor than other LGRBs." I consider their conclusion misleading, as one would not expect the afterglow properties Xu et al. (2009) study, such as decay slopes and the optical-to-X-ray luminosity ratio, to be different in Type I and Type II GRBs (Nakar 2007a; Nakar & Granot 2007; Nysewander et al. 2009a). I show here that the afterglow luminosity, on the other hand, differs strongly from that of all Type II GRBs.

From the afterglow luminosity perspective, in retrospect, I have discussed this GRB within the Type I sample, as it shows an intrinsically extremely faint afterglow that is as much an outlier in comparison to the Type II GRB afterglows as GRB 060121 is an outlier compared to the rest of the Type I GRB afterglows. If this truly is a Type II event, what we are left with is a uniquely subluminous GRB, one that is faint in the prompt emission, in the afterglow *and* in the SN emission, the latter implying that only a small amount of energy is deposited in the subrelativistic ejecta too, in strong contrast to the other subluminous local universe events. Therefore, if the progenitor is of similar mass as a typical Type II GRB collapsar, most of the kinetic and rest mass energy of the collapsing core must fall rapidly without significant emission through the event horizon of the central engine. The alternative possibility is that this is a merger event, probably from a rapid channel (Belczynski et al. 2006, 2010), that for some reason does not show a typical sub-second spike of emission, but a more extended light curve with significant lag, and is otherwise typically subluminous in terms of prompt and afterglow emission.

Chapter 6

Conclusions and Outlook

In this work, I have compiled a large amount of optical/NIR photometry of *Swift*-era GRB afterglows, creating a total sample of 76 Type II GRBs (as well as three more pre-*Swift* events), considering events up to the end of 2009 September, as well as a sample of 37 Type I GRBs up to the end of 2009 December. Following methods originally devised for Zeh et al. (2006a) and Kann et al. (2006b), I analyzed the light curves and SEDs. Here, most of the Type II GRB afterglow sample was selected to have high-quality data (Golden Sample) which allowed me to perform a detailed analysis of the SEDs. I also added additional GRB afterglows for which the SED could not be fit freely but could be constrained under reasonable assumptions (Silver Sample) as well as GRBs afterglows for which no SED information could be derived but which still yielded viable light curves (Bronze Sample). For the Type I GRBs, on the other hand, I could not afford to be so selective, and used all available events which yielded at least some analyzable data, though almost half of these have no optical afterglow detections at all, and many have either no redshift or insecure associations. In such cases, I performed reasonable assumptions, and a compariosn between the sample with secure redshifts and those without yields no strong differences. I also collected data on the energetics of the all these GRBs, as well as host galaxy offsets for the Type I GRBs.

In a first step, I used the sample of *Swift*-era Type II GRB afterglows to compare them to the pre-*Swift* sample taken from Kann et al. (2006b) (and expanded in this work), and looked for correlations between the optical afterglow luminosity and parameters of the prompt emission. To summarize, I come to the following results for this part of the work:

- As has been found before, observed optical afterglows in the *Swift* era are typically fainter than those of the pre-*Swift* era. The rapid localization and follow-up capabilities available today allow observers access to this fainter population.

- In terms of luminosity, I do not find a statistically significant difference between the pre-*Swift* and the *Swift*-era afterglows, the relative faintness of the *Swift*-era afterglows can typically be attributed to a larger mean redshift. I caution, though, that several selection biases still apply.

- I find that SMC-like dust is usually preferred and that the line-of-sight extinctions through the GRB host galaxies are usually low, verifying and expanding my results in Kann et al. (2006b). Still, at least one clear case (GRB 070802) of high A_V in my sample exists.

- The trend seen in Kann et al. (2006b) of lower extinction at higher redshifts is confirmed in my new sample, which increases the number of $z > 3$ GRBs from 1 to 17. But the correlation is only weak, and it is still unclear if this is due to a true evolution or to a selection bias.

- The clustering of optical afterglow luminosities at one day reported by Kann et al. (2006b), Liang & Zhang (2006) and Nardini et al. (2006) is found to be less significant than before, indeed, the spread of magnitudes actually increases in luminosity space due to the discovery of exceptionally over- as well as underluminous events. As the *Swift* sample is less biased than earlier samples, this indicates that the clustering found in pre-*Swift* data may be the result of selection effects only. The bimodal distribution when splitting the afterglows into two redshift bins (divided along the mean redshift found for pre-*Swift* GRBs) is confirmed though, but the total sample itself is not found to be bimodally distributed anymore, in agreement with several other recent results.

- At very early times, the apparent magnitude spread is much larger than at later times but, intriguingly, half the afterglows strongly cluster within three magnitudes. Basically, there seem to be three classes: optical afterglows with additional early emission components, afterglows which are dominated by the constant-blastwave-energy forward shock at early times already, and optically faint afterglows that show plateau phases or later rebrightenings (possibly due to energy injections into the forward shock or an off-axis viewing geometry). The forward-shock dominated afterglows make up 60% of the sample that had early detections (or late, definite peaks), and the afterglows with additional emission components, which are the most luminous ones, are also the most rare. While there is a trend between the peak time and the peak luminosity of afterglows with fast initial rises, a strong correlation such as the one claimed by Panaitescu & Vestrand (2008) from a much smaller sample is not observed.

- A trend is visible between the isotropic energy release in gamma-rays and the optical luminosity at a fixed late time in the rest frame. The scatter is large, probably due to circumburst density variations, but low-luminosity events support the reality of this trend, found to be significant a a few σ level by rank correlation tests.

In a second step, I combined the pre-*Swift* and *Swift*-era Type II GRB afterglow samples (as I found no significant intrinsic differences) for a total of 95 events, and used this as a "background" sample against which I characterized the Type I Afterglow sample. I have achieved the following results:

- Observationally, the optical afterglows of Type I GRBs are significantly fainter than those of Type II GRBs. Many Type I GRBs do not have any optical detections at all, and often these non-detections reach upper limits much deeper than the magnitudes of my (admittedly biased) Type II GRB afterglow sample at similar times. Type II GRBs not detected to similar depths are usually dark GRBs (though it remains unclear if such events are strongly extinguished or intrinsically much fainter).

- The luminosity distribution of Type I GRB afterglows shows a larger scatter than that of Type II GRBs. The fact that many Type I GRBs have upper limits on their optical

afterglows only implies that the luminosity distribution is even broader than what I have found. I find that the afterglows of Type I GRBs are, in the mean, 5 mags fainter than those of Type II GRBs. This is further support that Type I and Type II GRBs have different progenitors, exploding in different environments.

- Using the knowledge of the energetics and typical afterglow luminosities of Type I GRBs, I explore theoretically why their afterglows are even fainter than predicted by Panaitescu et al. (2001). The main reasons seem to be that Panaitescu et al. (2001) overestimated the energy release, also, generally the circumburst density is smaller than expected.

- Type I GRB afterglows extend the correlation between isotropic energy release and optical afterglow luminosity to smaller energies and lower luminosities. The slope is identical, but I find a different normalization, which can be explained by a strong difference in the density of the external medium into which the jets propagate.

- Another tentative correlation that confirms expectations is found between the host galaxy offset and the afterglow luminosity. If confirmed by additional data, it may be used as a rough redshift indicator, though projection effects can play an important role. I find only marginal evidence for the claim of Troja et al. (2008) that all GRBs with extended emission have small host galaxy offsets.

- A trend between the duration and the isotropic energy release is not detected in a significant way.

- I focus especially on three anomalous GRBs, which have been assumed to be Type I GRBs, in the light of the results on their optical luminosities.

  1. GRB 060121 is found to resemble Type II GRBs much more than Type I GRBs, but would then have an extremely short prompt emission spike.

  2. GRB 060614, notwithstanding its extreme duration, is in good agreement with the upper end of the Type I GRB distribution in terms of energetics and afterglow luminosity, and thus seems to represent an extreme case of an Extended Soft Emission Component.

  3. GRB 060505 remains a puzzling object. The measurement of a significant spectral lag would place it with the Type II GRBs (in agreement with the environment), whereas the total lack of a SN, the large offset from the Amati relation and the very low optical afterglow luminosity I derive are more akin to Type I GRBs. This leads to the question if the existence of significant spectral lag truly is a surefire indication that a GRB is a Type II event.

Several further results of my study are presented in Appendix B.

At the time the two studies based on pre-*Swift* data (Zeh et al. 2006a; Kann et al. 2006b) were published, this "phase" of GRB studies had been mostly wrapped up, with only a small amount of additional data and results on pre-2005 GRBs having been published since then. The *Swift*-era is far from being finished, though, the satellite may remain functional until ≈ 2017 (and a similar lifetime may be possible for *AGILE* and *Fermi* assuming extended missions are financed), allowing a transition to future missions (such as SVOM, e.g., Götz et al. 2009b and possibly EXIST, e.g., Grindlay et al. 2010). The total sample of high-quality afterglows is expected to at least double until then. Recent years have seen a proliferation of rapid response telescopes, especially in the 1 – 2m class (the Robonet telescopes, Bode et al. 2004 or the P60, Cenko et al. 2006), as well as instruments dedicated to GRB research (e.g., GROND, Greiner et al. 2008). A search for optical emission independent of the GRBs themselves will become possible soon through deep wide-field survey projects (Palomar Transient Factory, Pan-STARRS, Skymapper and finally LSST), and in the second half of the decade, once the JWST is put into orbit and the 30m class telescopes come online, GRBs will fulfill their promise as beacons of the high-redshift universe.

A colleague of mine, Daniele Malesani (Dark Cosmology Center, Copenhagen), once said: "If you have seen one GRB, you have seen *one* GRB". The lesson of the last years has been that the afterglows of GRBs are as diverse as the prompt emission itself, the exploration of new time domains *Swift* has allowed us has brought evidence that the "simple" version of the standard fireball model is incomplete and that we are from from deciphering the cosmic mystery GRBs remain until this very day. In the coming years, I plan the extend the reach of my sample, and research further aspects of GRB afterglows such as evidence for or against chromatic breaks, rebrightenings in afterglows and color evolution at early phases.

Bibliography

Abadie, J., Abbott, B. P., Abbott, R., et al. 2010, Astroph. J., 715, 1453

Abdo, A. A., Ackermann, M., Ajello, M., et al. 2009a, Astroph. J., 706, L138

Abdo, A. A., Ackermann, M., Ajello, M., et al. 2009b, Nature, 462, 331

Abdo, A. A., Ackermann, M., Ajello, M., et al. 2010, Astroph. J., 712, 558

Abdo, A. A., Ackermann, M., Arimoto, M., et al. 2009c, Science, 323, 1688

Abdo, A. A., Ackermann, M., Asano, K., et al. 2009d, Astroph. J., 707, 580

Achterberg, A., Gallant, Y. A., Kirk, J. G., & Guthmann, A. W. 2001, Mon. Not. R. Astron. Soc., 328, 393

Ackermann, M., Ajello, M., Baldini, L., et al. 2010a, Astroph. J., 717, L127

Ackermann, M., Asano, K., Atwood, W. B., et al. 2010b, Astroph. J., 716, 1178

Akerlof, C., Balsano, R., Barthelmy, S., et al. 1999, Nature, 398, 400

Aloy, M. A., Janka, H., & Müller, E. 2005, Astron. & Astroph., 436, 273

Amati, L. 2006, Mon. Not. R. Astron. Soc., 372, 233

Amati, L. 2008, in American Institute of Physics Conference Series, Vol. 966, Relativistic Astrophysics, ed. C. L. Bianco & S.-S. Xue, 3–6

Amati, L. 2009, Proceedings of "44th Rencontres de Moriond", La Thuile (Val d'Aosta, Italy) on "Very High Energy Phenomena in the Universe", in press (arXiv:0908.1339)

Amati, L., Della Valle, M., Frontera, F., et al. 2007, Astron. & Astroph., 463, 913

Amati, L., Frontera, F., & Guidorzi, C. 2009a, Astron. & Astroph., 508, 173

Amati, L., Frontera, F., & Guidorzi, C. 2009b, Astron. & Astroph., 508, 173

Amati, L., Frontera, F., Tavani, M., et al. 2002, Astron. & Astroph., 390, 81

Amati, L., Guidorzi, C., Frontera, F., et al. 2008, Mon. Not. R. Astron. Soc., 391, 577

Andersen, M. I., Hjorth, J., Pedersen, H., et al. 2000, Astron. & Astroph., 364, L54

Aoki, K., Totani, T., Hattori, T., et al. 2009, Publ. Astron. Soc. Japan, 61, 387

Band, D., Matteson, J., Ford, L., et al. 1993, Astroph. J., 413, 281

Barat, C. & Lestrade, J. P. 2007, Astroph. J., 667, 1033

Barthelmy, S. D., Chincarini, G., Burrows, D. N., et al. 2005, Nature, 438, 994

Belczynski, K., Holz, D. E., Fryer, C. L., et al. 2010, Astroph. J., 708, 117

Belczynski, K., Perna, R., Bulik, T., et al. 2006, Astroph. J., 648, 1110

Belczynski, K., Stanek, K. Z., & Fryer, C. L. 2007, Astroph. J., submitted (arXiv:0712.3309)

Belczynski, K., Taam, R. E., Rantsiou, E., & van der Sluys, M. 2008, Astroph. J., 682, 474

Bellm, E. C., Hurley, K., Pal'shin, V., et al. 2008, Astroph. J., 688, 491

Berger, E. 2007, Astroph. J., 670, 1254

Berger, E. 2009, Astroph. J., 690, 231

Berger, E. 2010, Astroph. J., submitted (arXiv:1007.0003)

Berger, E., Cenko, S. B., Fox, D. B., & Cucchiara, A. 2009, Astroph. J., 704, 877

Berger, E., Fox, D. B., Kulkarni, S. R., et al. 2005a, Astroph. J., 629, 328

Berger, E., Fox, D. B., Price, P. A., et al. 2007a, Astroph. J., 664, 1000

Berger, E., Kulkarni, S. R., Fox, D. B., et al. 2005b, Astroph. J., 634, 501

Berger, E., Price, P. A., Cenko, S. B., et al. 2005c, Nature, 438, 988

Berger, E., Shin, M., Mulchaey, J. S., & Jeltema, T. E. 2007b, Astroph. J., 660, 496

Berger, E., Shin, M., Mulchaey, J. S., & Jeltema, T. E. 2007c, Astroph. J., 660, 496

Bersier, D., Fruchter, A. S., Strolger, L., et al. 2006, Astroph. J., 643, 284

Beskin, G., Karpov, S., Bondar, S., et al. 2010, Astroph. J., 719, L10

Beuermann, K., Hessman, F. V., Reinsch, K., et al. 1999, Astron. & Astroph., 352, L26

Bhat, P. N., Fishman, G. J., Meegan, C. A., et al. 1992, Nature, 359, 217

Bhattacharya, D. 2001, Bulletin of the Astronomical Society of India, 29, 107

Blake, C. H., Bloom, J. S., Starr, D. L., et al. 2005, Nature, 435, 181

Blandford, R. D. & Znajek, R. L. 1977, Mon. Not. R. Astron. Soc., 179, 433

Bloom, J. S., Frail, D. A., & Sari, R. 2001, Astron. J., 121, 2879

Bloom, J. S., Kulkarni, S. R., & Djorgovski, S. G. 2002, Astron. J., 123, 1111

Bloom, J. S., Perley, D. A., Chen, H., et al. 2007, Astroph. J., 654, 878

Bloom, J. S., Perley, D. A., Li, W., et al. 2009, Astroph. J., 691, 723

Bloom, J. S., Prochaska, J. X., Pooley, D., et al. 2006, Astroph. J., 638, 354

Bode, M. F., Cardiff U., U. Hertfordshire, et al. 2004, in Bulletin of the American Astronomical Society, Vol. 36, Bulletin of the American Astronomical Society, 1400–+

Boër, M., Atteia, J. L., Damerdji, Y., et al. 2006, Astroph. J., 638, L71

Bradley, J., Dai, Z. R., Erni, R., et al. 2005, Science, 307, 244

Burrows, D. N., Grupe, D., Capalbi, M., et al. 2006, Astroph. J., 653, 468

Burrows, D. N., Romano, P., Falcone, A., et al. 2005, Science, 309, 1833

Butler, N. R., Kocevski, D., & Bloom, J. S. 2009, Astroph. J., 694, 76

Butler, N. R., Kocevski, D., Bloom, J. S., & Curtis, J. L. 2007a, Astroph. J., 671, 656

Butler, N. R., Kocevski, D., Bloom, J. S., & Curtis, J. L. 2007b, Astroph. J., 671, 656

Butler, N. R., Li, W., Perley, D., et al. 2006, Astroph. J., 652, 1390

Campana, S., Guidorzi, C., Tagliaferri, G., et al. 2007a, Astron. & Astroph., 472, 395

Campana, S., Mangano, V., Blustin, A. J., et al. 2006a, Nature, 442, 1008

Campana, S., Tagliaferri, G., Lazzati, D., et al. 2006b, Astron. & Astroph., 454, 113

Campana, S., Tagliaferri, G., Malesani, D., et al. 2007b, Astron. & Astroph., 464, L25

Castro-Tirado, A. J., Bremer, M., McBreen, S., et al. 2007, Astron. & Astroph., 475, 101

Castro-Tirado, A. J., de Ugarte Postigo, A., Gorosabel, J., et al. 2008, Nature, 455, 506

Castro-Tirado, A. J., Jelínek, M., Pandey, S. B., et al. 2006, Astron. & Astroph., 459, 763

Cenko, S. B., Berger, E., Nakar, E., et al. 2008a, Astroph. J., submitted (arXiv:0802.0874)

Cenko, S. B., Fox, D. B., Moon, D., et al. 2006, Publ. Astron. Soc. Pacific, 118, 1396

Cenko, S. B., Fox, D. B., Penprase, B. E., et al. 2008b, Astroph. J., 677, 441

Cenko, S. B., Frail, D. A., Harrison, F. A., et al. 2010, Astroph. J., submitted (arXiv:1004.2900v2)

Cenko, S. B., Kelemen, J., Harrison, F. A., et al. 2009, Astroph. J., 693, 1484

Chandra, P., Cenko, S. B., Frail, D. A., et al. 2008, Astroph. J., 683, 924

Chevalier, R. A. & Li, Z.-Y. 1999, Astroph. J., 520, L29

Chevalier, R. A. & Li, Z.-Y. 2000, Astroph. J., 536, 195

Chornock, R., Berger, E., Levesque, E. M., et al. 2010, Astroph. J., submitted (arXiv:1004.2262)

Christensen, L., Hjorth, J., & Gorosabel, J. 2004, Astron. & Astroph., 425, 913

Cobb, B. E., Bailyn, C. D., van Dokkum, P. G., & Natarajan, P. 2006, Astroph. J., 645, L113

Cobb, B. E., Bloom, J. S., Perley, D. A., et al. 2010, Astroph. J., 718, L150

Coburn, W. & Boggs, S. E. 2003, Nature, 423, 415

Colgate, S. A. 1968, Canadian Journal of Physics, 46, 476

Conselice, C. J., Vreeswijk, P. M., Fruchter, A. S., et al. 2005, Astroph. J., 633, 29

Costa, E., Frontera, F., Heise, J., et al. 1997, Nature, 387, 783

Covino, S., Campana, S., Conciatore, M. L., et al. 2010, Astron. & Astroph., in press (arXiv:1007.4769)

Covino, S., D'Avanzo, P., Klotz, A., et al. 2008, Mon. Not. R. Astron. Soc., 388, 347

Covino, S., Lazzati, D., Ghisellini, G., et al. 1999, Astron. & Astroph., 348, L1

Coward, D. M., Guetta, D., Burman, R. R., & Imerito, A. 2008, Mon. Not. R. Astron. Soc., 386, 111

Cucchiara, A., Jones, T., Charlton, J. C., et al. 2009, Astroph. J., 697, 345

Curran, P. A., Evans, P. A., de Pasquale, M., Page, M. J., & van der Horst, A. J. 2010, Astroph. J., 716, L135

Dai, X. 2009, Astroph. J., 697, L68

Dai, X., Garnavich, P. M., Prieto, J. L., et al. 2008a, Astroph. J., 682, L77

Dai, X., Halpern, J. P., Morgan, N. D., et al. 2007, Astroph. J., 658, 509

Dai, X., Stanek, K. Z., & Garnavich, P. M. 2008b, in American Institute of Physics Conference Series, Vol. 1065, American Institute of Physics Conference Series, ed. Y.-F. Huang, Z.-G. Dai, & B. Zhang, 93–97

Dai, Z. G. & Cheng, K. S. 2001, Astroph. J., 558, L109

D'Avanzo, P., D'Elia, V., & Covino, S. 2008, GCN Circular 8350

D'Avanzo, P., Malesani, D., Covino, S., et al. 2009, Astron. & Astroph., 498, 711

de Pasquale, M., Oates, S. R., Page, M. J., et al. 2007, Mon. Not. R. Astron. Soc., 377, 1638

De Pasquale, M., Schady, P., Kuin, N. P. M., et al. 2010, Astroph. J., 709, L146

de Ugarte Postigo, A., Castro-Tirado, A. J., Gorosabel, J., et al. 2005, Astron. & Astroph., 443, 841

de Ugarte Postigo, A., Castro-Tirado, A. J., Guziy, S., et al. 2006, Astroph. J., 648, L83

de Ugarte Postigo, A., Goldoni, P., Thöne, C. C., et al. 2010, Astron. & Astroph., 513, A42+

D'Elia, V., Fiore, F., Goldoni, P., et al. 2010, Mon. Not. R. Astron. Soc., 401, 385

D'Elia, V., Fiore, F., Perna, R., et al. 2009, Astron. & Astroph., 503, 437

Della Valle, M., Benetti, S., Mazzali, P., et al. 2008, Central Bureau Electronic Telegrams, 1602, 1

Della Valle, M., Chincarini, G., Panagia, N., et al. 2006, Nature, 444, 1050

Deng, W., Huang, Y., & Kong, S. 2010, Research in Astronomy and Astrophysics, submitted (arXiv:1003.0099)

Dewi, J. D. M., Podsiadlowski, P., & Sena, A. 2006, Mon. Not. R. Astron. Soc., 368, 1742

Donaghy, T. Q., Lamb, D. Q., Sakamoto, T., et al. 2006, Astroph. J., submitted (astro-ph/0605570)

Eichler, D., Guetta, D., & Manis, H. 2009, Astroph. J., 690, L61

Eichler, D., Livio, M., Piran, T., & Schramm, D. N. 1989, Nature, 340, 126

Elíasdóttir, Á., Fynbo, J. P. U., Hjorth, J., et al. 2009, Astroph. J., 697, 1725

Ellison, S. L., Vreeswijk, P., Ledoux, C., et al. 2006, Mon. Not. R. Astron. Soc., 372, L38

Evans, P. A., Beardmore, A. P., Page, K. L., et al. 2009, Mon. Not. R. Astron. Soc., 397, 1177

Evans, P. A., Beardmore, A. P., Page, K. L., et al. 2007, Astron. & Astroph., 469, 379

Fan, Y. & Piran, T. 2006, Mon. Not. R. Astron. Soc., 369, 197

Fan, Y., Zhang, B., Xu, D., Liang, E., & Zhang, B. 2010, ArXiv e-prints

Fenimore, E. E., Ricker, G., Atteia, J., et al. 2004, GCN Circular 2735

Ferrero, P., Kann, D. A., Klose, S., et al. 2008, in American Institute of Physics Conference Series, Vol. 1000, American Institute of Physics Conference Series, ed. M. Galassi, D. Palmer, & E. Fenimore, 257–260

Ferrero, P., Kann, D. A., Zeh, A., et al. 2006, Astron. & Astroph., 457, 857

Ferrero, P., Klose, S., Kann, D. A., et al. 2009, Astron. & Astroph., 497, 729

Ferrero, P., Sanchez, S. F., Kann, D. A., et al. 2007, Astron. J., 134, 2118

Filippenko, A. V. 1997, Annu. Rev. Astro. Astroph., 35, 309

Fiore, F., D'Elia, V., Lazzati, D., et al. 2005, Astroph. J., 624, 853

Fiore, F., Guetta, D., Piranomonte, S., D'Elia, V., & Antonelli, L. A. 2007, Astron. & Astroph., 470, 515

Fong, W., Berger, E., & Fox, D. B. 2010, Astroph. J., 708, 9

Ford, L. A., Band, D. L., Matteson, J. L., et al. 1995, Astroph. J., 439, 307

Fox, D. B., Frail, D. A., Price, P. A., et al. 2005, Nature, 437, 845

Fox, D. W., Price, P. A., Soderberg, A. M., et al. 2003a, Astroph. J., 586, L5

Fox, D. W., Yost, S., Kulkarni, S. R., et al. 2003b, Nature, 422, 284

Frail, D. A., Cameron, P. B., Kasliwal, M., et al. 2006, Astroph. J., 646, L99

Frail, D. A., Kulkarni, S. R., Nicastro, L., Feroci, M., & Taylor, G. B. 1997, Nature, 389, 261

Frank, S., Bentz, M. C., Stanek, K. Z., et al. 2007, Astroph.. & Space Sc., 312, 325

Freedman, D. L. & Waxman, E. 2001, Astroph. J., 547, 922

Friedman, A. S. & Bloom, J. S. 2005a, Astroph. J., 627, 1

Friedman, A. S. & Bloom, J. S. 2005b, Astroph. J., 627, 1

Fruchter, A. S., Levan, A. J., Strolger, L., et al. 2006, Nature, 441, 463

Fryer, C. L., Hungerford, A. L., & Young, P. A. 2007, Astroph. J., 662, L55

Fryer, C. L., Young, P. A., & Hungerford, A. L. 2006, Astroph. J., 650, 1028

Fynbo, J. P. U., Jakobsson, P., Prochaska, J. X., et al. 2009, Astroph. J. Suppl, 185, 526

Fynbo, J. P. U., Sollerman, J., Hjorth, J., et al. 2004, Astroph. J., 609, 962

Fynbo, J. P. U., Starling, R. L. C., Ledoux, C., et al. 2006a, Astron. & Astroph., 451, L47

Fynbo, J. P. U., Watson, D., Thöne, C. C., et al. 2006b, Nature, 444, 1047

Gal-Yam, A., Fox, D. B., Price, P. A., et al. 2006, Nature, 444, 1053

Galama, T. J., Vreeswijk, P. M., van Paradijs, J., et al. 1998, Nature, 395, 670

Galama, T. J. & Wijers, R. A. M. J. 2001, Astroph. J., 549, L209

Gehrels, N., Barthelmy, S. D., Burrows, D. N., et al. 2008, Astroph. J., 689, 1161

Gehrels, N., Chincarini, G., Giommi, P., et al. 2004, Astroph. J., 611, 1005

Gehrels, N., Norris, J. P., Barthelmy, S. D., et al. 2006, Nature, 444, 1044

Gehrels, N., Ramirez-Ruiz, E., & Fox, D. B. 2009, Annu. Rev. Astro. Astroph., 47, 567

Gehrels, N., Sarazin, C. L., O'Brien, P. T., et al. 2005, Nature, 437, 851

Gendre, B., Galli, A., & Boër, M. 2008, GCN Circular 7730

Gendre, B., Klotz, A., Palazzi, E., et al. 2010, Mon. Not. R. Astron. Soc., 405, 2372

Ghirlanda, G., Ghisellini, G., & Lazzati, D. 2004, Astroph. J., 616, 331

Ghirlanda, G., Ghisellini, G., & Nava, L. 2010, Astron. & Astroph., 510, L7+

Ghirlanda, G., Nava, L., Ghisellini, G., Celotti, A., & Firmani, C. 2009, Astron. & Astroph., 496, 585

Ghirlanda, G., Nava, L., Ghisellini, G., & Firmani, C. 2007, Astron. & Astroph., 466, 127

Ghirlanda, G., Nava, L., Ghisellini, G., Firmani, C., & Cabrera, J. I. 2008, Mon. Not. R. Astron. Soc., 387, 319

Ghisellini, G. 2010, invited talk at the conference: X-Ray Astronomy 2009, Present Status, multi-wavelength approach and future perspectives, September 2009, Bologna, arXiv:1002.1784

Giuliani, A., Mereghetti, S., Fornari, F., et al. 2008, Astron. & Astroph., 491, L25

Golenetskii, S., Aptekar, R., Mazets, E., et al. 2004, GCN Circular 2754

Gomboc, A., Kobayashi, S., Guidorzi, C., et al. 2008, Astroph. J., 687, 443

Gorosabel, J., Castro-Tirado, A. J., Guziy, S., et al. 2006, Astron. & Astroph., 450, 87

Gorosabel, J., Castro-Tirado, A. J., Tanvir, N. R., et al. 2010, GCN Circular 11125

Götz, D., Laurent, P., Lebrun, F., Daigne, F., & Bošnjak, Ž. 2009a, Astroph. J., 695, L208

Götz, D., Paul, J., Basa, S., et al. 2009b, in American Institute of Physics Conference Series, Vol. 1133, American Institute of Physics Conference Series, ed. C. Meegan, C. Kouveliotou, & N. Gehrels, 25–30

Graham, J. F., Fruchter, A. S., Levan, A. J., et al. 2009, Astroph. J., 698, 1620

Granot, J., Königl, A., & Piran, T. 2006, Mon. Not. R. Astron. Soc., 370, 1946

Granot, J., Ramirez-Ruiz, E., & Perna, R. 2005, Astroph. J., 630, 1003

Greiner, J., Bornemann, W., Clemens, C., et al. 2008, Publ. Astron. Soc. Pacific, 120, 405

Greiner, J., Clemens, C., Krühler, T., et al. 2009a, Astron. & Astroph., 498, 89

Greiner, J., Klose, S., Reinsch, K., et al. 2003, Nature, 426, 157

Greiner, J., Krühler, T., Fynbo, J. P. U., et al. 2009b, Astroph. J., 693, 1610

Greiner, J., Krühler, T., McBreen, S., et al. 2009c, Astroph. J., 693, 1912

Grindlay, J., Gehrels, N., Bloom, J., et al. 2010, Invited talk at SPIE Conference "Astronomical Telescopes and Instrumentation 2010", to appear in Proceedings SPIE (2010) (arXiv:1008.3394)

Grindlay, J., Portegies Zwart, S., & McMillan, S. 2006, Nature Physics, 2, 116

Grupe, D., Burrows, D. N., Patel, S. K., et al. 2006, Astroph. J., 653, 462

Grupe, D., Gronwall, C., Wang, X., et al. 2007, Astroph. J., 662, 443

Guetta, D. & Della Valle, M. 2007, Astroph. J., 657, L73

Guetta, D. & Granot, J. 2004, in Astronomical Society of the Pacific Conference Series, Vol. 312, Astronomical Society of the Pacific Conference Series, ed. M. Feroci, F. Frontera, N. Masetti, & L. Piro, 377−+

Guetta, D. & Stella, L. 2009, Astron. & Astroph., 498, 329

Guidorzi, C., Clemens, C., Kobayashi, S., et al. 2009a, Astron. & Astroph., 499, 439

Guidorzi, C., Melandri, A., Mundell, C. G., et al. 2009b, GCN Circular 10027

Guidorzi, C., Vergani, S. D., Sazonov, S., et al. 2007, Astron. & Astroph., 474, 793

Haislip, J. B., Nysewander, M. C., Reichart, D. E., et al. 2006, Nature, 440, 181

Hao, H., Stanek, K. Z., Dobrzycki, A., et al. 2007, Astroph. J., 659, L99

Hartmann, D. H. & Narayan, R. 1996, Astroph. J., 464, 226

Heise, J., in't Zand, J., Kippen, R. M., & Woods, P. M. 2001, in Gamma-ray Bursts in the Afterglow Era, ed. E. Costa, F. Frontera, & J. Hjorth, 16

Higdon, J. C. & Lingenfelter, R. E. 1990, Annu. Rev. Astro. Astroph., 28, 401

Hjorth, J., Sollerman, J., Gorosabel, J., et al. 2005a, Astroph. J., 630, L117

Hjorth, J., Sollerman, J., Møller, P., et al. 2003, Nature, 423, 847

Hjorth, J., Watson, D., Fynbo, J. P. U., et al. 2005b, Nature, 437, 859

Holland, S. T., Sbarufatti, B., Shen, R., et al. 2010, Astroph. J., 717, 223

Huang, K. Y., Urata, Y., Filippenko, A. V., et al. 2005, Astroph. J., 628, L93

Huang, Y. F., Cheng, K. S., & Gao, T. T. 2006, Astroph. J., 637, 873

Ioka, K., Kobayashi, S., & Zhang, B. 2005, Astroph. J., 631, 429

Ioka, K. & Nakamura, T. 2001, Astroph. J., 554, L163

Iwamoto, K., Mazzali, P. A., Nomoto, K., et al. 1998, Nature, 395, 672

Jakobsson, P., Fynbo, J. P. U., Ledoux, C., et al. 2006a, Astron. & Astroph., 460, L13

Jakobsson, P., Hjorth, J., Ramirez-Ruiz, E., et al. 2004, New Astronomy, 9, 435

Jakobsson, P., Levan, A., Fynbo, J. P. U., et al. 2006b, Astron. & Astroph., 447, 897

Jaunsen, A. O., Hjorth, J., Björnsson, G., et al. 2001, Astroph. J., 546, 127

Jaunsen, A. O., Rol, E., Watson, D. J., et al. 2008, Astroph. J., 681, 453

Jin, Z. P. & Fan, Y. Z. 2007, Mon. Not. R. Astron. Soc., 378, 1043

Jóhannesson, G., Björnsson, G., & Gudmundsson, E. H. 2007, Astron. & Astroph., 472, L29

Kalemci, E., Boggs, S. E., Kouveliotou, C., Finger, M., & Baring, M. G. 2007, Astroph. J. Suppl, 169, 75

Kaneko, Y., Ramirez-Ruiz, E., Granot, J., et al. 2007, Astroph. J., 654, 385

Kann, D. A. 2006, GCN Circular 5875

Kann, D. A. 2007, GCN Circular 6209

Kann, D. A., Covino, S., & Malesani, D. 2006a, GCN Circular 4913

Kann, D. A., Cusano, F., & Ludwig, F. 2009a, GCN Circular 9842

Kann, D. A., Filgas, R., & Högner, C. 2007a, GCN Circular 6206

Kann, D. A., Högner, C., & Ertel, S. 2008a, GCN Circular 7696

Kann, D. A., Högner, C., & Ertel, S. 2008b, GCN Circular 7688

Kann, D. A., Högner, C., Ertel, S., & Schulze, S. 2008c, GCN Circular 7701

Kann, D. A., Högner, C., & Filgas, R. 2007b, GCN Circular 6917

Kann, D. A., Högner, C., Filgas, R., & Klose, S. 2008d, GCN Circular 7705

Kann, D. A., Högner, C., Laux, U., & Filgas, R. 2007c, GCN Circular 6926

Kann, D. A., Klose, S., & Zeh, A. 2006b, Astroph. J., 641, 993

Kann, D. A., Klose, S., Zhang, B., et al. 2010, Astroph. J., 720, 1513

Kann, D. A., Klose, S., Zhang, B., et al. 2008e, Astroph. J., submitted (arXiv:0804.1959v1)

Kann, D. A. & Laux, U. 2009, GCN Circular 10077

Kann, D. A., Laux, U., & Ertel, S. 2008f, GCN Circular 7865

Kann, D. A., Laux, U., & Ertel, S. 2008g, GCN Circular 7823

Kann, D. A., Laux, U., & Filgas, R. 2007d, GCN Circular 6930

Kann, D. A., Laux, U., & Stecklum, B. 2009b, GCN Circular 9436

Kann, D. A., Laux, U., Stecklum, B., & Klose, S. 2007e, GCN Circular 6545

Kann, D. A. & Malesani, D. 2006, GCN Circular 5866

Kann, D. A. & Manohar, S. 2006a, GCN Circular 5278

Kann, D. A. & Manohar, S. 2006b, GCN Circular 5279

Kann, D. A. & Manohar, S. 2006c, GCN Circular 5284

Kann, D. A., Masetti, N., & Klose, S. 2007f, Astron. J., 133, 1187

Kann, D. A., Palazzi, E., Masetti, N., & Maiorano, E. 2006c, GCN Circular 5025

Kann, D. A., Schulze, S., & Hoegner, C. 2008h, GCN Circular 8423

Kann, D. A., Schulze, S., Hoegner, C., Klose, S., & Greiner, J. 2008i, GCN Circular 8420

Kann, D. A., Schulze, S., & Updike, A. C. 2008j, GCN Circular 7627

Kann, D. A. & Stecklum, B. 2006, GCN Circular 4909

Kann, D. A. & Wilson, A. C. 2007, GCN Circular 6629

Kann, D. A., Zeh, A., & Ludwig, F. 2004, GCN Circular 2614

Kasliwal, M. M., Cenko, S. B., Kulkarni, S. R., et al. 2008, Astroph. J., 678, 1127

Kawai, N., Kosugi, G., Aoki, K., et al. 2006, Nature, 440, 184

Kelly, P. L., Kirshner, R. P., & Pahre, M. 2008, Astroph. J., 687, 1201

King, A., Olsson, E., & Davies, M. B. 2007, Mon. Not. R. Astron. Soc., 374, L34

Kirk, J. G., Guthmann, A. W., Gallant, Y. A., & Achterberg, A. 2000, Astroph. J., 542, 235

Kiuchi, K., Sekiguchi, Y., Shibata, M., & Taniguchi, K. 2010, Physical Review Letters, 104, 141101

Klebesadel, R. W., Strong, I. B., & Olson, R. A. 1973, Astroph. J., 182, L85

Klose, S., Ferrero, P., Kann, D. A., Stecklum, B., & Laux, U. 2005a, GCN Circular 4207

Klose, S., Stecklum, B., Fuhrmann, B., Ludwig, F., & Greiner, J. 2005b, GCN Circular 3609

Klotz, A., Boër, M., Atteia, J. L., & Gendre, B. 2009, Astron. J., 137, 4100

Klotz, A., Boër, M., Atteia, J. L., et al. 2005, Astron. & Astroph., 439, L35

Kocevski, D., Bouvier, A., McEnery, J., et al. 2009, GCN Circular 10128

Kocevski, D. & Butler, N. 2008, Astroph. J., 680, 531

Kocevski, D., Modjaz, M., Bloom, J. S., et al. 2007, Astroph. J., 663, 1180

Kocevski, D., Thöne, C. C., Ramirez-Ruiz, E., et al. 2010, Mon. Not. R. Astron. Soc., 404, 963

Königl, A. & Granot, J. 2002, Astroph. J., 574, 134

Kouveliotou, C., Meegan, C. A., Fishman, G. J., et al. 1993, Astroph. J., 413, L101

Kouveliotou, C., Woosley, S. E., Patel, S. K., et al. 2004, Astroph. J., 608, 872

Krimm, H. A., Hurkett, C., Pal'shin, V., et al. 2006, Astroph. J., 648, 1117

Krimm, H. A., Yamaoka, K., Sugita, S., et al. 2009, Astroph. J., 704, 1405

Krühler, T., Greiner, J., Afonso, P., et al. 2009, Astron. & Astroph., 508, 593

Krühler, T., Küpcü Yoldaş, A., Greiner, J., et al. 2008a, Astroph. J., 685, 376

Krühler, T., Küpcü Yoldaş, A., Greiner, J., et al. 2008b, Astroph. J., 685, 376

Kuin, N. P. M., Landsman, W., Page, M. J., et al. 2009, Mon. Not. R. Astron. Soc., 395, L21

Kulkarni, S. R. 2005, arXiv:astro-ph/0510256

Kulkarni, S. R., Djorgovski, S. G., Odewahn, S. C., et al. 1999, Nature, 398, 389

Kulkarni, S. R., Djorgovski, S. G., Ramaprakash, A. N., et al. 1998, Nature, 393, 35

Kumar, P. & Narayan, R. 2009a, Mon. Not. R. Astron. Soc., 395, 472

Kumar, P. & Narayan, R. 2009b, Mon. Not. R. Astron. Soc., 395, 472

Kumar, P. & Panaitescu, A. 2008, Mon. Not. R. Astron. Soc., 391, L19

La Parola, V., Mangano, V., Fox, D., et al. 2006, Astron. & Astroph., 454, 753

Lamb, D. Q., Donaghy, T. Q., & Graziani, C. 2005, Astroph. J., 620, 355

Lapi, A., Kawakatu, N., Bosnjak, Z., et al. 2008, Mon. Not. R. Astron. Soc., 386, 608

Lazzati, D., Morsony, B. J., & Begelman, M. C. 2010, Astroph. J., 717, 239

Le Floc'h, E., Duc, P., Mirabel, I. F., et al. 2003, Astron. & Astroph., 400, 499

Lee, W. H. & Ramirez-Ruiz, E. 2007, New J. Phys., 9, 17

Lee, W. H., Ramirez-Ruiz, E., & van de Ven, G. 2010, Astroph. J., 720, 953

Leloudas, G., Sollerman, J., Levan, A. J., et al. 2010, Astron. & Astroph., in press (arXiv:1002.3164)

Levan, A. J., Tanvir, N. R., Fruchter, A. S., et al. 2006, Astroph. J., 648, L9

Levan, A. J., Tanvir, N. R., Hjorth, J., et al. 2009, GCN Circular 10154

Levan, A. J., Tanvir, N. R., Jakobsson, P., et al. 2008, Mon. Not. R. Astron. Soc., 384, 541

Levesque, E. M., Berger, E., Kewley, L. J., & Bagley, M. M. 2010, Astron. J., 139, 694

Li, A., Liang, S. L., Kann, D. A., et al. 2008, Astroph. J., 685, 1046

Li, L. 2008, Mon. Not. R. Astron. Soc., 388, 1487

Li, L. & Paczyński, B. 1998, Astroph. J., 507, L59

Li, W., Filippenko, A. V., Chornock, R., & Jha, S. 2003, Astroph. J., 586, L9

Liang, E., Racusin, J. L., Zhang, B., Zhang, B.-B., & Burrows, D. N. 2008, Astroph. J., 675, 528

Liang, E. & Zhang, B. 2006, Astroph. J., 638, L67

Liang, E., Zhang, B., Virgili, F., & Dai, Z. G. 2007a, Astroph. J., 662, 1111

Liang, E., Zhang, B., & Zhang, B. 2007b, Astroph. J., 670, 565

Liang, S. L. & Li, A. 2009, Astroph. J., 690, L56

Liang, S. L. & Li, A. 2010, Astroph. J., 710, 648

Lipkin, Y. M., Ofek, E. O., Gal-Yam, A., et al. 2004, Astroph. J., 606, 381

Lithwick, Y. & Sari, R. 2001, Astroph. J., 555, 540

Lü, H.-J., Liang, E., Zhang, B.-B., & Zhang, B. 2010, Astroph. J., submitted (arXiv:1001.0598)

MacFadyen, A. I. & Woosley, S. E. 1999, Astroph. J., 524, 262

Maiolino, R., Schneider, R., Oliva, E., et al. 2004, Nature, 431, 533

Malesani, D., Covino, S., D'Avanzo, P., et al. 2007, Astron. & Astroph., 473, 77

Malesani, D., de Ugarte Postigo, A., Levan, A. J., et al. 2009a, GCN Circular 10156

Malesani, D., Fynbo, J. P. U., Hjorth, J., et al. 2009b, Astroph. J., 692, L84

Malesani, D., Tagliaferri, G., Chincarini, G., et al. 2004, Astroph. J., 609, L5

Mangano, V., Holland, S. T., Malesani, D., et al. 2007, Astron. & Astroph., 470, 105

Margutti, R., Chincarini, G., Covino, S., et al. 2007, Astron. & Astroph., 474, 815

Marisaldi, M., Fuschino, F., Longo, F., et al. 2009, GCN Circular 10022

Mazets, E. P. & Golenetskii, S. V. 1981, Astroph.. & Space Sc., 75, 47

Mazzali, P. A., Deng, J., Nomoto, K., et al. 2006a, Nature, 442, 1018

Mazzali, P. A., Deng, J., Pian, E., et al. 2006b, Astroph. J., 645, 1323

Mazzali, P. A., Valenti, S., Della Valle, M., et al. 2008, Science, 321, 1185

McBreen, S., Foley, S., Watson, D., et al. 2008, Astroph. J., 677, L85

McBreen, S., Krühler, T., Rau, A., et al. 2010, Astron. & Astroph., 516, A71

McGlynn, S., Clark, D. J., Dean, A. J., et al. 2007, Astron. & Astroph., 466, 895

Medvedev, M. V. & Loeb, A. 1999, Astroph. J., 526, 697

Meegan, C. A., Fishman, G. J., Wilson, R. B., et al. 1992, Nature, 355, 143

Melandri, A., Mundell, C. G., Kobayashi, S., et al. 2008, Astroph. J., 686, 1209

Mészáros, P. 2001, Science, 291, 79

Mészáros, P. 2006, Rept. Prog. Phys., 69, 2259

Mészáros, P. & Rees, M. J. 1997, Astroph. J., 476, 232

Mészáros, P. & Rees, M. J. 1999a, Mon. Not. R. Astron. Soc., 306, L39

Mészáros, P. & Rees, M. J. 1999b, Mon. Not. R. Astron. Soc., 306, L39

Metzger, M. R., Djorgovski, S. G., Kulkarni, S. R., et al. 1997, Nature, 387, 878

Mirabal, N., Halpern, J. P., An, D., Thorstensen, J. R., & Terndrup, D. M. 2006, Astroph. J., 643, L99

Modjaz, M., Stanek, K. Z., Garnavich, P. M., et al. 2006, Astroph. J., 645, L21

Molinari, E., Vergani, S. D., Malesani, D., et al. 2007, Astron. & Astroph., 469, L13

Monfardini, A., Kobayashi, S., Guidorzi, C., et al. 2006, Astroph. J., 648, 1125

Moriya, T., Tominaga, N., Tanaka, M., et al. 2010, Astroph. J., 719, 1445

Mundell, C. G., Melandri, A., Guidorzi, C., et al. 2007a, Astroph. J., 660, 489

Mundell, C. G., Steele, I. A., Smith, R. J., et al. 2007b, Science, 315, 1822

Nakagawa, Y. E., Yoshida, A., Sugita, S., et al. 2006, Publ. Astron. Soc. Japan, 58, L35

Nakar, E. 2007a, Physics Reports, 442, 166

Nakar, E. 2007b, Advances in Space Research, 40, 1224

Nakar, E. & Granot, J. 2007, Mon. Not. R. Astron. Soc., 380, 1744

Nakar, E. & Piran, T. 2005, Astroph. J., 619, L147

Nardini, M., Ghisellini, G., & Ghirlanda, G. 2008, Mon. Not. R. Astron. Soc., 386, L87

Nardini, M., Ghisellini, G., Ghirlanda, G., et al. 2006, Astron. & Astroph., 451, 821

Nava, L., Ghirlanda, G., Ghisellini, G., & Celotti, A. 2010, Astron. & Astroph., submitted (arXiv:1004.1410)

Norris, J. P. & Bonnell, J. T. 2006, Astroph. J., 643, 266

Norris, J. P., Gehrels, N., & Scargle, J. D. 2010, Astroph. J., 717, 411

Norris, J. P., Marani, G. F., & Bonnell, J. T. 2000, Astroph. J., 534, 248

Nousek, J. A., Kouveliotou, C., Grupe, D., et al. 2006, Astroph. J., 642, 389

Nysewander, M., Fruchter, A. S., & Pe'er, A. 2009a, Astroph. J., 701, 824

Nysewander, M., Reichart, D. E., Crain, J. A., et al. 2009b, Astroph. J., 693, 1417

Oates, S. R., Page, M. J., Schady, P., et al. 2009, Mon. Not. R. Astron. Soc., 395, 490

O'Brien, P. T., Willingale, R., Osborne, J., et al. 2006, Astroph. J., 647, 1213

Oechslin, R. & Janka, H. 2006, Mon. Not. R. Astron. Soc., 368, 1489

Ofek, E. O., Cenko, S. B., Gal-Yam, A., et al. 2007, Astroph. J., 662, 1129

Ohno, M., Fukazawa, Y., Takahashi, T., et al. 2008, Publ. Astron. Soc. Japan, 60, 361

O'Shaughnessy, R., Belczynski, K., & Kalogera, V. 2008, Astroph. J., 675, 566

Paczynski, B. 1986, Astroph. J., 308, L43

Paczyński, B. 1998, Astroph. J., 494, L45

Page, K. L., Willingale, R., Osborne, J. P., et al. 2007, Astroph. J., 663, 1125

Panaitescu, A. 2006, Mon. Not. R. Astron. Soc., 367, L42

Panaitescu, A. 2007, Mon. Not. R. Astron. Soc., 380, 374

Panaitescu, A., Kumar, P., & Narayan, R. 2001, Astroph. J., 561, L171

Panaitescu, A., Mészáros, P., Burrows, D., et al. 2006a, Mon. Not. R. Astron. Soc., 369, 2059

Panaitescu, A., Mészáros, P., Gehrels, N., Burrows, D., & Nousek, J. 2006b, Mon. Not. R. Astron. Soc., 366, 1357

Panaitescu, A. & Vestrand, W. T. 2008, Mon. Not. R. Astron. Soc., 387, 497

Pastorello, A., Zampieri, L., Turatto, M., et al. 2004, Mon. Not. R. Astron. Soc., 347, 74

Pei, Y. C. 1992, Astroph. J., 395, 130

Pelangeon, A. & Atteia, J. 2008, GCN Circular 7760

Pellizza, L. J., Duc, P., Le Floc'h, E., et al. 2006, Astron. & Astroph., 459, L5

Perley, D. A., Bloom, J. S., Butler, N. R., et al. 2008a, Astroph. J., 672, 449

Perley, D. A., Bloom, J. S., Klein, C. R., et al. 2010, Mon. Not. R. Astron. Soc., 406, 2473

Perley, D. A., Bloom, J. S., Modjaz, M., et al. 2008b, GCN Circular 7889

Perley, D. A., Bloom, J. S., Modjaz, M., Poznanski, D., & Thoene, C. C. 2007a, GCN Circular 7140

Perley, D. A., Cenko, S. B., Bloom, J. S., et al. 2009a, Astron. J., 138, 1690

Perley, D. A., Li, W., Chornock, R., et al. 2008c, Astroph. J., 688, 470

Perley, D. A., Metzger, B. D., Granot, J., et al. 2009b, Astroph. J., 696, 1871

Perley, D. A., Thoene, C. C., & Bloom, J. S. 2007b, GCN Circular 6774

Pian, E., Mazzali, P. A., Masetti, N., et al. 2006, Nature, 442, 1011

Piran, T. 1997, in Unsolved Problems in Astrophysics, 343–377

Piran, T. 2005, Rev. Mod. Phys., 76, 1143

Piranomonte, S., D'Avanzo, P., Covino, S., et al. 2008, Astron. & Astroph., 491, 183

Pontzen, A., Hewett, P., Carswell, R., & Wild, V. 2007, Mon. Not. R. Astron. Soc., 381, L99

Porciani, C., Viel, M., & Lilly, S. J. 2007, Astroph. J., 659, 218

Prochaska, J. X., Bloom, J. S., Chen, H., et al. 2006a, Astroph. J., 642, 989

Prochaska, J. X., Bloom, J. S., Chen, H., et al. 2004, Astroph. J., 611, 200

Prochaska, J. X., Chen, H., & Bloom, J. S. 2006b, Astroph. J., 648, 95

Prochaska, J. X., Ellison, S., Foley, R. J., Bloom, J. S., & Chen, H. . 2005, GCN Circular 3332

Prochaska, J. X., Sheffer, Y., Perley, D. A., et al. 2009, Astroph. J., 691, L27

Prochter, G. E., Prochaska, J. X., Chen, H., et al. 2006, Astroph. J., 648, L93

Quimby, R. M., Rykoff, E. S., Yost, S. A., et al. 2006, Astroph. J., 640, 402

Racusin, J. L., Karpov, S. V., Sokolowski, M., et al. 2008, Nature, 455, 183

Racusin, J. L., Liang, E. W., Burrows, D. N., et al. 2009, Astroph. J., 698, 43

Rau, A., Savaglio, S., Krühler, T., et al. 2010, Astroph. J., 720, 862

Rees, M. J. 1995, Publ. Astron. Soc. Pacific, 107, 1176

Rees, M. J. & Mészáros, P. 1992, Mon. Not. R. Astron. Soc., 258, 41P

Resmi, L. & Bhattacharya, D. 2008, Mon. Not. R. Astron. Soc., 388, 144

Rhoads, J. E. 1997, Astroph. J., 487, L1

Rhoads, J. E. 1999, Astroph. J., 525, 737

Richardson, D., Branch, D., & Baron, E. 2006, Astron. J., 131, 2233

Richardson, D., Branch, D., Casebeer, D., et al. 2002, Astron. J., 123, 745

Rol, E., van der Horst, A., Wiersema, K., et al. 2007, Astroph. J., 669, 1098

Romano, P., Campana, S., Chincarini, G., et al. 2006, Astron. & Astroph., 456, 917

Roming, P. W. A., Schady, P., Fox, D. B., et al. 2006a, Astroph. J., 652, 1416

Roming, P. W. A., Vanden Berk, D., Pal'shin, V., et al. 2006b, Astroph. J., 651, 985

Rossi, A., de Ugarte Postigo, A., Ferrero, P., et al. 2008, Astron. & Astroph., 491, L29

Rosswog, S. 2005, Astroph. J., 634, 1202

Rosswog, S., Ramirez-Ruiz, E., & Davies, M. B. 2003, Mon. Not. R. Astron. Soc., 345, 1077

Rowlinson, A., O'Brien, P. T., Tanvir, N. R., et al. 2010a, Mon. Not. R. Astron. Soc., in press (arXiv:1007.2185)

Rowlinson, A., Wiersema, K., Levan, A. J., et al. 2010b, Mon. Not. R. Astron. Soc., 1138

Ruiz-Velasco, A. E., Swan, H., Troja, E., et al. 2007, Astroph. J., 669, 1

Rykoff, E. S., Aharonian, F., Akerlof, C. W., et al. 2009, Astroph. J., 702, 489

Rykoff, E. S., Mangano, V., Yost, S. A., et al. 2006, Astroph. J., 638, L5

Rykoff, E. S., Swan, H., Schaefer, B., & Quimby, R. 2005, GCN Circular 3382

Salmonson, J. D. 2000, Astroph. J., 544, L115

Salvaterra, R., Cerutti, A., Chincarini, G., et al. 2008, Mon. Not. R. Astron. Soc., 388, L6

Salvaterra, R., Della Valle, M., Campana, S., et al. 2009, Nature, 461, 1258

Salvaterra, R., Devecchi, B., Colpi, M., & D'Avanzo, P. 2010, Mon. Not. R. Astron. Soc., 406, 1248

Sari, R. & Piran, T. 1999a, Astroph. J., 517, L109

Sari, R. & Piran, T. 1999b, Astroph. J., 517, L109

Sari, R., Piran, T., & Narayan, R. 1998, Astroph. J., 497, L17

Sato, G., Yamazaki, R., Ioka, K., et al. 2007, Astroph. J., 657, 359

Sato, R., Kawai, N., Suzuki, M., et al. 2003, Astroph. J., 599, L9

Savaglio, S. 2006, New Journal of Physics, 8, 195

Savaglio, S., Glazebrook, K., & Le Borgne, D. 2009, Astroph. J., 691, 182

Sazonov, S. Y., Lutovinov, A. A., & Sunyaev, R. A. 2004, Nature, 430, 646

Schady, P., de Pasquale, M., Page, M. J., et al. 2007a, Mon. Not. R. Astron. Soc., 380, 1041

Schady, P., Mason, K. O., Page, M. J., et al. 2007b, Mon. Not. R. Astron. Soc., 377, 273

Schady, P., Page, M. J., Oates, S. R., et al. 2010, Mon. Not. R. Astron. Soc., 401, 2773

Schaefer, B. E. 2006, Astroph. J., 642, L25

Schaefer, B. E. & Xiao, L. 2006, Astroph. J., submitted (arXiv:astro-ph/0608441)

Schlegel, D. J., Finkbeiner, D. P., & Davis, M. 1998, Astroph. J., 500, 525

Shao, L. & Dai, Z. G. 2005, Astroph. J., 633, 1027

Shen, R., Kumar, P., & Robinson, E. L. 2006, Mon. Not. R. Astron. Soc., 371, 1441

Smartt, S. J. 2009, Annu. Rev. Astro. Astroph., 47, 63

Soderberg, A. M., Berger, E., Kasliwal, M., et al. 2006a, Astroph. J., 650, 261

Soderberg, A. M., Berger, E., Page, K. L., et al. 2008, Nature, 453, 469

Soderberg, A. M., Kulkarni, S. R., Berger, E., et al. 2004a, Astroph. J., 606, 994

Soderberg, A. M., Kulkarni, S. R., Berger, E., et al. 2004b, Nature, 430, 648

Soderberg, A. M., Kulkarni, S. R., Fox, D. B., et al. 2005, Astroph. J., 627, 877

Soderberg, A. M., Kulkarni, S. R., Nakar, E., et al. 2006b, Nature, 442, 1014

Soderberg, A. M., Kulkarni, S. R., Price, P. A., et al. 2006c, Astroph. J., 636, 391

Sollerman, J., Fynbo, J. P. U., Gorosabel, J., et al. 2007, Astron. & Astroph., 466, 839

Sollerman, J., Jaunsen, A. O., Fynbo, J. P. U., et al. 2006, Astron. & Astroph., 454, 503

Spergel, D. N., Verde, L., Peiris, H. V., et al. 2003, Astroph. J. Suppl, 148, 175

Stanek, K. Z., Gnedin, O. Y., Beacom, J. F., et al. 2006, Acta Astronomica, 56, 333

Stanek, K. Z., Matheson, T., Garnavich, P. M., et al. 2003, Astroph. J., 591, L17

Starling, R. L. C., Rol, E., van der Horst, A. J., et al. 2009, Mon. Not. R. Astron. Soc., 400, 90

Starling, R. L. C., van der Horst, A. J., Rol, E., et al. 2008, Astroph. J., 672, 433

Starling, R. L. C., Wiersema, K., Levan, A. J., et al. 2010, Mon. Not. R. Astron. Soc., submitted (arXiv:1004.2919)

Starling, R. L. C., Wijers, R. A. M. J., Wiersema, K., et al. 2007, Astroph. J., 661, 787

Steele, I. A., Mundell, C. G., Smith, R. J., Kobayashi, S., & Guidorzi, C. 2009, Nature, 462, 767

Stefanescu, A., Kanbach, G., Słowikowska, A., et al. 2008, Nature, 455, 503

Stefanescu, A., Slowikowska, A., Kanbach, G., et al. 2007, GCN Circular 6492

Stratta, G., Basa, S., Butler, N., et al. 2007a, Astron. & Astroph., 461, 485

Stratta, G., D'Avanzo, P., Piranomonte, S., et al. 2007b, Astron. & Astroph., 474, 827

Stratta, G., Fiore, F., Antonelli, L. A., Piro, L., & De Pasquale, M. 2004, Astroph. J., 608, 846

Stratta, G., Maiolino, R., Fiore, F., & D'Elia, V. 2007c, Astroph. J., 661, L9

Sudilovsky, V., Savaglio, S., Vreeswijk, P., et al. 2007, Astroph. J., 669, 741

Sudilovsky, V., Smith, D., & Savaglio, S. 2009, Astroph. J., 699, 56

Tagliaferri, G., Antonelli, L. A., Chincarini, G., et al. 2005a, Astron. & Astroph., 443, L1

Tagliaferri, G., Goad, M., Chincarini, G., et al. 2005b, Nature, 436, 985

Tanvir, N. R., Fox, D. B., Levan, A. J., et al. 2009, Nature, 461, 1254

Tanvir, N. R., Levan, A. J., Rol, E., et al. 2008a, Mon. Not. R. Astron. Soc., 388, 1743

Tanvir, N. R., Rol, E., Levan, A., et al. 2008b, Astroph. J., submitted (arXiv:0812.1217)

Tanvir, N. R., Vergani, S., Hjorth, J., et al. 2010, GCN Circular 11123

Tejos, N., Lopez, S., Prochaska, J. X., et al. 2009, Astroph. J., 706, 1309

Tejos, N., Lopez, S., Prochaska, J. X., Chen, H., & Dessauges-Zavadsky, M. 2007, Astroph. J., 671, 622

Thöne, C. C., Fynbo, J. P. U., & Jørgensen, U. G. 2006, GCN Circular 5179

Thöne, C. C., Fynbo, J. P. U., Östlin, G., et al. 2008a, Astroph. J., 676, 1151

Thöne, C. C., Greiner, J., Savaglio, S., & Jehin, E. 2007, Astroph. J., 671, 628

Thöne, C. C., Kann, D. A., Johannesson, G., et al. 2010, Astron. & Astroph., in press (arXiv:0806.1182v3)

Thöne, C. C., Wiersema, K., Ledoux, C., et al. 2008b, Astron. & Astroph., 489, 37

Tominaga, N., Maeda, K., Umeda, H., et al. 2007, Astroph. J., 657, L77

Troja, E., King, A. R., O'Brien, P. T., Lyons, N., & Cusumano, G. 2008, Mon. Not. R. Astron. Soc., 385, L10

Updike, A. C., Haislip, J. B., Nysewander, M. C., et al. 2008, Astroph. J., 685, 361

Usov, V. V. 1992, Nature, 357, 472

van den Heuvel, E. P. J. 2007, in American Institute of Physics Conference Series, Vol. 924, The Multicolored Landscape of Compact Objects and Their Explosive Origins, ed. T. di Salvo, G. L. Israel, L. Piersant, L. Burderi, G. Matt, A. Tornambe, & M. T. Menna, 598–606

van Paradijs, J., Groot, P. J., Galama, T., et al. 1997, Nature, 386, 686

Vergani, S. D., Petitjean, P., Ledoux, C., et al. 2009, Astron. & Astroph., 503, 771

Vestrand, W. T., Borozdin, K., Casperson, D. J., et al. 2004, Astronomische Nachrichten, 325, 549

Vestrand, W. T., Wozniak, P. R., Wren, J. A., et al. 2005, Nature, 435, 178

Vestrand, W. T., Wren, J. A., Wozniak, P. R., et al. 2006, Nature, 442, 172

Villasenor, J. S., Lamb, D. Q., Ricker, G. R., et al. 2005, Nature, 437, 855

Virgili, F. J., Liang, E., & Zhang, B. 2009, Mon. Not. R. Astron. Soc., 392, 91

Volnova, A. A., Pozanenko, A. S., Rumyantsev, V. V., et al. 2010, Astron. Bulletin, in press

Vreeswijk, P. M., Ellison, S. L., Ledoux, C., et al. 2004, Astron. & Astroph., 419, 927

Wainwright, C., Berger, E., & Penprase, B. E. 2007, Astroph. J., 657, 367

Wang, W. ., Kakazu, Y., Schmidt, B. P., et al. 2006, GCN Circular 4653

Watson, D., Fynbo, J. P. U., Ledoux, C., et al. 2006, Astroph. J., 652, 1011

Watson, D., Hjorth, J., Fynbo, J. P. U., et al. 2007, Astroph. J., 660, L101

Wei, D. M., Yan, T., & Fan, Y. Z. 2006, Astroph. J., 636, L69

Wiersema, K., van der Horst, A. J., Kann, D. A., et al. 2008, Astron. & Astroph., 481, 319

Willingale, R., O'Brien, P. T., Osborne, J. P., et al. 2007, Astroph. J., 662, 1093

Willis, D. R., Barlow, E. J., Bird, A. J., et al. 2005, Astron. & Astroph., 439, 245

Woosley, S. E. 1993, Astroph. J., 405, 273

Woosley, S. E. & Bloom, J. S. 2006, Annu. Rev. Astro. Astroph., 44, 507

Woźniak, P. R., Vestrand, W. T., Panaitescu, A. D., et al. 2009, Astroph. J., 691, 495

Woźniak, P. R., Vestrand, W. T., Wren, J. A., Evans, S., & White, R. R. 2005, GCN Circular 3414

Woźniak, P. R., Vestrand, W. T., Wren, J. A., et al. 2006, Astroph. J., 642, L99

Wyithe, S., Oh, S. P., & Pindor, B. 2010, Mon. Not. R. Astron. Soc., submitted, arXiv:1004.2081

Xu, D., Starling, R. L. C., Fynbo, J. P. U., et al. 2009, Astroph. J., 696, 971

Yonetoku, D., Murakami, T., Nakamura, T., et al. 2004, Astroph. J., 609, 935

Yoon, S., Langer, N., & Norman, C. 2006, Astron. & Astroph., 460, 199

Yost, S. A., Alatalo, K., Rykoff, E. S., et al. 2006, Astroph. J., 636, 959

Yost, S. A., Swan, H. F., Rykoff, E. S., et al. 2007, Astroph. J., 657, 925

Yuan, F., Rykoff, E. S., Schaefer, B. E., et al. 2008, in American Institute of Physics Conference Series, Vol. 1065, American Institute of Physics Conference Series, ed. Y.-F. Huang, Z.-G. Dai, & B. Zhang, 103–106

Zeh, A., Kann, D. A., Klose, S., & Hartmann, D. H. 2005a, Nuovo Cimento C Geophysics Space Physics C, 28, 617

Zeh, A., Kann, D. A., Klose, S., Manning, A., & Riddle, C. 2005b, GCN Circular 3646

Zeh, A., Klose, S., & Hartmann, D. H. 2004, Astroph. J., 609, 952

Zeh, A., Klose, S., & Kann, D. A. 2006a, Astroph. J., 637, 889

Zeh, A., Riddle, C., Klose, S., Kann, D. A., & Hartmann, D. H. 2006b, in American Institute of Physics Conference Series, Vol. 836, Gamma-Ray Bursts in the Swift Era, ed. S. S. Holt, N. Gehrels, & J. A. Nousek, 464–466

Zhang, B. 2007, Chin. J. Astron. Astroph., 7, 1

Zhang, B., Fan, Y. Z., Dyks, J., et al. 2006, Astroph. J., 642, 354

Zhang, B., Liang, E., Page, K. L., et al. 2007a, Astroph. J., 655, 989

Zhang, B., Liang, E., Page, K. L., et al. 2007b, Astroph. J., 655, 989

Zhang, B. & Mészáros, P. 2004, International Journal of Modern Physics A, 19, 2385

Zhang, B., Zhang, B., Liang, E., et al. 2007c, Astroph. J., 655, L25

Zhang, B., Zhang, B., Virgili, F. J., et al. 2009, Astroph. J., 703, 1696

Zhang, B., Zhang, B.-B., Liang, E.-W., et al. 2007d, Astroph. J., 655, L25

Zhang, W., Woosley, S. E., & MacFadyen, A. I. 2003, Astroph. J., 586, 356

Zheng, W., Deng, J., & Wang, J. 2009, Research in Astronomy and Astrophysics, 9, 1103

Zou, Y. C., Dai, Z. G., & Xu, D. 2006, Astroph. J., 646, 1098

Appendix A

Tables

Table A.1: Results of the SED Fitting for the Golden Sample, Part 1

GRB	Filters	No Extinction		MW Dust		
		χ^2_{dof}	β_0	χ^2_{dof}	β	A_V
990510	$BVR_ci^GI_cJHK_S$	1.83	0.61 ± 0.04	1.95	0.69 ± 0.09	-0.06 ± 0.06
011211	BVR_cI_cJK	1.57	0.72 ± 0.04	1.3	0.84 ± 0.09	-0.09 ± 0.06
030323	R_cI_cJH	0.94	0.85 ± 0.03	0	1.22 ± 0.27	-0.35 ± 0.25
050319	VR_CI_CK	0.38	1.00 ± 0.06	0.71	0.94 ± 0.33	0.06 ± 0.31
050408	$UBVR_cI_cZJHK$	3.12	1.61 ± 0.14	3.27	1.17 ± 0.60	0.33 ± 0.44
050416A	$U_3U_2UBVR_CI_Cz'K_S$	0.39	1.15 ± 0.17	0.91	1.20 ± 0.45	0.11 ± 0.38
050502A	$R_ci'JHK_s$	0.76	0.95 ± 0.06	0.39	0.46 ± 0.22	0.40 ± 0.18
050525A	$U_1UBVR_cJHKS_{3.6}S_{4.5}S_{8.0}S_{24.0}$	12.7	1.02 ± 0.03	13.7	1.12 ± 0.07	-0.11 ± 0.06
050730	$i'I_cJK$	0.71	0.82 ± 0.04	0.89	0.88 ± 0.09	-0.08 ± 0.10
050801	BVR_CI_CJK	3.53	1.28 ± 0.10	4.43	1.40 ± 0.17	-0.07 ± 0.07
050802	$UBVR_CI_C$	0.9	0.78 ± 0.05	1.01	0.76 ± 0.06	0.05 ± 0.07
050820A	$g'VR_cI_cz'JHK$	1.09	0.96 ± 0.03	1.12	0.98 ± 0.04	0.02 ± 0.02
050824	$U_1UBVR_CI_CK$	0.79	0.65 ± 0.07	0.97	0.70 ± 0.29	-0.05 ± 0.19
050904	$YJHK$	0.05	1.00 ± 0.09	0.01	0.99 ± 0.10	0.02 ± 0.08
050922C	BVR_cI_c	0.02	0.56 ± 0.01	0.04	0.56 ± 0.01	0.00 ± 0.01
060124	BVR_cI_c	15.13	0.54 ± 0.11	0.9	0.57 ± 0.03	0.17 ± 0.03
060206	$R_cI_ci'z'JHK_s$	0.25	0.77 ± 0.01	0.24	0.81 ± 0.04	-0.03 ± 0.03
060418	$UBVr'R_ci'I_cz'JHK$	2.11	0.98 ± 0.02	2.06	0.88 ± 0.07	0.07 ± 0.05
060526	$r'R_ci'I_cJHK_s$	0.08	0.65 ± 0.06	0.07	0.70 ± 0.18	-0.05 ± 0.16
060607A	$g'Vr'R_ci'I_cJHK$	0.88	0.98 ± 0.08	0.98	0.85 ± 0.26	0.10 ± 0.18
060904B	$U_2U_1UBVR_cI_cJK$	1.14	1.21 ± 0.03	1.04	1.31 ± 0.13	-0.11 ± 0.13
060908	$BVr'R_Ci'I_Cz'JHK$	0.17	0.30 ± 0.06	0.18	0.33 ± 0.15	-0.02 ± 0.08
061007	$UBVR_Ci'JHK$	9.08	1.93 ± 0.03	10.4	1.87 ± 0.05	0.05 ± 0.03
061126	$UBVR_cI_cJHK_S$	3.57	0.97 ± 0.03	4.16	0.96 ± 0.11	0.01 ± 0.08
070125	$UBg'Vr'R_ci'I_cJHK$	1.88	0.86 ± 0.02	2.12	0.85 ± 0.03	0.00 ± 0.02
070419A	$Bg^GVr'R_Ci'I_Cz'JHK$	1.52	1.01 ± 0.10	1.5	0.60 ± 0.36	0.35 ± 0.29
070802	$Bg_GVr_GR_ci_GI_cz_Gz^GJ_GH_GK_G$	6.88	2.98 ± 0.04	4.78	2.24 ± 0.16	0.52 ± 0.11
071003	$g'VR_ci'I_cz'K_S$	1.09	1.09 ± 0.09	1.14	1.32 ± 0.27	-0.18 ± 0.20
071010A	$UBVR_cI_cJHK$	20.4	1.51 ± 0.07	15.08	0.88 ± 0.40	0.52 ± 0.32
071031	$Vr_GR_ci_GI_cz_GJJ_GH_GKK_G$	0.37	0.66 ± 0.06	0.25	0.76 ± 0.11	-0.08 ± 0.07
071112C	$U_1UBVR_CI_CJHK_S$	1.04	0.94 ± 0.08	0.75	0.05 ± 0.56	0.79 ± 0.49
080129	$i_Gz_GJ_GH_GK_G$	0.81	0.69 ± 0.05	1.21	0.68 ± 0.09	0.01 ± 0.07

080210	$Bg_Gg'Vr_GR_Ci_Gz_GJ_GH_GK_G$	6.25	1.90 ± 0.08	5.91	1.53 ± 0.15	0.35 ± 0.12
080310	$Bg^GVr'R_ci'I_cz'JHK$	2.67	0.87 ± 0.03	2.48	1.00 ± 0.08	-0.10 ± 0.05
080319B	$UBVr'R_ci'I_cz'JHK_S$	0.73	0.21 ± 0.03	0.72	0.14 ± 0.08	0.05 ± 0.06
080319C	$UBVR_ci'z'$	7.4	3.10 ± 0.08	2.68	3.64 ± 0.16	-0.29 ± 0.06
080330	$UBg'Vr'R_ci'I_cz'JJ_GHH_GKK_G$	0.46	0.75 ± 0.04	0.43	0.53 ± 0.16	0.16 ± 0.11
080413A	VR_cI_cJHK	0.28	0.81 ± 0.08	0.21	0.91 ± 0.17	-0.08 ± 0.12
080710	$U_2U_1Bg_GVr_GR_Ci_Gi_GI_Cz_GJJ_GH_GK_G$	0.77	0.99 ± 0.03	0.83	1.11 ± 0.14	-0.10 ± 0.12
080913	$JJ_GH_GK_G$	0.41	1.16 ± 0.17	0.05	1.13 ± 0.17	0.08 ± 0.09
080916C	$i_Gz_GJJ_GHH_GK_SK_G$	0.45	0.38 ± 0.10	0.52	0.36 ± 0.12	0.03 ± 0.10
080928	$UBg_GVr_GR_Ci_Gz_GJ_GH_GK_G$	0.49	1.30 ± 0.07	0.19	1.08 ± 0.14	0.14 ± 0.08
081008	$Bg_GVr_GR_Ci_GI_Cz_GJJ_GH_GKK_G$	1.30	0.73 ± 0.06	0.98	1.01 ± 0.14	-0.22 ± 0.10
090102	$UBg_GVR_Ci_Gz_GJ_GH_GHK_G$	0.44	0.97 ± 0.05	0.49	1.04 ± 0.41	-0.06 ± 0.34
090313	$r'R_ci'I_cz'JHK_S$	1.69	1.65 ± 0.08	0.87	2.05 ± 0.18	-0.33 ± 0.13
090323	$i'i_Gz_GJ_GH_GK_G$	2.88	1.14 ± 0.02	1.60	1.28 ± 0.06	-0.13 ± 0.05
090328	$Ug_Gr_Gi_Gi'z_GJ_GH_GK_G$	1.25	1.41 ± 0.04	1.26	1.26 ± 0.14	0.12 ± 0.11
090424	$U_1UBg_GVr_Gr'R_Ci_GI_Cz_GJJ_GH_GKK_G$	2.65	1.58 ± 0.03	1.92	1.10 ± 0.15	0.42 ± 0.13
090902B	$Ug_GVr_Gr'i_Gi'z_GJJ_GH_GK_GK$	2.18	0.87 ± 0.04	2.16	0.96 ± 0.07	-0.06 ± 0.04
090926A	$Bg_Gg'Vr_Gr'R_Ci_Gi'I_Cz_GJJ_GH_GK_G$	2.64	1.07 ± 0.05	2.15	1.28 ± 0.09	-0.18 ± 0.06

Table A.2: Results of the SED Fitting for the Golden Sample, Part 2

GRB	LMC Dust			SMC Dust		
	χ^2_{dof}	β	A$_V$	χ^2_{dof}	β	A$_V$
990510	1.81	0.36 ± 0.18	0.16 ± 0.11	0.21	0.17 ± 0.15	0.22 ± 0.07
011211	1.82	0.51 ± 0.24	0.13 ± 0.14	0.45	0.41 ± 0.15	0.14 ± 0.06
030323	0.03	0.15 ± 0.51	0.35 ± 0.26	0.03	0.46 ± 0.28	0.13 ± 0.09
050319	0.17	0.64 ± 0.52	0.12 ± 0.17	0.31	0.74 ± 0.42	0.05 ± 0.09
050408	1.1	0.01 ± 0.47	1.06 ± 0.31	0.59	0.28 ± 0.27	0.74 ± 0.15
050416A	0.56	0.84 ± 0.38	0.33 ± 0.24	0.46	0.92 ± 0.30	0.21 ± 0.14
050502A	0.35	0.43 ± 0.22	0.24 ± 0.10	0.16	0.76 ± 0.16	0.05 ± 0.05
050525A	11.27	0.53 ± 0.10	0.42 ± 0.08	8.42	0.52 ± 0.08	0.36 ± 0.05
050730	0.5	0.45 ± 0.28	0.21 ± 0.16	0.03	0.52 ± 0.05	0.10 ± 0.02
050801	4.7	1.29 ± 0.25	-0.01 ± 0.13	3.69	0.69 ± 0.34	0.30 ± 0.18
050802	0.06	0.36 ± 0.26	0.21 ± 0.13	0.74	0.39 ± 0.35	0.10 ± 0.10
050820A	0.67	0.91 ± 0.03	0.04 ± 0.02	0.06	0.72 ± 0.03	0.07 ± 0.01
050824	0.76	0.44 ± 0.24	0.17 ± 0.19	0.59	0.45 ± 0.18	0.14 ± 0.13
050904	0.03	0.92 ± 0.35	0.05 ± 0.20	0.03	1.31 ± 1.20	-0.10 ± 0.40
050922C	0.03	0.53 ± 0.05	0.02 ± 0.02	0.02	0.51 ± 0.05	0.01 ± 0.01
060124	13.48	0.13 ± 0.38	0.19 ± 0.17	29	0.30 ± 1.13	0.05 ± 0.26
060206	0.31	0.75 ± 0.09	0.01 ± 0.05	0.27	0.73 ± 0.05	0.01 ± 0.02
060418	1.54	0.69 ± 0.11	0.20 ± 0.08	1.74	0.78 ± 0.09	0.12 ± 0.05
060526	0.04	0.35 ± 0.62	0.16 ± 0.33	0.05	0.51 ± 0.32	0.05 ± 0.11
060607A	0.85	0.65 ± 0.30	0.15 ± 0.13	0.87	0.72 ± 0.27	0.08 ± 0.08
060904B	1.08	1.13 ± 0.12	0.07 ± 0.12	0.93	1.11 ± 0.10	0.08 ± 0.08
060908	0.19	0.29 ± 0.28	0.01 ± 0.15	0.18	0.24 ± 0.20	0.03 ± 0.10
061007	6.19	1.07 ± 0.19	0.48 ± 0.10	9.5	1.62 ± 0.14	0.13 ± 0.05
061126	3.52	0.84 ± 0.12	0.09 ± 0.09	2.77	0.82 ± 0.09	0.10 ± 0.06
070125	1.77	0.73 ± 0.08	0.07 ± 0.04	0.96	0.59 ± 0.10	0.11 ± 0.04
070419A	1.5	0.46 ± 0.47	0.46 ± 0.39	1.54	0.48 ± 0.48	0.42 ± 0.37
070802	2.84	1.07 ± 0.31	1.18 ± 0.19	6.44	2.31 ± 0.21	0.34 ± 0.11
071003	0.99	0.45 ± 0.52	0.43 ± 0.35	0.1	0.35 ± 0.11	0.40 ± 0.06
071010A	2.78	0.37 ± 0.21	0.90 ± 0.16	1.61	0.61 ± 0.12	0.64 ± 0.09
071031	0.36	0.89 ± 0.37	-0.14 ± 0.22	0.27	0.34 ± 0.30	0.14 ± 0.13
071112C	0.92	0.41 ± 0.42	0.44 ± 0.34	1	0.63 ± 0.29	0.23 ± 0.21
080129	1.22	0.72 ± 0.35	-0.02 ± 0.18	1.18	0.76 ± 0.26	-0.03 ± 0.09
080210	4.36	0.44 ± 0.32	0.71 ± 0.15	6.16	1.19 ± 0.29	0.21 ± 0.08
080310	1.95	0.34 ± 0.19	0.30 ± 0.10	0.92	0.42 ± 0.12	0.19 ± 0.05
080319B	0.72	0.11 ± 0.11	0.07 ± 0.08	0.76	0.13 ± 0.10	0.05 ± 0.07
080319C	8.87	4.20 ± 0.68	-0.43 ± 0.25	0.8	0.98 ± 0.42	0.59 ± 0.12
080330	0.33	0.27 ± 0.20	0.32 ± 0.13	0.35	0.42 ± 0.15	0.19 ± 0.08
080413A	0.37	0.87 ± 0.74	-0.04 ± 0.46	0.17	0.52 ± 0.37	0.13 ± 0.17
080710	0.47	0.75 ± 0.12	0.17 ± 0.08	0.29	0.80 ± 0.09	0.11 ± 0.04
080913	0.04	0.79 ± 0.45	0.21 ± 0.24	0.05	3.02 ± 2.17	-0.58 ± 0.67
080916C	0.45	0.08 ± 0.47	0.16 ± 0.24	0.52	0.23 ± 0.51	0.05 ± 0.16
080928	0.31	0.90 ± 0.29	0.23 ± 0.17	0.55	1.32 ± 0.22	-0.01 ± 0.10
081008	1.41	0.86 ± 0.36	-0.09 ± 0.22	1.19	0.38 ± 0.23	0.17 ± 0.11
090102	0.38	0.63 ± 0.36	0.23 ± 0.24	0.35	0.74 ± 0.22	0.12 ± 0.11
090313	1.98	1.36 ± 0.60	0.16 ± 0.32	0.96	0.74 ± 0.40	0.34 ± 0.15

090323	3.84	1.11 ± 0.32	0.02 ± 0.18	1.35	0.74 ± 0.15	0.16 ± 0.06
090328	1.18	1.20 ± 0.17	0.17 ± 0.14	1.10	1.17 ± 0.17	0.18 ± 0.13
090424	1.49	0.97 ± 0.15	0.50 ± 0.12	1.56	1.12 ± 0.12	0.35 ± 0.09
090902B	2.04	0.58 ± 0.16	0.15 ± 0.08	1.49	0.52 ± 0.12	0.13 ± 0.04
090926A	2.86	1.07 ± 0.27	0.00 ± 0.15	2.43	0.72 ± 0.17	0.13 ± 0.06

Filters that are not used for the fit (e.g, due to Lyman α dampening) are not included. The degrees of freedom of the fit are always number of filters minus three for the fits with extinction, and minus two for the fit without extinction. β_0 is the spectral slope without extinction correction. $U_{1,2,3}$ denote the *Swift* UVOT UVW1, UVM2 and UVW2 filters, respectively. $S_{3.6,4.5,8.0,24.0}$ denote *Spitzer Space Telescope* IRAC 3.6μm, 4.5μm, 8.0μm and MIPS 24.0μm filters, respectively. A superscript G denotes a Gunn filter. A subscript G denotes *GROND* dichroic filters. The results on GRB 050904 are taken from Kann et al. (2007f), the results on GRB 060526 are from Thöne et al. (2010).

Table A.3: Corrected Apparent and Absolute Magnitudes of Type II Afterglows

GRB	dRc	R_C (at 1 day)	M_B (at 1 day)	R_C (at 4 days)	M_B (at 4 days)	Type
990510	-1.60	17.95 ± 0.15	-24.73 ± 0.16	20.83 ± 0.16	-21.85 ± 0.16	B
011211	-2.18	$19.22^{+0.14}_{-0.16}$	$-23.53^{+0.15}_{-0.16}$	21.92 ± 0.32	-20.83 ± 0.32	B
030323	-3.38	$17.80^{+0.19}_{-0.20}$	$-24.96^{+0.20}_{-0.22}$	20.80 ± 0.24	-21.96 ± 0.25	B
050319	-3.20	$18.09^{+0.08}_{-0.12}$	$-24.77^{+0.14}_{-0.16}$	$20.41^{+0.18}_{-0.20}$	$-22.43^{+0.21}_{-0.23}$	B
050408	-2.00	$20.73^{+0.27}_{-0.28}$	$-21.99^{+0.28}_{-0.29}$	$22.40^{+0.29}_{-0.30}$	$-20.32^{+0.30}_{-0.31}$	A
050416A	$+0.83$	24.35 ± 0.48	-18.54 ± 0.49	$\cdots$	$\cdots$	A
050502A	-3.56	$22.30^{+0.31}_{-0.32}$	$-20.55^{+0.31}_{-0.32}$	$\cdots$	$\cdots$	B
050525A	$+0.73$	20.40 ± 0.36	-22.39 ± 0.37	23.15 ± 0.40	-19.64 ± 0.41	A
050730	-3.75	$18.83^{+0.10}_{-0.11}$	$-23.95^{+0.10}_{-0.11}$	$\cdots$	$\cdots$	B
050801	-1.82	$21.05^{+0.36}_{-0.35}$	$-21.38^{+0.38}_{-0.36}$	$\cdots$	$\cdots$	B
050802	-1.77	$20.80^{+0.29}_{-0.28}$	$-21.94^{+0.30}_{-0.29}$	$\cdots$	$\cdots$	B
050820A	-2.64	17.71 ± 0.05	-25.13 ± 0.05	19.21 ± 0.05	-23.63 ± 0.05	B
050824	$+0.19$	21.39 ± 0.13	-21.37 ± 0.13	22.60 ± 0.13	-20.16 ± 0.13	A
050904	-5.05	18.13 ± 0.15	-24.78 ± 0.15	21.50 ± 0.20	-21.41 ± 0.20	B
050922C	-1.91	19.80 ± 0.06	-22.98 ± 0.06	22.24 ± 0.30	-20.54 ± 0.30	B
060124	-2.55	17.67 ± 0.15	-25.13 ± 0.15	19.55 ± 0.20	-23.25 ± 0.20	B
060206	-3.54	$17.78^{+0.10}_{-0.11}$	$-25.06^{+0.10}_{-0.11}$	$20.45^{+0.19}_{-0.20}$	$-22.39^{+0.19}_{-0.20}$	B
060418	-1.45	19.91 ± 0.21	$-22.63^{+0.21}_{-0.22}$	21.80 ± 0.20	$-21.03^{+0.20}_{-0.19}$	B
060526	-3.00	$18.30^{+0.19}_{-0.11}$	$-24.48^{+0.21}_{-0.14}$	$21.80^{+0.22}_{-0.16}$	$-20.98^{+0.24}_{-0.18}$	B
060607A	-3.14	$\cdots$	$\cdots$	$\cdots$	$\cdots$	B
060904B	$+0.84$	22.00 ± 0.20	-20.95 ± 0.19	23.40 ± 0.40	-19.55 ± 0.40	A
060908	-1.44	22.50 ± 0.50	-20.62 ± 0.50	$\cdots$	$\cdots$	B
061007	-1.58	$20.91^{+0.34}_{-0.35}$	$-22.02^{+0.34}_{-0.35}$	$\cdots$	$\cdots$	A
061126	-0.57	20.92 ± 0.14	-21.94 ± 0.14	23.43 ± 0.32	-19.43 ± 0.32	A
070125	-1.33	17.52 ± 0.12	-25.28 ± 0.12	20.20 ± 0.21	-22.60 ± 0.21	B
070419A	-0.50	23.10 ± 0.51	-19.70 ± 0.51	24.33 ± 0.51	-18.44 ± 0.50	A
070802	-5.88	19.55 ± 0.30	-23.38 ± 0.31	$\cdots$	$\cdots$	B
071003	-2.07	17.67 ± 0.12	-25.07 ± 0.12	19.97 ± 0.30	-22.77 ± 0.30	B
071010A	-1.10	$18.62^{+0.17}_{-0.16}$	$-24.18^{+0.17}_{-0.16}$	$21.72^{+0.17}_{-0.16}$	$-21.08^{+0.17}_{-0.16}$	A
071031	-2.73	19.20 ± 0.57	-23.53 ± 0.58	$\cdots$	$\cdots$	B
071112C	$+0.11$	$22.60^{+0.42}_{-0.41}$	$-20.21^{+0.43}_{-0.42}$	$\cdots$	$\cdots$	A
080129	-3.59	$16.54^{+0.10}_{-0.11}$	$-26.29^{+0.10}_{-0.11}$	19.60 ± 0.30	-23.23 ± 0.30	B
080210	-4.35	$18.93^{+0.28}_{-0.27}$	$-23.83^{+0.29}_{-0.28}$	$\cdots$	$\cdots$	B
080310	-2.67	18.67 ± 0.13	$-24.08^{+0.13}_{-0.14}$	21.62 ± 0.22	-21.13 ± 0.22	B
080319B	$+0.15$	20.25 ± 0.15	-22.45 ± 0.15	22.35 ± 0.20	-20.35 ± 0.20	A
080319C	-3.44	$\cdots$	$\cdots$	$\cdots$	$\cdots$	B
080330	-1.37	21.40 ± 0.30	-21.38 ± 0.30	$\cdots$	$\cdots$	B
080413A	-2.56	$20.40^{+0.47}_{-0.37}$	$-22.38^{+0.48}_{-0.38}$	$\cdots$	$\cdots$	B
080710	$+0.26$	20.90 ± 0.13	-21.96 ± 0.13	23.30 ± 0.11	-19.56 ± 0.11	A
080913	-5.25	18.73 ± 0.13	-24.22 ± 0.14	20.30 ± 0.40	-22.65 ± 0.40	B
080916C	-3.26	19.09 ± 0.11	-23.65 ± 0.11	21.20 ± 0.50	-21.54 ± 0.50	B
080928	-1.82	20.30 ± 0.19	-22.63 ± 0.19	$\cdots$	$\cdots$	B
081008	-2.03	19.27 ± 0.32	-23.47 ± 0.33	$\cdots$	$\cdots$	B
090102	-1.39	$22.52^{+0.32}_{-0.33}$	$-20.32^{+0.33}_{-0.34}$	$\cdots$	$\cdots$	B
090313	-4.58	17.17 ± 0.35	-25.67 ± 0.37	$\cdots$	$\cdots$	B
090323	-3.92	$17.59^{+0.16}_{-0.15}$	-25.25 ± 0.16	20.25 ± 0.21	-22.59 ± 0.27	B

090328	+0.58	19.98 ± 0.33	-22.98 ± 0.33	22.50 ± 0.30	$-20.46^{+0.37}_{-0.38}$	A
090423	−4.64	18.90 ± 0.27	-23.86 ± 0.27	21.58 ± 0.40	-21.18 ± 0.40	B
090424	+0.95	21.54 ± 0.23	-21.36 ± 0.23	23.13 ± 0.30	-19.77 ± 0.30	A
090902B	−1.80	19.35 ± 0.17	-23.43 ± 0.17	20.71 ± 0.17	-22.07 ± 0.17	B
090926A	−2.27	16.79 ± 0.14	-26.04 ± 0.15	18.62 ± 0.18	$-24.21^{+0.18}_{-0.19}$	B
050401	−5.06	18.90 ± 0.25	-23.82 ± 0.25	20.25 ± 0.35	-22.47 ± 0.35	B
051109A	−2.08	18.90 ± 0.12	-23.85 ± 0.12	$\cdots$	$\cdots$	B
051111	−1.52	20.10 ± 0.15	-22.70 ± 0.15	$\cdots$	$\cdots$	B
060210	−9.85	$\cdots$	$\cdots$	$\cdots$	$\cdots$	B
060502A	−1.99	20.10 ± 0.30	-22.81 ± 0.30	$\cdots$	$\cdots$	B
060906	−3.37	18.15 ± 0.50	-24.31 ± 0.50	$\cdots$	$\cdots$	B
060927	−5.74	19.70 ± 0.62	-23.16 ± 0.62	$\cdots$	$\cdots$	B
070208	−1.82	20.50 ± 0.40	-22.32 ± 0.40	$\cdots$	$\cdots$	A
071020	−2.80	18.00 ± 0.30	-24.86 ± 0.30	$\cdots$	$\cdots$	B
071025	−7.94	18.45 ± 0.42	-24.44 ± 0.42	$\cdots$	$\cdots$	B
071122	−0.80	20.21 ± 0.30	-22.61 ± 0.30	$\cdots$	$\cdots$	A
080721	−3.68	$18.15^{+0.26}_{-0.25}$	$-24.72^{+0.26}_{-0.25}$	$20.43^{+0.28}_{-0.27}$	$-22.44^{+0.28}_{-0.27}$	B
080810	−3.52	17.50 ± 0.10	-25.28 ± 0.10	20.50 ± 0.50	-22.28 ± 0.50	B
081203A	−2.00	20.00 ± 0.18	-22.80 ± 0.18	22.90 ± 0.33	-19.90 ± 0.33	B
050315	−1.64	20.04 ± 0.15	-22.76 ± 0.15	$\cdots$	$\cdots$	B
050318	−0.91	21.04 ± 0.40	-21.76 ± 0.40	$\cdots$	$\cdots$	B
050603	−2.51	18.44 ± 0.20	-24.36 ± 0.20	$\cdots$	$\cdots$	B
050908	−2.90	19.30 ± 0.50	-23.50 ± 0.50	$\cdots$	$\cdots$	B
060512	+2.03	23.20 ± 0.20	-19.60 ± 0.20	$\cdots$	$\cdots$	A
060605	−3.61	20.90 ± 0.20	-22.03 ± 0.20	$\cdots$	$\cdots$	B
060707	−2.96	19.84 ± 0.30	-22.96 ± 0.30	$\cdots$	$\cdots$	B
060714	−2.42	19.91 ± 0.20	-22.89 ± 0.20	$\cdots$	$\cdots$	B
060729	+1.54	19.34 ± 0.10	-23.46 ± 0.10	21.15 ± 0.10	-21.65 ± 0.10	A
061121	−0.68	20.45 ± 0.07	-22.35 ± 0.07	22.02 ± 0.20	-20.78 ± 0.20	A
070110	−2.08	19.16 ± 0.30	-23.64 ± 0.30	21.15 ± 0.30	-21.65 ± 0.30	B
070411	−2.62	20.18 ± 0.10	-22.62 ± 0.10	22.78 ± 0.50	-20.02 ± 0.50	B
070612A	+1.21	19.80 ± 0.20	-23.00 ± 0.20	23.21 ± 0.50	-19.59 ± 0.50	A
070810A	−1.89	22.26 ± 0.40	-20.54 ± 0.40	$\cdots$	$\cdots$	B

First block: Additional pre-*Swift* Golden Sample; second block: Golden Sample; third block: Silver Sample; fourth block: Bronze Sample. *dRc* is the magnitude shift, see K06. Times are after the GRB in the $z = 1$ frame ($2\times$ the rest-frame time. Type A: $z < 1.4$; Type B: $z \geq 1.4$. See K06 for more information on the two types.

Table A.4: Early Afterglow Peak or Limit Magnitudes

Type	GRB	Time	R_C Magnitude
Peak + Fast Decay	990123	0.0004440	7.60 ± 0.02
	080319B	0.0006359	5.18 ± 0.02
	061121	0.0007647	14.19 ± 0.16
	060526	0.0014088	12.18 ± 0.14
	060729	0.0014365	17.20 ± 0.14
	050904	0.0016318	6.48 ± 0.24
	080129	0.0022666	13.51 ± 0.10
	070802	0.0155854	15.34 ± 0.07
Limit + Fast Decay	080413A	0.0001546	9.55 ± 0.08
	071020	0.0002060	10.64 ± 0.05
	061126	0.0002495	11.23 ± 0.01
	060908	0.0004103	12.51 ± 0.04
	090102	0.0005246	11.61 ± 0.20
	090424	0.0013043	13.78 ± 0.10
Peak + Slow Decay	080810	0.0007660	9.04 ± 0.12
	061007	0.0010277	8.04 ± 0.13
	060607A	0.0010565	10.98 ± 0.05
	060714	0.0011901	15.10 ± 0.27
	081008	0.0013476	11.04 ± 0.03
	060418	0.0017900	12.98 ± 0.05
	060605	0.0020854	11.59 ± 0.10
	071025	0.0021328	10.45 ± 0.06
	070810A	0.0023068	14.84 ± 1.00
	071112C	0.0023744	16.79 ± 0.10
	080210	0.0024286	11.44 ± 0.30
	050730	0.0028513	11.80 ± 0.30
	080319C	0.0029180	13.83 ± 0.02
	081203A	0.0031460	9.89 ± 0.01
	070208	0.0032076	17.35 ± 0.20
	050820A	0.0033973	11.97 ± 0.02
	060210	0.0035812	8.00 ± 0.08
	071010A	0.0054710	15.06 ± 0.10
	071031	0.0070640	15.27 ± 0.07
	070419A	0.0070725	17.87 ± 0.15
	060904B	0.0071057	17.19 ± 0.09
	090313	0.0071958	10.95 ± 0.05
	060729	0.0086297	18.00 ± 0.10
	060707	0.0114726	15.90 ± 0.17
	060206	0.0171000	12.57 ± 0.03
	080928	0.0172837	14.56 ± 0.28
	080710	0.0274666	16.45 ± 0.05
	060906	0.0521760	15.35 ± 0.18
	030429	0.0841990	15.83 ± 0.08
	070612A	0.1133787	18.05 ± 0.20
Limit + Slow Decay	060927	0.0000685	9.03 ± 0.20
	050401	0.0002119	11.57 ± 0.29

	050502A	0.0002242	10.44 ± 0.11
	051109A	0.0002554	12.54 ± 0.20
	051111	0.0003312	11.14 ± 0.03
	071003	0.0003949	10.34 ± 0.02
	050319	0.0009090	12.94 ± 0.14
	050525A	0.0009513	13.20 ± 0.24
	080721	0.0010968	9.10 ± 0.01
	060502A	0.0011465	16.41 ± 0.07
	050922C	0.0011617	12.55 ± 0.03
	060512	0.0015863	17.46 ± 0.17
	080913	0.0016264	15.25 ± 0.03
	050802	0.0024857	14.33 ± 0.25
	050824	0.0080368	18.33 ± 0.35
Plateau + Peak	080310	0.0020151	13.99 ± 0.07
	080330	0.0032251	15.70 ± 0.13
	060124	0.0036178	13.61 ± 0.11
	070411	0.0059173	14.07 ± 0.10
	070110	0.0300253	16.66 ± 0.26
	021004	0.0529879	13.67 ± 0.12
	071122	0.0575405	18.82 ± 0.38
	970508	2.1210965	19.33 ± 0.10
Limit + Plateau	050801	0.0002186	12.87 ± 0.05
	050908	0.0013855	15.42 ± 0.10
	050416A	0.0017643	19.55 ± 0.30
	041006	0.0034965	17.78 ± 0.10
	090423	0.0037297	15.57 ± 0.11
	040924	0.0117394	17.63 ± 0.10

See text for more details on the basic types. Time in days after the GRB trigger in $z = 1$ frame, either peak time or earliest detection. Magnitude is either peak magnitude or magnitude of earliest detection in the $z = 1$ frame. Errors do not include error of dRc.

Notes on special cases:

GRB 080319B: Complex multi-peaked structure during prompt GRB emission, last and brightest peak given. Followed by very steep decay, probably due to curvature effect radiation, then a less steep decay of a probable reverse shock (Racusin et al. 2008; Beskin et al. 2010; Bloom et al. 2009; Woźniak et al. 2009).

GRB 061121: Peak associated with the main prompt emission peak (Page et al. 2007).

GRB 060526: Associated with a bright prompt emission flare, also seen as a giant X-ray flare (Thöne et al. 2010).

GRB 060729: First of three peaks, fast rise and decline.

GRB 050904: Comes after plateau phase, possibly associated with the prompt emission, but steep decay typical of a reverse shock later.

GRB 080129: Extremely fast optical flare, possibly associated with the prompt emission (Greiner et al. 2009c).

GRB 070802: Steep rise and decay, but seems superposed on a forward shock peak (Krühler et al. 2008b).

GRB 080413A: The situation for this afterglow is somewhat unclear. While the first point lies on an extrapolation of the late decay (which has a typical value for a forward shock), the second point is significantly fainter, and it is followed by a small optical flare associated with a prompt emission peak,

implying a steep decay between the first and second data point (Yuan et al. 2008).

GRB 080810: The decay after the peak is very slow, forming a plateau before breaking into a typical forward-shock decay.

GRB 060714, GRB 071025: There is a second peak after the first one reaching almost the same magnitude level.

GRB 070810A, GRB 080210, GRB 060707, GRB 070612A: Data situation is sparse and the given value may not represent the true peak.

GRB 071112C: The very earliest data point implies a very early steep decay. The peak is followed by a plateau.

GRB 050730: The very earliest data points imply a very early steep decay.

GRB 080319C: Followed by an early optical flare, possibly an energy injection.

GRB 081203A: The peak is possibly followed by a steep decay, but Kuin et al. (2009) do not publish the data shown in their figure, and the *Swift* observations stop at a critical point.

GRB 050820A: Preceded and partially superposed by flares linked to the prompt emission (Vestrand et al. 2006).

GRB 060210: The peak is preceded by an early plateau phase.

GRB 060904B: Value given for the second peak. There is a very early complex variability (Rykoff et al. 2009), and the second flare is followed by a plateau probably due to an energy injection.

GRB 060729: Second of three peaks, followed by a plateau phase, a decay, and another optical rebrightening (Grupe et al. 2007).

GRB 060206: Late, very bright peak probably due to a strong energy injection (Woźniak et al. 2006).

GRB 060906: Late peak after an early plateau and a decay (Cenko et al. 2009).

GRB 060927: Possibly a peak, as decay is slower between the first two points than later. Followed by a strong rebrightening (Ruiz-Velasco et al. 2007).

GRB 050502A: Possible very early plateau or peak, as there is hardly any decay between the first two points (Yost et al. 2006).

GRB 051111: The early decay is slightly steeper than later, probably due to a tail component associated with the prompt emission Yost et al. (2007); Butler et al. (2006).

GRB 071003: Followed by a small chromatic bump and a later, strong rebrightening (Perley et al. 2008c).

GRB 050319: Followed by a plateau phase (Quimby et al. 2006).

GRB 050525A: Later followed by a plateau phase (Klotz et al. 2005).

XRF 080330: Long, slow rollover preceded by early complex variability.

GRB 070110: Follows an early, sparsely sampled decay, goes over into a long rollover.

GRB 021004: Complex evolution, early plateau, then decay to second plateau, then rise to the peak given here.

GRB 970508: Very faint ($R_C \approx 20.9$) early plateau starting < 0.15 days after the GRB, which goes over into a very strong, late rebrightening.

Table A.5:   Results on Type I GRBs

GRB	β	A_V	dRc	mag	$M_B(AG)$	k	$M_R(SN)$
050509B	0.6	0	+3.68	> 28.95	> -13.9	$< 2.5 \times 10^{-3}$	> -12.7
050709	1.12	0.67	+4.15	25.3 ± 0.2	-17.6 ± 0.2	$< 1.5 \times 10^{-3}$	> -12.1
050724	0.76	0	+3.43	23.9 ± 0.1	-18.95 ± 0.13	< 0.06	> -16.1
050813	0.6	0	+0.81	> 24.3	> -18.5	< 0.29	> -17.8
050906	0.6	0	+2.10	> 28.0	> -14.8	< 0.08	> -16.4
050911	0.6	0	+4.41	> 30.19	> -12.6	$\cdots$	$\cdots$
051105A	0.6	0	+1.73	> 25.35	> -17.5	$\cdots$	$\cdots$
051210	0.6	0	-0.83	> 23.70	> -19.1	$\cdots$	$\cdots$
051211A	0.6	0	+1.73	> 23.43	> -19.8	$\cdots$	$\cdots$
051221A	0.62	0	+1.52	23.82 ± 0.2	-19.0 ± 0.2	< 0.60	> -18.6
051227	0.6	0	+0.00	27.17 ± 1.03	-15.6 ± 1.0	$\cdots$	$\cdots$
060121	0.6	0.5	-6.67	18.5 ± 0.5	-24.3 ± 0.5	$\cdots$	$\cdots$
060121	0.6	1.1	-4.11	21.0 ± 0.3	-21.8 ± 0.3	$\cdots$	$\cdots$
060313	0.6	0	+0.00	22.72 ± 0.07	-20.08 ± 0.07	$\cdots$	$\cdots$
060502B	0.6	0	+3.09	> 27.28	> -15.5	$< 3.8 \times 10^{-3}$	> -13.1
060505	1.1	0	+6.16	26.6 ± 0.3	-16.35 ± 0.3	$< 3.3 \times 10^{-4}$	> -10.5
060614	0.41	0.28	+4.67	24.04 ± 0.05	-18.71 ± 0.05	$< 6.0 \times 10^{-3}$	> -13.6
060801	0.6	0	-0.31	> 24.94	> -17.9	$\cdots$	$\cdots$
061006	0.6	0	+2.06	25.32 ± 0.2	-17.5 ± 0.2	$\cdots$	$\cdots$
061201	0.6	0	+5.32	28.9 ± 0.4	-13.9 ± 0.4	$< 3.3 \times 10^{-3}$	> -13.0
061210	0.6	0	+2.22	> 25.6	> -17.2	$\cdots$	$\cdots$
061217	0.6	0	+0.47	> 22.5	> -20.3	$\cdots$	$\cdots$
070209	0.6	0	+1.73	$\cdots$	$\cdots$	$\cdots$	$\cdots$
070406	0.6	0	+1.73	> 26.0	> -16.8	$\cdots$	$\cdots$
070429B	0.6	0	+0.26	> 25.1	> -17.7	$\cdots$	$\cdots$
070707	0.6	0	+0.00	23.46 ± 0.05	-19.34 ± 0.05	$\cdots$	$\cdots$
070714B	0.6	0	+0.21	23.95 ± 0.21	-18.85 ± 0.21	$\cdots$	$\cdots$
070724A	0.6	1.29	+0.31	> 25.4	> -17.4	< 0.06	> -16.1
070729	0.6	0	+1.73	$\cdots$	$\cdots$	$\cdots$	$\cdots$
070809	1.1	1.45	+2.55	26.62 ± 0.25	-16.3 ± 0.25	$\cdots$	$\cdots$
070810B	0.6	0	+1.78	> 27.0	> -15.8	$\cdots$	$\cdots$
071112B	0.6	0	+1.73	> 26.6	> -16.2	$\cdots$	$\cdots$
071227	0.6	0	+2.40	26.20 ± 0.30	-16.6 ± 0.3	$\cdots$	$\cdots$
080503	1.1	0	+0.00	25.06 ± 0.18	-17.89 ± 0.18	$\cdots$	$\cdots$
080905A	0.6	0	+5.11	29.32 ± 0.30	-13.48 ± 0.30	$< 5.5 \times 10^{-3}$	> -13.6
090510	0.79	0.24	-0.14	25.5 ± 0.5	-17.4 ± 0.5	$\cdots$	$\cdots$
090515	0.6	0	+2.26	28.68 ± 0.25	-14.12 ± 0.25	$\cdots$	$\cdots$
0901109B	0.6	0	+1.73	28.4 ± 0.5	-14.4 ± 0.5	$\cdots$	$\cdots$

Excepting GRB 060121, if the slope is $\beta = 0.6$, then this is the assumed value. If the Table gives extinction in the host frame as $A_V = 0$, then this is the assumed value, except for GRB 050724 and GRB 060505, where no extinction is found in the SED. dRc is the magnitude shift to $z = 1$. mag is the R_C magnitude of the afterglow (or upper limit thereon) at 1 day after the GRB in the $z = 1$ frame. $M_B(AG)$ is the absolute B-band magnitude of the afterglow at one day after the burst (for the $z = 1$ frame). k is the upper limit on a SN contribution in comparison to the light curve of SN 1998bw. This has only been obtained for GRBs with deep late detections or upper limits (see

Figure B.2). $M_R(SN)$ is the limit on the absolute R_C-band luminosity of a contributing SN at peak. No redshift at all is known for GRBs 051105A, 051211A, 051227, 060313, 070209, 070406, 070707, 070729, 071112B, 080503, and 091109B. A shift $dRc = +1.73$ implies that I assume $z = 0.5$, a shift $dRc = +0.00$ implies I assume $z = 1$. For GRB 060121, two lines are given: $z = 4.6$ (upper line) and $z = 1.7$ (lower line).

Appendix B

Additional Results on the Afterglows of Type I and Type II GRBs

B.1 Does the high number of Mg II foreground absorbers depend on afterglow flux?

Prochter et al. (2006), studying medium- and high-resolution spectra of bright GRB afterglows, found a high number of strong ($W_r(2796) > 1$ Å) intervening Mg II absorption systems, 4 ± 2 times more than along the lines of sight to quasars studied in the SDSS. Such a discrepancy was not found in intervening C IV systems (Sudilovsky et al. 2007; Tejos et al. 2007), and multiple explanations have been proposed (see, e.g., Porciani et al. 2007, for an overview). Differing beam sizes of quasars and GRBs (Frank et al. 2007) as an explanation cannot account for the case of GRB 080319B, where high-S/N multi-epoch data show no temporal variations over several hours (D'Elia et al. 2010, see also Pontzen et al. 2007; Vergani et al. 2009)[1]. Sudilovsky et al. (2009) simulated the effect of dust in the foreground absorbers on quasar detection efficiency and ruled out a strong contribution from this factor (see also Cucchiara et al. 2009). Cucchiara et al. (2009) compared properties of foreground Mg II systems along quasar and GRB sightlines and found no significant differences, concluding that the GRB systems are probably not associated with material ejected near the GRB at relativistic velocities (intrinsic origin). Tejos et al. (2009) and Vergani et al. (2009) also studied the incidence of weak Mg II systems, and both came to the conclusion that the incidence of weak systems is similar along quasar and GRB afterglow sightlines, implying that the best explanation is that the GRB afterglows of the echelle sample have been amplified by gravitational lensing (see also Wyithe et al. 2010, but see Cucchiara et al. 2009). Both studies also find that the excess is smaller than originally deduced from the original small sample by Prochter et al. (2006), but the significance that the excess is real has increased with increasing sample size and redshift path.

All GRBs in the UVES sample of Vergani et al. (2009) are included in my Golden Sample (with GRB 021004 being part of the pre-*Swift* Golden Sample, and GRB 060607A not having any data at 0.5 rest-frame days, therefore I will not include it in this discussion), and two further GRBs with echelle spectra (Keck HIRES) from the sample of Tejos et al. (2009) are also part of our Silver Sample. Furthermore, a GRB with published UVES spectroscopy not included in the sample of Vergani et al.

---

[1] Hao et al. (2007) claimed variable equivalent widths of foreground absorber Mg II lines seen in multi-epoch spectra of the GRB 060206 afterglow, but this was later refuted by Thöne et al. (2008b) and Aoki et al. (2009) using high-S/N Subaru and WHT data.

(2009) is XRF 080330, which also shows a very strong Mg II foreground absorber (D'Elia et al. 2009), and another strong foreground system is seen in the afterglow of GRB 090313, as measured by X-Shooter (de Ugarte Postigo et al. 2010). That all of these GRBs are in my samples is not surprising, only very bright afterglows can be successfully observed with echelle spectrographs, and will therefore very likely also have extensive photometric follow-up (and a redshift, of course), allowing inclusion in my sample (though this situation is now changing with X-Shooter, see de Ugarte Postigo et al. 2010). While the telescopes capable of deriving echelle spectra of GRBs (VLT/UVES+X-Shooter, Magellan/MIKE, and Keck/HIRES) are all concentrated in one hemisphere (Chile and Hawaii), and thus some GRBs with bright afterglows are missed because they have become too faint once they are observable (GRB 061007 being a good example), the isotropic distribution of GRBs should ensure that the echelle sample is mostly unbiased.

First, I create two samples. The first one, the "UVES" sample, contains the nine GRBs from the sample of Vergani et al. (2009) (excluding, as mentioned, GRB 060607A), furthermore GRB 051111 and GRB 080810 (Tejos et al. 2009, while these are from the Silver Sample, the extinction correction is small in both cases, so the insecurity in the luminosity is not large) XRF 080330 (D'Elia et al. 2009) and GRB 090313 (de Ugarte Postigo et al. 2010). The "non-echelle" sample contains all other GRBs from the Golden Samples, for a total of 54 GRBs. Note that this sample still includes several GRBs with echelle observations. But in the cases of GRB 020813 (Fiore et al. 2005), GRB 050502A (Prochaska et al. 2005) and especially GRB 071003 (Perley et al. 2008c), the resulting spectra had very low S/N. GRB 081008 was also observed by UVES (D'Avanzo et al. 2008), but no information has been published on whether a foreground system exists or not. In the case of GRB 030329 (Thöne et al. 2007), the GRB is so close that there are no intervening absorbers, and gravitational lensing is very unlikely. I find the mean absolute B magnitude of the UVES sample to be $\overline{M_B} = -23.72 \pm 0.41$, while the other sample has $\overline{M_B} = -23.05 \pm 0.25$, implying the the UVES sample is brighter only at the 1.4σ level, which is not statistically relevant ($P = 0.28$). On the other hand, the UVES sample can be brighter by, at the 2σ level, up to 1.63 mags, which is a factor of $4.5\times$, which lies above the amplification of $1.7\times$ inferred by Porciani et al. (2007), therefore I am not able to rule at such a rather subtle amplification with any significance either.

A second point is that the sample selection as I am using it now just contains information about the afterglows which were, or were not, observed with high-resolution spectrographs, which can be due to nothing but luck (declination and explosion time). A more precise analysis needs to compare afterglows with strong foreground absorbing system with those that definitely do not have any. Therefore, I create two subsamples of the UVES sample. The "strong sample" contains GRBs 021004, 050820A, 051111, 060418, 080319B, 080330 and 090313, while the "weak sample" contains GRBs 050730[2], 050922C, 071031, 080310, 080413A and 080810[3]. I find $\overline{M_B} = -23.65 \pm 0.66$ for the strong sample, and $\overline{M_B} = -23.80 \pm 0.49$ for the weak sample, implying they are identical ($P = 0.95$), with the weak sample actually being marginally brighter (though I caution that these are low-number statistics here). I come to the conclusion that if the Mg II statistics are influenced by lensing, the effect is not statistically relevant, on the other hand, I can also not rule out a small amplification factor with any significance either. Clearly, the sample of high-S/N, high-res afterglow spectra must be increased before further conclusions can be drawn, X-Shooter will make an important contribution here (de Ugarte Postigo et al. 2010).

Also note that on the issue of dust reddening by foreground systems, I don't find any evidence for large absorption in any of the GRBs in the UVES sample, with the highest values being found for

---

[2]Tejos et al. (2009) find one "Very Strong" foreground absorber for this event from Magellan MIKE spectroscopy, but Vergani et al. (2009) give an upper limit for this system below the $W_r(2796) > 1$ Å cutoff after correcting for sky contamination using UVES data.

[3]There is tentative evidence for a very weak ($W_r(2796) < 0.07$ Å) Mg II foreground system in the spectrum which was too weak to even be included in the sample of Tejos et al. (2009) (N. Tejos, private communication). Of course, this does not influence the fact that GRB 080810 belongs to the weak sample.

GRB 060418 ($A_V = 0.20 \pm 0.08$), where one foreground absorbing system may contribute significantly (Ellison et al. 2006; Vergani et al. 2009), and GRB 090313 ($A_V = 0.34 \pm 0.15$). The latter value is based on GCN data only so far, though, but there is corroborating evidence for dust found in the spectrum (de Ugarte Postigo et al. 2010).

B.2   Does an Upper Limit on the Forward Shock Luminosity Exist?

Compared to K06, the luminosity range of my afterglow sample has slightly expanded, both to lower and higher luminosities, but this must be seen in the context of a much larger sample. In the K06 sample, the afterglow of GRB 021004 dominated the luminosity distribution over a long period of time. In the present sample, several more GRBs are added which parallel the evolution of the afterglow of GRB 021004. The large early luminosity of the afterglow of GRB 050904 has been discussed in by myself in Kann et al. (2007f). Its light curve evolution is clearly anomalous, featuring an early rise, a plateau and a superposed sharp peak. Multiple papers (e.g., Racusin et al. 2008; Woźniak et al. 2009; Beskin et al. 2010; Kumar & Panaitescu 2008; Kumar & Narayan 2009b) discuss the extreme prompt optical flash of GRB 080319B. Finally, the derived very high extinction for GRB 060210 is unsure, implying that the afterglow, which seems to show a standard (not rapid, like GRB 050904 and GRB 080319B) decay after a short plateau and peak, may be much less luminous. Excluding these special events, the early afterglow of GRB 061007 (Mundell et al. 2007a; Schady et al. 2007a) is the most luminous in the sample, although it decays rapidly. Between 0.01 and 0.5 days, the afterglow of GRB 090313 is the most luminous, though I caution that so far, only an extensive GCN data set exists. It is then exceeded by the last strong rebrightening of GRB 080129, which is then followed after about 1.5 days by the afterglow of GRB 090926A, which shows a very similar evolution to that of GRB 021004.

In Figure 4.3 in the main section, I have also plotted as a boundary a power-law decay and attach it to the brightest afterglow detections at times from hours to days (it is $\alpha \approx 1$). At early times, this slope is exceeded, and at least for GRB 990123, GRB 050904 and GRB 080319B, additional emission components dominate over the forward shock afterglow (e.g., Akerlof et al. 1999; Nakar & Piran 2005; Boër et al. 2006; Wei et al. 2006; Zou et al. 2006; Beskin et al. 2010; Kumar & Panaitescu 2008; Kumar & Narayan 2009b). This may also be the case for GRB 061007, although this burst's afterglow showed a remarkable, unbroken broadband (from gamma-rays to optical) power-law decay from very early times onward (Mundell et al. 2007a; Schady et al. 2007a). Beyond ≈ 2 days, the light curves usually become steeper due to jet breaks. This upper boundary may imply that there exists an upper limit for the luminosity of forward-shock-generated afterglow emission in the optical bands. Jóhannesson et al. (2007) have studied a large sample of synthetic afterglows created by using the standard fireball model and find that the luminosity function of afterglows (in wavebands from the X-rays to the radio) can be described by a log-normal distribution with an exponential cutoff at high luminosities, which may be considered a theoretical prediction of this result, although they do not explicitly state that. Determining the actual luminosity distribution from the data is clearly non-trivial, especially trying to discern between, e.g., a regular power-law distribution and one that needs an exponential cutoff at high luminosities (as a power-law distribution itself will trend toward zero, just not as sharply as the exponential cutoff). Furthermore, determining the slope of the power-law is complicated by selection effects such as Eddington bias at low luminosities, as well as all the selection effects I have pointed out earlier concerning my optically selected sample.

In standard afterglow theory, the optical flux generally depends on the isotropic kinetic energy $E_{k,iso}$, the ambient density (n for an ISM or A^* for a wind), and the shock microphysics parameters p (electron spectral index), ε_e (fraction of energy in electrons) and ε_B (fraction of energy in magnetic fields). This upper limit therefore is relevant to a combination of these parameters and cannot be used to pose a limit for each individual parameter. On the other hand, if one makes the assumption

that the microphysics parameters do not vary significantly among bursts, this upper limit may suggest that bursts do not have an exceptionally large $E_{\rm k,iso}$ and the fireball is usually not expanding into an ambient medium of very high density. Jóhannesson et al. (2007) also find that variation of the initial energy release is one of the main drivers of the luminosity distribution (the others are the microphysical parameters, but they should not vary overly much from burst to burst). It may be possible that a very high circumburst density, as one would find within a molecular cloud, is connected to very large gas and dust column densities, and thus to a large line-of-sight extinction, which prevents a detection the afterglow or at least its addition to my sample. Note that Jóhannesson et al. (2007) find that a range of circumburst densities has little influence on the afterglow luminosity, but they only vary the density between 0.1 and 10 cm^{-3}. I also find that several of the GRBs that populate the region of the upper limit only reach it due to additional injections of energy into the external shock, e.g. GRB 021004 (de Ugarte Postigo et al. 2005), GRB 060206 (Woźniak et al. 2006; Monfardini et al. 2006), GRB 070125 (Updike et al. 2008; Chandra et al. 2008), GRB 080129 (Greiner et al. 2009c) and GRB 090926A (Cenko et al. 2010; Rau et al. 2010). For GRB 050603 and especially GRB 991208 (see K06), the lack of early afterglow data makes the situation less clear. The afterglow of GRB 050820A has a relatively slow decay and a very late break. Therefore, several factors may account for the potential existence of this upper luminosity limit, and the afterglow sample will have to increase strongly to reach further conclusions, as these bright events are very rare.

B.3 A New Population of Low-Luminosity GRBs at Low Redshifts?

There is clear evidence for one Type II sub-population that probably extends the $L_{\rm opt} - E_{\rm iso}$ correlation (Chapter 4.3.3) to significantly lower energy values. These are the so-called low-luminosity SN bursts, GRB 980425, GRB 031203 and XRF 060218 (Pian et al. 2006; Soderberg et al. 2006b; Liang et al. 2007a; Guetta & Della Valle 2007; Virgili et al. 2009)[4]. In all these three cases, while luminous, basically unreddened SN emission was detected, there were no or only marginal indications of a "classical" optical afterglow (e.g., Galama et al. 1998; Malesani et al. 2004; Campana et al. 2006a; Pian et al. 2006; Ferrero et al. 2006; Cobb et al. 2006; Mirabal et al. 2006; Modjaz et al. 2006; Sollerman et al. 2006; Kocevski et al. 2007). On the other hand, the prompt emission energy release of these GRBs is orders of magnitude beneath typical Type II events and thus, they cannot be readily compared with each other. The SN emission and, in the case of GRB 031203, the bright host galaxy (Prochaska et al. 2004; Mazzali et al. 2006b; Margutti et al. 2007) prevent the derivation of definite limits on afterglow emission, thus, they can not be included in my study.

Recently, systematic photometric and spectroscopic observations of GRB host galaxies (see, e.g., Perley et al. 2009a for first results from the Keck survey) have started to reveal a population of GRBs that are intermediate in luminosity, both in terms of prompt emission and afterglow, lying between most of the GRBs in my optically selected sample and the local universe low-luminosity events mentioned above. These GRBs are defined by low fluence, usually soft spectra (several are XRFs), usually a simple prompt emission light curve, faint or non-existent afterglows and low redshifts ($z \lesssim 1$). Recently, the existence of this population was inferred theoretically by comparing the distribution of measured redshifts with what is expected if the GRB rate follows the star formation history of the universe (Coward et al. 2008). Several examples are included in my sample (XRF 050416A, XRF 060512, GRB 070419A) and have been mentioned in the main section, although these still have afterglows that are relatively bright observationally. Another example is XRF 050824, although this event has an even brighter optical afterglow. I searched the literature for further examples of these

---

[4]The recently discovered XRF 100316D (Chornock et al. 2010; Starling et al. 2010; Fan et al. 2010) does not yet have enough analyses published to be further included here.
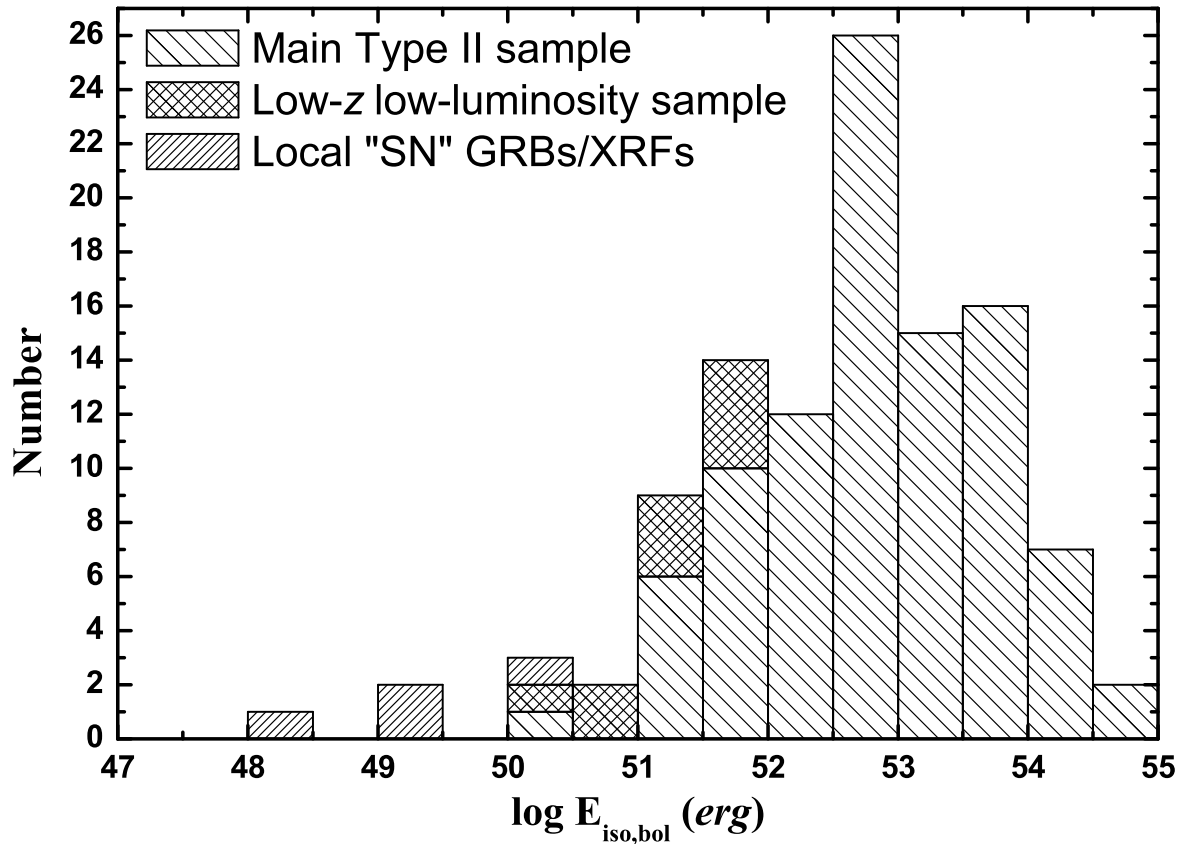
Figure B.1: *Distribution of bolometric isotropic energies for all the GRBs of the "optically selected" main sample of my work and the low-z low-luminosity events for which there is no optical afterglow information. Here, I also differentiate between the four local "SN" GRBs/XRFs and the new sample which is being uncovered mostly by host galaxy observations. These form an intermediate population between the optically selected sample and the local events with spectroscopic SN signatures.*

low-redshift events. Similar to my main Type II sample, I compiled their energetics (see Table 6 of Paper I). This contains ten events from the *Swift* era and three pre-*Swift* events. Next to GRB 980425 and GRB 031203 I also added XRF 020903. The latter burst did have a faint afterglow and showed a spectroscopic (albeit of low significance) and photometric SN signature (Soderberg et al. 2004a, 2005; Bersier et al. 2006). Due to limited publicly available photometry (or no afterglow detection at all), these GRBs cannot be included in my main sample either.

Fiore et al. (2007) speculate that many bright *Swift* GRBs without optical afterglows could be low-z, dust obscured events. Such events clearly exist, e.g., GRB 051022 was mentioned in Chapter 4.1.4. But the GRBs I am considering here are clearly a different population, although here too, evidence for dust obscuration does exist, e.g. GRB 060202, which had a bright X-ray afterglow, was dark even in the K band (Wang et al. 2006), while the X-ray faint GRB 050223 was situated in a dusty, red galaxy (Pellizza et al. 2006). Intrinsic faintness or dust obscuration is undecided in the other cases, but I point out again that this population has low-luminosity prompt emission. This population may partly be responsible for an excess of dark bursts at low gamma-ray peak fluxes, reported by Dai (2009).

In Fig. B.1 I show the distribution of the bolometric isotropic energies for the "optically selected" main sample of my work (which also includes the K06 bursts), the four SN GRBs/XRFs and the low-z low-luminosity sample. All in all, the isotropic energy releases are distributed over six orders

of magnitude without gaps, with only GRB 980425 being over one order of magnitude less energetic than the next faintest event (XRF 020903). Clearly, the three samples are quite distinct from each other. The mean (logarithmic) bolometric isotropic energy of the optically selected sample is $\overline{E_{\mathrm{iso,bol}}} = 52.88 \pm 0.09$, it is $\overline{E_{\mathrm{iso,bol}}} = 51.30 \pm 0.16$ for the low-z sample and $\overline{E_{\mathrm{iso,bol}}} = 49.22 \pm 0.43$ for the "SN" sample. A K-S test finds that the optically selected GRBs and the low-z GRBs do not stem from the same sample with high significance ($P = 2.7 \times 10^{-6}$). This low probability is hardly surprising, as the low-z sample was selected according to the criteria of low fluence and low redshift, necessarily implying a low isotropic energy release. Note that the five faintest GRBs (in terms of prompt energy release) in the optical sample all lie at $z < 1$. Next to XRF 060512, XRF 050416A, GRB 070419A and XRF 050824 (all mentioned above) this includes XRF 071010A. The latter event, though, has an observationally bright optical afterglow (Covino et al. 2008). I move the first four into the low-z sample, and now find $\overline{E_{\mathrm{iso,bol}}} = 52.96 \pm 0.08$ for the rest of the optically selected sample and $\overline{E_{\mathrm{iso,bol}}} = 51.21 \pm 0.14$ for the larger low-z sample, and the difference becomes even more significant ($P = 7.4 \times 10^{-9}$). On the other hand, the almost continuous distribution of energy releases may indicate that all events are part of a single population that can be described by a single power-law luminosity function.

As pointed out above, most of these low-z events are only now being identified as such due to host galaxy spectroscopy campaigns. These are, of course, biased to low redshift events, both due to host galaxies being observationally brighter and due to effects like the "redshift desert" when the [O II] line moves into the airglow region of the spectrum at $z \gtrsim 1$. Still, it is intriguing that many of the GRBs with new redshift information are not the bright, dust-enshrouded events Fiore et al. (2007) predicted, but a population that falls beneath the "standard energy reservoir" as already pointed out by Kocevski & Butler (2008). These events, being optically dim or even dark, are only observable due to the X-ray localization capabilities of *Swift* (with the flux sensitivity playing a lesser role) which allows discovery of the host galaxy in many cases (though the significance of some of the associations may be questionable). With more host galaxy observation results likely to be published in the future, it is expected that this sample will continue to grow. As most of these redshifts were not found until months after the event, searches for SN signatures have not been undertaken, so it is as yet unclear if these events are also subluminous (or perhaps superluminous) in terms of their SN explosions (assuming that they truly are related to the deaths of massive stars). But the clear association of events that are even fainter with powerful broad-lined Type Ic SNe indicates that the basic collapsar mechanism will probably also underlie this new population. Future observatories, such as *SVOM* and especially *EXIST*, are predicted to yield much higher detection rates of these subluminous GRBs.

B.4   Upper Limits on a SN-Light Component in Type I GRB Afterglows

To establish magnitude limits on any contribution of SN light in the late afterglows of Type I GRBs, I shift their afterglow light curves to a redshift of $z = 0.1$. In most cases, the shift to $z = 0.1$ is smaller in z-space than a shift to $z = 1$, implying a smaller uncertainty through the unknown β. Another reason for performing this analysis at $z = 0.1$ and not at $z = 1$ where I usually compare all the GRB afterglows is that at the latter redshift, the R_C-band light curve of the SN template in the observer rest-frame may provide inaccurate flux measurements given the UV-deficiency exhibited by Type Ic SNe such as those which are found to be associated with (Type II) GRBs (Filippenko 1997). My sample for this search consists of those Type I GRBs that have a known redshift (which, in some cases, is derived only from associating the GRB with a nearby bright galaxy or a cluster) and late detections/upper limits: GRB 050509B, GRB 050709, GRB 050724, GRB 050813, GRB 050906, GRB 051221A, GRB 060502B, GRB 060505, GRB 060614 (the latter two being the "SN-less long GRBs"), GRB 061201, GRB 080905A, and GRB 090515. I then compare the detections/upper limits

with the template light curve of SN 1998bw (Galama et al. 1998), see Zeh et al. (2004) for details of the method and descriptions of the parameters k and s, which measure the GRB-SN luminosity in units of the luminosity of SN 1998bw at peak and the light curve stretching in comparison to the SN 1998bw light curve, respectively. In my comparison, I conservatively assume that the late optical emission from the Type I GRBs is due only to SN light and there is no contribution from afterglow emission. In the case of deep (host-galaxy subtracted) detections, I fit the template to pass through the brighter 1σ error bar of the faintest data point, and in the case of an upper limit, I fit the template to pass through the most restrictive upper limit. As I have no information at all about the stretch factor s, I assume it to be 1 in all cases. If the stretch factor is smaller than SN 1998bw, such as XRF 060218/SN 2006aj (Ferrero et al. 2006) or the photometric SN bump of XRF 050824 (Sollerman et al. 2007) the luminosity limit typically would be slightly less constraining. My fitting then results in a value of the luminosity factor k, e.g., $k = 0.1$ implies a SN that has 0.1 times the peak luminosity of SN 1998bw in the same band at the same redshift. As there have been no signs of SN bumps in the light curves of Type I GRB afterglows, these k values can be seen as conservative upper limits on any SN contribution.

The appearance of such SN light, both photometrically and spectroscopically, in a GRB afterglow is the main observational evidence for the origin of the burst being a collapsing massive star. Its non-detection within about the first 2 weeks down to deep luminosity limits is therefore usually considered as a strong argument in favor of the identification of the burst under consideration as a Type I GRB, especially if one considers Type I GRBs as those that do not originate from the deaths of massive stars. Only recently has it become obvious that other explosion channels of single stars that do not produce bright SNe may be realized, namely stars that collapse more or less directly to a black hole (Fryer et al. 2006, 2007; Moriya et al. 2010). This has been suggested as an explanation for the "SN-less long GRBs" GRB 060505 and GRB 060614 (Fynbo et al. 2006b; Gal-Yam et al. 2006; Della Valle et al. 2006; Thöne et al. 2008a; McBreen et al. 2008) and has been predicted based on theoretical grounds even before the detection of these two events (Woosley 1993; Fryer et al. 2006, 2007; Tominaga et al. 2007).

The results from my analysis of SN limits, including GRB 060505 and GRB 060614, are shown in Figure B.2 and given in Table A.5. The limits for GRB 051221A and GRB 050813 are not very strict, as both GRBs lie at a redshift ($z = 0.5 - 0.7$) where it also becomes challenging to detect the SN signature in Type II GRB afterglows (Zeh et al. 2004). Furthermore, in both cases, observations were not extended to a time when a hypothetical accompanying SN would have probably peaked (assuming a similar rise time as SN 1998bw). The limits for GRBs 060614, 080905A, 060502B, 061201, 050509B, 050709, and 060505 are much stricter, and fainter than any Type II SN known (not to mention broad-lined Type Ic SNe; Ferrero et al. 2006, and references therein). The limits for GRBs 050724, 050906, and 070724A are intermediate between the two extremes, fainter than broad-lined Type Ic SNe, but still comparable to fainter Type II SNe (note that the redshift of GRB 050906 is not secure). My limits are in accordance with those found by other authors before for GRBs 050509B (Hjorth et al. 2005a), 050709 (Hjorth et al. 2005b; Fox et al. 2005), 050724 (Malesani et al. 2007), 050906 (Levan et al. 2008), 050813 (Ferrero et al. 2007), 051221A (Soderberg et al. 2006a), 060505 (Ofek et al. 2007; Fynbo et al. 2006b), 060614 (Gal-Yam et al. 2006; Fynbo et al. 2006b; Della Valle et al. 2006), and 080905A (Rowlinson et al. 2010b). The limits for GRBs 060502B and 061201 stated here are derived for the first time by myself, and my limits for GRB 070724A are much shallower than what Kocevski et al. (2010) derive, since I correct for the high extinction along the line of sight. Additionally, D'Avanzo et al. (2009) report a limit of $M_B = -15.1$ for any classical SN light following GRB 071227. This compilation further substantiates the observation that Type I GRBs are not associated with the deaths of massive stars and their accompanying SNe and must derive from progenitors that produce only very small amounts of ^{56}Ni, such as the mergers of compact objects. The missing bright late-time SN signal of Type I GRBs is thus a substantial phenomenological difference compared to the late-time evolution of Type II GRBs (see also Hjorth et al. 2005a; Fox et al. 2005). On the other hand, even
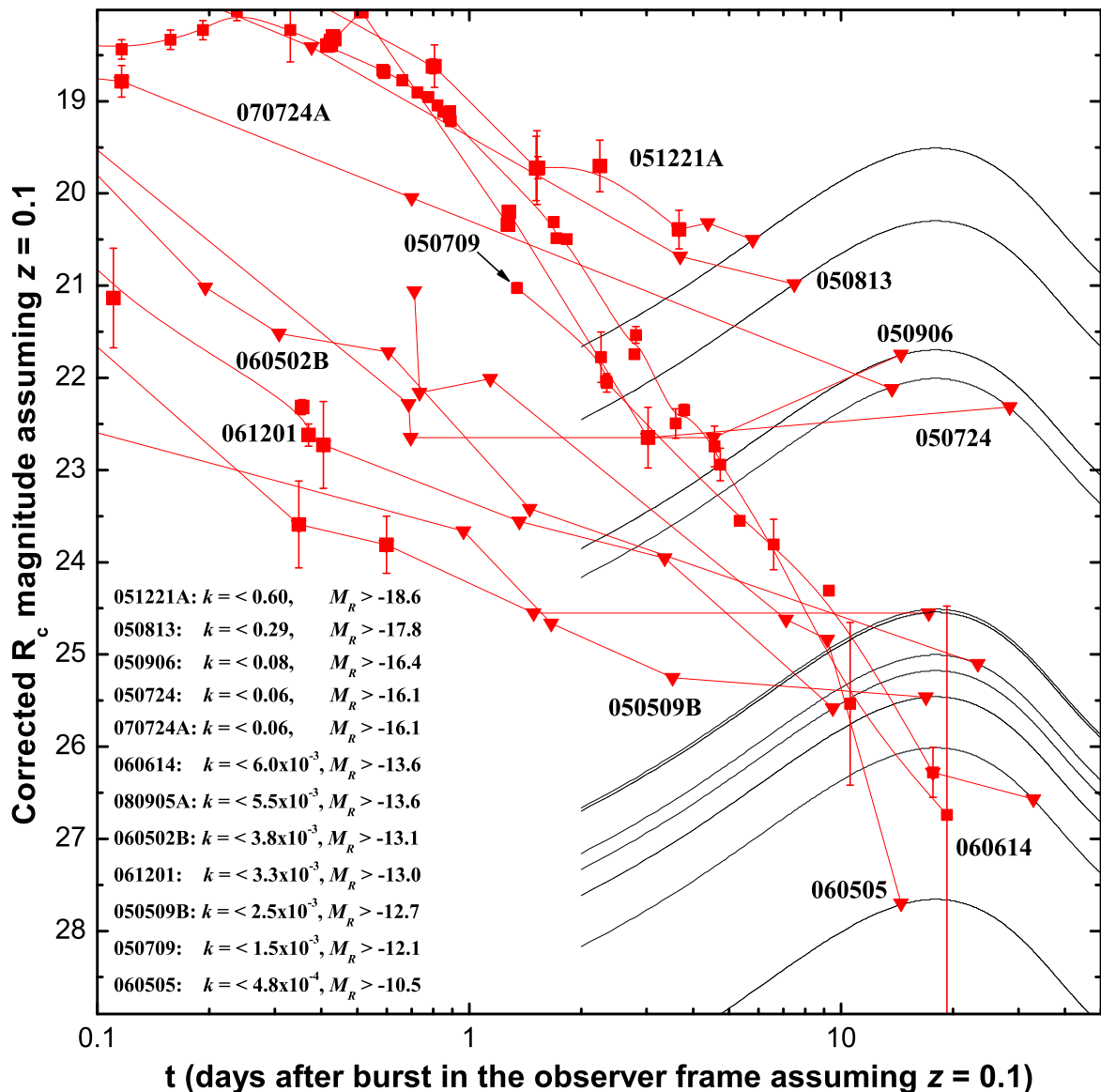
Figure B.2: *Deep late detections or upper limits of Type I GRB afterglows, all shifted to $z = 0.1$, and compared with the R-band light curve of SN 1998bw at $z = 0.1$. I conservatively assume that the late detections derive from SN light only and there is no more afterglow contribution. For GRBs 051221A and 050813, the limits on an accompanying SN are not very strong, but all other Type I GRBs in this figure, including the temporally long events GRB 060505 and GRB 060614, give extremely stringent limits on any accompanying SN emission. The faintest upper limits are less luminous than any confirmed SNe at peak.*

the very strict limit, $M_R \gtrsim -10.5$, on a SN accompanying GRB 060505 (Ofek et al. 2007, and my own work), which yield $M(^{56}Ni) \lesssim 1 \times 10^{-4}~M_\odot$, cannot exclude a collapsar with a very low jet energy deposition (Tominaga et al. 2007). Furthermore, the less-constraining upper limits cannot exclude SNe similar to the faintest local core-collapse events (cf. Richardson et al. 2002; Pastorello et al. 2004). Still, there must exist a broad gap in peak luminosity between these faint SNe (if they exist at all) and the traditional SNe associated with Type II GRBs.

It must be stressed that only in two cases detections of the optical transient at the time of the

suspected SN maximum at $t > 10$ days have been reported in the literature (for GRB 050709 and GRB 060614; even though, after host subtraction, with a large error bar for the latter), but no late-time follow-up observations weeks after the suspected SN peak have been published so far. This leaves open the question if this positive detection was the late afterglow light or in fact an underlying faint SN component, even though the error bar is small enough for GRB 050709 only to tackle this question seriously. In all other cases only upper limits are available at the suspected SN maximum around $(1 + z) \times 15...20$ days after the corresponding burst, if at all.

Clearly, the upper limits which can set will be misleading if the light curve evolution of any kind of SN following a Type I GRB differs substantially from the one of GRB-SNe of Type II GRBs, i.e., with respect to peak time and stretch factor. Such a case has been modeled as well, the so-called "mini-SN" (Li & Paczyński 1998) or "macronova" (Kulkarni 2005), where the ejection of neutron-rich matter from the merger even powers a usually short-lived (hours to days) but possibly very bright (comparable to typical SNe) transient. In Paper II, I and my colleagues compare deep upper limits of GRB 050509B with the analytical models of Li & Paczyński (1998) and derive limits on the two main parameters which exclude the existence of such bright transients at least for some Type I GRBs. This expands the work of Hjorth et al. (2005a), and later, a similar study was published on GRB 070724A (Kocevski et al. 2010), though it ignores the strong line-of-sight extinction (Berger et al. 2009, my work). As the mini-SN computations were done by Sylvio Klose, I will not discuss them further here.

Appendix C

The Diversity of GRBs and their afterglows

In this appendix, I will present the results of various scientific investigations into the nature of GRBs I was additionally involved in beyond the main scope of my thesis work. While always involving the study of GRBs, the topics are diverse and therefore do not allow a connecting chain of argumentation.

C.1   The peculiar XRF 060218 – a Transition Object?

The project to comprehensively analyze the afterglow light curves of GRBs began with the study of the late-time evolution of light curves to look for the contribution of supernova emission. Typically, the afterglow should have faded at times greater than a week after the GRB, and supernova emission should become dominant, unless the GRB was too distant (SN emission is strongly suppressed in the UV, and at large redshifts what is observed in the optical bands is the rest-frame UV light) or the host galaxy was very bright. The results from the initial search were presented by Zeh et al. (2004) and expanded in Zeh et al. (2005a). It was found that all GRBs at $z \lesssim 0.7$ which had observations at late times exhibited "bumps" in their light curves which could be fit successfully by using the model light curve of the "archetypal" GRB-SN, SN 1998bw. SN bumps were found to beyond $z = 1$ for GRBs 021211 and 000911. Andreas Zeh developed an analytical function which described the SN 1998bw light curve evolution, which was modified by two further parameters: k is the luminosity normalization, with $k = 1$ implying the peak luminosity of the SN is identical to that of SN 1998bw in the same photometric band. The stretch factor s allows the possibility to have the SN evolve faster or slower than SN 1998bw while keeping the overall light curve shape. At the beginning of my thesis work, I used my results on host galaxy extinction, as derived from the GRB afterglows, to correct the SN luminosities for the extinction along the line of sight (Zeh et al. 2006b).

After the highly successful observing campaign of GRB 030329/SN 2003dh with the VLT (Hjorth et al. 2003), a proposal was submitted to observe one nearby GRB-associated SN in detail (PI: Elena Pian), of which I was part of. With the launch of *Swift*, it was hoped that the number of nearby events similar to GRB 980425/SN 1998bw and GRB 031203/SN 2003lw would increase. In retrospect, this hope has been dashed, because only two such events have been discovered in the *Swift*-era so far (over 5 years), namely XRF 060218/SN 2006aj, and the recent XRF 100316D/SN 2010bh.

The two pre-*Swift* events were unremarkable from the point of view of their prompt emission (if one discounts the fact that they were underluminous). XRF 060218, on the other hand, was a unique event, until the very similar XRF 100316D was detected. It triggered *Swift* as a long-duration "image trigger" (where coded-mask images of the same field are compared internally to look for new sources), was detected only at low energies, mostly in the X-ray band (and was thus a true X-ray Flash, unlike
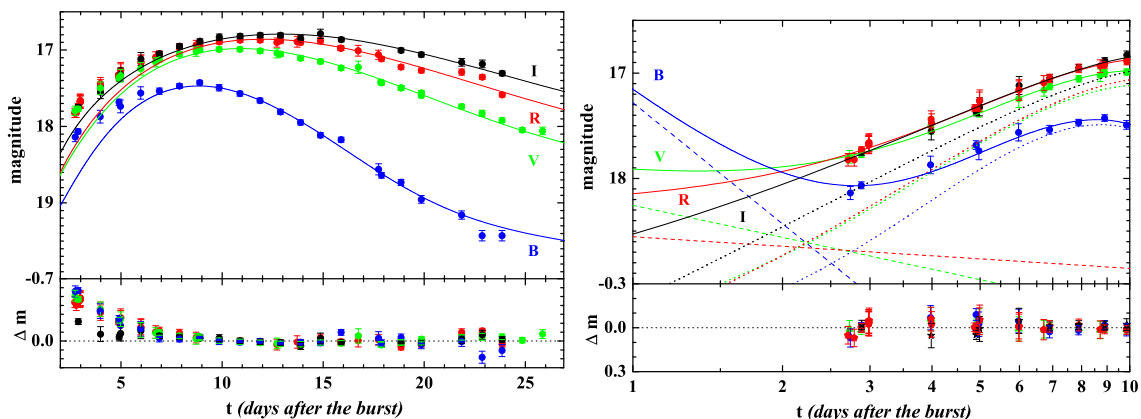
Figure C.1: *The light curves of SN 2006aj in the BVRI filters, associated with XRF 060218. The time is measured from the* Swift *trigger time.* Left: *The light curves have been fitted with an SN 1998bw model, with both the normalization k and the stretch factor s left as free parameters (and not coupled between filters). Clearly, from about nine days onward, the fit is good, but the early data are too blue, as can be seen from the residuals, and they have been omitted from the fit.* Right: *A zoom-in into the first ten days, plotted in a logarithmic timescale to enhance clarity for the early data. Here, the fit has been done with an "afterglow" component (power-law decay) and the SN 1998bw component. The solid lines show the combined fit, which is now able to fit all data well, while the dashed lines show the power-law component, and the dotted lines show the SN component. Figures taken from Ferrero et al. (2006).*

some of the GRBs presented in Chapter C.2), and lasted for about 2700 seconds. Further observations with *Swift* revealed a "flare" which peaked at about half a day after the trigger, with a spectral peak in the ultraviolet range. This has been interpreted as the shock-breakout of the supernova. The *Swift* observations are described in Campana et al. (2006a).

The peculiar nature of the source led to some initial confusion, until the first spectroscopy revealed it to be extragalactic, lying at $z = 0.0335$ (Mirabal et al. 2006). With this knowledge, we triggered our VLT program and began a systematic observation campaign, shortly thereafter announcing the discovery of SN 2006aj. The results of the spectroscopic campaign are presented by Pian et al. (2006), with theoretical interpretations by Mazzali et al. (2006a). My involvement in this phase was relatively minor, I collected data and kept track of the luminosity evolution of the developing SN.

Next to spectroscopy, we also obtained high-quality photometry of the developing SN (until it got too close to the sun). Adding data from the Liverpool Telescope (LT) and the Katzmann Automatic Imaging Telescope (KAIT) to the VLT data set, we undertook an analysis of the photometric SN evolution in comparison to SN 1998bw, and also compared SN 2006aj with other GRB SNe and a sample of extinction-corrected "stripped-envelope SNe" (the types IIb, Ib and Ic, all having lost most or all of their hydrogen envelope) as collected by Richardson et al. (2006). Our results have been presented in Ferrero et al. (2006) as well as the PhD thesis of Dr. Patrizia Ferrero. For the study, I performed the SN fits to the data of SN 2006aj. As can be seen in Figure C.1, the modified light curve of SN 1998bw gives a good fit to SN 2006aj, but only after about 10 days. At earlier times, there is an additional component, which is seen best in the B band, which can be modeled with a fading power-law. This is not a GRB afterglow, but the fading shock-breakout peak which was seen by *Swift UVOT* (Campana et al. 2006a). Next to SN 2006aj, I also collected data on several further stripped-envelope SNe, in order to model them with the SN 1998bw light curve and place them in the context of GRB-SNe. SN 1994I is usually seen as the "canonical" Type Ic SN (with "narrow" lines), even though it has a faster evolution to peak than most known Type Ic events. SN 2002ap is the
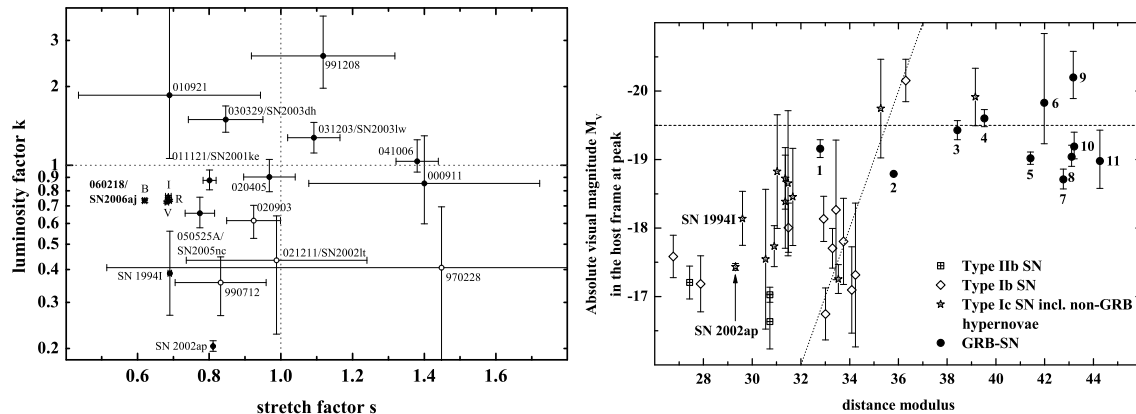
Figure C.2: Left: *The luminosity factor k plotted against the stretch factor s for GRB-associated SNe and "SN bumps" (with $k, s = 1, 1$ marking SN 1998bw). Filled dots are corrected for the extinction along the line of sight in the host galaxy, empty dots are not. All values are measured in the observed R_C band. For XRF 060218/SN 2006aj, we plot the derived values for all four colors, with the exception of a slightly faster B band evolution, the values cluster tightly. Furthermore, we plot the "canonical" Type Ic SN 1994I and the broad-lined Type IC SN 2002ap, which was not associated with a GRB.* Right: *The absolute magnitudes M_V at peak of the GRB-SNe in comparison with the stripped-envelope SNe sample of Richardson et al. (2006). The dotted line represents the typical peak luminosity of Type Ia SNe, which is seen to be comparable to GRB-SNe. The slanted line represents a constant observed peak magnitude. 1 is GRB 980425/SN 1998bw, 2 is XRF 060218/SN 2006aj, 3 is GRB 031203/SN 2003dh, 4 is GRB 030329/SN 2003lw. All peak luminosities have been corrected for host galaxy extinction. Figures taken from Ferrero et al. (2006).*

best-observed broad-lined Type Ic SN to date, it was not associated with a GRB. I also compiled data on the peculiar Type Ib SN 2005bf, but we ended up not using it. I also re-analyzed the SN bumps presented in earlier works (Zeh et al. 2004, 2005a, 2006b) using additional photometry and improved host galaxy extinction measures.

In Figure C.2, left panel, SN 2006aj is compared with the other GRB-SNe in terms of the parameters k and s. It can be seen that there is scatter around the $(k, s = 1, 1)$ value of SN 1998bw (measured in the observed R_C band). SN 2006aj is found to be less luminous, and also "faster" (reaching the peak luminosity earlier) than SN 1998bw. Except for a small offset for the B band, the relative photometric evolution in the different bands is identical to SN 1998bw. The two nearby Type Ic SNe are seen to be fainter and faster than SN 1998bw, especially SN 2002ap, which is less luminous than any GRB-SN. Also, the few cases where no extinction correction could be applied are always less luminous than the other GRB-SNe, indicating that the scatter in luminosity would be reduced if corrections were applied. In the right panel, the GRB-SNe for which an extinction correction could be applied are plotted in peak luminosity vs. distance. It can be seen that as a class, GRB-associated SNe are highly luminous, rivaling Type Ia SNe, and exceeding non-GRB stripped envelope SNe by one to two magnitudes except for some cases. Furthermore, there is no luminosity evolution evident, distant events are not significantly more luminous than the "local" spectroscopically confirmed GRB-SNe.

Since our study, only a few more GRB-SNe have been discovered. Photometric bumps have been found for the pre-*Swift* GRB 040924 (Soderberg et al. 2006c; Wiersema et al. 2008, see Chapter 3.3.1), the *Swift* XRF 050824 (Sollerman et al. 2007, see Chapter C.2). Two possible cases are GRB 070419A and GRB 070518 (Dai et al. 2008a,b). For GRB 081007, a SN (SN 2008hw) has been spectroscopically and photometrically confirmed at $z = 0.53$ (Della Valle et al. 2008). The very bright GRB 090618 ($z = 0.54$) shows a late photometric bump (R. L. C. Starling, private communication, 2010), and

GRB 091127 ($z = 0.49034$) is also associated with a photometric bump, named SN 2009nz (Cobb et al. 2010). Finally, the nearby ($z = 0.059$) XRF 100316D is associated with the spectroscopically confirmed SN 2010bh, yet another broad-lined Type Ic SN (Chornock et al. 2010).

C.2 X-ray Flashes can be X-Ray-Rich GRBs at moderate Redshifts

Since their discovery with *BeppoSAX* (Heise et al. 2001) and the confirmation that they are cosmological sources as well (Soderberg et al. 2004a), several different models have been proposed to explain their properties (very low peak energies, often simple light curve shapes, in case afterglows are discovered, they often have long early plateau phases). Initially, it was thought the sources lay at very high redshift, being "normal" GRBs shifted into the X-ray regime. A leading model explains their properties geometrically: The observer lies off the jet axis, which is able to explain the multiple properties given above (e.g., Lamb et al. 2005). Observational evidence for off-axis models has been found (e.g., Fynbo et al. 2004; Granot et al. 2005; Guidorzi et al. 2009a), and the statistical properties of larger samples detected by *HETE* and *Swift* show that XRFs, soft GRBs (so-called X-ray righ GRBs, XRRs) and "classical" GRBs form a continuum. Several studies in which I was involved have shown that while the high-redshift theory does not seem tenable, clearly, some XRFs result from medium-redshift XRR GRBs.

Stratta et al. (2007a) report on the *HETE* XRF 040912. This event was optically dark (no optical afterglow was detected even in deep observations), and observed extensively at TLS, I contributed the data reduction and analysis to the paper. The X-ray afterglow was localized by the *Chandra* X-ray observatory, which led to the discovery of a host galaxy. Spectroscopy revealed that this galaxy lies at $z = 1.563$. While the analysis of the prompt emission found that this is unambiguously an XRF, a comparison with other XRFs and XRR GRBs in the rest-frame shows that most events are XRR GRBs after correcting for the redshift, only XRF 020903 and XRF 060218 (Chapter C.1) are *intrinsic* XRFs.

A comprehensive analysis of the *Swift* XRF 050824 has been performed by Sollerman et al. (2007). This event has one of the best-observed optical afterglows for an XRF. Starting already ten minutes after the trigger, it is seen to decay with a power-law, in contrast to the expectations of the off-axis model. Furthermore, the decay of the light curve is very shallow, indicating a long-lasting energy injection into the afterglow. This injection may also be responsible for small-scale variability around the power-law. My fitting of the light curve data revealed a possible shallow break, from a slope of of $\alpha_1 = 0.57 \pm 0.02$ to $\alpha_2 = 0.81 \pm 0.06$ at $t_b = 0.53 \pm 0.23$ days after the GRB. The slope change $\Delta\alpha = 0.24 \pm 0.06$ is in good agreement with this being a cooling break. The late afterglow shows a bump which can be modeled with a bright but fast SN: $k = 1.05 \pm 0.42$ and $s = 0.52 \pm 0.14$. This is faster than any of the GRB-SNe presented in Ferrero et al. (2006) (Chapter C.1).

A further *Swift* XRF with excellent optical observations is XRF 071010A, at $z = 0.985$ analyzed by Covino et al. (2008). In this case, observations started even earlier than for XRF 050824, just two minutes after the trigger, and revealed a smoothly rising afterglow which peaked about 7 minutes after the trigger, rolling over into a typical power-law decay. This situation can be interpreted as the onset of the forward-shock afterglow in the optical (e.g. Molinari et al. 2007). Again, similar to XRF 050824, the optical light curve favors an on-axis interpretation. At about 0.6 days, a strong rebrightening is seen, both in the optical and the X-rays, probably due to a discrete energy injection. This is followed at one day by an achromatic steepening, a clear jet break, and one of the few really good cases in the *Swift* era (see also Chapter C.4). My analysis of the SED also showed that the afterglow was reddened by a moderate amount of SMC dust ($A_V = 0.64 \pm 0.09$), one of the most significant dust detections so far.

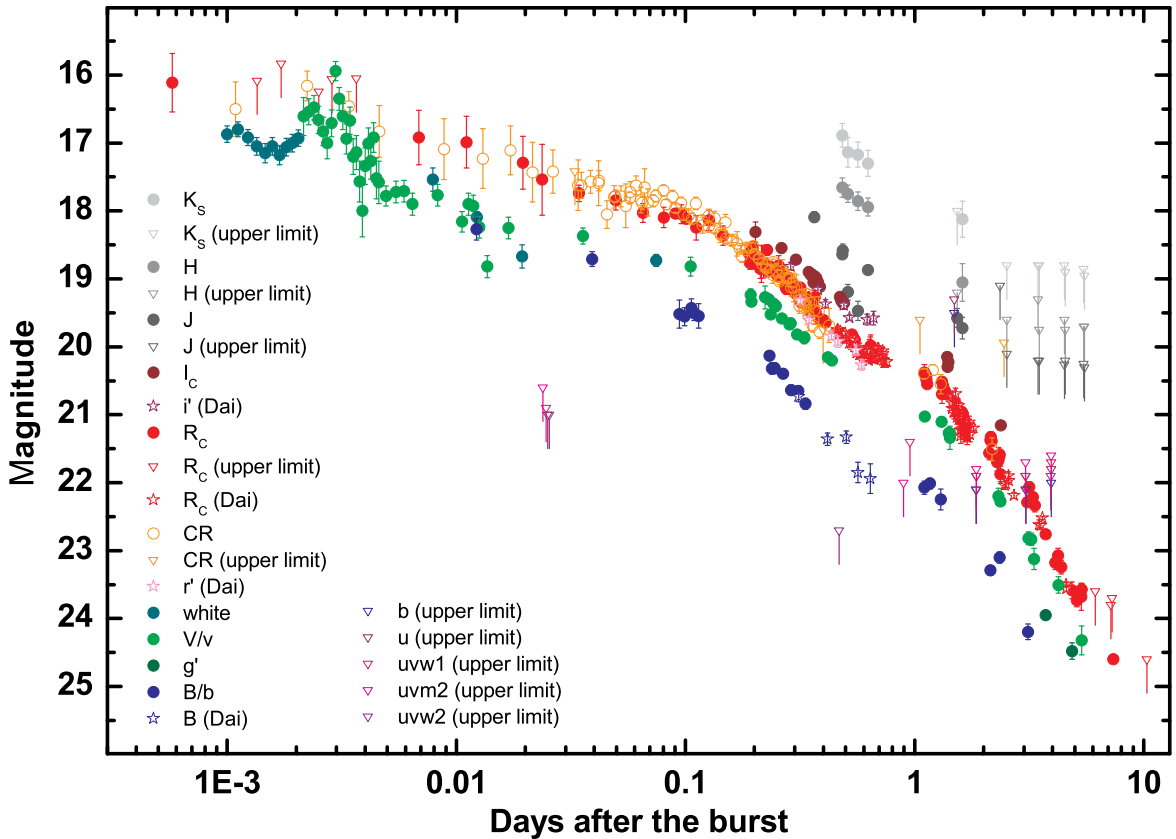Interestingly, the opposite case is also possible, GRBs which are not XRFs in terms of their prompt

Figure C.3: *The multicolor light curves of the high-redshift GRB 060526. At early times, two distinct, sharp flares can be seen in the UVOT observations. After a following plateau phase, the light curve experiences a series of rebrightenings, "bumps" and "wiggles". At very late times, no host galaxy is discovered down to extremely deep levels with the VLT and the HST (not shown). Figure taken from Thöne et al. (2010).*

emission properties can show the signature of an off-axis jet in their afterglow. One example is GRB 080710 (Krühler et al. 2009), to which I contributed TLS observations which filled a hole in the light curve between the GROND (the Gamma-ray Burst Optical and Near-Infrared Detector, a camera on the 2.2m ESO telescope at La Silla Observatory which takes images in seven filters at the same time, Greiner et al. 2008) observations. The afterglow is seen to slowly rise, peaking only about 0.02 days (≈ 1700 s) after the trigger, which is very uncommon.

C.3   The highly variable Afterglow of GRB 060526

While the basic fireball theory predicts a smooth afterglow evolution, detailed observations often reveal variability on short timescales, such as in the famous case of GRB 030329 (e.g., Lipkin et al. 2004). Acquiring such detailed observations often features a certain element of chance. Next to being bright, it is "helpful" if the afterglow is well observable (in the ecliptic plane as well at such a right ascension that it is highest near local midnight) and occurs during dark time, when interfering moonlight is low. All these factors were given for GRB 030329, making it the most well-observed GRB afterglow ever. Similarly favorable conditions were given for the *Swift* GRB 060526. Due to inclement weather, no TLS observations could be obtained for over two days, and even then, only 40 minutes in R_C were observed, which yielded one good detection (at seven days, I also obtained a deep but non-constraining
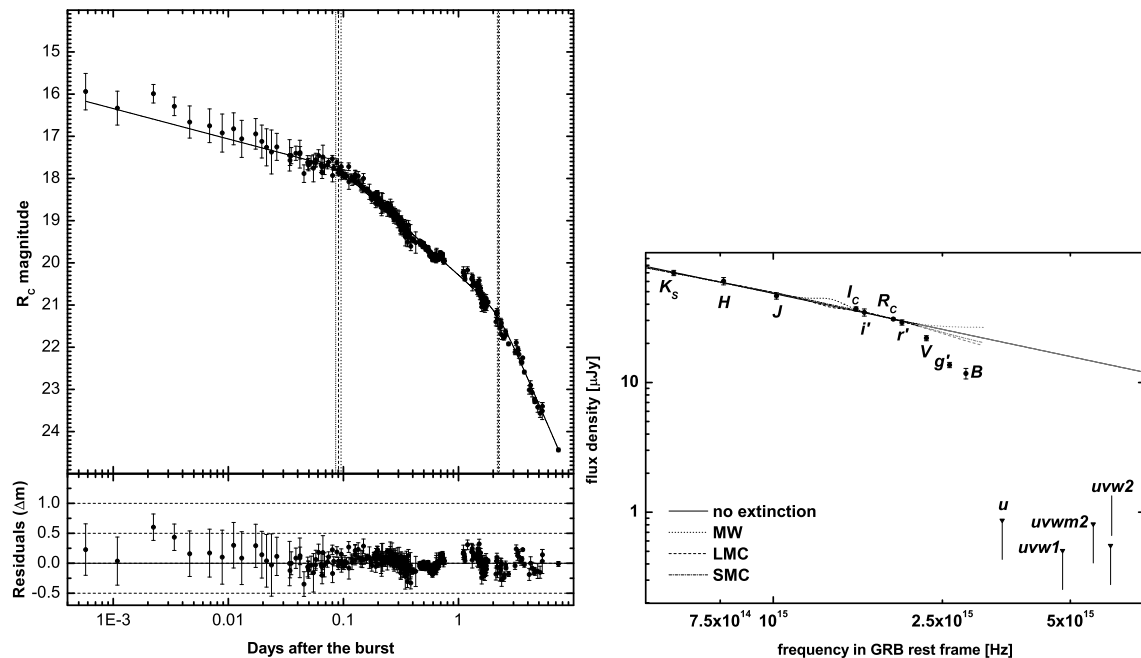
Figure C.4: *Left*: *The R_C-band light curve of GRB 060526 fit with a a double smoothly broken power law, using data starting at 0.046 days. The residuals of the fit show an early optical flare (seen much more clearly in the* UVOT *data, Figure C.3) and later strong variations of up to 0.3 magnitudes. The dashed vertical lines mark the break times, the dotted lines the 1σ region of uncertainty. The second break is soft ($n \approx 4$) and is thus seen as a smooth rollover. Right*: *The SED of the afterglow of GRB 060526 in uvw2 uvm2 uvw1 uBg'Vr'R_Ci'I_CJHK$_S$, measured at the beak time of 2.2 days, and fits with no extinction (straight black line), MW extinction (dotted line), LMC extinction (dashed line) and SMC extinction (thick dash-dotted line). Data beyond 2.2×10^{15} Hz (Vg'Bu uvw1 uvm2 uvw2) were not included in the fit due to Lyman forest blanketing, the gray curves represent extrapolations. The* UVOT *u and UV filters are upper limits only. The flux density scale is measured at the break time. Clearly, there is very little dust along this line of sight. The figures are taken from Thöne et al. (2010).*

upper limit). I also performed a light curve analysis with the available GCN data, which confirmed a break reported earlier (Thöne et al. 2006). Even beforehand, optical variability was reported, these data were published in Dai et al. (2007).

Christina C. Thöne, then at the Dark Cosmology Center in Copenhagen (who had obtained multicolor data with the Danish 1.54m telescope on La Silla, as well as high signal-to-noise VLT low-to-mid-resolution spectroscopy) and myself decided to gather as much optical data as possible and study the broadband evolution of the optical light curve, and we were highly successful. Our data set is one of the most comprehensive ever published on a GRB afterglow, featuring a total of 412 data points in fourteen photometric bands (plus unfiltered data calibrated to R_C). It ranges from just 36 seconds after the GRB (from the Watcher robotic telescope, as well as high time-resolution *Swift* UVOT data starting at 86 seconds) to over 1000 days later, an extremely deep ($F775W_{AB} \geq 28.5$) upper limit on the host galaxy (one of the deepest non-detections of a host ever). In total, 17 telescopes were involved, mostly mid-size ground based telescopes, but including rapid robotic follow-up telescopes (Watcher and ROTSE-III), "big glass" (VLT and Keck) and satellites (*Swift* and the Hubble Space Telescope). I performed the data analysis for the TLS, MIRO, Keck and PAIRITEL observations (the latter together with my summer student Amelia C. Wilson).

The complete data set, which also includes the data from Dai et al. (2007), is shown in Figure

C.3, and consists of over 500 data points. At early times, strong and rapid variability is visible. The Watcher data shows an elevated level in comparison to the back-extrapolation of the later decay (Figure C.4), but the real variability is only resolved by the UVOT data, which has been taken in event mode, a special photon-counting mode, which allows long exposures (finding charts) to be split into shorter exposures with no breaks due to read-out time. The *white* observation, together with the first v band data points, shows two small peaks before a very sharp peak is seen in v which rises and decays extremely rapidly. It is temporally concurrent with a powerful flare in X-rays which is also seen in the *BAT* and thus represents a "Vestrand-Blake" prompt emission flare as seen for GRB 041219A (Vestrand et al. 2005; Blake et al. 2005). A second flare, at smaller S/N, is temporally offset from a flare seen only in X-rays, possibly due to hard-to-soft evolution. The light curve (in R_C, the best-sampled band) after 0.046 days shows less abrupt variations. I have fit it with a double smoothly broken power-law (the equation was derived by Steve Schulze), finding the following parameters: $\alpha_{plateau} = 0.288 \pm 0.026$, $\alpha_1 = 0.971 \pm 0.008$, $\alpha_2 = 2.524 \pm 0.052$, $t_{b1} = 0.090 \pm 0.005$ days, $t_b = 2.216 \pm 0.049$ days, $n_1 = 10$ had to be fixed, and $n = 4.278 \pm 0.726$. The fit is shown on the left side of Figure C.4. The later data still shows deviations from the power law decay of up to 0.3 magnitudes, leading to a high $\chi^2 = 964$ for 309 degrees of freedom. This small-scale variability was originally described by Dai et al. (2007), though with a much smaller data set. An analysis of separate parts of the light curve revealed that it could be fit with a set of either single or smoothly broken power laws. In some cases, the "bumps" showed steep decays, up to $\alpha = 6.7 \pm 3.5$. Such steep decays indicate processes not involving the forward shock, but possibly stemming from further central engine activity, as also suggested by Dai et al. (2007). These authors also first described that the X-ray light curve shows a break which is probably achromatic, indicating the late break is a true jet break ("probably", because the late X-ray data is sparse and low S/N). After the break, the data shows a "step-ladder" structure which is indicative of energy injections into the afterglow. Indeed, one of our team, Gudlaugur Jóhanesson, has fitted the broadband afterglow with his numerical code, which integrates energy injections into the afterglow. He finds the early light curve is well-modeled with a total of six injections. But even this model is not able to fit the short-term variability, again hinting at an additional superposed component.

Furthermore, I studied the SED of the afterglow, as shown on the right side of Figure C.4. The data on the blue side is strongly affected by Lyman blanketing. The rest of the data is almost a pure power law, and extinction is found to be minimal, as is often the case for high redshift GRBs (Kann et al. 2006b, 2010). Further analysis presented in the Thöne et al. (2010) which I was not directly involved in concerns the search for a host galaxy as well as a full analysis of the obtained spectroscopy. All in all, the GRB showcases nicely all the information one can derive out of a rich broadband data set.

C.4   Examples of optical Jet Breaks in the *Swift* Era

As pointed out in Chapter 2, finding jet breaks in GRB afterglows is important for the derivation of the true energetics of the event, which can be used in cosmological studies. In our study of pre-*Swift* optical afterglows (Zeh et al. 2006a), we found that in almost all cases where follow-up was dense and went deep, and the contamination by a bright host galaxy was not a problem, an achromatic (within the optical/NIR regime) break was found. When the *Swift*-era began, there was the hope that X-ray afterglows would reveal a multitude of jet breaks. Since the break is a geometric and hydrodynamic effect, it is expected to be achromatic, a break in the optical band should happen at the same time in the X-ray band. Intriguingly, this result did not materialize. The first well-observed *Swift* GRBs showed that while breaks were found in the X-rays, they were chromatic, occurring at different times than in the optical (Panaitescu et al. 2006a) or not at all (Sato et al. 2007). Studies of X-ray afterglows alone revealed only a relatively small number of jet break candidates (Panaitescu 2007; Racusin et al.
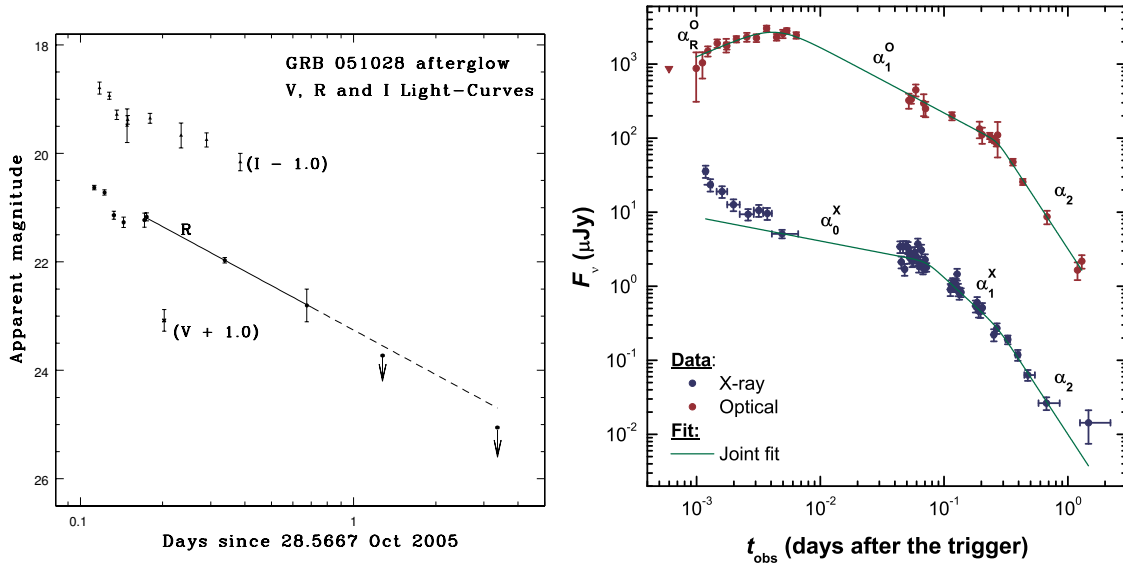
Figure C.5: Left: *The optical light curve of the* HETE *GRB 051028, as presented in Castro-Tirado et al. (2006). The two late upper limits lie beneath the extrapolation of the power-law decay, indicating that a break in the light curve must have occurred.* Right: *The optical and X-ray light curves of GRB 060605 (Ferrero et al. 2009). In the fit, the parameter α_2 as well as the last break time (where α_1^X/α_1^O transition to α_2) are shared. While the evolution before this break is markedly different in the two wavebands, the late decay is achromatic. Together with the steep decay index $\alpha_2 = 2.56 \pm 0.13$, this is a clear sign of a jet break.*

2009), and this number is reduced even more if one combines this with optical data (Liang et al. 2008).

Within this chapter, I have already presented several GRBs whose afterglows had clear jet break signatures. In the case of XRF 071010A (Chapter C.2) and GRB 060526 (Chapter C.3), these have even found to be achromatic between the optical and the X-rays. Here, I will present further afterglow studies in which I was involved in which found evidence for probably jet breaks.

GRB 051028 was one of the last GRBs localized by the *HETE* satellite. It was only seen with the *WXM* instrument, which yielded a large error box ($33' \times 18'$). As this is still covered by the TLS Schmidt camera, we initiated follow-up observations as soon as the afterglow position became observable. It was well-placed for observations, and the weather was fair as well, so we observed the whole night. *Swift* XRT found an X-ray afterglow, which allowed the optical afterglow to be discovered by the William Herschel Telescope (WHT) on La Palma. Reduction and analysis of our images, performed in part by myself, revealed further afterglow detections (we also obtained follow-up during the next two days, yielding upper limits only, which are unpublished), including the only published V band detection. This detection led to an estimate of the redshift to lie between 3 and 4, but spectroscopy was not obtained. Two late, deep upper limits from the WHT show that the initial power-law decay must have broken to a steeper decay, as they lie significantly beneath the extrapolation of this decay (Figure C.5). This is probably due to a jet break, but no precise values could be obtained. Furthermore, the (sparsely sampled) X-ray light curve seems to show no break until at least ten days after the event, but there is a gap in the observations where the optical break occurs. Our analysis is published in Castro-Tirado et al. (2006).

The main motivation behind our study of the high-*z Swift* GRB 060605 (Ferrero et al. 2009) was our integral field spectroscopy obtained with that Calar Alto 3.5m telescope. This has been discussed in detail in the PhD thesis of Dr. Patrizia Ferrero, and I will only focus on the afterglow light curve, which I studied together with Steve Schulze. No TLS data was obtained for this GRB, but
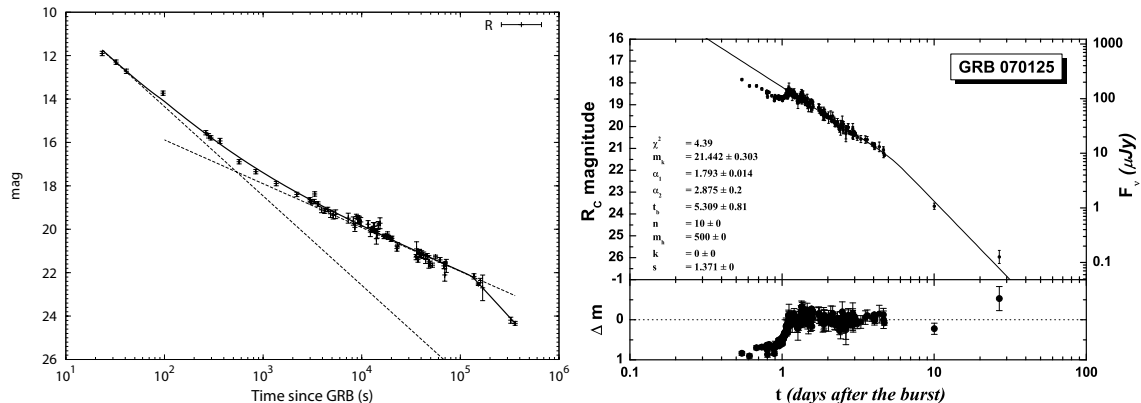
Figure C.6: Left: *The R_C band afterglow of GRB 061126, corrected for the host galaxy contribution. It is modeled with a double-broken power law. The early steep decay is probably due to a reverse shock flash, but the peak precedes even the earliest detection (Perley et al. 2008a). At ≈ 1.5 days, a break is seen which is a jet break candidate. Figure taken from Gomboc et al. (2008).* Right: *A fit to the R_C light curve of GRB 070125, using the combined data sets from Updike et al. (2008), Chandra et al. (2008) and Dai et al. (2008a). Post-break data is scarce, but a clear break is seen in the light curve. The parameters of the fit are given in the figure, I followed Cenko et al. (2008b) and assumed a negligible host galaxy contribution (tidal tail starburst). The break is also evident in the X-rays, implying it is very probably a jet break.*

we published the *Swift* UVOT data in our study, combining them with late R_C−band observations (Jinsong Deng et al., in preparation). To create a well-sampled light curve, we shifted the UVOT detections to the R_C band assuming achromacy. While this procedure can be risky, early observations by the ROTSE-III telescope (Rykoff et al. 2009), which were published after we finalized our study, fully confirmed our light curve. The optical afterglow exhibits a break to a steep decay at 0.27 days after the trigger, and a comparison with the X-ray light curve shows that they evolve achromatically after the break, a sure sign that this is a jet break (Figure C.5). Especially considering the redshift we derived for this GRB, $z = 3.773 \pm 0.001$, this break is very early in comparison to the sample of Zeh et al. (2006a), indicating strong collimation. I also studied the SED of this event, but due to the redshift, only the R_C band is unaffected by Lyman dropout (no observations in redder bands have been reported). The UVOT data is strongly suppressed, and the afterglow is not detected in the u band or even further blueward. Therefore, no analysis of the dust properties is possible.

GRB 061126 was a bright *Swift* GRB which I observed at two epochs with the TLS telescope (Kann & Malesani 2006; Kann 2006). Two comprehensive studies have been published on this event. Perley et al. (2008a) focused on the early afterglow of the GRB, and also found that while the SED shows little signs of extinction, it is strongly depressed in comparison to the X-ray afterglow, indicating that either gray dust is required, or an additional component increases the flux of the X-rays. Gomboc et al. (2008), which also includes the TLS data, find additional evidence to support the latter scenario. My analysis of the SED using both data sets confirms the results of Perley et al. (2008a). Furthermore, after subtraction of the host galaxy, I found evidence for an optical break (Figure C.6), which I had already found from the TLS observations (Kann 2006). (Actually, I had made a mistake during the preliminary analysis, underestimating the magnitude. The full analysis of later data showed, though, that the break actually did occur before the second TLS epoch.) This break is not seen in the X-rays, which can be fit with a single power-law decay, giving another example of a chromatic break. This example shows that it can be misleading to use the X-ray regime alone to search for jet breaks, and also to look for dust extinction through joint X-ray-optical fits.

GRB 070125 was a very bright GRB localized by the *IPN* (Bellm et al. 2008). A very bright

afterglow was discovered, leading to an extensive observing campaign (TLS could not observe as it was bright time and the Schmidt camera was not mounted) (Updike et al. 2008; Chandra et al. 2008). The spectra of the afterglow showed very few lines and small column densities (Cenko et al. 2008b; Updike et al. 2008; Fynbo et al. 2009), which, together with deep limits on any host galaxy (Dai et al. 2008a) led to the interpretation that this GRB had exploded in a halo environment, possibly a starburst in a tidal tail (Cenko et al. 2008b). The early afterglow showed a very strong rebrightening, probably due to an energy injection, and my analysis showed that is one of the most luminous afterglows ever discovered (Updike et al. 2008). Afterglow follow-up was dense until about four days after the trigger, but then became very sparse due to interference from the bright moon. But the few late detections and upper limits, also in the X-ray regime, show that a strong break occurred (at $t_b = 5.31 \pm 0.81$ days, according to my analysis of the joint data sets), and the probable achromaticity implies that this is a jet break. Using this time and the prompt emission parameters to calculate the collimation-corrected energy release shows that GRB 070125 was one of the most energetic GRBs ever detected.

C.5   Are the Afterglows of GRBs with High-Energy Detections special?

With the launch of *AGILE* and *Fermi*, it was clear that GRBs would be discovered which featured emission in the high MeV (> 50) to GeV range. So far, the only GRBs with high-energy detections had been *CGRO EGRET* events, and none of them was localized or had a discovered afterglow. Therefore, it was of interest to check if GRBs with *AGILE GRID/Fermi LAT* detections are fundamentally different from other GRBs when it comes to their afterglows. A correct approach to this would be to create a comparison sample of GRBs which were in the *GRID/LAT* field of view but have no detections. The inherent problem is that, so far, only a single GRB has been simultaneously localized by *Fermi LAT* and *Swift BAT* (the extremely luminous Type I GRB 090510), all other *LAT* GRBs with detected afterglows owe their localization to *LAT* itself (so far, no *AGILE GRID*-detected GRB has had a *GRID* localization exclusively), and only one GRB so far (GRB 091010, localized by *SuperAGILE* and *Swift XRT*) has been well-localized and has upper limits only from both *GRID* (Marisaldi et al. 2009) and *LAT* (Kocevski et al. 2009), but no optical afterglow (Guidorzi et al. 2009b). Therefore, a first comparison will involve the global afterglow sample I have created, independent of the fact that some of these GRBs might have been detected at high MeV/GeV energies had the technology been available. A second important point (though not so much for my own studies) is that only with a redshift, and thus accurate distance information, a full interpretation of the high energy results is possible (such as the derivation of upper limits on the quantum gravity mass scale, Abdo et al. 2009b).

     GRB 080514B was a rather short ($T_{90} = 7$ s) GRB with a complex emission profile and a high peak flux. It was localized by the *SuperAGILE* detector, but only in one dimension. Due to its brightness, it triggered several other satellites, and the annulus derived from *SuperAGILE* and *Mars Odyssey* data lay almost vertical to the *SuperAGILE* error strip, creating a small error box. It was the first GRB which *AGILE* detected with *GRID*, and the analysis of this data revealed that the high-energy emission was delayed with respect to the soft gamma rays, something which is now recognized as a common feature. The *AGILE* observations are described in Giuliani et al. (2008). As soon as the error box was published, the localization was followed up by *Swift*. Even before an XRT position was known, an optical afterglow was discovered by the IAC80 telescope in Spain. It was later detected at several epochs by GROND. We gathered all available optical data, including *Swift* UVOT (as well as XRT) data as well as Keck host galaxy observations. The light curve data is rather sparse, but it allowed us, thanks to the UVOT UV data, to determine a photometric redshift of $z = 1.8^{+0.4}_{-0.3}$ (Figure C.7). This is in excellent agreement with the "*pseudo-z*" obtained from gamma-ray data (Pelangeon & Atteia 2008), but lies right between the two redshift estimates from X-ray data (Gendre et al.
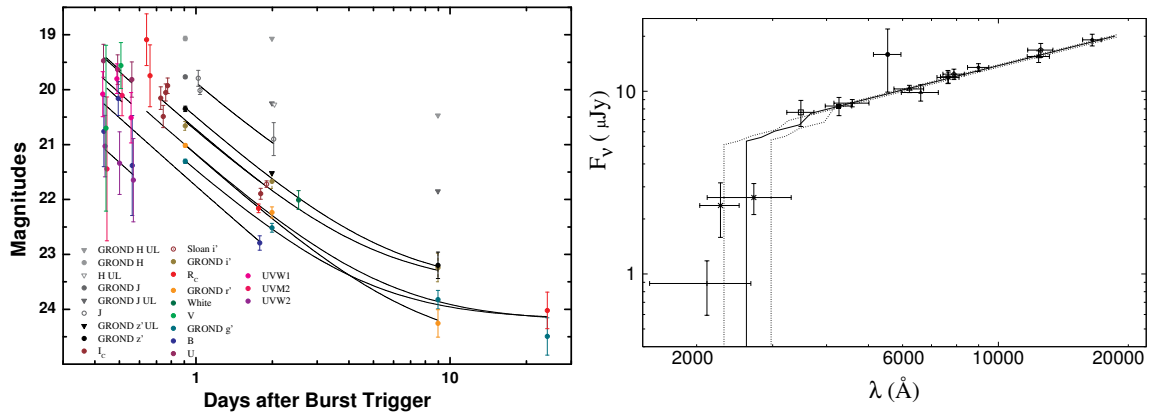
Figure C.7: Left: *The light curve of the afterglow of the* AGILE *GRB 080514B. All data can be fit by a single power-law with a late host galaxy component.* Right: *The SED of the afterglow of the* AGILE *GRB 080514B. With the exception of the UVOT v band (a marginal detection) the SED is described by a pure power-law, without evidence for dust extinction, up to ≈ 3000 Å. The UVOT UV filters, though, are strongly depressed, indicating the effect of Lyman α absorption. This dropout can be used to determine a photometric redshift, we find $z = 1.8^{+0.4}_{-0.3}$. Figures taken from Rossi et al. (2008).*

2008). My analysis of the light curve revealed no break, the slope ($\alpha = 1.67 \pm 0.07$) does not allow a determination if it is pre- or post-break. I found no evidence for any dust extinction from the SED, it is an almost astonishingly smooth power law. A comparison with my afterglow sample showed that the afterglow of GRB 080514B was neither exceptionally bright or faint, nor did we find any other properties which set it apart. We concluded the high energy detection was due to the brightness of the GRB.

With the launch of *Fermi*, the detection of high-energy emission from GRBs has become more common (e.g. Abdo et al. 2009c,b,a,d, 2010; Ackermann et al. 2010a), with a total of 19 *LAT* GRBs so far (see http://fermi.gsfc.nasa.gov/ssc/resources/observations/grbs/grb_table/). The GROND/TLS team has been at the forefront of optically following up these special GRBs (which are all bright, sometimes exceptionally so), with the discovery of the first afterglow of a *LAT* GRB, that of GRB 080916C, which also allowed a photometric redshift determination and revealed that this GRB is one of the most energetic ever discovered (Greiner et al. 2009a). The next well-localized *LAT* GRB, GRB 090323, is the first to have a spectroscopic redshift ($z = 3.568$, Cenko et al. 2010). Within the "bolometric" energy band (1 keV - 10 MeV in the GRB rest frame), it even has a slightly higher energy release than GRB 080916C. The afterglow was discovered by GROND, and I obtained multiple epochs of follow-up with the TLS telescope, including the latest and deepest afterglow detection (Appendix C) achieved here so far. Further observations were obtained by GROND for the *LAT* GRBs GRB 090328, GRB 090510 (a Type I GRB), GRB 090902B (also late VLT observations) and GRB 090926A. Our team obtained spectroscopy for GRB 090323, GRB 090328, GRB 090510, and GRB 090926A. While the spectroscopy of GRB 090323 and the afterglow observations of GRB 090926A will be published in separate papers (see Rau et al. 2010, for the latter), all other data has been combined in McBreen et al. (2010), where we present a comprehensive analysis of the optical/NIR data of these GRBs. Next to the reduction and analysis of the TLS data of GRB 090323, I also analyzed the SEDs of the GRBs (confirming the results made by the GROND team in Garching) and compared the afterglow luminosities with my afterglow sample. The afterglow of GRB 090323 is among the most luminous of all afterglows, whereas the others are closer to the center of the *Swift* luminosity distribution. Observationally, as an ensemble, the *LAT* afterglows are brighter than *Swift* afterglows, resembling the afterglows of the *BeppoSAX/BATSE/HETE* sample. See Chapters 4 and 5 for more details.

C.6   GRBs are the most luminous electromagnetic sources in the universe

In the gamma-ray band, GRBs can outshine the complete gamma-ray sky for short periods of time, making them easy to detect. The case is different in the optical, where it has been found that most optical afterglows are faint even at early times (Roming et al. 2006a). The observational faintness notwithstanding, the absolute luminosities of GRB afterglows can be very high, though only for very short times. The prompt flash of GRB 990123 (Akerlof et al. 1999), which was theoretically observable with binoculars from $z = 1.6$, already illustrates this point. But in the *Swift*-era, two further afterglows have beaten this record.

GRB 050904 has already been mentioned in the history section (Chapter 1) as being the most distant discovered GRB at the time (Kawai et al. 2006). Astonishingly, the 25cm robotic TAROT telescope in France detected an optical flash during the prompt emission (Boër et al. 2006). These authors compared their measurement directly with the prompt flash of GRB 990123, finding that it was brighter but just calling the two events "comparable". I decided to research this aspect further (Kann et al. 2007f). In the course of compiling my database (Chapter 4), I also compiled all available data on GRB 050904. In a first step, I obtained light curve fits that yielded comparable but more precise results than those obtained before (Tagliaferri et al. 2005a; Haislip et al. 2006), and I created a composite light curve by shifting data from different filters to a common (J) zero point (no spectral changes were found) (Figure C.8). Due to its high redshift, it was mostly observed in the NIR ($YJHK$). Detections were also made in $I_C z$, but these are affected by Lyman α absorption. The NIR SED is a smooth power-law, indicating the the dust extinction along the line of sight is negligible. In such a case, it can be assumed that the power-law can be extrapolated into the rest-frame UV region which is affected by the Lyman α absorption, allowing the derivation of the observed R_C magnitude of the afterglow in the hypothetical case of a completely transparent universe. This shifted light curve was then transformed to $z = 1$ (see Chapter 4). For the peak of the optical flash, I derived, at $z = 1$, $R_C = 6.48^{+0.27}_{-0.28}$ (all errors in the process have been propagated, but the error is dominated by the original measurement error from Boër et al. 2006), which is more than a magnitude brighter than the flash of GRB 990123 (if at $z = 1$). In terms of absolute magnitude, I find $M_R = -37.6 \pm 0.3$, which is equivalent to $6.4 \cdot 10^{16} L_{\odot R}$. This is at least several dozen times more luminous (in the R_C band only) than the most luminous persistent source known, the BAL quasar APM 08279+5255, is in the bolometric bandpass. I also reviewed the existing literature on GRB 050904 and compared it with the known properties of "typical" GRBs. I found that while the GRB is among the most energetic known (both in terms of prompt emission and afterglow), it is not so exceptional that a new type of progenitor (e.g., a Pop III star) would be necessary.

Several years later, serendipity yielded a direct view into the most luminous explosion ever detected. *Swift* had detected a GRB, GRB 080319A, triggering a multitude of robotic telescopes to follow it up. Twenty-seven minutes later and just 14° away, GRB 080319B exploded, allowing several wide-field telescopes (Pi-of-the-Sky, TORTORA and RAPTOR-Q) to observe the GRB location as it was occurring, and multiple robotic telescopes (ROTSE, RAPTOR-P and -T, PAIRITEL, REM, P60, *Swift* UVOT) to be on target before the prompt emission ended (Bloom et al. 2009; Racusin et al. 2008; Woźniak et al. 2009). What was discovered was astounding. GRB 080319B had the second-highest fluence of any GRB in the last 20 years, and it was accompanied by a prompt flash which reached naked-eye visibility ($R_C \approx 5.3$) (although bright moonlight prevented an actual visual observation), earning it the moniker "the naked-eye GRB". I was part of a study led by the Berkeley GRB group (Bloom et al. 2009). I fit the late afterglow data with a supernova component (see also Kann et al. 2008j for preliminary results), finding that the accompanying supernova, which is clearly seen as a bump in the $i'z'$ bands, is highly luminous, though this depended on the final host galaxy magnitude. Tanvir et al. (2008b), using even later observation that show almost pure host galaxy
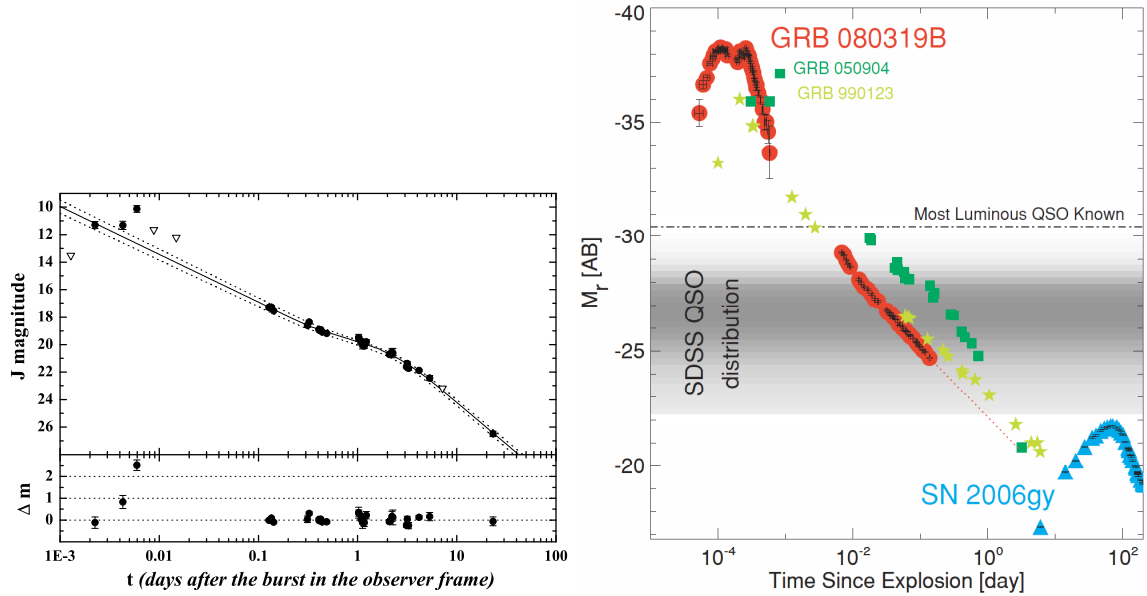
Figure C.8: Left: *The composite J−band light curve of GRB 050904. At early times, it exhibits a rapid rise, short plateau, and an optical flash which exceeds the back-extrapolation of the late afterglow. The later data first show a steep decay (typical for a reverse shock flash), a "standard" decay and a break to a late, steep decay, probably a jet break (the X-ray data are too sparse to check achromaticity). Taken from Kann et al. (2007f).* Right: *A comparison between the luminosities (given in AB magnitudes in the r′ filter) of the prompt flashes of the afterglows of GRBs 990123, 050904 and 080319B, as well as other very luminous sources which have been used as "backlighting" to study the surrounding environment. The prompt flash of GRB 080319B is the most luminous optical source ever detected. Taken from Bloom et al. (2009).*

light, found the host is brighter than I had assumed and the SN therefore more similar to SN 1998bw. A transformation to $z = 1$ (which is very precise, as the GRB occurred at $z = 0.937$ anyway) shows that the prompt flash reached $R_C = 5.14$ at peak, over a magnitude brighter than the prompt flash of GRB 050904. A comparison (Figure C.8) shows the extreme luminosity in comparison with other highly luminous sources. We found that *Swift* would have been able to significantly detect this GRB up to almost $z = 11$, and ground-based rapid follow-up NIR telescopes like PAIRITEL would have easily detected it in the K band up to $z = 17$. Of course, the prompt flash of GRB 080319B is an extremely exceptional event, but it indicates that it *is* possible to detect GRBs and their afterglows deep into the age of reionization – possibly the only cosmic source which will give us this possibility to study the ISM and IGM at such high redshifts.

C.7   The odd one out – the optically flaring Galactic source of GRB 070610

In the final section of this chapter, I will present some results on a highly peculiar source which initially "masqueraded" as a normal Gamma-Ray Burst but turned out to be a so-far unique Galactic transient source.

GRB 070610 triggered *Swift*, which was not able to slew to it immediately, though. The prompt emission is completely unremarkable, consisting of a 5 s long symmetrical peak, the spectrum is adequately fit by a power-law. It is also not an outlier in the Hardness-Ratio−T_{90} diagram. The *Swift* observations are described in Kasliwal et al. (2008).

Rapid optical observations were obtained by the 1.3m telescope at the Skinakas observatory on Crete. Serendipitously, it was observing a nearby source, allowing it to be on the nearby target extremely rapidly for a telescope this size, in just 28 seconds. The first observations revealed a faint source which was not visible in archival images (which was found in a very crowded field without the help of an XRT localization), and 300 seconds after the trigger, observations began with the fiber-fed photon counting detector OPTIMA-Burst. These revealed that at 7 minutes after the GRB trigger, the source emitted a complex multi-peaked optical flare (Stefanescu et al. 2007).

In Tautenburg, the GRB occurred during dusk, and was followed up immediately with the Rapid Response Mode as soon as the telescope was activated, leading to a delay of 640 seconds after the trigger, and thus missing the optical flare detected by OPTIMA-Burst. When I analyzed the data the following day (consisting of two sequences of $6 \times I_C$, $3 \times R_C$ and $3 \times V$, 120 seconds each), I discovered two further optical flares, one in the I_C and one in the R_C band. This behavior was highly untypical for normal GRB afterglows. The source lies in the Galactic plane, behind high extinction, which would have implied that the flares reached roughly 13th magnitude if the source was extragalactic and behind the plane. Finally, the first *Swift* XRT data showed that the X-ray source associated with the flaring optical counterpart remained flat with superposed small flares. All these clues led me to propose that this was a new Galactic source, and it has also been designated as SWIFT J195509.6+261406 (SWIFT J1955 in short).

A large collaboration led by Alberto Castro-Tirado and including the TLS GRB team began a broadband observational campaign which included X-ray (public *Swift* data and a late XMM-Newton observation) optical/NIR (photometry, including adaptive optics $H-$band imaging, and spectroscopy), millimeter and radio observations. These are described in Castro-Tirado et al. (2008). At the same time, further observations were obtained with OPTIMA-Burst (Stefanescu et al. 2008), and a third team also obtained optical/NIR and radio observations (Kasliwal et al. 2008).

These observations found that the source did not fade, but became optically extremely variable within a day after the trigger. Flares were detected which peaked at 14th magnitude (Figure C.9), and Stefanescu et al. (2008) detected two of these with very high time resolution, showing shapes reminiscent of prompt GRB emission. Spectroscopy was unfortunately obtained too late (Castro-Tirado et al. 2008) or targeted the wrong source (Kasliwal et al. 2008, the initially submitted version). After three days of activity, the source finally started fading, but some smaller late-time flares were still observed with large-aperature telescopes (Kasliwal et al. 2008; Castro-Tirado et al. 2008). Deep late-time observations in the X-rays, the optical and the NIR revealed no quiescent counterpart in any waveband. Radio observations of the line-of-sight were used to establish with high confidence that the source is indeed within the Galactic plane (Castro-Tirado et al. 2008, note that if it lay beyond the Galaxy, the energy requirements would become extreme). Up to date, no further outburst has been detected, nor have any similar sources been found.

As impressive as the observations are, the fact that they resemble, as a whole, no known source, makes the theoretical interpretation difficult. Kasliwal et al. (2008) find a certain resemblance to the "fast X-ray nova" V4641 Sgr, a binary system with a black hole and a main sequence star, and add SWIFT J1955 to this class. Castro-Tirado et al. (2008) point out several problems with this interpretation, such as the lack of any radio emission and the very strong constraint on any stellar companion from deep NIR emissions. The flaring properties are also markedly different, both in magnitude and in variability (Stefanescu et al. 2008). The conclusion of both our team and Stefanescu et al. (2008) is that the source is a magnetar, an "optical SGR", possibly an "old" one which is making the transition to the Dim Isolated Neutron star phase. This is also supported by my analysis of the distribution of flare magnitudes (Figure C.9), which shows a truncated log-normal (in flux density) distribution, like that found for the high-energy flares of true SGRs. The actual mechanism of the optical flaring remains unexplained, though Stefanescu et al. (2008) suggest it may be the result ion-driven aurorae in the powerful magnetic field of the neutron star.

Clearly, the discovery of SWIFT J1955 shows that after four decades of work to establish the
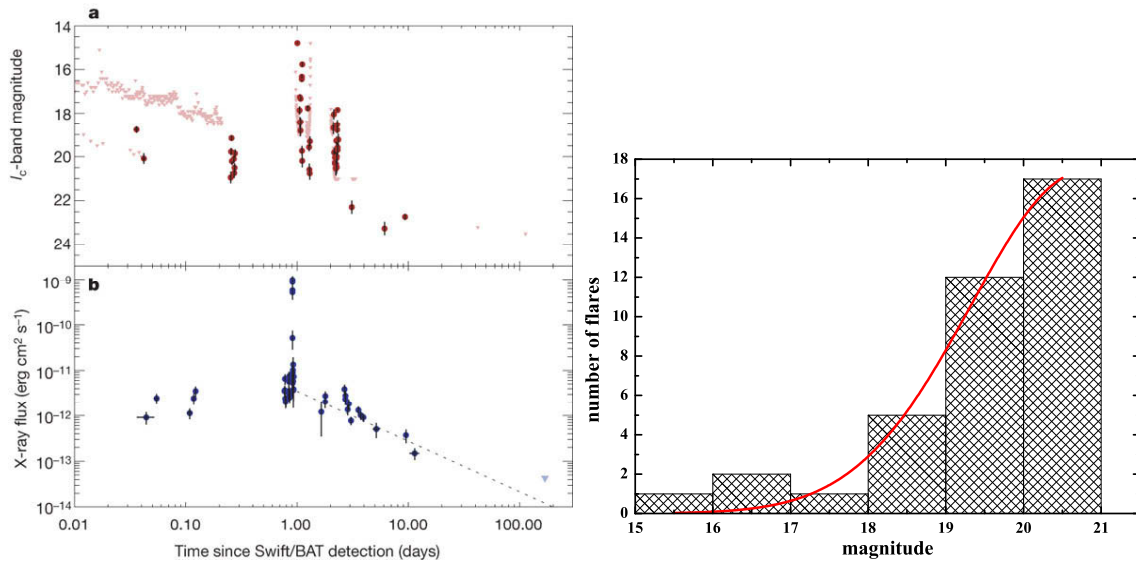
Figure C.9: Left: *Light curves of the transient associated with GRB 070610 in the I_C band (top) and the X-rays (bottom). Pink triangles are upper limits, darker circles are detections – the first two are from Tautenburg. Clearly, the light curve is highly variable in both bands (unfortunately, no optical observations were obtained during the bright X-ray flare), showing short-timescale flares (duration less than a few minutes) during which the source can increase by more than five magnitudes. This behavior is not known from any extragalactic GRB afterglow, implying, along with the position in the Galactic plane, that the source is a new Galactic transient of unknown nature.* Right: *Distribution of the flare magnitudes in the I_C band. An adequate fit can be obtained with a truncated log-normal (in flux density) distribution, similar to that of SGR flares. Several further observational results also favor a magnetar interpretation. Figures taken from Castro-Tirado et al. (2008).*

extragalactic distance scale, some GRBs have "returned home" to our own Galaxy. The fact that no further similar source has been identified though shows that the contamination rate can not be very high. Further research into the nature of this mysterious transient will require very deep observations with the likes of *Chandra* or *HST WFC3 IR* to either detect a quiescent counterpart or establish even stricter limits on it.

Appendix D

GRB observations with the Tautenburg Schmidt Telescope

In the following, I list the GRB observations with the 1.34m Schmidt telescope of the Thüringer Landessternwarte Tautenburg I was involved in, most of them have been published in some way. In most cases, my involvement consisted in both obtaining the observations as well as reducing and analyzing the data.

- GRB 040624 was an *INTEGRAL* GRB far off the Galactic plane which was observed in $R_C I_C$ 0.5 days after the burst. Upper limits only, published in a GCN (Kann et al. 2004).

- XRF 040912 was an optically dark *HETE II* X-ray Flash. Multiple epochs of deep upper limits in $BVR_C I_C$ were obtained and are published in Stratta et al. (2007a).

- XRF 040916, a *HETE II* X-ray Flash, was observed about one day after the GRB in $VR_C I_C$. Later analysis shows it was detected in R_C, in agreement with other data. Not published.

- GRB 041006, a *HETE II* GRB with many optical observations, was observed 1.4 days after the event in R_C. The data is included in Kann et al. (2010).

- GRB 050712 was a *Swift* GRB faintly detected in R_C, with an upper limit one day later. Data are only published in a GCN (Zeh et al. 2005b).

- GRB 050714A was a faint *INTEGRAL* GRB in the Galactic plane, and the first time the TLS Rapid-Response Mode (RRM, Klose et al. 2005b) was triggered (follow-up was delayed due to the ongoing observations not being immediately interrupted). I was not involved in the initial observations, but obtained later deep data in multiple colors, as well as I_C-band data with the Calar Alto 2.2m observatory. A publication in preparation was abandoned when it was realized the initial (possibly fading) afterglow candidate lay strongly outside the final revised XRT error circle. It has a stellar PSF and may be a slightly variable red dwarf.

- GRB 051008 was a bright *Swift* GRB observed at multiple epochs in I_C (one hour after the event) and R_C (three weeks). No transient source (either afterglow or supernova) is detected. This is a very dark burst. A paper I was involved in has been published (Volnova et al. 2010), but the TLS data are not included.

- GRB 051028 was a *HETE II* GRB successfully detected in $VR_C I_C$. The observations have been published in Castro-Tirado et al. (2006).

- "GRB 051102" turned out to be a false trigger of the *HETE II* satellite. It was the second RRM observation, showing that data acquisition could begin within five minutes of receiving the position alert. As it was a false trigger, nothing of interest was found except a faint asteroid, and no circular was issued.

- GRB 051103, localized by the IPN, is most likely a superflare from an SGR in M81. TLS observations VR_C gave upper limits only, published only in a GCN (Klose et al. 2005a).

- GRB 051105 was a faint *Swift* Type I GRB observed on two epochs in R_C. Only upper limits were obtained, they are published in Kann et al. (2008e).

- GRB 051117 was only observed at a late time, ruling out a host galaxy which had been suggested from UVOT observations. The derived upper limit is the deepest I have ever achieved with our telescope (24th magnitude in R_C). The result was only published in a GCN (Kann et al. 2006c).

- GRB 060105 was observed at late times to search for a host galaxy. Only an upper limit could be found, published in a GCN (Kann & Manohar 2006a).

- GRB 060109 was observed at late times to search for a host galaxy. Only an upper limit could be found, published in a GCN (Kann & Manohar 2006b).

- GRB 060124 was an extremely long *Swift* GRB (see Romano et al. 2006, for the *Swift* observations). The afterglow was discovered by myself. Multiple epochs of VR_CI_C observations were obtained. Analysis is not yet completed, and a paper led by myself is in preparation.

- GRB 060323 was a faint *Swift* GRB with a very faint afterglow. An initial candidate reported by myself (Kann & Stecklum 2006) turned out to be a faint galaxy near the actual afterglow, which is detected in R_CI_C and possibly V (Kann et al. 2006a). A publication was planned (L. Vetere et al.) but has been strongly delayed and it is unclear if it will be finished.

- GRB 060502B was a *Swift* Type I GRB observed 0.11 days after the event. Only a moderately shallow upper limit in R_C was obtained due to bad observing conditions. In this GCN, I suggested for the first time that the elliptical galaxy at a large offset might be the host galaxy, as later also argued by Bloom et al. (2007). The TLS data will be published in Kann et al. (2008e).

- GRB 060515 was observed at late times to search for a host galaxy. Only an upper limit could be found, published in a GCN (Kann & Manohar 2006c).

- GRB 060526 was observed at two epochs in R_C, resulting in a detection and a late, deep upper limit. Data are published in Thöne et al. (2010).

- GRB 061126 was observed at two epochs in R_C, resulting in nine data points, which are published in Gomboc et al. (2008).

- GRB 070311 was an *INTEGRAL* GRB which featured a large, late-time optical flare (Guidorzi et al. 2007). My TLS observation, yielding a faint detection in R_C, showed the initial rise was not due to an SN component (Kann et al. 2007a), making me suggest that it might be an optical flare due to late central engine activity (Kann 2007). A paper led by myself is in preparation.

- GRB 070411 was observed immediately in RRM, starting 342 seconds after the burst trigger. It was close to the horizon and sinking, but in total, 18 R_C detections were achieved. The afterglow was discovered independently of the *Swift* team by Steve Schulze and myself, but our GCN was submitted a bit slower. The data have been presented (along with further rapid follow-up) in Ferrero et al. (2008), a more detailed publication is planned.

- GRB 070610 was initially thought to be a *Swift* GRB close to the Galactic plane, but RRM observations (slightly delayed as the GRB occurred during twilight just as the telescope was turned on) from Tautenburg, which showed a short-time optical flare, led me to propose this to be a new Galactic source. Further observations worldwide confirmed this interpretation, and the TLS observations (among many others) have been published in the journal *Nature* (Castro-Tirado et al. 2008).

- GRB 070616 was a very long *Swift* GRB. It happened behind the Galactic plane, and very close to a foreground star. Only upper limits in I_C could be derived (Kann et al. 2007e; Kann & Wilson 2007), no publications beyond the GCNs are planned.

- GRB 071010B was a bright *Swift* GRB with an amateur-discovered afterglow. TLS observations in R_C confirmed the afterglow. I obtained multiple observations of the slowly fading afterglow over a week, also with other telescopes, which reveal a late break in the light curve. A publication led by myself is in preparation.

- GRB 071013 was a *Swift* GRB for which no XRT position was obtainable. Multiple observations in R_C revealed no variable sources (Kann et al. 2007b,c,d). Further late follow-up was obtained which will be compared with image subtraction methods to the first epochs in the future, and a final report will be issued.

- GRB 080430, a low-redshift *Swift* GRB, could not be observed directly with RRM due to inclement weather. I obtained a clear detection a day later. The data will appear in an upcoming publication (A. de Ugarte Postigo et al., in preparation).

- GRB 080506, a *Swift* event, was successfully detected in VR_CI_CZ 0.3 days after the GRB, and in R_C one day after that. So far published only in GCNs (Kann et al. 2008b,a).

- GRB 080507 was an *AGILE* GRB not reported until over a day after the trigger. Follow-up observations in R_C (Kann et al. 2008c,d) led me to discover the afterglow. So far, no publications beyond the GCNs are planned.

- GRB 080603A was an *INTEGRAL* GRB which was observed in R_C 1.5 days after the GRB. Late-time observations were obtained for the purpose of image subtraction, as there are several galaxies close to the GRB position. A paper is in preparation (C. Guidorzi et al.).

- GRB 080603B was a *Swift* GRB which was detected 1.2 days after the event in R_C (Kann et al. 2008g). A deep upper limit at 5 days (Kann et al. 2008f) shows that a late break must have been occurred. No publication beyond the GCNs is planned.

- GRB 080605 was a *Swift* GRB which was observed in RRM mode, starting 354 seconds after the event. while the afterglow was first announced by the *Swift* team, there was a delay in the distribution of GCNs and it was discovered independently by UVOT, myself as well as the Liverpool telescope. A nearby, very red source led to source confusion, late-time observations have been obtained to perform image-subtraction. A paper is in preparation (A. Melandri et al.).

- GRB 080710 was a low-redshift *Swift* GRB detected in R_CI_C 0.73 days after the event. The data are included in Krühler et al. (2009).

- GRB 081024B was the first *Fermi* Type I GRB detected at GeV energies by LAT. TLS observations obtained 0.9 days after the event indicate a possible afterglow, but the variability of this source is in dispute (Kann et al. 2008h). Additional observations were obtained several months later to look for variability with image subtraction methods, this analysis has not been performed yet. A final report will then be issued.

- GRB 081025 was a *Swift* GRB detected during a slew and thus reported with a large delay. It was observed in RRM mode when the position was sent out, almost 0.4 days after the GRB. Only upper limits in R_CI_C could be derived (Kann et al. 2008i).

- GRB 090323 was a very bright *Fermi* GRB at moderately high redshift localized by LAT. TLS observations in R_C were performed at multiple epochs, yielding a total of ten detections which are published in McBreen et al. (2010). This is the highest redshift GRB (with spectroscopically determined redshift, GRB 051028 probably lies at a similar distance) successfully detected in Tautenburg, and also the latest (nine days) and deepest ($R_C = 23.70 \pm 0.37$) detection so far.

- GRB 090424 was a very bright *Swift* GRB observed in R_C at about 0.25 days after the GRB. A total of ten detections were achieved, they are published in Kann et al. (2010).

- GRB 090426 was a short, possibly Type I *Swift* GRB. It was faintly detected in $R_C I_C$. A publication within a compilation paper, together with GROND data (A. Nicuesa Guelbenzu et al.) is in preparation.

- GRB 090529 was a *Swift* GRB observed 0.3 days after the event, yielding one detection in I_C and three detections in R_C (Kann et al. 2009b). A publication led by L. Xin is in preparation, which includes an additional R_C detection at 0.45 days which may imply a rebrightening.

- GRB 090817 was an event localized by *INTEGRAL* in the Galactic plane. I, among several other teams, performed late-time observations (in R_C, eight days after the GRB) which showed that an object at the XRT position was a star and not variable (Kann et al. 2009a).

- GRB 091020 was a *Swift* GRB observed $0.16 - 0.22$ days after the event, yielding a total of 15 detections, three each in $BVR_C I_C Z$, one of the best multicolor data sets obtained so far with this telescope of an afterglow. At 5.2 days, the afterglow was detected again, faintly with $R_C = 23.62 \pm 0.31$. A paper is in preparation (J. Racusin et al.).

- GRB 091024 was an extremely long *Swift/Fermi* GRB in the Galactic plane. Only a rather shallow limit at 0.6 days could be obtained in R_C (Kann & Laux 2009).

Acknowledgements

"I know the sun and the moon — The names of stars — Their movement and purpose — I mark the place of Polaris on these impossible heights
This here is my place, it is my work — I was made the maker of the sky"

  – *Amorphis, Skyforger*

"We... Are... A Blaze... In The Northern Sky..."

  – *Darkthrone, Kathaarian Life Code*

Ehrenwörtliche Erklärung

Ich erkläre hiermit ehrenwörtlich, dass ich die vorliegende Arbeit selbständig, ohne unzulässige Hilfe Dritter und ohne Benutzung anderer als der angegebenen Hilfsmittel und Literatur angefertigt habe. Die aus anderen Quellen direkt oder indirekt übernommenen Daten und Konzepte sind unter Angabe der Quelle gekennzeichnet.

Bei der Auswahl und Auswertung folgenden Materials haben mir die nachstehend aufgeführten Personen in der jeweils beschriebenen Weise unentgeldlich geholfen:

1. Dr. habil. Sylvio Klose: Betreuung der vorliegenden Arbeit, Programmierung (Berechnung der Helligkeitskorrektur, mini-SN Parameter, Monte-Carlo Analysen, K-S Test).

2. Dr. Andreas Zeh programmierte die Fit-Routinen unter *Origin*, die für das Fitten der Lichtkurven (inklusive der Supernova-Komponente) und SEDs verwendet wurden.

3. Dipl.-Phys. Steve Schulze sowie Amelia C. Wilson halfen bei der Berechnung der bolometrischen isotropen Energien der GRBs.

4. Prof. Dr. Bing Zhang trug zur theoretischen Interpretation des mittleren Helligkeitsunterschieds zwischen Type I und Typ II GRB Nachglühen bei.

5. Etliche Ko-Autoren trugen mit Datenanalyse sowie Kommentaren zu den Papers bei.

Weitere Personen waren an der inhaltlich-materiellen Erstellung der vorliegenden Arbeit nicht beteiligt. Insbesondere habe ich hierfür nicht die entgeltliche Hilfe von Vermittlungs bzw. Beratungsdiensten (Promotionsberater oder andere Personen) in Anspruch genommen. Niemand hat von mir unmittelbar oder mittelbar geldwerte Leistungen für Arbeiten erhalten, die in Zusammenhang mit dem Inhalt der vorgelegten Dissertation stehen.

Die Arbeit wurde bisher weder im In- noch im Ausland in gleicher oder ähnlicher Form einer anderen Prüfungsbehörde vorgelegt.

Die geltende Promotionsordnung der Physikalisch-Astronomischen Fakultät ist mir bekannt.

Ich versichere ehrenwörtlich, dass ich nach bestem Wissen die reine Wahrheit gesagt und nichts verschwiegen habe.

Tautenburg, den 31. August 2010   David Alexander Kann

Lebenslauf

Zur Person:

Name: Kann
Vorname: David Alexander
Geburtsdatum: 15.02.1977
Geburtsort: Trier

Werdegang:

Aug. 1983 - Jul. 1987	Pestalozzi-Grundschule, Trier
Aug. 1987 - Jul. 1996	Max-Planck Gymnasium, Trier
1996	Abschluß: Abitur
Apr. 1998 - Okt. 2004	Physik-Studium an der Friedrich-Schiller-Universität, Jena
2004	Diplomarbeit "Gamma-Ray Bursts and Cosmic Dust at High Redshifts" an der Thüringer Landessternwarte Tautenburg, Betreuer: Dr. habil. Sylvio Klose
	Abschluß: Diplom-Physiker
seit Apr. 2005:	Doktorand an der Thüringer Landessternwarte Tautenburg Betreuer: Dr. habil. Sylvio Klose Titel: "The Afterglows of *Swift*-era Short and Long Gamma-Ray Bursts"

Tautenburg, den 31. August 2010   David Alexander Kann